

https://dspace.org/

Iron and Malaria

Van Zyl, Robyn L.

1997-02-07
https://hdl.handle.net/10539/31660
Van Zyl, R. L. Iron and Malaria. University of the Witwatersrand; Johannesburg.1997.

Downloaded from a DSpace repository. https://dspace.org/

IRON AND MALARIA

Robyn Lynne van Zyl

A thesis submitted to the Faculty of Medicine,
University of the Witwatersrand, in fulfilment
of requirements for the degree
of
Doctor of Philosophy

Johannesburg, 1997

DECLARATION

I, Robyn Lynne van Zyl declare that this thesis is my own work. It is being submitted for the degree of Doctor of Philosophy at the University of the Witwatersrand, Johannesburg. It has not been submitted before for any degree or examination at this or any other University.

RlvanZyl

.....

7th day of February , 1997

DEDICATION

This thesis is dedicated to the memory of my grandmother, Dorothy Mary Tregear, who passed away in May, 1995. Thank you for all the confidence, love and encouragement you gave me.

PUBLICATIONS AND PRESENTATIONS

Portions of this thesis have been published in full or been submitted:

van Zyl RL, Havlik I, Monteagudo FSE. The effect of iron chelators and classical antimalarials on the *in vitro* growth of *Plasmodium falciparum*. Journal of Antimicrobial Chemotherapy 1992;30:273-278.

van Zyl RL, Havlik I, Hempelmann E, MacPhail AP, McNamara L. Malaria pigment and extracellular iron: Possible target for iron chelating agents. Biochemical Pharmacology 1993;45(Pt 7):1431-1436.

van Zyl RL, Havlik I. The effect of different variables on the antimalarial activity of desferrioxamine. Transactions of the Royal Society of Tropical Medicine and Hygiene 1997:submitted.

van Zyl RL, Havlik I. The *in vitro* effects of ferric and ferrous iron chelating agents on the growth of *Plasmodium falciparum*. Biochemical Pharmacology 1997:submitted.

van Zyl RL, Havlik I. The effect of iron chelating agents on the uptake of diferric transferrin by *Plasmodium falciparum*-infected erythrocytes. Biochimica Biophysica Acta 1997:submitted.

Portions of this thesis have been presented at congresses and published in conference proceedings:

van Zyl RL, Jairam K, Havlik I, Monteagudo FSE. The combined effect of iron chelators and classical antimalarials on the *in vitro* growth of *Plasmodium falciparum*. The 24th South African Pharmacological Society Congress, Johannesburg, 1990:27.

Havlik I, van Zyl RL. The combined effect of iron chelators and classical antimalarials

on the *in vitro* growth of *Plasmodium falciparum*. The 6th South-east Asian/Western Pacific Regional Meeting of Pharmacologists, Hong Kong, 1991.

van Zyl RL, Havlik I. Iron and Malaria. The 26th South African Pharmacological Society Congress, Bloemfontein, 1992:81.

van Zyl RL, Havlik I. Iron and Malaria. Journal of the South African Veterinary Association 1993;64(Pt 4):187-188. The Parasitological Society of Southern Africa, Lake St Lucia, 1993.

Havlik I, van Zyl RL, Hempelmann E, MacPhail AP, McNamara L. Malaria pigment: Possible target for iron chelating agents. Transactions of the Royal Society of Tropical Medicine and Hygiene 1993;87(Pt 4):368. The Residential Meeting of the Royal Society of Tropical Medicine and Hygiene, Scotland, 1993.

Havlik I, van Zyl RL. Iron and Malaria. Plzensky Lekarsky Sbornik 1993;68(Suppl):67. A symposium on Chelating agents in Pharmacology, Toxicology and Therapeutics, the Czek Republic, 1993.

van Zyl RL, Havlik I. Effect of iron chelators on the uptake of iron into *Plasmodium falciparum*-infected erythrocytes. Canadian Journal of Physiology and Pharmacology 1994;72(Suppl 1):189. The XIIth International Congress of Pharmacology, Canada, 1994.

van Zyl RL, Herweg BNES, Leseticky L, Havlik I. The effect of chelating agents on the *in vitro* growth of *Plasmodium falciparum* malaria parasite. The 28th South African Pharmacological Society Congress, Cape Town, 1994.

van Zyl RL, Havlik I. The effect of chloroquine and iron chelating agents on ferriprotoporphyrin-IX induced haemolysis of *Plasmodium falciparum* infected erythrocytes. The 29th South African Pharmacological Society Congress, Bloemfontein, 1995:53.

ABSTRACT

Malaria is one of the most devastating infections found in man and the resurgence of drug resistance has prompted the search for novel chemotherapeutic strategies. Clinical observations have exposed the susceptibility of malaria parasites to iron deficiency, thus the metabolism of iron in parasitized erythrocytes could be a potential antimalarial target.

In *in vitro* experiments, the parasites accumulated approximately four times more non-transferrin-bound iron than diferric transferrin. Both forms were accumulated in a concentration- and time-dependant manner, with more iron being associated with the trophozoite stage than the ring stage. The ferric iron chelating agent, desferrioxamine inhibited the uptake of transferrin and non-transferrin-bound iron in a concentration dependent manner. 2,2'-Bipyridyl, a ferrous iron chelating agent also inhibited the uptake of non-transferrin-bound iron, but did not affect the uptake of diferric transferrin. This indicated that the parasite does not accumulate diferric transferrin by transferrin-receptor mediated endocytosis, but rather by a non-specific endocytotic pathway.

A large quantity of the accumulated iron was associated with the parasite haemozoin. Desferrioxamine effectively reduced the amount of iron associated with the haemozoin, whilst 2,2'-bipyridyl did not, which indicates that the haemozoin-associated iron is in the ferric state. The parasitized erythrocytes were more susceptible to haemolysis by the haemozoin subunits than the uninfected erythrocytes. The presence of chloroquine and 2,2'-bipyridyl potentiated the haemolysis induced by the subunits, whilst desferrioxamine protected the parasitized erythrocytes.

The plasma chelating agents and aminocarboxylate compounds were not as effective in inhibiting parasite growth, as desferrithiocin, bathophenanthroline, desferrioxamine and 2,2'-bipyridyl which avidly chelate iron. The additive interaction between the latter two agents and chloroquine, quinine and pyrimethamine, completely eliminated the malaria infection. As did the combination of two lipophilic ferrous or two hydrophilic ferric iron chelating agents, as well as the combination of a hydrophilic ferric and lipophilic ferrous iron chelating agent. Whilst the combination of hydrophilic ferric and hydrophilic ferrous

iron chelating agents antagonised each others antimalarial actions. Variables such as inoculum size, extracellular pH, cation supplementation and stage dependency, all affected the antimalarial activity of the iron chelating agents.

Thus, the unique pathways involved in the iron metabolism of *P. falciparum*-infected erythrocytes, could be potential targets for new antimalarial drugs, which are membrane permeable and avidly chelate iron.

ACKNOWLEDGEMENTS

I would like to express my gratitude and appreciation to the following people and institutions:

I am indebted to my supervisor Prof I Havlik for his help, advice and latitude.

My loving Mother for her endless patience, support and advice.

My Dad for his love and encouragement.

Denise and Norman for their friendship and "worldly" education.

Bev and Daniela for their advice in preparing this manuscript.

Prof AP MacPhail and Mrs L McNamara, Department of Medicine, for technical advice.

Dr Leseticky from the Charles University, Prague, for the alkyl derivatives of EDTA.

The technical staff of the Pharmacology Department for always being there.

Ms J Freese (National Malaria Research Programme of the Medical Research Council) and Dr Walliker (University of Edinburgh) for the malaria strains.

The SA Blood Transfusion Service for the blood supply.

The University of the Witwatersrand and FRD for financial support.

TABLE OF CONTENTS

	Page
DECLARATION	ii
DEDICATION	iii
PUBLICATIONS AND PRESENTATIONS	iv
ABSTRACT	vi
ACKNOWLEDGEMENTS	viii
TABLE OF CONTENTS	ix
LIST OF FIGURES	xv
LIST OF TABLES	xviii
LIST OF ABBREVIATIONS	xix
1.0 GENERAL INTRODUCTION	**1**
1.1 The problem of malaria	2
1.2 The malaria parasite	2
1.2.1 Parasite life cycle	3
1.3 Immunopathology	3
1.4 Iron, an indispensable micronutrient	6
1.4.1 Chemistry of iron	7
1.4.2 Iron metabolism in man	7
1.4.2.1 Distribution of iron in the body	8
1.4.2.2 Iron absorption	9
1.4.2.3 Iron excretion	12
1.4.2.4 Transport and storage iron proteins	12
1.4.3 Iron chelating agents	16
1.5 Aims of this thesis	16
2.0 METHODOLOGY	**18**
2.1 In vitro cultivation of *P. falciparum*	19
2.1.1 Strains	19
2.1.2 Cryopreservation and initiation of cultures	19
2.1.2.1 Cryopreservation	19
2.1.2.2 Initiation of cultures	20
2.1.3 Cultivation procedure	20
2.1.3.1 Assessment of parasite growth	21
2.1.3.2 Erythrocyte preparation	21
2.1.3.3 Preparation of complete culture medium	21
2.1.3.4 Plasma preparation	22
2.1.3.5 Synchronization	22
2.2 Labelling technique for iodination of diferric transferrin	22
2.2.1 Method for preparing diferric transferrin	23
2.2.1.1 Apotransferrin preparation	23
2.2.1.2 Diferric transferrin preparation	23
2.2.1.3 Removal of excess iron from transferrin solution	23
2.2.1.4 Diferric transferrin determination	23

2.2.1.5 Analysis 24
2.2.2 Iodination of ^{59}Fe-transferrin 24
2.2.2.1 Protein iodination 25
2.2.2.2 Dialysis 25
2.2.2.3 Analysis 26
2.2.3 Radial immunodiffusion technique 26
2.2.3.1 Procedure 26
2.2.3.2 Analysis 27
2.2.4 6 M urea polyacrylamide gel electrophoresis 27
2.2.4.1 Gel preparation 27
2.2.4.2 Gel analysis 29
2.3 Uptake of ^{59}Fe into parasitized-erythrocytes 29
2.3.1 Uptake of double labelled diferric transferrin 30
2.3.1.1 Preparation of microculture tubes 30
2.3.1.2 Harvesting 31
2.3.1.3 Gamma counting and data evaluation 31
2.3.2 Uptake of ferric citrate 32
2.3.2.1 Preparation of ^{59}Fe-citrate 32
2.3.2.2 Experimental procedure 32
2.4 Investigation of malaria haemozoin 32
2.4.1 Iron incorporation into haemozoin 32
2.4.1.1 Preparation of parasitized and uninfected erythrocytes 32
2.4.1.2 Haemozoin isolation 33
2.4.1.3 Haemozoin electrophoresis 33
2.4.2 *In vitro* effect of desferrioxamine on radiolabelled haemozoin 36
2.4.3 Effect of iron chelating agents on the isolated ^{59}Fe-haemozoin 37
2.4.3.1 Preparation of iron chelating agents 37
2.4.3.2 Procedure 37
2.4.4 Incorporation of $^{59}FeCl_3$ into isolated haemozoin 37
2.4.5 UV-VIS spectrophotometric analysis of the effects of desferrioxamine on isolated labelled-haemozoin and haemin 38
2.4.5.1 Effects of desferrioxamine on isolated labelled-haemozoin 38
2.4.5.2 Effect of desferrioxamine on haemin 39
2.5 Haemin induced haemolysis 39
2.5.1 Haemin preparation 39
2.5.2 Preparation of drugs 40
2.5.3 Preparation of uninfected erythrocytes 40
2.5.4 Preparation of parasitized erythrocytes 40
2.5.5 Haemolytic procedure 41
2.5.6 Data evaluation 41
2.6 Hypoxanthine incorporation assay 42
2.6.1 Basis of hypoxanthine uptake studies 42
2.6.1.1 Preparation of drugs 42
2.6.1.2 Preparation of uninfected control erythrocytes 44
2.6.1.3 Preparation of parasitized erythrocytes 44
2.6.1.4 Preparation of microculture plates 44
2.6.1.5 Labelling of parasite DNA 44
2.6.1.6 Harvesting the parasite DNA and beta scintillation counting 46

2.6.1.7 Evaluation of dpm results 46
2.6.1.8 Dose-response curves 47
2.6.2 Modifications of the hypoxanthine incorporation assay 47
2.6.2.1 Drug combinations 47
2.7 Statistical analysis 48

3.0 PASSAGE OF IRON INTO *P. FALCIPARUM*-INFECTED ERYTHROCYTES **49**
3.1 Introduction 50
3.1.1 Acquisition of iron 52
3.1.1.1 Plasma diferric transferrin 52
3.1.1.2 Non-transferrin-bound iron 55
3.1.1.3 Erythrocytic haemoglobin 56
3.1.1.4 Intraerythrocytic iron pool 56
3.1.1.5 Erythrocytic ferritin 58
3.1.2 Iron chelating agents and iron uptake 59
3.2 Aims 61
3.3 Experimental design 61
3.4 Results 61
3.4.1 Uptake of iron 61
3.4.1.1 Uptake of diferric transferrin 61
3.4.1.2 Uptake of ferric citrate 64
3.4.2 Effect of iron chelating agents on iron uptake 64
3.4.2.1 Differic transferrin as the iron source 64
3.4.2.2 Combined effect of desferrioxamine and 2,2'-bipyridyl on diferric transferrin uptake 67
3.4.2.3 Ferric citrate as the iron source 68
3.5 Discussion 71
3.5.1 Plasma diferric transferrin 73
3.5.2 Uptake of non-transferrin bound iron 74
3.5.3 Effect of 2,2'-bipyridyl on iron uptake 75
3.5.4 Effect of desferrioxamine on iron uptake 77

4.0 INVESTIGATION OF MALARIA HAEMOZOIN **79**
4.1 Introduction 80
4.1.1 Degradation of haemoglobin 80
4.1.2 Protein component of haemozoin 83
4.1.3 Haem moiety of haemozoin 83
4.1.4 Haemin as a haemolytic agent 86
4.1.4.1 Oxidation and peroxidation 86
4.1.4.2 Cytoskeletal stability 86
4.1.4.3 Enzyme inhibition 87
4.1.4.4 Cation leakage 87
4.1.5 Effect of antimalarials on haemin induced haemolysis 87
4.2 Aims 88
4.3 Experimental design 88

4.4 Results 89
4.4.1 Incorporation of transferrin bound iron into malaria parasites. 89
4.4.2 *In vitro* effect of desferrioxamine on parasite haemozoin. 89
4.4.3 Effect of desferrioxamine and 2,2'-bipyridyl on isolated labelled haemozoin. 90
4.4.4 UV-VIS spectrophotometric analysis of the effects of desferrioxamine on isolated haemozoin and haemin. 91
4.4.4.1 Effects of desferrioxamine on isolated labelled-haemozoin. 91
4.4.4.2 Effects of desferrioxamine on haemin. 92
4.4.5 Haemin induced haemolysis 94
4.4.5.1 Haemin induced haemolysis. 94
4.4.5.2 Effect of chloroquine and haemin on haemolysis. 94
4.4.5.3 Effect of desferrioxamine and haemin on haemolysis. 98
4.4.5.4 Effect of 2,2'-bipyridyl on haemin induced haemolysis. 98
4.5 Discussion 100
4.5.1 Incorporation of transferrin bound iron into malaria parasites 100
4.5.2 Effect of iron chelating agents on haemozoin 104
4.5.2.1 Effect of desferrioxamine 104
4.5.2.2 Effect of 2,2'-bipyridyl 105
4.5.3 The deleterious effects of haemin on erythrocytic membranes 105
4.5.4 Effect of chloroquine on haemin induced haemolysis 106
4.5.5 Inhibition of haemin induced haemolysis by desferrioxamine 107
4.5.6 Effect of 2,2'-bipyridyl on haemin induced haemolysis 108

5.0 THE INDIVIDUAL AND COMBINED EFFECT OF CHELATING AGENTS AND CLASSICAL ANTIMALARIALS ON THE *IN VITRO* GROWTH OF *P. FALCIPARUM* **110**
5.1 Introduction 111
5.1.1 Human plasma 111
5.1.2 Pharmacological chelating agents 113
5.1.2.1 Desferrioxamine, a hydroxamate chelating agent 113
5.1.2.2 Desferrithiocin 116
5.1.2.3 Aminocarboxylate compounds 117
5.1.2.4 Nitrilotriacetic acid 119
5.1.2.5 Ferrous chelating agents 119
5.1.3 Classical antimalarials 120
5.1.3.1 Pyrimethamine 121
5.1.3.2 Quinoline containing antimalarials 122
5.1.4 The combined effect of iron chelating agents and classical antimalarials on the growth of *P. falciparum*. 124
5.2 Aims 125
5.3 Experimental design 125
5.4 Results 125
5.4.1 Effect of desferrioxamine, 2,2'-bipyridyl and classical antimalarials on *P. falciparum* isolates 125
5.4.2 Effect of various chelating agents on the *in vitro* growth of the chloroquine-resistant FCR-3 strain 127

5.4.3 Combined effect of iron chelating agents and classical antimalarials on the growth of the FCR-3 strain 128
5.4.4 Combined effect of ferric and/or ferrous iron chelating agents on parasite growth 132
5.5 Discussion 136
5.5.1 Effect of desferrioxamine, 2,2'-bipyridyl and classical antimalarials on the growth of *P. falciparum* isolates 136
5.5.2 Effect of various iron chelating agents on the *in vitro* growth of the chloroquine-resistant FCR-3 strain 137
5.5.2.1 Citrate 137
5.5.2.2 Ascorbate 137
5.5.2.3 Apotransferrin 138
5.5.2.4 Aminocarboxylate compounds 138
5.5.2.5 Nitrilotriacetic acid 140
5.5.2.6 Desferrioxamine 140
5.5.2.7 Desferrithiocin 141
5.5.2.8 Bathophenanthroline and 2,2'-bipyridyl, ferrous iron chelating agents 142
5.5.3 Combined effect of iron chelating agents and classical antimalarials on the growth of the FCR-3 strain 143
5.5.4 Combined effect of ferrous and/or ferric iron chelating agents on parasite growth 145
5.5.4.1 Combined effect of two ferric chelating agents on parasite growth 145
5.5.4.2 The combined effect of two ferrous chelating agents on parasite growth 146
5.5.4.3 The combined effect of bathophenanthroline, a ferrous iron chelating agent and a ferric iron chelating agent, desferrioxamine or desferrithiocin, on parasite growth 147
5.5.4.4 The combined effect of 2,2-bipyridyl, a ferrous iron chelating agent and a ferric iron chelating agent, desferrioxamine or desferrithiocin, on parasite growth 148

6.0 THE EFFECT OF DIFFERENT VARIABLES ON THE ANTI-MALARIAL ACTIVITY OF THE IRON CHELATING AGENTS . . . 151
6.1 Introduction 152
6.1.1 Inoculum size 152
6.1.2 Extracellular pH 152
6.1.3 Transition metals 153
6.1.4 Stage dependency and recrudescence 154
6.1.4.1 Stage-dependency effects of iron chelating agents 154
6.1.4.2 Recrudescence 156
6.2 Aims 156
6.3 Experimental Plan 156
6.3.1 Effect of inoculum size on drug efficacy 156
6.3.2 Effect of pH on drug efficacy 157
6.3.3 Effect of cation-chelates on parasite growth 157
6.3.4 Stage-specificity of iron chelating agents, desferrioxamine and

2,2'-bipyridyl 158
6.3.4.1 Microscopic examination of the stage-specificities of desferrioxamine and 2,2'-bipyridyl 158
6.3.4.2 Rate of inhibition of parasite growth by desferrioxamine and 2,2'-bipyridyl 158
6.3.4.3 Morphological examination 159
6.3.4.4 Recrudescence of desferrioxamine-treated parasites 159
6.4 Results 159
6.4.1 Effect of inoculum size on the efficacy of chloroquine and iron chelating agents 159
6.4.2 Effect of pH on the efficacy of the iron chelating agents, desferrioxamine and 2,2'-bipyridyl 160
6.4.3 Effect of cation-chelates on parasite growth 161
6.4.4 Stage-specificity of desferrioxamine and 2,2'-bipyridyl on the intraerythrocytic life cycle of malaria 164
6.4.4.1 Microscopic examination of the stage-specificities of desferrioxamine and 2,2'-bipyridyl 164
6.4.4.2 Inhibition of ^{3}H-hypoxanthine incorporation into parasite DNA by desferrioxamine and 2,2'-bipyridyl 167
6.4.4.3 Morphological changes induced by desferrioxamine and 2,2'-bipyridyl . 170
6.4.4.4 Recrudescence of desferrioxamine pre-treated parasites 170
6.5 DISCUSSION 172
6.5.1 Effect of inoculum size on drug efficacy 172
6.5.2 Effect of pH on drug efficacy 173
6.5.3 Effect of cation-chelates on parasite growth 174
6.5.3.1 Cation supplementation 174
6.5.3.2 Effect of cation-desferrioxamine chelates 175
6.5.3.3 Effect of cation-2,2'-bipyridyl chelates 176
6.5.4 Stage-specific effects and recrudescence 177
6.5.4.1 Stage dependent effects of desferrioxamine 177
6.5.4.2 Stage-dependent effects of 2,2'-bipyridyl 181
6.5.4.3 Combined effect of desferrioxamine and 2,2'-bipyridyl 182

7.0 GENERAL DISCUSSION **184**

APPENDICES **190**
Appendix A 191
Appendix B 194
Appendix C 196
Appendix D 197
Appendix E 198

REFERENCES **201**

LIST OF FIGURES

Figure		Page
1.1	The intraerythrocytic life cycle of *P. falciparum* malaria parasite	4
1.2	The intraerythrocytic gametocytes, rings and late schizont stages of the chloroquine-sensitive 3D7-A strain	4
1.3	Distribution of body iron in the various compartments	8
1.4	The absorption of iron into intestinal mucosal cells and its storage in ferritin or delivery to the blood plasma	10
1.5	Regulation of intracellular iron homeostasis	15
2.1	Radioactive iodination of diferric transferrin using the Bolton and Hunter Reagent	24
2.2	Concentration of Bolton and Hunter Reagent	25
2.3	Radial immunodiffusion gel with Coomassie Blue stained diffusion bands	28
2.4	The 6 M urea PAGE gel to determine the purity of the iodinated diferric transferrin solution	30
2.5	Microscope photographs of the steps involved in haemozoin isolation	34
2.6	Biorad linear gradient maker used to pour the 6-20% polyacrylamide gel	35
2.7	The tritiated hypoxanthine assay in relation to the intraerythrocytic life cycle of the *P. falciparum* malaria	43
2.8	The layout of the 96-well microculture plate for the ^{3}H-hypoxanthine incorporation assay	45
2.9	An isobologram indicating different drug interactions	49
3.1	Possible mechanisms of iron acquisition by the malaria parasite.	51
3.2	Transferrin-receptor mediated endocytosis.	53
3.3	The redox-mediated process for iron uptake from the transferrin-transferrin-receptor complex.	54
3.4	Possible mechanism by which 2,2'-bipyridyl inhibits the uptake of diferric transferrin	60
3.5	The time-dependant uptake of iron and transferrin by ring-infected and control erythrocytes.	62
3.6	The time-dependant uptake of iron and transferrin by trophozoite-infected and control erythrocytes	63
3.7	Concentration-dependant uptake of diferric transferrin and ferric citrate after 4 hours by trophozoite-infected and control erythrocytes	65
3.8	The time-dependant uptake of ferric citrate by the ring-, trophozoite-infected and control erythrocytes.	66
3.9	The temperature dependant uptake of ferric citrate by trophozoite-infected and control erythrocytes at 4°C and 37°C	67
3.10	The time dependant uptake of diferric transferrin and ferric citrate	

by trophozoite-infected and control erythrocytes at 37°C 68
3.11 The dose dependent effect of desferrioxamine on iron and transferrin uptake by trophozoite-infected and control erythrocytes at 37°C 69
3.12 The dose dependent effect of 2,2'-bipyridyl on iron and transferrin uptake by trophozoite-infected and control erythrocytes at 37°C 70
3.13 The effect of desferrioxamine and 2,2'-bipyridyl on the uptake of ferric citrate into trophozoite-infected and control erythrocytes 72

4.1 Pathway of haemoglobin degradation and haemozoin formation, with possible mechanisms by which chloroquine and iron chelating agents, such as desferrioxamine could inhibit parasite growth 81
4.2 The structure of haemozoin as proposed by Slater *et al.* (1991) 84
4.3 Molecular structure of the iron (III) ferriprotoporphyrin-IX complexes 85
4.4 The distribution of ^{59}Fe in trophozoite-infected erythrocytes 90
4.5 A 6-20% gradient SDS electrophoretic gel of haemozoin and haemoglobin obtained from ^{59}Fe-labelled trophozoite-infected and control erythrocytes, with corresponding one minute gamma counts 91
4.6 The *in vitro* effects of desferrioxamine on the haemozoin ^{59}Fe content 92
4.7 The effects of various concentrations of desferrioxamine and 2,2'-bipyridyl on isolated ^{59}Fe-labelled haemozoin. 93
4.8 Concentration dependent effect of haemin induced haemolysis against the FCR-3 parasitized and uninfected erythrocytes, which were incubated at 37°C for 2 hours in the dark 95
4.9 The haemolytic effect of chloroquine and haemin on the uninfected and parasitized erythrocytes after 2 hours of incubation. 96
4.10 The effect of pre-treating erythrocytic membranes with chloroquine for 30 minutes before the addition of haemin (2 hours) 97
4.11 Effect of desferrioxamine on haemin induced haemolysis 99
4.12 Effect of 2,2;-bipyridyl on haemin induced haemolysis. 101
4.13 Proposed structure of the haemozoin crystal as determined from this study 103

5.1 The iron-catalysed Haber-Weiss reaction, where equation A is the Fenton reaction 113
5.2 The chemical structure of desferrioxamine 113
5.3 The chemical structure of desferrithiocin 116
5.4 The chemical structure of diethylene triamino pentaacetic acid and ethylene bis (oxy-ethylene nitrilo) tetraacetic acid 117
5.5 The chemical structure of ethylene diamino tetraacetic acid and the alkyl derivatives, 1,2-diaminooctyl tetraacetic acid, 1,2-diaminododecyl tetraacetic acid and 1,2-diaminohexadecyl tetraacetic acid. 118
5.6 The chemical structure of nitrilotriaacetic acid 119
5.7 The chemical structure of bathophenanthroline sulphonate and 2,2'-bipyridyl 119
5.8 Chemical structure of chloroquine, quinine and pyrimethamine 121

5.9 The *de novo* synthesis of folate in *P. falciparum* and the potential sites of inhibition of pyrimethamine, sulphonamides and desferrioxamine 122
5.10 The correlation between the number of carbon atoms in the R-group and the antimalarial activity of the EDTA alkyl derivatives 128
5.11 Dose-response curves showing the combined effects of chloroquine with desferrioxamine and 2,2'-bipyridyl on the growth of *P. falciparum* FCR-3 strain. 129
5.12 Dose-response curves showing the combined effects of quinine with desferrioxamine and 2,2'-bipyridyl on the growth of *P. falciparum* FCR-3 strain. 130
5.13 Dose-response curves showing the combined effects of pyrimethamine with desferrioxamine and 2,2'-bipyridyl on the growth of *P. falciparum* FCR-3 strain. 131
5.14 The isobolograms of the ferric iron chelating agents desferrioxamine and desferrithiocin against other iron chelating agents 133
5.15 The isobolograms of the ferrous iron chelating agents 2,2'-bipyridyl and bathophenanthroline against other iron chelating agents 134
5.16 The isobologram showing the antagonistic drug interaction between desferrioxamine and 2,2'-bipyridyl in both the chloroquine-sensitive 3D7-A and chloroquine-resistant FCR-3 strains. 135
5.17 The effect of a time interval between the addition of desferrioxamine and 2,2'-bipyridyl 135
5.18 The influence of ferrous (B) and ferric (D) iron chelating agents on the equilibrium of iron 146

6.1 The dependence of the IC_{50} of desferrioxamine and 2,2'-bipyridyl on inoculum size. 160
6.2 Dependence of the IC_{50} of desferrioxamine and 2,2'-bipyridyl on the extracellular medium pH. 161
6.3 The *in vitro* effect of cation-chelates on parasites growth. 163
6.4 Morphological changes occurring through-out the life cycle of the parasite, with drugs added at time 0 (ring stage) 165
6.5 Morphological changes occurring through-out the life cycle of the parasite, with drugs added at time 24 (trophozoite stage) 166
6.6 Morphological changes occurring through-out the life cycle of the parasite, with drugs added at time 32 (schizont stage) 168
6.7 ^{3}H-hypoxanthine incorporation into desferrioxamine and 2,2'-bipyridyl treated cultures. 169
6.8 Morphological changes induced after 4 days of treatment 172

E1 The dose-response curves generated for plates A and B 198
E2 The dose-response curves generated for plates C and D 198
E3 The dose-response curves generated for plates E and F 199
E4 The dose-response curves generated for plates G and H 199

LIST OF TABLES

Table **Page**

3.1 The combined effect of desferrioxamine and 2,2'-bipyridyl on the uptake of diferric transferrin by parasitized and control erythrocytes. 71

4.1 The effect of time and temperature on haemin induced haemolysis of FCR-3 parasitized erythrocytes. 95

5.1 Effect of various iron chelating agents and classical antimalarials on the *P. falciparum* isolates 126
5.2 The effect of chelating agents on the growth of the FCR-3 strain. 127

6.1 The IC_{50} of the iron chelating agents and cations alone and combined in equimolar concentrations 162

E1 Data used to generate the isobolograms. 200

LIST OF ABBREVIATIONS

APS	Ammonium persulfate
ATP	Adenosine triphosphate
K_a	Association constant
ATPase	Adenosine triphosphatase
BIPY	2,2'-Bipyridyl
BPS	Bathophenanthroline sulphonate
CO_2	Carbon dioxide
cpm	Counts per minute
°C	Degree Celsius
dATP	Deoxyadenosine triphosphate
DDDTA	1,2-diaminododecyl tetraacetic acid
DFO	Desferrioxamine
DHDTA	1,2-diaminohexadecyl tetraacetic acid
DHFR	Dihyrdrofolate reductase
DMSO	Dimethylsulphoxide
DNA	Deoxyribonucleic acid
dNTP	Deoxynucleotriphosphates
DOTA	1,2-diaminooctyl tetraacetic acid
dpm	Disintegrations per minute
dTMP	Deoxythymidine monophosphate
DTPA	Diethylene triamino pentaacetic acid
dTTP	Deoxythymidine triphosphate
dUMP	Deoxyuridine monophosphate
EDTA	Ethylene diamino tetraacetic acid
EGTA	Ethylene bis(oxy-ethylene nitrilo) tetraacetic acid
g	Centrifugation in gravity
H_2O_2	Hydrogen peroxide
HEPES	4-(2-hydroxyethyl)-1-piperazinethane sulphoric acid
IC_{50}	50% Inhibitory concentration
kgf/cm^2	Kilogram force per unit area

μCi	Microcurie
μl	Microlitre
μm	Micrometre
μM	Micromolar
mg	Milligram
mM	Millimolar
mol	Moles
NADP	Nicotamide adenine dinucleotide
NADPH	Nicotamide adenine dinucleotide, reduced
p	Value of significance
PBS	Phosphate buffered saline
r^2	The square of the regression correlation/coefficient
RPMI	Roswell Park Memorial Institute
s.d.	Standard deviation
SDS	Sodium dodecyl sulphate
TEMED	N,N,N',N'-tetramethylenediamine
Tris	Hydrozymethylaminomethane
UV-VIS	Ultraviolet-visible
v/v	Volume per volume
V	Volt
w/v	Weight per volume

CHAPTER ONE

GENERAL INTRODUCTION

1.1 THE PROBLEM OF MALARIA

Malaria is one of the most devastating and geographically widespread infections found in man. In Africa alone, over one million infant deaths can be directly attributed to malaria (Greenwood *et al.*, 1991). Earlier in the century, the widespread application of effective insecticides and antimalarial drugs led to a decline in the incidence of malaria and the disease was eradicated from some countries. However, over the past two decades, global resistance to both insecticides and antimalarial drugs has emerged. The incidence of malaria has increased rapidly and the geographic occurrence has become more widespread. The phenomenon of drug resistance in *P. falciparum* was first documented in 1910 when quinine failed to eliminate an infection. In South Africa, chloroquine resistance was first detected in 1985 and is now well established in this country (Sharp and Freese, 1995). Efforts to develop a malaria vaccine are underway, but face formidable obstacles, because the parasite can change its form very quickly, by altering its highly polymorphic antigens (Howard and Pasloske, 1993). Some researchers believe that even if a vaccine is successfully developed, the logistics of administering a vaccine and regular boosters would probably be neither practical nor economically feasible in the developing world (Milon, 1994). The life cycle of the parasite involves many biochemical steps, each of which is controlled by a defined set of parasite and host molecules, which could serve as potential sites for specific drug targeting. Thus, it has become necessary to further investigate the biochemistry and morphology of the malaria parasite.

1.2 THE MALARIA PARASITE

Malaria is caused by a single-celled protozoan of the *Plasmodium* species. Four species known to infect humans are, namely, *P. falciparum, P. vivax, P. ovale* and *P. malariae.* Clinical symptoms associated with malaria infections include chills, shivering, severe headaches, fever and jaundice. Of these four species, *P. falciparum* is responsible for over 90% of infections contracted in southern Africa (Medfile, 1991). The most severe clinical consequences of *P. falciparum* are anaemia, renal failure and cerebral malaria. Anaemia is probably more common than cerebral malaria in African children, but the latter usually

occurs as a result of delayed diagnosis and treatment of the infection. Symptoms associated with cerebral malaria are drowsiness, convulsion, coma and if left untreated, death.

1.2.1 PARASITE LIFE CYCLE

The life cycle of the parasite is complex, with proliferation occurring in two hosts, namely man and the adult female *Anopheles* mosquito. In man, the infection begins when sporozoites are injected into the blood by a mosquito. The sporozoites then migrate to and invade the liver hepatocytes and develop into merozoite-forming schizonts. The intraerythrocytic stage of the life cycle begins when the merozoites invade the erythrocytes to form rings, then trophozoites and finally erythrocytic schizonts (Figure 1.1). The schizonts, as in the hepatic stage, develop into merozoites, which are released from the erythrocytes to invade further erythrocytes or develop into gametocytes (Figure 1.2). The latter are ingested by a feeding mosquito and then develop into sexual forms, i.e. microgametes (male) and macrogametes (female), which fuse to form a zygote. In the gut wall, the zygote develops into a motile ookinete and then oocyst, from which large numbers of sporozoites are released. The sporozoites then invade the salivary glands from which they are injected into the human host when the mosquito feeds (Roitt *et al.*, 1989).

The rupturing of the erythrocytes during the asexual, intraerythrocytic stage of development is believed to be responsible for the clinical manifestations of the infection, such as the characteristic chills and fevers.

1.3 IMMUNOPATHOLOGY

The pathogenesis of *P. falciparum* malaria is also related to the capacity of the parasite to reproduce at an extremely rapid rate, where in just 48 hours, a single merozoite can divide produce 16 protozoa.

To sustain such an explosive replication rate, the parasite requires a sufficient supply of

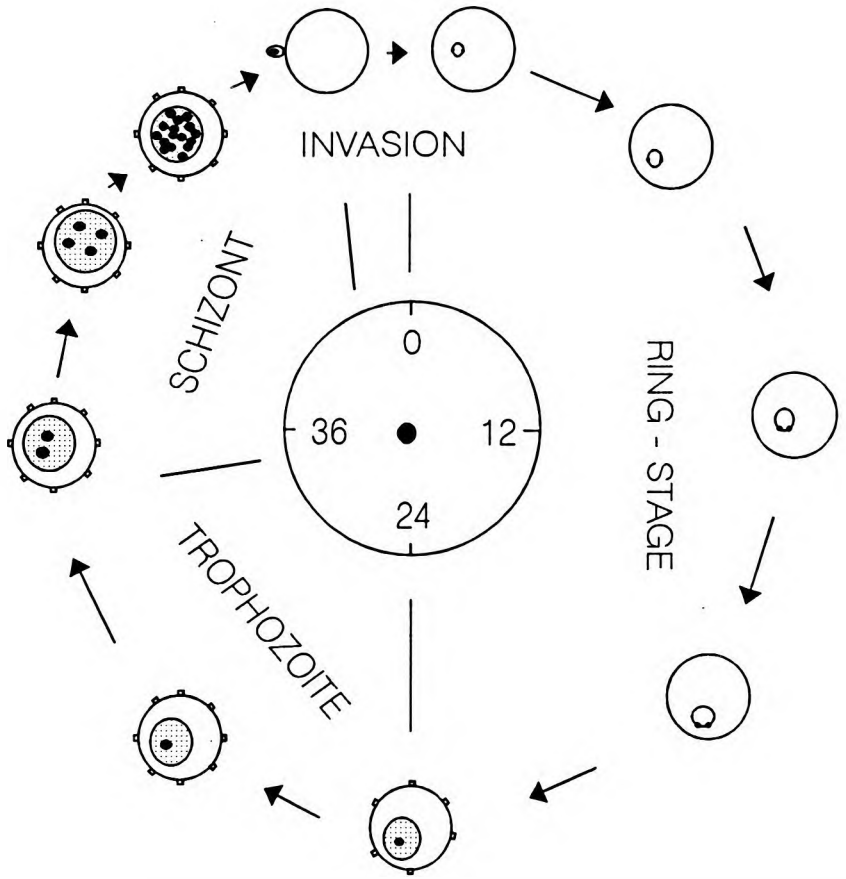


Figure 1.1: The intraerythrocytic life cycle of the *P. falciparum* malaria parasite.

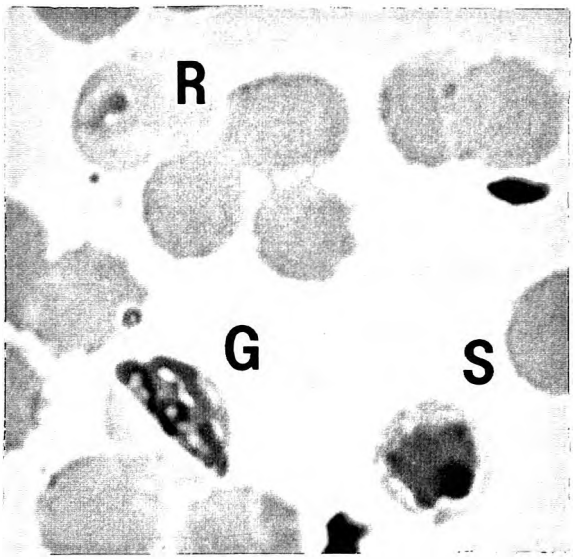


Figure 1.2: The intraerythrocytic gametocytes (G), ring (R) and late schizont (S) stages of the chloroquine-sensitive 3D7-A strain.

nutrients to maintain the biochemical processes involved (e.g. DNA replication and protein synthesis). To achieve this the parasite manipulates its microenvironment and competes with the host for these nutrients. Malaria infections are known to cause disturbances in the mineral homeostasis of the host, such that hypocalcaemia and hypophosphataemia are common complications in acute *P. falciparum* malaria (Davies *et al.*, 1993).

To acquire non-penetrating ferric ions, microorganisms normally produce their own potent metal ligands, termed siderophores. These are low molecular weight, water soluble structures that scavenge extracellular iron with high affinity (Cabantchik, 1995). However, the malaria parasite does not appear to produce such molecules, and the intracellular parasite has no obvious means for mobilizing bioavailable iron from the host or the extracellular milieu. It has however, been proposed that the parasite incorporates transferrin-bound iron or iron from the host haemoglobin (see Chapter 3.1.1.2 and 3.1.1.3) (Pollack and Fleming, 1984; Gabay and Ginsburg, 1993).

To compete with the parasite for nutrients, the host induces the mobilization of macrophages which produce cytokines, namely tumour necrosis factor, interleukin-1 and 6 (Graninger *et al.*, 1992). These in turn orchestrate widespread metabolic changes and mediate an enhanced level of activity of the immune system. The activated immune system increases the hepatic synthesis of transferrin, a transport protein that avidly binds iron and withholds iron from the invading pathogens. Aremu (1989) reported that in uncomplicated malaria, the mean serum transferrin concentration and mean serum iron is elevated above the control value, with a decreased mean saturation of serum transferrin with iron. The increase in serum transferrin may be accounted for by the fact that haemolysis of the parasitized erythrocytes and the resultant iron release, stimulates transferrin synthesis, thus enabling the mobilization of the increased serum iron. However, Graninger *et al.* (1992) found significantly lower serum transferrin concentrations in malaria-infected patients compared to the uninfected controls. In cerebral malaria patients, microvascular obstruction by *P. falciparum*-infected erythrocytes results in local ischaemia and microhaemorrhage, with the release of free haemoglobin and iron. The liberation of haem iron elevates transferrin saturation, diminishing the capacity of this antioxidant protein to protect the central nervous system from lipid peroxidant damage. This delays the rate of

recovery to full consciousness by comatosed children (Gordeuk *et al.*, 1995).

In addition to increased transferrin concentrations, many other serum proteins increase in concentration during the infection, such as haptoglobin which complexes free haemoglobin and ceruloplasmin, a copper binding protein (Graninger *et al.*, 1992). The increase in these metal-binding proteins, results in a decrease of free iron and copper which in turn decreases the possibility of these metals from catalysing the free radical generating Fenton reaction (Das *et al.*, 1993). Similarly, deficiencies in magnesium and zinc also provide the host with some protection against the *Plasmodium* infection (Ginsburg *et al.*, 1986; Hess *et al.*, 1995). Thus, the ability of the host to withhold certain essential nutrients, especially iron, from the pathogenic microorganism, has become an important component of the hosts defense system and has been termed "nutritional immunity" (Weinberg, 1975).

1.4 IRON, AN INDISPENSABLE MICRONUTRIENT

The importance of iron in our existence is perhaps best summarised by the quotation from R. Kipling's "Cold Iron", which was cited by Aisen in his article on the physiochemical aspects of iron metabolism (Aisen, 1977).

"Gold is for the mistress - silver for the maid -
Copper for the craftsman cunning at his trade!
'Good!' said the Baron, sitting in his hall,
'But iron' - Cold Iron - is master of them all."

It has been observed that without iron, life in any form, is in all likelihood impossible. Iron is needed by almost all living organisms, including malaria parasites, where it is essential in oxidation-reduction and other cellular reactions. Save for the lactic acid bacteria, there is no way that living cells, whether prokaryotic or eukaryotic, anaerobic or aerobic, heterotrophic or auxotrophic, can survive without iron.

1.4.1 CHEMISTRY OF IRON

It is believed that this dependence on iron is largely due to a unique combination of properties, such as its co-ordination number, structure, ligand type, ligand equilibrium, ligand dynamics and especially the following four properties:

(1) Iron is universally abundant. It is the second most abundant metal and the fourth most abundant element in the earth's crust. The increased tendency for more iron to be created than other elements, is due to it having the most stable nucleus of all the elements.

(2) Iron is a member of the first transition triad, which is characterized by the $3d^2 4s^2$ ground state configuration, and exists in two oxidative states in aqueous solutions, ferrous (Fe^{2+}) and ferric (Fe^{3+}).

(3) Iron has a range of oxidation/reduction potentials (+350 mV to -500 mV), allowing it to participate in a broad spectrum of chemical reactions (Cotton and Wilkinson, 1980). Some of these reactions include the catalysis of oxidation and hydrogen peroxide, the decomposition of peroxide and superoxide, oxidative phosphorylation and the transport of oxygen by haemoglobin and other related compounds. All proliferating cells require iron as a cofactor for the enzyme ribonucleotide reductase, which is necessary for the production of DNA. In the latter reaction, if no iron is available, no DNA is produced, resulting in cell death. No other metal can substitute for iron in this reaction.

Thus, iron has evolved to play a vital and multiple role in the biochemistry and survival of living cells.

1.4.2 IRON METABOLISM IN MAN

Iron metabolism in man consists of a series of processes involving the entry of iron into the body through its absorption, its transport and storage throughout the body, its utilization for the formation of haemoglobin and other iron-containing compounds, and its eventual excretion (Figure 1.3).

1.4.2.1 Distribution of iron in the body

The normal iron distribution in a 70 kg male adult totals approximately 3,7 g, with about 70% of the total iron circulating as ferrous iron in erythrocyte haemoglobin. Another 25% is stored in the reticuloendothelial system, in the liver, spleen and bone marrow. Here the ferric iron is stored as the protein complexes, ferritin and haemosiderin. Iron complexed by haemoglobin and ferritin is inert and/or thermodynamically non-reversible (May and Williams, 1980). Only about 0,1% of the total body iron is found circulating in the plasma bound thermodynamically reversibly to transferrin, such that it is 30% saturated with ferric iron (May and Williams, 1980). The remainder of the body iron is distributed between the muscle myoglobin, cytochromes and iron-containing enzymes (Figure 1.3).

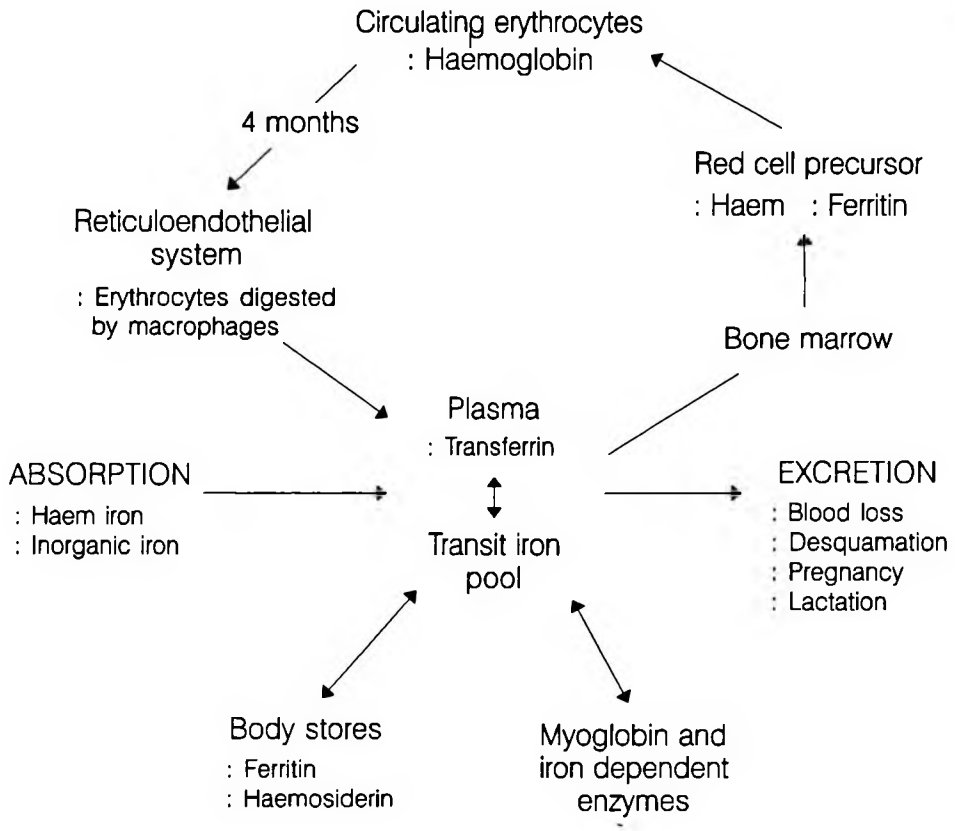


Figure 1.3: Distribution of body iron in the various compartments. Once iron is absorbed, it is in a virtually closed system since iron excretion is minimal (Adapted from May and Williams, 1980).

The iron content of the body depends on the balance between iron absorption and iron loss/excretion, where the former is attuned to the body's requirements for metabolic processes and growth.

1.4.2.2 Iron absorption

In healthy individuals the iron required for the daily production of new erythrocytes is drawn from the stores laid down when old red cells are destroyed (Conrad and Umbreit, 1993); such that only a small but critical fraction of iron is obtained from the diet (Babior and Stossel, 1994). The body's daily requirements of iron is easily provided by a dietary intake of leafy green vegetables, which is rich in inorganic iron, whilst haem iron is more easily absorbed from haem-containing foods, such as liver.

In the early 1980's, it was believed that mucosal transferrin acted as a shuttle by being secreted into the intestinal lumen to bind inorganic iron and then re-enter the cell to facilitate absorption (Morgan, 1980).

But recently, Conrad *et al.* (1993) propose the following sequence of events to be involved in the absorption of inorganic iron from ingested food (Figure 1.4). Firstly, the iron is solubilized in the acidic pH of the stomach, where it combines with mucins, which are macromolecular proteins able to chelate a multiple number of iron molecules. The mucins make the iron soluble and available for absorption in the more alkaline small intestine. Iron chelates of ascorbate, fructose and histidine can also donate iron to mucins at these elevated pHs.

Integrins which transverse the surface of the absorptive mucosal cells facilitate the transfer of iron through the cell membrane and for binding with the 56 kilodalton mobilferrin (Conrad *et al.*, 1993). The latter cytosolic protein serves as a shuttle for iron in the cell, and has a dissociation constant of 10^{-6} M^{-1}. It competitively binds other transition metals (Ca^{2+}, Cu^{2+}, Zn^{2+}, Pb^{2+}), but with lower affinities. The mobilferrin then either stores the iron in ferritin or delivers it to the apotransferrin-transferrin-receptor complex or directly to the plasma apotransferrin for circulation in the blood plasma (Figure 1.4) (Conrad and

Umbreit, 1993).

In contrast, haem enters the mucosal cell as an intact metallo-porphyrin, with the iron being released from the porphyrin ring by the mucosal haem oxygenase enzyme (Figure 1.4) (Babior and Stossel, 1994). The iron then enters the cell's transient iron pool to be either stored in ferritin or to enter the blood plasma, with the possibility of mucin being the cytoplasmic iron carrier (Conrad and Umbreit, 1993).

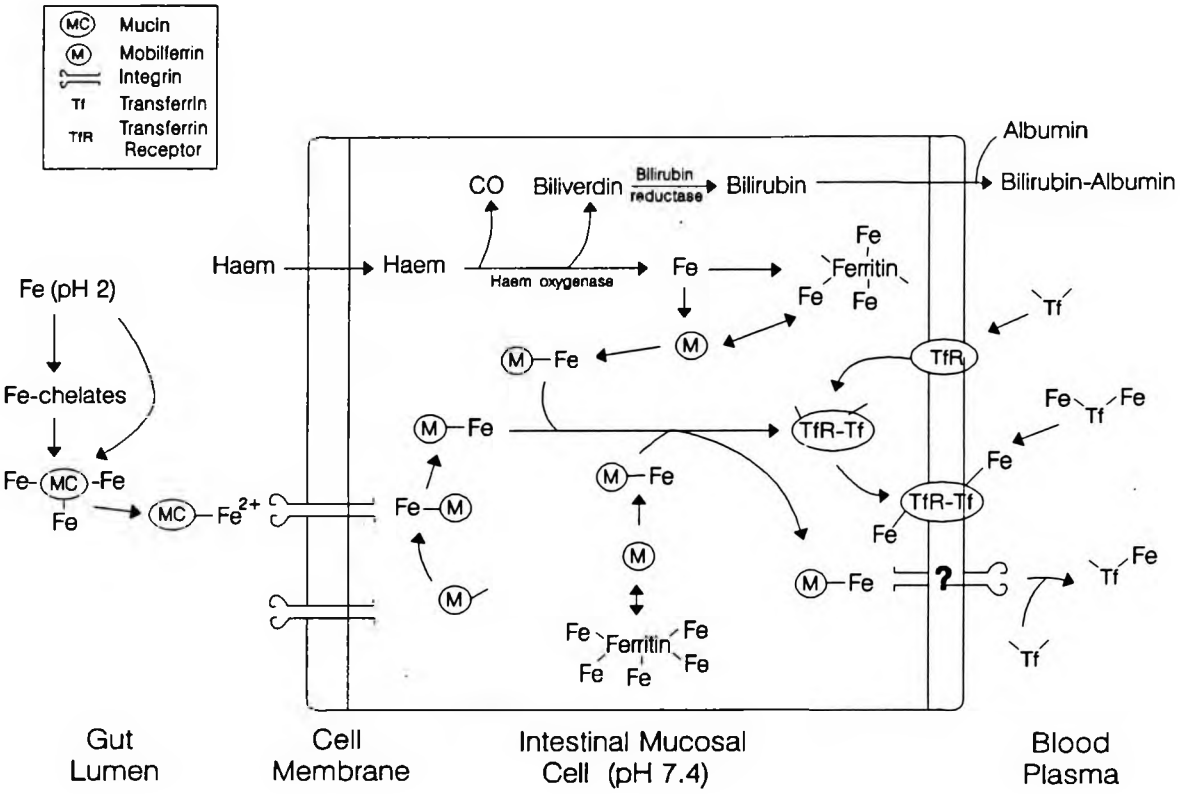


Figure 1.4: The absorption of iron into intestinal mucosal cells and its storage in ferritin or delivery to the blood plasma (Adapted from Conrad and Umbreit, 1993).

1.4.2.2.1 Variations in iron absorption

If the intake and absorption of iron is either decreased or increased, two conditions may

develop.

Firstly, iron deficiency. This will inevitably occur after excessive blood loss or following extended intervals of inadequate iron intake, which is largely due to the poor availability of iron in the cereal-based diets. The latter being the major cause of iron deficiency in most developing countries, such as Africa (Sayers *et al.*, 1973).

As a result of the reduced iron uptake, the iron stores in ferritin and tissue become depleted, although haemoglobin synthesis and metabolic processes are not affected. But once the iron stores are depleted such that when the amount of circulating iron decreases, haemoglobin and therefore erythrocyte production are affected. If this unfavourable balance continues for a lengthy period, anaemia can develop (Bridges and Seligman, 1995).

Conversely, iron overload occurs when there is increased intestinal absorption for example in idiopathic haemochromatosis, thalassaemia, when excessive amounts of bioavailable iron are ingested or as a result of inappropriate parenteral therapy and multiple blood transfusions. A very rare cause of iron overload is an inherited deficiency of transferrin (Bridges and Seligman, 1995).

The presence of excess ingested iron that exceeds the body's need and excretion rate, will affect the ability of the mucosa to control iron absorption and the capacity of transferrin to bind the plasma iron. With transferrin 100% saturated with iron, a plasma iron fraction is formed and is referred to as non-transferrin bound iron. It is assumed that this non-transferrin plasma iron represents a heterogenous group of small molecular weight iron compounds which may be non-specifically bound to albumin and other serum proteins (Hershko and Peto, 1987). With the reticuloendothelial storage capacity exceeded, the iron is complexed in haemosiderin and deposited in the liver, heart and other organs (Bridges and Seligman, 1995). However, this form of iron is potentially very toxic and damage to the latter organs could be contributed to lipid peroxidation, i.e. the effect of free radicals generated by this redox-active iron (Wapnick *et al.*, 1968; Hershko and Peto, 1987).

1.4.2.3 Iron excretion

The presence of a specific or regulated mechanism of iron excretion is unknown. The loss from the body, probably depends on the ferritin iron content of cells lost by desquamation, which are mostly from the intestinal tract and skin. Blood loss can also significantly affect the body's iron balance. Urinary loss is negligible, reflecting the fact that all circulating iron is protein-bound (Babior and Stossel, 1994; Morgan, 1980). In men, only a small amount of iron (1 mg/day) is lost, whilst in women additional losses occur through menstruation, during pregnancy and lactation (Conrad and Umbreit, 1993).

1.4.2.4 Transport and storage iron proteins

1.4.2.4.1 Transferrin

Plasma transferrin (half-life of 7 to 10 days) is responsible for the transport of iron from the intestinal mucosa, reticuloendothelial system and liver parenchymal cells, to all proliferating cells in the body (Pippard and Hoffbrand, 1989).

The β_1-globulin human transferrin consists of a single polypeptide chain of 679 amino acid residues and two N-linked complex type glycan chains, which results in a molecular weight of approximately 80 kilodaltons (Thorstensen and Romslo, 1990). The transferrin gene is located at q21→25 on chromosome 3, with the protein being synthesized in the liver (Yang *et al.*, 1984). The transferrin molecule is folded into two globular homologous domains, namely the N- and C-terminal domains, with each domain possessing a specific metal binding site (Thorstensen and Romslo, 1990). Transferrins are capable of binding many metal ions such as Cu^{2+}, $Co^{2+/3+}$, Zn^{2+}, Ni^{2+}, Al^{3+} and Fe^{3+}, with the latter having the highest affinity constant of approximately 10^{26} M^{-1}, at a neutral or slightly alkaline pH (Bridges and Seligman, 1995). Iron predominantly binds to the N-terminal binding site, in the serum of healthy individuals. Under physiological conditions the effective affinity constants of the N- and C-terminal sites are 1 and 6.10^{22} M^{-1}, respectively. The relevance of this difference is still a matter of debate (de Jong *et al.*, 1990).

The transferrin-iron complex binds to the cell surface through a specific, high-affinity receptor, the transferrin-receptor. Virtually all cells express transferrin-receptors and utilize the endocytic clathrin transferrin cycle for iron uptake (See Chapter 3.1.1.1)

(Klausner *et al.*, 1993); although alternative pathways are now being postulated and investigated (see Chapter 3.1.1.1 and 3.1.1.2).

The transferrin-receptor is an integral transmembrane glycoprotein composed of two identical subunits of approximately 95 kilodaltons, which are linked by a disulphide bridge to form a dimer (Thorstensen and Romslo, 1990). The transferrin-receptor structural gene locus is located at q12→qtr on chromosome 3, with the mRNA encoding a peptide of 760 amino acid residues (McClelland *et al.*, 1984). The post-transcription of the transferrin-receptor mRNA is regulated by the intracellular iron concentrations, such that increased concentrations, will result in a decrease in the post-transcription of the transferrin-receptor mRNA, and thus prevent further iron uptake (see Chapter 1.4.4.3). At physiological pH, each receptor can bind two molecules of transferrin with a very high affinity constant of 5.10^8 M^{-1}; although its affinity for apotransferrin is much lower. On the other hand, at a pH of approximately 5, apotransferrin forms a very stable complex with the receptor (Arosio *et al.*, 1994).

1.4.2.4.2 Ferritin and haemosiderin

Ferritin is the primary iron storage protein found in all cells of the body and provides a reserve of iron which may be used for haem synthesis. The soluble protein consists of a spherical apoprotein shell (approximate molecular weight of 480 kilodaltons) enclosing a core of ferric hydroxyphosphate (up to 4000 iron atoms) (Babior and Stossel, 1994). Human ferritin is made up from 24 subunits of two immunological distinct types, high-subunits (molecular weight of 21 kilodaltons) and low-subunits (molecular weight of 19 kilodaltons); which are encoded for by genes on chromosomes 11 and 19, respectively. However, pseudogenes are located on 12 different chromosomes, which accounts for the heterogeneity of ferritin from different tissues, such as the liver, with low-rich ferritin and red cells, with high-rich ferritin (Pippard and Hoffbrand, 1989). Arosio *et al.* (1994) showed that the high- and low-chains have distinct functional specificities. High-chains promote iron oxidation via the functionality of its ferroxidase centre during iron incorporation; while low-chains promote iron hydrolysis/mineralization inside the protein coat.

The small amount of ferritin, normally found in the serum contains little iron and consists

almost exclusively of low-subunits. Glycosylated serum ferritin has an approximate half-life of 30 hours (Pippard and Hoffbrand, 1989). The concentration of serum ferritin is directly related to body iron stores, whilst the synthesis of intracellular ferritin is modulated by the intracellular iron content, as describe in Chapter 1.4.4.3 (Klausner *et al.*, 1993).

The catabolic pathways of ferritin appear to proceed via the fusion of endocytic vesicles with primary lysosomes to produce secondary lysosomes, in which proteolytic digestion of the protein occurs, leaving the stable iron core and partial protein degradation product, haemosiderin (Halliday *et al.*, 1994). The latter protein-iron complex is water soluble, non -crystalline and has an amorphous structure, with a higher iron to protein ratio than ferritin (37%:20%) (Pippard and Hoffbrand, 1989).

1.4.2.4.3 Role of iron in coordinating cellular transferrin receptor and ferritin synthesis

Ferritin homeostasis in mammalian cells is maintained by the co-ordinate regulation of the expression of the transferrin receptor and ferritin (Klausner *et al.*, 1993). By controlling the level of expression of these two proteins, the cell can determine the amount of iron acquired (proportional to the number of transferrin receptors) and sequestered (proportional to cytoplasmic ferritin levels). As seem in Figure 1.5, the mRNA stability, translation of iron storage and transport protein mRNAs are regulated by the interaction of iron responsive element binding proteins (IRE-BP), with a conserved coding sequence in the mRNA, called iron responsive elements (IRE).

The latter are present at the untranslated region at the 5' end of ferritin and 3' end of transferrin receptor mRNA. In the presence of iron, a [4Fe-4S]-cluster is inserted into the IRE-BP to convert it to a cytoplasmic aconitase enzyme. This conformational change of the IRE-BP, results in the IRE-BP detaching from the mRNA and thereby initiating ferritin translation. At the same time, the stability of the transferrin receptor mRNA decreases, resulting in diminished receptor synthesis and iron uptake. Conversely, in iron deprivation states, the [4Fe-4S]-cluster-free IRE-BP is able to specifically bind to the IREs; which results in decreased translation of the ferritin mRNA and increased stability and

consequently increased translation of transferrin receptor mRNA. These molecular changes result in more iron being extracted from the plasma to be utilized for metabolic processes and less being sequestered and stored in ferritin (Klausner *et al.*, 1993; Kühn *et al.*, 1994).

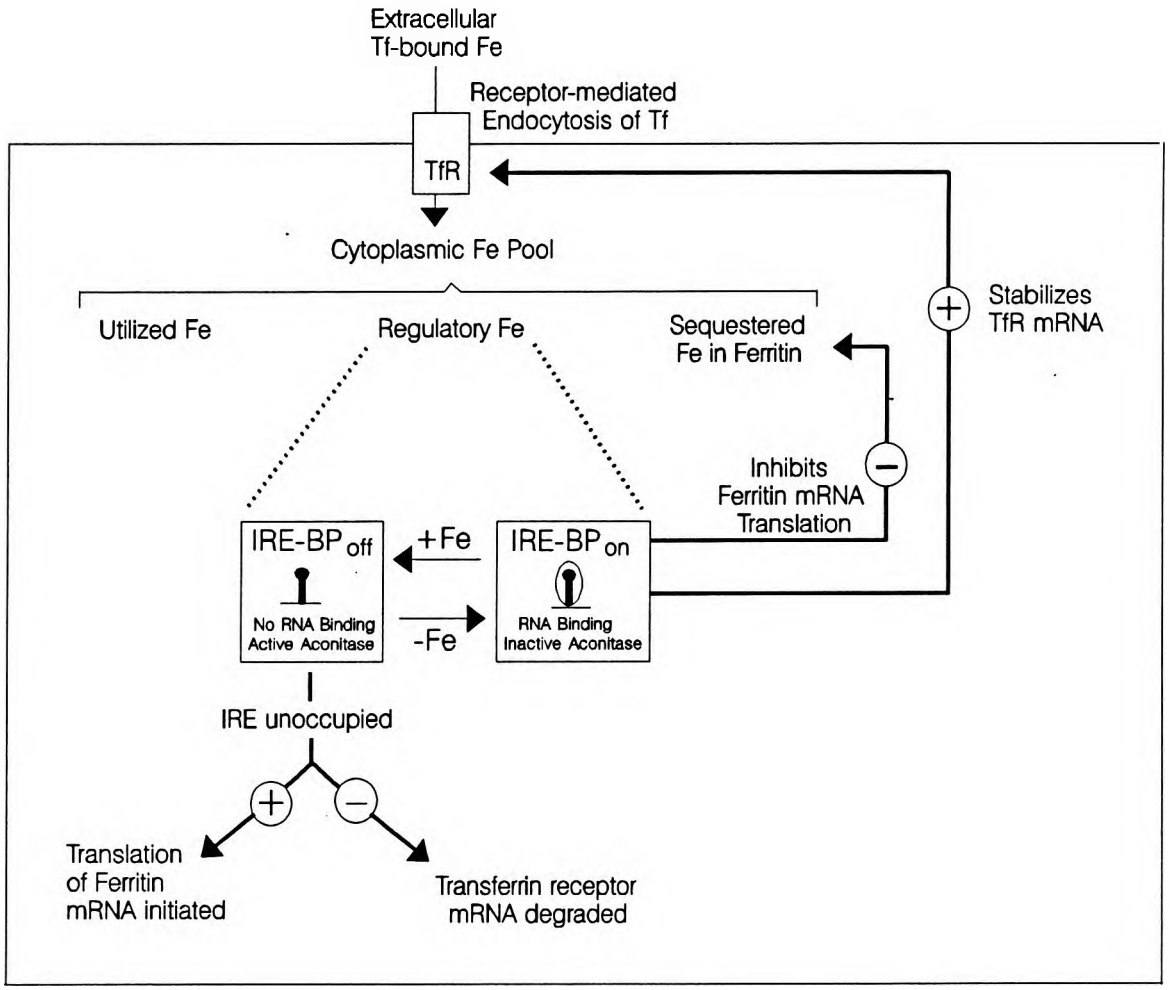


Figure 1.5 Regulation of intracellular iron homeostasis. A scarcity of iron uptake inhibits ferritin mRNA translation and stabilizes transferrin receptor mRNA. Such that less ferritin is synthesised and the number of transferrin receptors increase. The converse is true when iron is abundant (Adapted from Klausner *et al.*, 1993).

1.4.3 IRON CHELATING AGENTS

Several clinical studies indicate that iron deficiency may have an important inhibitory effect on the progression of malarial infections (Nurse, 1979 and Oppenheimer, 1989). Thus, any iron-dependant process in the parasites metabolism could be a potential target for the development of new antimalarial drugs.

In China, iron chelating agents, for example the plant-derived coumarins, have been used for hundreds of years to treat malaria (Yang *et al.*, 1992). More recently, desferrioxamine B (DFO), a natural hydroxamate siderophore isolated from *Streptomyces pilosus*, is effectively used to chelate extracellular plasma iron in iron overload patients. It can also be used to selectively starve the parasite of iron, thereby abolishing cell growth (Raventos-Suarez *et al.*, 1982). However, due to the hydrophilicity of desferrioxamine, it is poorly permeable into the parasitized erythrocytes. Thus, many synthetic compounds have been designed for optimal drug performance and to replace desferrioxamine. These compounds are:

(1) more lipophilic, enabling faster permeation into the parasitized erythrocytes;
(2) have greater binding affinity, to effectively compete for the iron, and
(3) inhibit all stages of the intraerythrocytic parasites (Porter *et al.*, 1988).

But to date, none of these compounds have replaced desferrioxamine in treating patients with uncomplicated malaria or with life threatening cerebral malaria (Bunnag *et al.*, 1992; Gordeuk *et al.*, 1992a).

1.5 AIMS OF THIS THESIS

The involvement of iron in the functioning of the immune system and in the biochemistry of the host and invading pathogen, highlights the necessity for further research into the importance of iron in the pathology of malaria. This thesis tries to encompass a number of aspects related to the metabolism of iron in the *P. falciparum* malaria parasite, and the

following will be examined:

1. The mechanism by which the parasite acquires its iron from the extracellular medium.

2. The process by which the parasite sequesters the reactive iron and the properties of the iron storage component.

3. The advantages of an iron deficient status will be exploited by inducing such a condition with the use of various iron chelating agents.

4. In order to try and increase the pharmacological benefits of the iron chelating agents, they will be combined with the classical antimalarials and other iron chelating agents.

5. Several variables which could influence the antimalarial activity of the iron chelating agents, and possibly optimize the potency and specificity of these drugs against the intraerythrocytic parasites.

All the experimental chapters will aid in determining the mechanism by which the iron chelating agents inhibit the intraerythrocytic parasite growth. By understanding more about the pharmacology of these agents, this information could contribute to the design of new iron chelating agents and antimalarial drugs.

CHAPTER TWO

METHODOLOGY

2.1 *IN VITRO* CULTIVATION OF *P. FALCIPARUM*

2.1.1 STRAINS

The following malaria strains were used for experimentation:

1) FCR-3: A chloroquine-resistant strain originally isolated from the Gambia and was kindly donated by J. Freese, National Research Programme of the Medical Research Council. This strain is known as the International Reference Strain.

2) 7G8: A chloroquine-resistant strain kindly donated by Dr D. Walliker from Edinburgh University.

3) FAB-6: Also known as RSA2, a chloroquine-sensitive strain characterized and kindly donated by J. Freese.

4) RSA-2: A chloroquine-sensitive strain isolated in 1985 from a patient in KwaZulu-Natal, and kindly donated by J. Freese.

5) 3D7-A: A chloroquine-sensitive strain isolated from a patient in the Netherlands and kindly donated by Dr D. Walliker from Edinburgh University.

2.1.2 CRYOPRESERVATION AND INITIATION OF CULTURES

2.1.2.1 CRYOPRESERVATION

To maintain the frozen stock numbers, cultures consisting mainly of ring-infected erythrocytes (parasitaemia > 5%), were cryopreserved as follows (Freese *et al.*, 1988).

The culture was centrifuged for 5 minutes at 400 *g* and the supernatant discarded. To the packed pellet 28% (v/v) glycerol in phosphate buffer saline (PBS) was added in a 1:1 ratio, where the PBS consisted of 120 mM NaCl, 8,32 mM $Na_2PO_4.2H_2O$ and 3,16 mM KH_2PO_4. The best available chemicals were used (See Appendix A). This suspension was then left to stand at room temperature for 5 minutes, before being aliquoted into sterile cryotubes, which were then stored in liquid nitrogen until required.

2.1.2.2 Initiation of cultures

To re-establish the *in vitro* culture, the frozen cryotube was removed from the liquid nitrogen and placed in a 37°C pre-warmed waterbath. The thawed suspension was then transferred to a calibrated centrifuge tube. To every millilitre of blood suspension, 0,1 ml of 2,05 mM NaCl was added whilst shaking the tube. The suspension was left to stand at room temperature for 5 minutes before 9 volumes of 270 μM NaCl was gently mixed in. The suspension was then centrifuged for 5 minutes at 400 *g*. To the packed pellet, 9 volumes of 34,22 μM NaCl and 45,42 μM glucose were added and the pellet was gently resuspended before being centrifuged (Freese *et al.*, 1988). Finally, freshly washed erythrocytes were added to the packed pellet before being resuspended in complete culture medium with 20% (v/v) plasma. This suspension was then incubated at 37°C and maintained as described in Chapter 2.1.3.

2.1.3 CULTIVATION PROCEDURE

Long-term *in vitro* cultivation of *P. falciparum* strains was carried out according to a modified version of the methods described by Jensen and Trager (1976) and Freese *et al.* (1988).

The parasitized erythrocytes were maintained at a 5% haematocrit and an approximate parasitaemia of 5-10%. The gametocyte forming cultures (i.e. the 7G8, FAB-6, RSA-2 and 3D7-A strains) were kept on an orbital shaker, but were allowed to stand static for a maximum of 1 to 2 hours, whilst being maintained. This orbital motion was not necessary for the FCR-3 strain, which has lost its ability to produce gametocytes. Parasite growth was monitored daily by preparing thin blood smears (Chapter 2.1.3.1).

To a culture consisting mainly of ring-infected erythrocytes, the parasites were either synchronized for experimental purposes (Chapter 2.1.3.5) or cryopreserved to maintain frozen stock numbers (Chapter 2.1.2.1). To the trophozoite/schizont-infected erythrocytes, washed erythrocytes (Chapter 2.2.3.2) were added. If the parasitaemia was greater than 10%, the culture was split into two flasks. The daily maintenance procedure involved

aspirating the spent medium and replacing it with pre-warmed complete culture medium (Chapter 2.1.3.3). The lids of the flasks were tightly closed before being incubated at 37°C. Sterile techniques (flaming and 70% absolute alcohol) were used throughout.

2.1.3.1 Assessment of parasite growth

The percentage parasitaemia and morphology were determined daily by microscopic examination of Giemsa stained thin blood smears. The smear was fixed with 100% methanol and left until dry before being stained with dilute Giemsa for 15 minutes. Giemsa stain was diluted 1:5 with a phosphate buffer (25,72 mM KH_2PO_4 and 40,62 mM $Na_2HPO_4.12H_2O$). The dried slide was then examined by light microscopy under oil immersion (1000x magnification). The percentage parasitaemia was calculated via the following formula:

$$\% \text{ Parasitaemia} = PC/(PC + EC) \times 100\%$$

Where: PC = Number of parasitized erythrocytes and EC = Number of uninfected erythrocytes.

2.1.3.2 Erythrocyte preparation

Human whole blood stored in citrate phosphate dextrose adenosine-1 was collected from a healthy donor or the Johannesburg Hospital Blood Transfusion Services and stored at 4°C for a maximum period of three weeks. Erythrocytes were washed three times with blood-PBS by centrifugation at 400 *g* for 5 minutes. The blood-PBS consisted of 136,89 mM NaCl, 4,02 mM KCl, 4,10 mM $Na_2HPO_4.2H_2O$ and 1,47 mM KH_2PO_4, which was sterilized by being autoclaved at 120°C for 20 minutes under a pressure of 1,75 kgf/cm^2. Care was taken to remove the buffy coat. The washed erythrocytes, resuspended in blood-PBS to prevent dehydration, were stored at 4°C for no longer than 48 hours.

2.1.3.3 Preparation of complete culture medium

The culture medium was prepared in autoclaved water with the following ingredients: 10,4 g/l RPMI 1640, 5,94 g/l HEPES buffer, 4,00 g/l glucose, 44,0 mg/l hypoxanthine and 50

mg/l gentamycin sulphate. The culture medium was sterilized through a Sterivex-GS 0,22 μm filter and stored at 4°C. When required the culture medium was saturated with CO_2 gas until the phenol red indicator turned yellow in colour. This step replaced the tedious task of gassing each culture with the traditional gas mixture of 3% O_2, 4% CO_2 and 93% N_2. In addition, this step aided in optimizing the growing conditions for the gametocyte forming strains. Complete culture medium for daily cultivation was prepared by adding 10% (v/v) human plasma (Chapter 2.1.3.4) and 29,75 mM $NaHCO_3$.

2.1.3.4 Plasma preparation

The plasma from at least 3 donors was pooled together and heat inactivated in a 56°C water bath for 1 hour. The inactivated plasma was centrifuged for 10 minutes at 800 *g*. Thereafter the supernatant was aliquoted into 10 and 40 ml volumes and stored at -20°C.

2.1.3.5 Synchronization

To obtain a culture consisting predominantly of ring-infected erythrocytes, the pelleted erythrocytes were treated with 10 volumes of 5% (w/v) D-sorbitol for 10-20 minutes at room temperature (Lambros *et al.*, 1979). The D-sorbitol selectively lysed the mature stages, leaving the ring-infected and uninfected erythrocytes intact. The suspension was then centrifuged for 5 minutes at 400 *g* and the resultant pellet was resuspended in complete culture medium and incubated at 37°C.

2.2 LABELLING TECHNIQUE FOR IODINATED DIFERRIC TRANSFERRIN

Human apotransferrin was diferrically loaded with ^{59}Fe and the transferrin protein iodinated with ^{125}I as described by L. MacNamara of the Department of Medicine, University of the Witwatersrand Medical School (personal communication) and Baynes *et al.* (1988). All disposable equipment and solutions that came into contact with the following procedures were discarded in designated bins and the non-disposable glassware soaked overnight in 3,5% (v/v) Contrad®.

2.2.1 METHOD FOR PREPARING DIFERRIC TRANSFERRIN

2.2.1.1 Apotransferrin preparation

An apotransferrin solution was prepared by dissolving lyophilised human apotransferrin in saline. To ensure complexation of the ferric iron and apotransferrin, optimal conditions were created. Firstly, 1 M Na_2CO_3 (20 μl) was added per mg apotransferrin, and then the pH was buffered with 0,2 M Tris/HCl (pH 7,3; 40 μl) per mg apotransferrin. The pH of the solution was then adjusted to between 7,4 and 7,6 using dilute NaOH and HCl.

2.2.1.2 Diferric transferrin preparation

To determine the volume of 1 mCi $^{59}FeCl_3$ required to prepare the diferric transferrin solution from an apotransferrin solution, the calculation in Appendix B.1 was used. Twice the calculated volume of $^{59}FeCl_3$, was added dropwise to the apotransferrin solution, which turned salmon-pink/red in colour as the iron-transferrin complex formed. The transferrin solution was adjusted to a pH of approximately 7,5 using dilute NaOH and HCl. The labelling technique was performed in a fume cupboard.

2.2.1.3 Removal of excess iron from transferrin solution

Excess iron was removed from the transferrin solution by passing it through a chloride AG1-X8 ion exchange column, which has a high binding affinity for iron. The ion exchange column was prepared by plugging a 10 ml syringe with gauze before packing it with AG1-X8 (3 ml). The column was then moistened with saline, before the transferrin solution was passed through and collected in a sterile, iron-free glass tube.

2.2.1.4 Diferric transferrin determination

Spectral analysis was performed on the transferrin solution to determine the ratio of diferric transferrin to apotransferrin present. A quartz cuvette was used to read the optical densities at 470 nm and 280 nm. The sample read at 280 nm, was diluted 1 in 10, due to the high concentration of diferric transferrin detected at this wavelength (Lestas, 1976). An optical density ratio was then calculated by the following formula:

O.D. 470 / 10(O.D. 280).

The optical density ratio should have been approximately 0,046, indicating transferrin saturation. But if it was less than 0,046, more $^{59}FeCl_3$ was added and the solution passed through the column again. If the ratio was more than 0,046, the solution was passed through a new column. The labelled diferric transferrin solution was stored for up to 3-4 weeks at 4°C.

2.2.1.5 Analysis

To check the radioactivity of the labelled-transferrin, 2 μl of solution was counted in the Packard gamma counter for 1 minute with background and cross-counting taken into account. The concentration of the transferrin solution was determined via radial immuno-diffusion (Chapter 2.2.3). The purity of the solution was determined by running a 6 M urea polyacrylamide gel (Chapter 2.2.4).

2.2.2 IODINATION OF ^{59}Fe-TRANSFERRIN

Iodination (^{125}I) of the diferric transferrin was performed using 0,5 mCi Bolton and Hunter Reagent solution in dry benzene containing 0,2% dimethyl formamide as described by Bolton and Hunter (1973). The basic chemistry involved in the technique is shown in Figure 2.1.

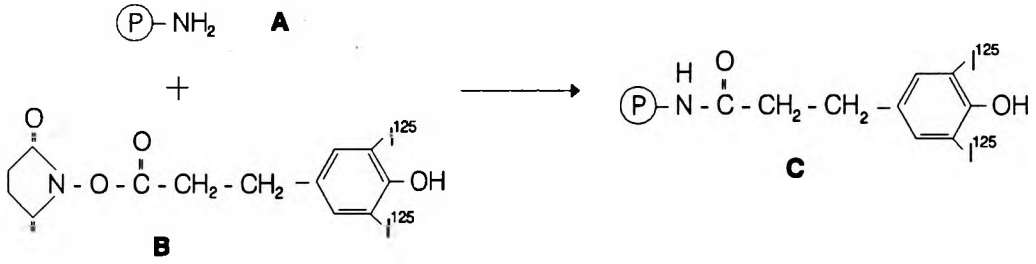


Figure 2.1: Radioactive iodination of diferric transferrin using the Bolton and Hunter Reagent. Indirect iodination was done via an active ester reaction in which the Bolton and Hunter reagent (B) is attached to a reactive amino group (A) in the transferrin polypeptide, to form the iodinated polypeptide (C). (Adapted from Bohinski, 1987).

Safety precautions included ingesting a few drops of Lugols iodine 3 to 12 hours before the experiment, wearing a lead apron and working behind lead blocks in a well ventilated fume cupboard.

2.2.2.1 Protein iodination

To obtain a concentrated form of ^{125}I, the benzene was evaporated off, using the set up as seen in Figure 2.2. At room temperature, a gentle stream of dry nitrogen was directed onto the surface of the liquid to allow for the evaporation of the benzene. This took approximately 15 to 20 minutes. The vial was then carefully removed from bottle with forceps and placed up to the lip in crushed ice. To this, 2 ml diferric transferrin solution was added and left to stand for 30 minutes with intermittent stirring with a thin glass rod.

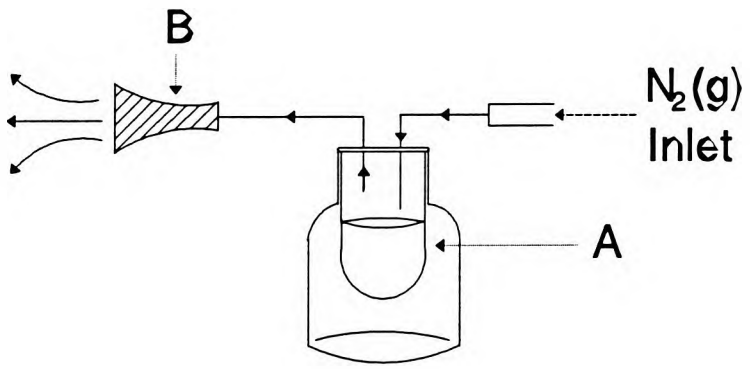


Figure 2.2: Concentration of Bolton and Hunter Reagent. Two hypodermic needles were inserted through the seal of the vial containing the Bolton and Hunter reagent (A) - one as the inlet for the nitrogen gas and the other as the outlet. The inlet needle was placed just above the liquid surface, whilst the outlet needle was placed higher than the inlet needle. A charcoal trap (B) was fitted to the outlet to ensure safer working conditions.

2.2.2.2 Dialysis

The iodinated diferric transferrin solution was dialysed in order to remove excess Bolton and Hunter Reagent. To maximise the rate of dialysis, Spectra/por 1® (Spectrum) with a

molecular weight cutoff of 60 000 to 80 000 was selected. About 20 cm of dialysis tubing was pre-soaked in blood-PBS (pH 7,4) for at least 5 minutes before use. At the one end of the tubing two knots were tied approximately 1 cm apart.

With as little handling as possible, the solution was removed from the vial into the dialysis tube with a pasteur pipette, then the other end of the tubing was knotted. The solution was stirred overnight at 4°C, whilst being dialysed against blood-PBS (pH 7,4). The double-labelled transferrin solution was removed from the dialysis tubing and placed into an iron-free glass tube. The solution was stored behind lead blocks at 4°C for a maximum period of 4 weeks.

2.2.2.3 Analysis

To determine the amount of radioactivity associated with the double-labelled transferrin, 2 μl of solution was counted in a Packard gamma counter for 1 minute, with background and cross-counting taken into account. The transferrin concentration was calculated via radial immunodiffusion (Chapter 2.2.3). The purity of the double-labelled solution was determined by running a 6 M urea polyacrylamide gel (Chapter 2.2.4).

2.2.3 RADIAL IMMUNODIFFUSION TECHNIQUE

The transferrin concentrations of both the ^{59}Fe-transferrin and ^{59}Fe-^{125}I-transferrin solutions were determined using goat anti-transferrin antibodies in the radial immunodiffusion technique (Baynes *et al.*, 1988).

2.2.3.1 Procedure

A glass plate was pre-cleaned with methanol and placed on a level surface. A tube of solid agarose gel (see Appendix B) was melted in a boiling bath and allowed to cool to approximately 56°C before 30 μl of transferrin antibody was added. The tube was inverted and poured onto the pre-flamed glass plate. Wells of constant size were cut into the solidified gel using a LKB mini immunoelectrophoresis vacuum cutting system.

Appropriate apotransferrin standards were prepared, i.e. 1000 μg/ml, 500 μg/ml, 100 μg/ml, 50 μg/ml and 25 μg/ml. The iodinated diferric transferrin solutions were diluted 1 in 10 before 8 μl of the samples and standards were added to the wells. The gel was left to develop in a moisture chamber at 4°C for 64 hours. Thereafter, the gel was placed on a level surface and covered with 1 wet and 5 dry filter papers. A glass plate along with a 1 kg weight was placed on top of the filter paper stack to absorb excess moisture. This step was repeated twice before washing the gel twice in 0,1 M NaCl for 15 minutes, and pressing it once as before. The gel was dried to a fine film in a pre-heated oven at 45°C for 2 hours and then stained for 10 minutes with Coomassie Blue (see Appendix B). The destained gel (See Appendix B) was rinsed in running water and air dried. Figure 2.3 shows an example of the resultant gel with the blue stained diffusion bands.

2.2.3.2 Analysis

The transferrin concentrations of the unknown samples were determined from a standard curve, which was constructed using the log of the apotransferrin concentrations versus the log of the diffusion diameter of each well.

2.2.4 6 M UREA POLYACRYLAMIDE GEL ELECTROPHORESIS

The gel was run in order to determine the purity of the double-labelled transferrin (Makey and Seal, 1976). All glassware was soaked overnight in 6 M HCl to remove all traces of iron and only wooden spatulas were used. Sodium Chelex-100, a weakly acidic chelating resin was used to ultrapurify the solutions, by chelating trace metal contaminants, such as copper, iron, calcium and magnesium, without altering the concentrations of the non-metallic ions.

2.2.4.1 Gel preparation

Powder-free gloves were worn to prevent grease marks from being left on the glass, and due to the high toxicity of acrylamide and bisacrylamide monomers. The glass plates were cleaned with soap, xylene and finally with methanol, then left to air dry.

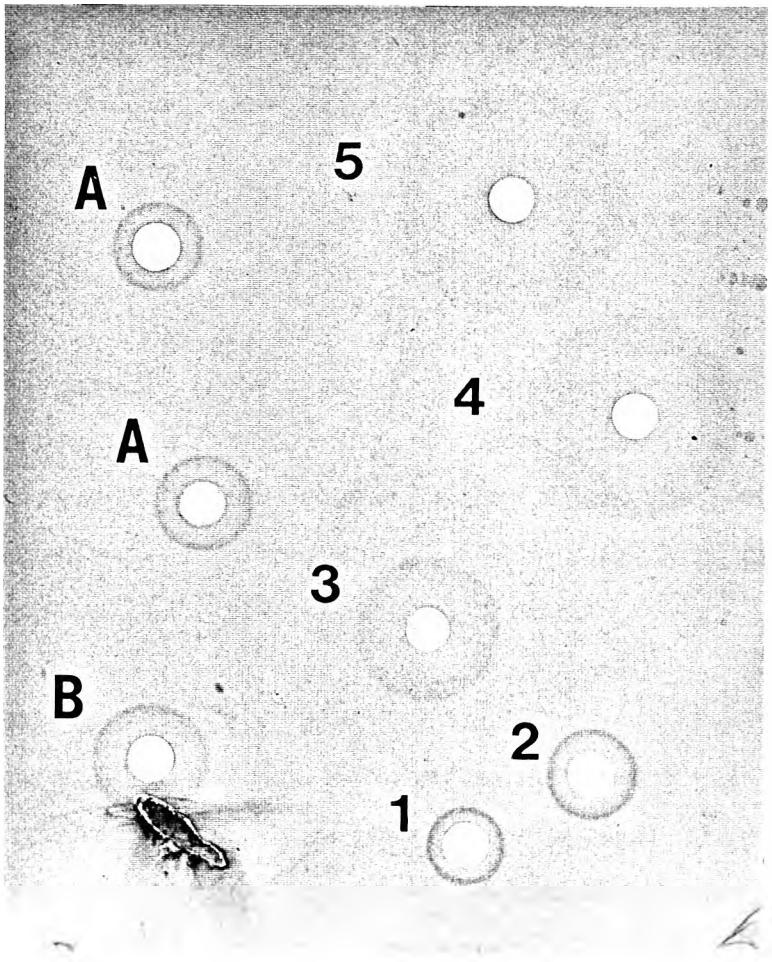


Figure 2.3: Radial immunodiffusion gel with Coomassie Blue stained diffusion bands. Where 1-5 deplict the increasing concentrations of the standards, A and B are the iodinated diferric transferrin and diferric transferrin samples, respectively.

Two spacers were sandwiched between the glass plates before the system was securely clamped into a gel pouring stand. The bottom of the plates were sealed with 2,5 ml acrylamide stock, 5 μl TEMED and a few granules of APS (See Appendix C). Whilst, this gel solution solidified, the urea, acrylamide, 20x Tris/ borate/EDTA buffer, distilled water and APS were mixed together and degassed (See Appendix C). TEMED was added to this

mixture, before the casting solution (See Appendix C) was poured between the plates. The comb was carefully placed between the plates to prevent the formation of air bubbles. After approximately 30 minutes, the comb was removed from the polymerized gel and the wells rinsed out with electrode buffer (See Appendix C). The plates were then removed from the stand and clipped into the electrophoretic apparatus. Sufficient electrode buffer was added to emerse approximately 5 cm of the gel in the bottom reservoir and the top reservoir was filled.

The samples (apotransferrin (1 mg/ml), single-labelled transferrin and iodinated diferric transferrin) were diluted in a 1:1 ratio with sample diluting buffer (See Appendix C). Each sample (30 μl) was added per well, with the iodinated diferric transferrin sample loaded in duplicate. The gel was run at a voltage of 180 V or 80 mA at 10°C for at least 6 hours for complete separation of the different transferrin species.

2.2.4.2 Gel analysis

The gel was removed from the glass plates and a lane carrying the iodinated diferric transferrin was cut from the gel and sliced into 2 mm wide pieces. The slices were placed into tubes in consecutive order and counted for 1 minute in a Packard gamma counter, with background and cross-counting taken into account. The counts were then plotted to establish whether there was an iron-iodine peak representing the double-labelled transferrin. The rest of the gel was Coomassie stained overnight (See Appendix C), and then destained (Figure 2.4).

2.3 UPTAKE OF ^{59}Fe INTO PARASITIZED-ERYTHROCYTES

To verify whether the malaria parasite acquired its iron from the extracellular milieu, the uptake of iron and transferrin into the parasite were examined using double labelled diferric transferrin and ferric citrate.

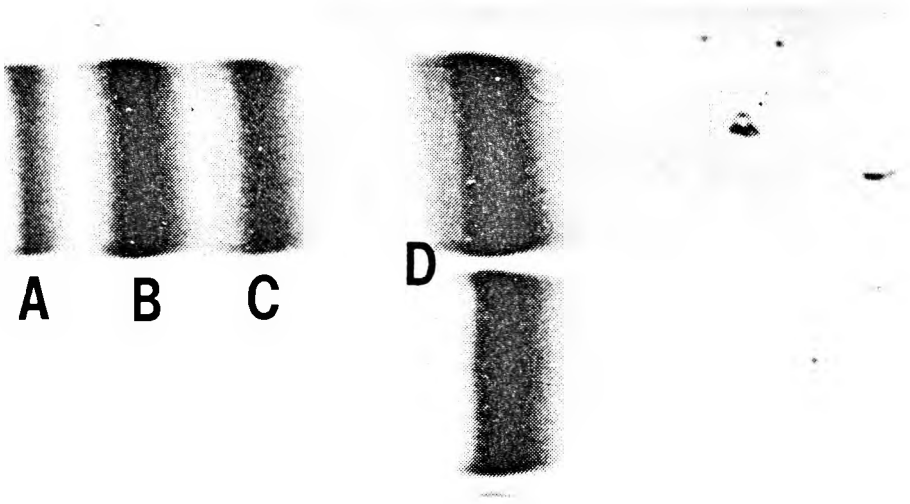


Figure 2.4: 6 M urea PAGE gel to determine the purity of the iodinated diferric transferrin solution. The top and bottom lanes contain 75% and 100% diferric transferrin (D), respectively. A is apotransferrin, B and C are monoferric transferrins with the iron bound at either the N- or C- binding sites. The gel ran from left to right. (Reproduced from Makey and Seal, 1976).

2.3.1 UPTAKE OF DOUBLE LABELLED DIFERRIC TRANSFERRIN

A modified version of the method described by Baynes *et al.* (1988) was used to examine the uptake of iodinated diferric transferrin into malaria parasitized erythrocytes.

2.3.1.1 Preparation of microculture tubes

To ensure that a synchronised culture was used, the culture was sorbitolled every cycle (Chapter 2.1.3.5). Slides were prepared and the percentage parasitaemia and morphology determined before centrifuging the culture for 5 minutes at 400 *g* at room temperature. The packed parasitized pellet was washed at least three times in culture medium to remove all traces of transferrin. Uninfected erythrocyte controls were prepared and treated as the parasitized erythrocytes. A haematocrit of 20% was prepared in culture medium and 0,5 ml of suspension was aliquoted out in triplicate into 5 ml tissue culture tubes (Celcult,

Sterilin). These were allowed to equilibrate during a pre-incubation period of 1 hour. If iron chelating agents were to be tested, 0,25 ml of drug (prepared in culture medium) was added to the suspension at this time. On completion of the pre-incubation period, the double-labelled transferrin was added to each tube. In all but the transferrin-concentration dependent experiments, a final concentration of 2,7 μg/ml (33,75 nM) iodinated diferric transferrin was used. This concentration was comparable to that found circulating in human plasma and was sufficient to obtain adequate radioactive counts. The lids of the tubes were left slightly ajar to permit the free flow of gases to the cultures. The tubes were incubated at 37°C in a candle jar, at a 45° angle to maximise the surface area of the suspension for optimal gaseous exchange.

2.3.1.2 Harvesting

At the desired time intervals, the uptake of transferrin was stopped and the parasites harvested by centrifuging the tubes at 400 *g* for 5 minutes at room temperature. The supernatant (S1) was collected, the pellet resuspended in ice cold blood-PBS (Chapter 2.1.3.2) and centrifuged again. The supernatant of the first wash was collected with S1 and counted as a control to indicate that radioactivity was present and that it had been taken up into the parasite. The pellet was washed twice, and the supernatants discarded. The erythrocytes were lysed with 0,5% (w/v) saponin in blood-PBS, with the final volume of 2 ml kept constant for all tubes. The tubes were stored overnight at 4°C to ensure total haemolysis.

2.3.1.3 Gamma counting and data evaluation

Tubes were counted for 1 minute in a Packard gamma counter and appropriate corrections made for background and cross-counting. The mean and standard deviation of each set were calculated. Thereafter, the counts per minute (cpm) were converted into pmoles of transferrin or iron per 0,1 ml pellet, using the standard control of counting 2 μl of the double labelled transferrin with each experiment. If 2 μl of a 33,75 pmol transferrin solution had A cpm, then a tube with B cpm would have, (33,75.B/A) pmol transferrin present per 0,1 ml pellet. The latter formula was also used to calculate the number of pmol of iron taken up. For each pmol of transferrin there were 2 pmol of iron, since the transferrin was diferric in nature. Thus, the number of pmol of iron present per 0,1 ml

pellet was (67,5.*B*/*A*).

2.3.2 UPTAKE OF FERRIC CITRATE

To determine whether the parasite accumulated iron via a transferrin independent uptake system as in HeLa cells, iron was bound to citrate (Sturrock *et al.*, 1990).

2.3.2.1 Preparation of ^{59}Fe-citrate

Ferric citrate was prepared by the addition of $^{59}FeCl_3$ to a 50-fold molar excess of the trisodium salt of citrate. The citrate was dissolved in blood-PBS (pH 7,6), sterilized through a 0,22 μm Millipore filter into an iron-free glass tube and stored for up to a month at 4°C. A 1:1 molar ratio of $^{59}FeCl_3$ and citrate was freshly prepared and allowed to stand for at least 20 minutes for the pale yellow chelate to form. Culture medium was added to this chelate solution to adjust the volume to that required (MacNamara, personal communication).

2.3.2.2 Experimental procedure

The ferric citrate experiments were conducted and evaluated as described for the diferric transferrin experiments in Chapter 2.3.1.

2.4 INVESTIGATION OF MALARIA HAEMOZOIN

2.4.1 IRON INCORPORATION INTO HAEMOZOIN

2.4.1.1 Preparation of parasitized and uninfected erythrocytes

Synchronous early ring-infected erythrocytes (approximately 10% parasitaemia) were washed three times with culture medium for 5 minutes at 400 *g* to remove traces of plasma transferrin, iron and gentamycin. Uninfected erythrocyte controls were prepared in parallel with the parasitized erythrocytes. The erythrocytes were resuspended at a 10% haematocrit

in culture medium supplemented with 25 mM $NaHCO_3$ and 168,75 nM diferric transferrin and then incubated at 37°C until required. The development of the parasite was monitored by preparing Giemsa-stained thin blood smears (Chapter 2.1.3.1). Once the parasites had progressed to the late trophozoite stage (Figure 2.5.A), the parasitized erythrocytes were washed three times in culture medium at 400 *g* for 5 minutes to remove the extracellular isotope. The supernatants were collected and counted for 1 minute in a Packard gamma counter.

2.4.1.2 Haemozoin isolation

The parasitized erythrocytic pellets were resuspended in 7,5 volumes of culture medium and then frozen at -70°C for at least 2 hours. The lysed erythrocyte suspension was thawed and centrifuged at 500 *g* for 10 minutes at 10°C to collect the isolated parasites (Figure 2.5.B). Before discarding the supernatant, 2 μl was collected for gamma counting. Trace amounts of haemoglobin were removed from the pellets by washing pellets in a 4:1 ratio of culture medium and 0,25 M sucrose-5 mM Tris solution (pH 7,4). Approximately four washes were required to obtain a pure dark-brown parasite pellet. Before the parasites were lysed for the isolation of the haemozoin, 2 μl of the parasite pellet was removed and gamma counted for 1 minute. The isolated parasites, were lysed by five cycles of freezing in liquid nitrogen and thawing in warm water. One millilitre of SDS-PBS buffer (0,1% (w/v) SDS to 10% (v/v) PBS) was added to the lysed parasites. The tubes were then vortexed before being centrifuged at 1000 *g* for 10 minutes at room temperature. The haemozoin pellet was washed with SDS-PBS buffer until only pure haemozoin crystals remained (Figure 2.5.C), which were stored at -70°C until required (Hempelmann and Marques, 1994). The wash supernatant and haemozoin pellet were gamma counted for 1 minute.

2.4.1.3 Haemozoin electrophoresis

SDS gradient gel electrophoresis was used to analyse the ^{59}Fe-loaded haemozoin (Hempelmann and Marques, 1994). A 6-20% linear gradient gel was prepared according to the method described by Hempelmann (1984).

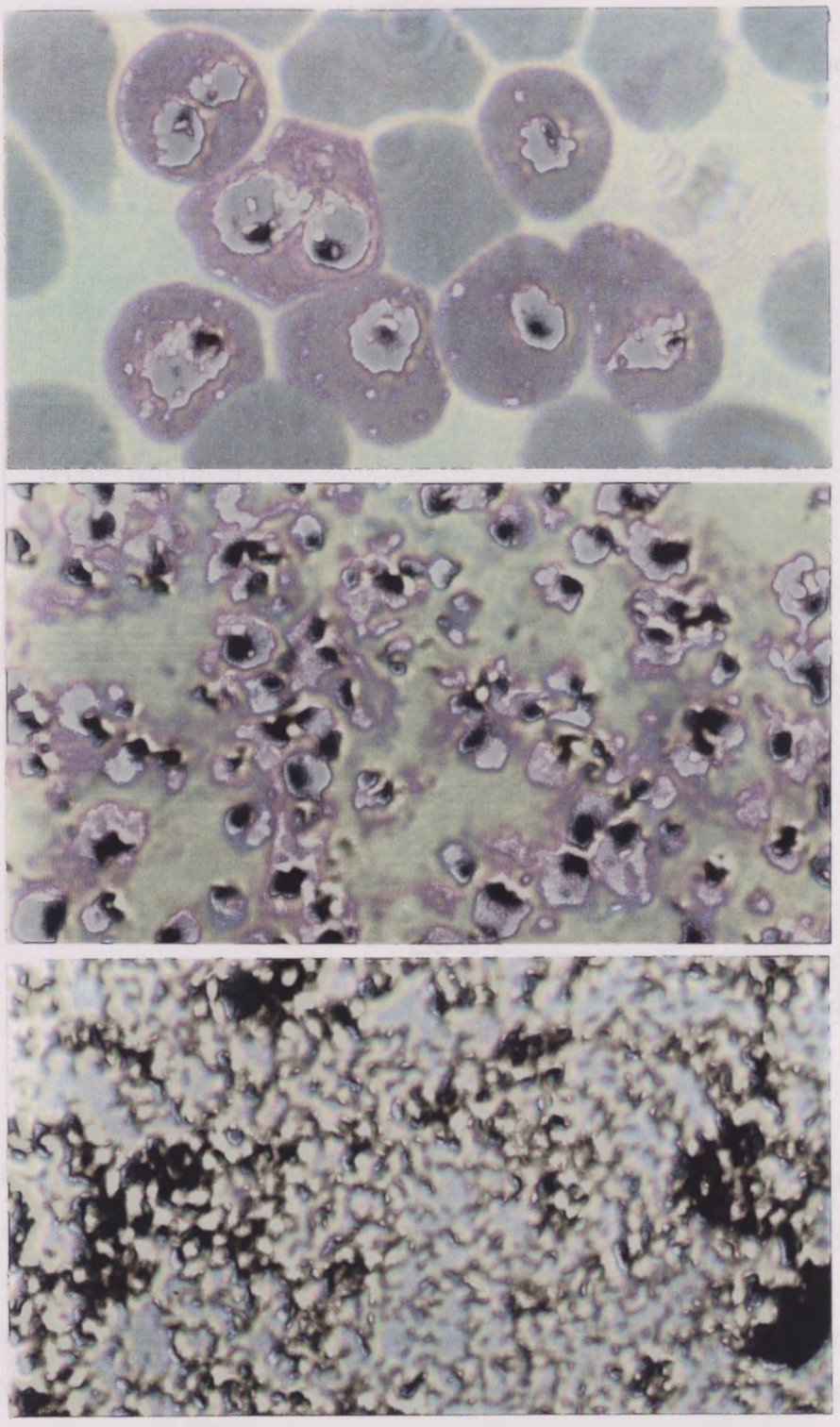


Figure 2.5: Microscope photographs of the steps involved in haemozoin isolation. (A) parasitized erythrocytes, (B) isolated parasites and (C) the isolated haemozoin crystals (1000x magnification). In (A), the trophozoite-infected erythrocytes were concentrated by the gelatine flotation method.

2.4.1.3.1 Electrophoretic apparatus and procedure

A Biorad linear gradient apparatus (Figure 2.6) was used to pour the 6-20% SDS polyacrylamide gel (Studier, 1973).

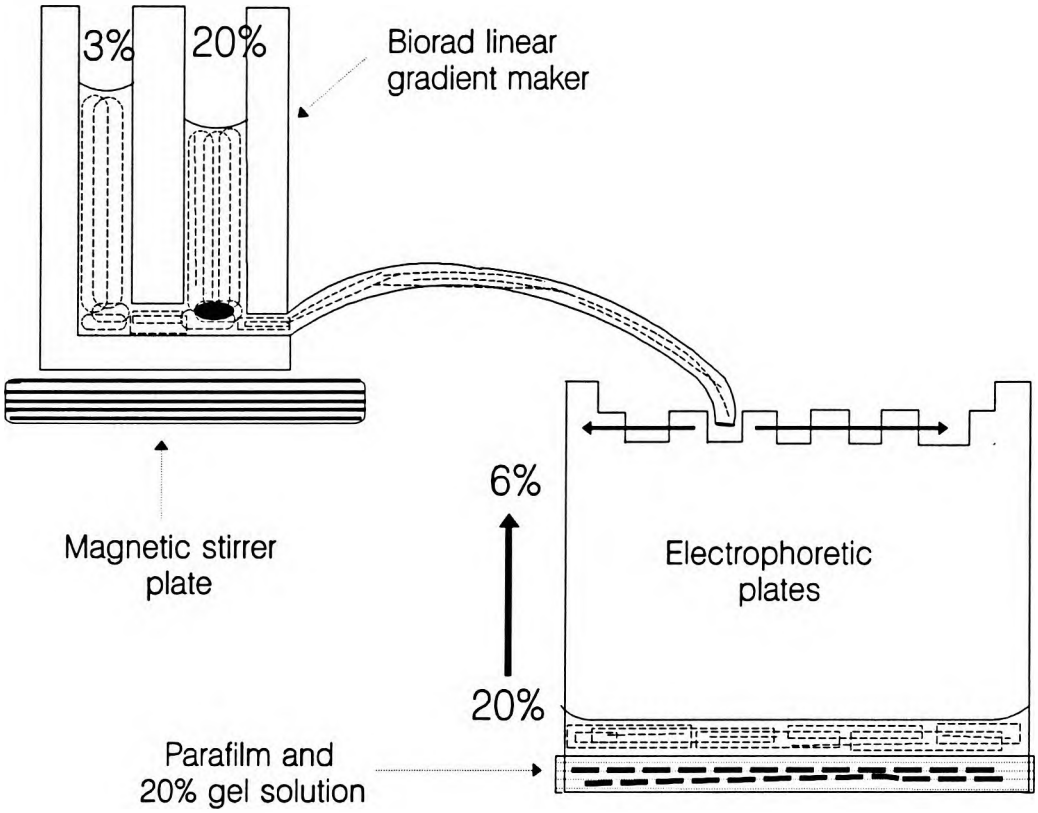


Figure 2.6: Biorad linear gradient maker used to pour the 6-20% polyacrylamide gel.

The plates were assembled as in Chapter 2.2.4.1, with grease and parafilm being placed across the bottom of the plates to prevent leakage of the gel solutions (Figure 2.6). To form a permanent seal, 20% gel solution and TEMED were mixed and added between the plates. Equal volumes of the 3% and 20% gel solutions were added to the Biorad linear gradient maker, with the 20% gel solution entering the assembly first, such that the acrylamide concentration steadily decreased from 20% to 6%.

Once the gel had polymerized, the reservoirs were filled with the appropriate buffers and 20 μl of sample (See Appendix D) was loaded in a mirror image (i.e. haemoglobin.haemozoin-haemozoin.haemoglobin). The gel was run at a voltage of 95 V for 4 hours at 4°C.

2.4.1.3.2 Gel analysis

The position of the brown coloured haemozoin and haemoglobin were measured, then one half of the gel was placed in destain solution (See Appendix D) for at least 3 hours, before being Coomassie stained (See Appendix D) overnight. The haemozoin and haemoglobin samples in the other half were each sliced into 2 mm wide pieces and sequentially counted for 1 minute, with the appropriate corrections taken into account.

2.4.2 *IN VITRO* EFFECT OF DESFERRIOXAMINE ON RADIOLABELLED HAEMOZOIN

Parasites were prepared as in Chapter 2.4.1.1, except 161,81 nM diferric transferrin was added to the parasitized erythrocytic suspension. An uninfected erythrocyte control was prepared in parallel with the parasitized erythrocytes. No desferrioxamine was added to the erythrocyte suspension. When the parasites had progressed to pigmented mid-late trophozoites, the parasitized and uninfected erythrocytes were centrifuged at 400 *g* for 5 minutes at 10°C. The supernatant was collected for gamma counting, and the pellets were washed twice in culture medium to remove traces of the diferric transferrin. The pellet was resuspended in 25 ml of culture medium and evenly aliquoted out into five tubes. To these 15 ml of the various desferrioxamine concentrations were added. The desferrioxamine concentrations were prepared in culture medium supplemented with 25 mM $NaHCO_3$. The parasitized erythrocytes were incubated with desferrioxamine for 2 hours at 37°C on an orbital shaker. At the end of the incubation period, the tubes were centrifuged at 400 *g* for 5 minutes at 10°C. The pellets were washed twice with culture medium and all the supernatants were collected for gamma counting.

The radiolabelled haemozoin was isolated as described in Chapter 2.4.1.3. The isolated

haemozoin pellets were gamma counted for 1 minute. The radioactivity associated with the haemozoin pellet was expressed as a percentage of the control.

2.4.3 EFFECT OF IRON CHELATING AGENTS ON THE ISOLATED ^{59}Fe-HAEMOZOIN

Iron chelating agents were added to the ^{59}Fe-haemozoin, to establish whether the incorporated radio-iron was accessible for chelation and to determine the ionic state of the incorporated iron.

2.4.3.1 Preparation of iron chelating agents

Various concentrations of desferrioxamine and 2,2'-bipyridyl were dissolved in a phosphate buffer (66,14 mM KH_2PO_4 and 0,265 mM $Na_2HPO_4.2H_2O$), pH 5,0. A pH of 5,0 was used to simulate the conditions in the parasite food vacuole which has a reported pH of 5,0 to 5,5.

2.4.3.2 Procedure

Radioactive haemozoin recovered from experiments in Chapter 2.4.1 was aliquoted out (3 μl of approximately 6000 cpm) and gamma counted for 1 minute (i.e. initial pellet). The various concentrations of iron chelating agents were added to the haemozoin and vortexed. After a 30 minute incubation period at room temperature, the tubes were centrifuged at 1000 *g* for 15 minutes at 10°C. The supernatants and pellets (i.e. final pellet) were gamma counted as before, and the resultant radioactivity associated with pellets and supernatants was expressed as a percentage of their respective initial pellets.

2.4.4 INCORPORATION OF $^{59}FeCl_3$ INTO ISOLATED HAEMOZOIN

Radioactive iron and isolated haemozoin were incubated together in order to determine whether an active metabolism was required for the iron to be incorporated into the haemozoin structure of the parasite.

The non-radioactive haemozoin was isolated from late trophozoite infected erythrocytes as described in Chapter 2.4.1.2; whilst the $^{59}FeCl_3$ was diluted with the phosphate buffer (pH 5,0) described in Chapter 2.4.3.1. The isolated haemozoin aliquots and $^{59}FeCl_3$ solution were then incubated at room temperature for two different time periods (30 minutes and 24 hours), before the tubes were centrifuged at 1000 *g* for 15 minutes at 10°C. The supernatants and pellets were separated, then gamma counted for 1 minute. The radioactivity associated with the pellets was expressed as a percentage of the initial cpm of $^{59}FeCl_3$ added.

2.4.5 UV-VIS SPECTROPHOTOMETRIC ANALYSIS OF THE EFFECTS OF DESFERRIOXAMINE ON ISOLATED LABELLED-HAEMOZOIN AND HAEMIN

2.4.5.1 Effects of desferrioxamine on isolated labelled-haemozoin

To determine whether the iron chelating actions of desferrioxamine could induce structural changes in the haemozoin crystals, the haemozoin spectrum was monitored.

2.4.5.1.1 Haemozoin and desferrioxamine preparation

The ^{59}Fe-haemozoin was prepared and isolated as described in Chapter 2.4.1. The stock concentration of desferrioxamine (2,5 mM) and dilutions were prepared in a phosphate buffer (pH 5,15) with a composition as described in Chapter 2.4.3.1.

2.4.5.1.2 Time drive

A UV-VIS spectrophotometric scan, using a Philips UV-VIS spectrophotometer, was run between 250-600 nm with the time interval set at 15 minutes, and the combination of phosphate buffer and 30 μM desferrioxamine was used as the baseline. ^{59}Fe-haemozoin (50 μl) was added to the baseline solution and scanned. After the sixth scan, the concentration of desferrioxamine was increased to 125 μM and the time interval changed to 90 minutes with the number of cycles changed from infinite to 15 cycles.

2.4.5.1.3 Solubilization of the haemozoin crystal

It was noted that the haemozoin (Chapter 2.4.5.1.2) did not dissolve or produce any colour alterations at the acidic pH of 5,15. Thus, the crystals were dissolved by the addition of 1 ml of 20% NaOH (final pH of 12,77) to the solution consisting of haemozoin, phosphate buffer (pH 5,15) and 125 μM desferrioxamine. The UV-VIS spectrometric scan was run between 300-700 nm and the concentration of desferrioxamine was further increased to 312,5 μM to intensify any possible spectral changes.

2.4.5.2 Effect of desferrioxamine on haemin

A haemin chloride (2,11 μM) solution prepared in phosphate buffer (pH 5,15) (Chapter 2.4.3.1) was scanned between 200 and 700 nm. Thereafter, the crystals were solubilized with the addition of 1 ml of 20% NaOH (pH 12,55). Desferrioxamine (final concentration of 2,68 mM) was then added to the haemin solution. The desferrioxamine stock solution was prepared as in Chapter 2.4.3.1. After incubating in the dark for 1 hour, the desferrioxamine and haemin (1,72 μM) solution was scanned as before. The spectra of the labelled-haemozoin obtained in Chapter 2.4.5.1.3 were compared to the haemin spectra.

2.5 HAEMIN INDUCED HAEMOLYSIS

Haemin (ferriprotoporphyrin-IX) has been implicated as the causative agent of haemolysis and to play an integral part in the antimalarial action of the quinoline drugs (Dutta and Fitch, 1983). Therefore, the interaction between haemin and chloroquine, desferrioxamine and 2,2'-bipyridyl in uninfected and parasitized erythrocytes were examined.

2.5.1 HAEMIN PREPARATION

Bovine haemin chloride was used as the haemin source and the stock powder was stored at -20°C in a desiccator. To avoid problems associated with polymerization of haemin in water, solutions were made up fresh in all experiments. Solubility problems were overcome by dissolving the stock solution in 0,02 M NaOH, which was kept on ice in the

dark for up to 2 hours (Fitch *et al.*, 1982). When required, the dilutions were prepared in blood-PBS (Chapter 2.1.3.2) and kept under the same conditions as the stock solution.

2.5.2 PREPARATION OF DRUGS

The various concentrations of desferrioxamine, 2,2'-bipyridyl and chloroquine were prepared in blood-PBS or isotonic buffer (141 mM NaCl and 10 mM Tris, pH 7,7) and kept on ice in the dark until required.

2.5.3 PREPARATION OF UNINFECTED ERYTHROCYTES

Fresh erythrocytes were obtained from healthy female donors and stored in heparinized tubes at 4°C for up to 3 days. For each experiment, erythrocytes were washed at least four times in isotonic buffer (pH 7,7) to ensure that the plasma and buffy coat were removed and only the erythrocytes remained. The washed erythrocytes were stored at 4°C until required.

2.5.4 PREPARATION OF PARASITIZED ERYTHROCYTES

Concentration of the mature trophozoite/schizont-infected erythrocytes (5-10% parasitaemia) was achieved by gelatine flotation (Jensen, 1978). The cultures were centrifuged at 400 *g* for 10 minutes to pellet the erythrocytes. To every 2 ml of packed cells, 6 ml of 1% (w/v) gelatine in culture medium and 12 ml culture medium were added. The suspension was centrifuged as before and the supernatant discarded. The pellet was resuspended in 5 ml of the 1% gelatine solution and 5 ml of culture medium, before being placed at 37°C to sediment the ring-infected and uninfected erythrocytes. After approximately 15-30 minutes, the supernatant, consisting of the trophozoite/ schizont-infected erythrocytes, was carefully removed and centrifuged at 400 *g* for 10 minutes. The ring-infected and uninfected erythrocytes were placed back into culture at 37°C. The pellet

containing the trophozoite-infected erythrocytes was washed at least three times in pre-warmed culture medium before being incubated at 37°C for 10 minutes. The cells were then washed a further three times in isotonic buffer (pH 7,7) to ensure the gelatine coating the cells was removed. In a preliminary study, it was found that six washes were adequate to remove all the gelatine.

2.5.5 HAEMOLYTIC PROCEDURE

The uninfected and parasitized erythrocytes were resuspended in isotonic buffer (pH 7,7) at a 0,5% haematocrit. Six eppendorfs were set up for the controls, whilst every concentration was done in triplicate. Each eppendorf contained 920 μl cellular suspension, 80 μl of the drug, blood-PBS or haemin. In combination studies, 40 μl of drug and 40 μl haemin were added to the suspension. The suspension was well mixed before being incubated at 37°C in the dark for 2 hours, unless otherwise stated. At approximately 30 minute intervals the cells were resuspended by gentle shaking. The combinations and conditions for each study were subject to change as stated in the figure legends. At the end of the incubation period, the erythrocytes were sedimented by micro-centrifugation at 1000 *g* for 1 minute at room temperature. After collecting the supernatant, the pellets were lysed with distilled water and vortexed. When parasitized erythrocytes were used, the lysed pellet was micro-centrifuged, as before, to pellet the haemozoin which as determined in a preliminary study, interferes with the absorbance readings.

2.5.6 DATA EVALUATION

The amount of haemoglobin in the supernatant and lysed pellet were routinely estimated by measuring the absorbance at 540 nm in an UV-VIS spectrophotometer. The following equation was used to calculate the % haemolysis (Dutta and Fitch, 1983):

$$\% \text{ Haemolysis} = \frac{Abs_{supnat} \times 100\%}{Abs_{supnat} + Abs_{lysed\ pellet}} - \% Hc$$

Where: Abs_{supnat} = the absorbance of the supernatant;

$Abs_{lysed\ pellet}$ = the absorbance of the lysed pellet;

% Hc = the percentage haemolysis of the control.

The % haemolysis was plotted against the concentration of drug or haemin to determine whether these drugs could induce or protect the parasitized and uninfected erythrocytes from haemolysis.

2.6 HYPOXANTHINE INCORPORATION ASSAY

Liquid scintillation spectroscopy was used to quantify the amount of tritiated hypoxanthine that was incorporated into the parasite DNA during the experiment. The radioisotope levels were used as an indicator of parasite growth and subsequently the efficacy of the drug being tested *in vitro*. This assay was performed in a sterile laminar flow hood to prevent contamination with bacteria or yeast as the complete culture medium used did not contain any antibiotics.

2.6.1 BASIS OF HYPOXANTHINE UPTAKE STUDIES

The basic method of tritiated hypoxanthine uptake as described by Desjardins *et al.* (1979) and illustrated in Figure 2.7 was used to monitor parasite growth.

2.6.1.1 Preparation of drugs

All stock solutions and dilutions were freshly prepared for each experiment and ONLY

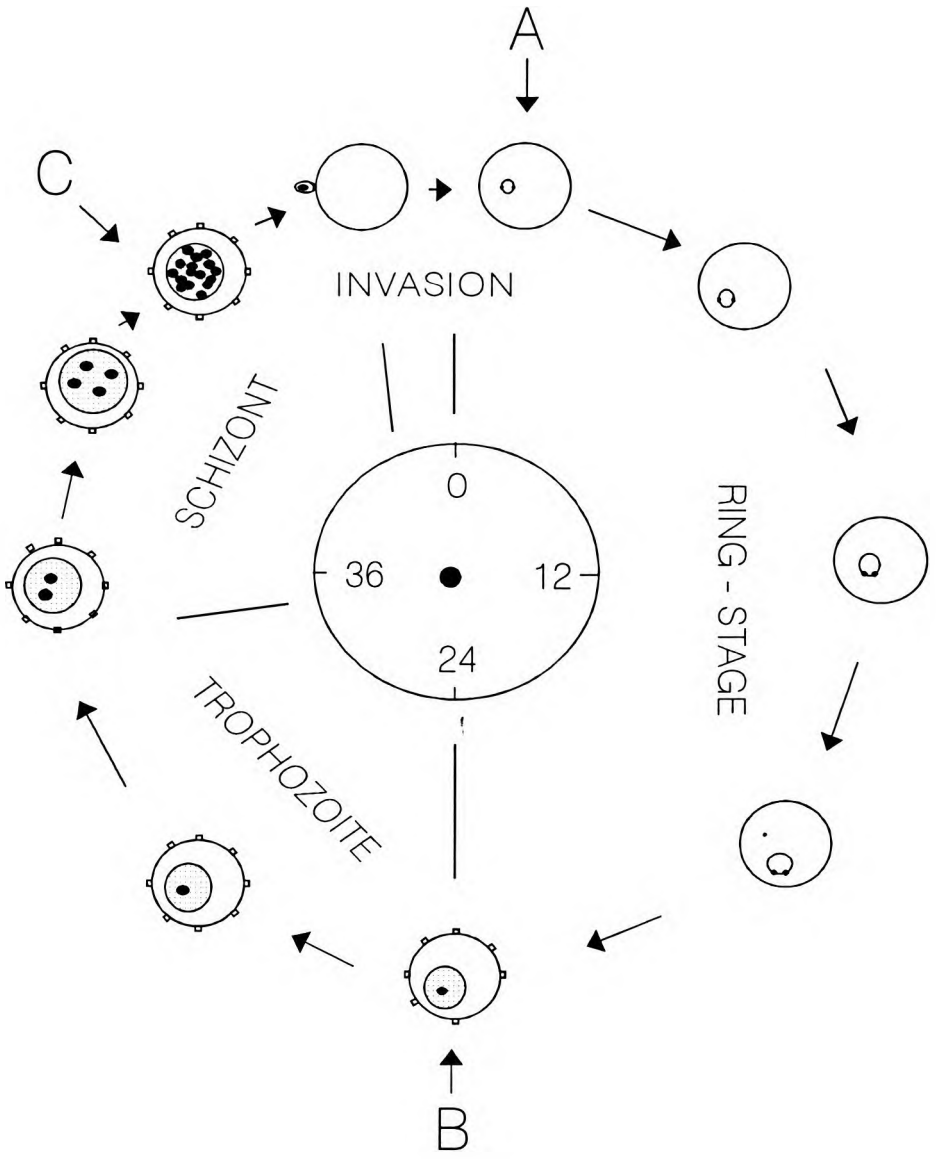


Figure 2.7: The tritiated hypoxanthine assay in relation to the intraerythrocytic life cycle of the *P. falciparum* malaria. (A) Drug addition; (B) ^{3}H-hypoxanthine addition; (C) Harvesting of parasite DNA.

wooden spatulas were used. The stock solutions were filter-sterilized through a 0,22 μm Millipore filter into sterile iron-free tubes.

Chloroquine diphosphate, quinine sulphate, desferrioxamine mesylate (Figure 5.2), bathophenanthroline sulfonate (Figure 5.3), trisodium citrate, ascorbic acid, all dissolved easily in hypoxanthine-free culture medium.

Pyrimethamine was dissolved in 10% DMSO and hypoxanthine-free culture medium; where the addition of up to 10% DMSO did not affect parasite growth. 2,2'-Bipyridyl was dissolved in hypoxanthine-free culture medium after 5 to 10 minutes of continuous vortexing. Nitrilotriacetic acid was dissolved in 2,4% DMSO/0,5% 0,02 M NaOH/ hypoxanthine-free culture medium, after 10 minutes of continuously vortexing.

Sodium ethylene diaminotetraacetic acid (EDTA) and the alkyl derivatives, 1,2-diaminooctyl tetraacetic acid (DOTA), 1,2-diaminododecyl tetraacetic acid (DDDTA) and 1,2-diaminohexadecyl tetraacetic acid (DHDTA), were all dissolved in 5% $NaHCO_3$ (pH 8,3), since this is the only solution in which the most lipophilic derivative, DHDTA was soluble. Thus, to standardize the aminocarboxylate group of drugs, ethylene bis(oxy-ethylene nitrilo) tetraacetic acid (EGTA) and diethylene triaminopentaacetic acid (DTPA) were also dissolved in 5% $NaHCO_3$ (pH 8,3).

2.6.1.2 Preparation of uninfected control erythrocytes

Uninfected human erythrocytes were washed at least three times in blood-PBS (Chapter 2.1.3.2), before being suspended at a 1% haematocrit in complete hypoxanthine-free culture medium.

2.6.1.3 Preparation of parasitized erythrocytes

Drug sensitivity tests using the hypoxanthine uptake assay were always started with early ring-infected erythrocytes (A in Figure 2.7). The synchronized culture was adjusted to 0,5% parasitaemia and 1,0% haematocrit.

2.6.1.4 Preparation of microculture plates

Flat bottomed, 96-well microculture plates were used (Figure 2.8). The prepared drug dilutions (25 μl) were added in triplicate, such that a total of 28 different drug dilutions could be tested in one plate. To the control wells (i.e. row H), 25 μl of hypoxanthine-free

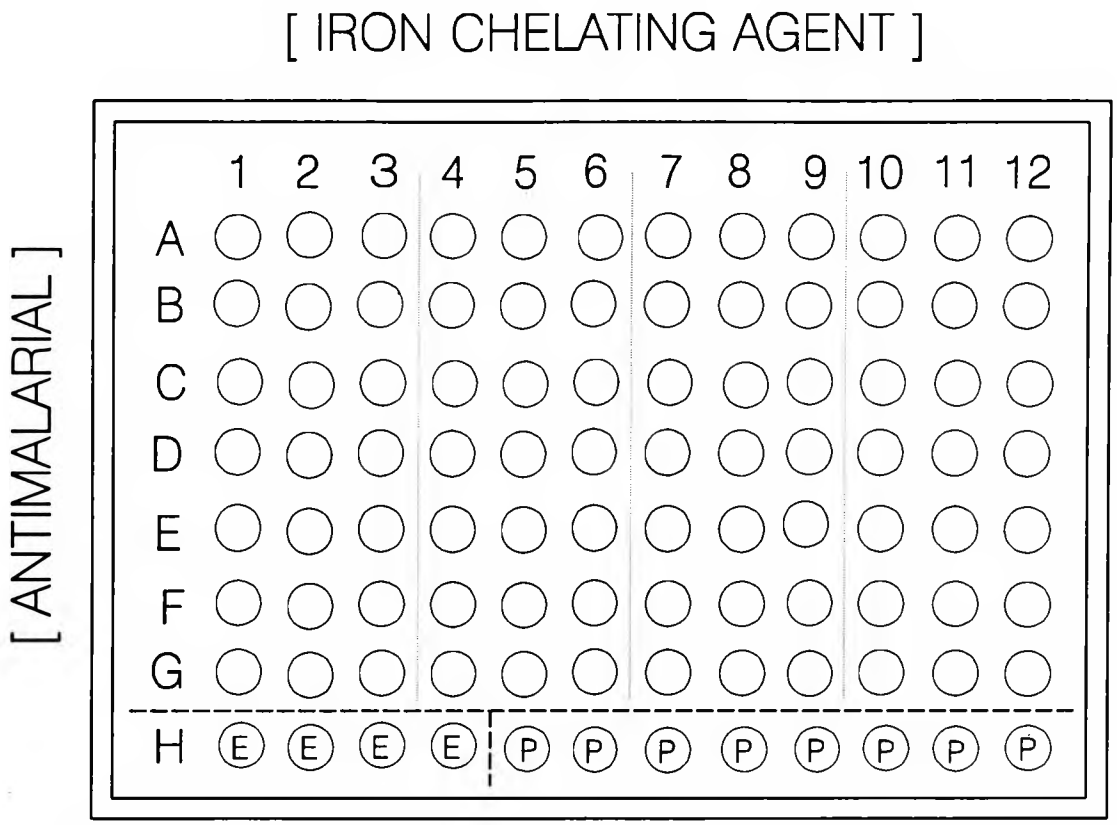


Figure 2.8: The layout of the 96-well microculture plate for the ^{3}H-hypoxanthine incorporation assay. E is the uninfected erythrocyte control and P is the parasitized erythrocyte control.

culture medium was added to maintain a fixed total volume in each well. A constant volume (200 μl) of parasitized erythrocyte suspension (Chapter 2.6.13) was added to each well, except to the first four wells of Row H, to which 200 μl of uninfected erythrocyte suspension (Chapter 2.6.1.2) was added. Thus, the first four wells of Row H served as the uninfected erythrocyte controls and the remainder of Row H served as the parasitized erythrocyte controls. The plates were then placed in a candle jar and incubated at 37°C for 24 hours.

2.6.1.5 Labelling of parasite DNA

The incorporation of beta emitting [G-^{3}H]-hypoxanthine into parasite DNA, was used as an index of parasite growth.

The [G-^{3}H]-hypoxanthine solution, dissolved in 50% ethanol (molecular grade) was stored at -20°C. Before the [G-^{3}H]-hypoxanthine was added to the microculture plates, the ethanol was evaporated from 0,2 ml of the stock sample, and 4,9 ml of hypoxanthine-free culture medium was added. Twenty four hours after the parasites had been added to the drug dilutions, 25 μl of the prepared isotope was added to each well to give a final isotope concentration of 0,5 μCi/well (B in Figure 2.7). The plates were returned to the candle jar and incubated for a further 18 hours at 37°C.

2.6.1.6 Harvesting the parasite DNA and beta scintillation counting

At the end of the 18 hour incubation period (C in Figure 2.7), each plate was harvested with a semi-automatic cell harvester (Titertek Cell Harvester, Flow Laboratory). The parasite DNA of each well was aspirated and deposited onto glass fibre filter paper, with each well being washed three times with distilled water. The filter paper was then allowed to air dry.

Two different methods for preparing the DNA samples for beta counting were used. Firstly, the dry circular disks were removed from the filter paper sheet and placed in a sequential order into glass vials containing 5 ml of Aquagel I® (a toluene based scintillation cocktail). Then each vial was beta counted for a period of 1 minute in a Packard Scintillation Counter.

Alternatively, the filter paper sheet along with 10 ml of Wallac Betaplate Scint® fluid were enclosed in a sample bag and heat sealed. The sheet, correctly aligned in a cassette, was placed in the Wallac Betaplate liquid scintillation counter and each sample counted for a period of 1 minute.

2.6.1.7 Evaluation of dpm results

The mean dpm values for the uninfected and parasitized erythrocyte controls were calculated and used in the following equation to determine the percentage parasite survival. The standard deviation of percentage parasite survival for each drug concentration was also calculated.

% Parasite survival = (D - EC) x (100/PEC)

Where: D = the mean dpm value of the parasitized erythrocytes at each drug dilution;
EC = the mean dpm value of the uninfected erythrocyte control;
PEC = the difference between the mean dpm values of the parasitized and uninfected erythrocyte controls.

2.6.1.8 Dose-response curves

To obtain dose response curves for the different drugs, the following two equations, from a non-linear regression data analysis curve fitting programme, Enzfitter® were used.

$$\text{Effect } (\%) = 100/(1+(C/IC_{50})^{P})$$
$$\text{Effect } (\%) = 100/(1+(10^{C}/IC_{50})^{-P})$$

Where: 100 = the maximum parasite inhibition achieved;
C = concentration of the drug used;
IC_{50} = 50% inhibition concentration of the drug;
P = the slope;
10 = the logarithmic factor.

From each dose response curve, the software calculated the inhibitory concentration at which 50% of the parasites were killed, i.e. the IC_{50} value. This value was used to determine whether the drug could potentially be used as an antimalarial.

2.6.2 MODIFICATIONS OF THE HYPOXANTHINE INCORPORATION ASSAY

2.6.2.1 Drug combinations

In order to determine whether it would be advantageous to add two drugs in combination,

the following studies were performed.

2.6.2.1.1 Type A: Fixed concentrations

Initially combination experiments were set up such that fixed concentrations of both drugs being tested were added to the plate as in Figure 2.8.

The microculture plates were pre-dosed with 25 μl of each chelating agent, antimalarial or combinations of these drugs. To this 170 μl uninfected or parasitized erythrocyte suspension was added and incubated, harvested and analysed as described in Chapter 2.6.1. It was not possible to generate isobolograms using this methodology, thus the method by which the dilutions were prepared, was altered, as described Chapter 2.6.2.1.2.

2.6.2.1.2 Type B: Fixed ratios

Drugs were dissolved and sterilized as in Chapter 2.6.1.1. Fixed ratios of the drugs were prepared as seen in Table E1 in Appendix E. The drugs were then mixed in a 1:1 ratio with further 1 in 4 serial dilutions, such that there were 14 dilutions in total. The uninfected and parasitized erythrocyte suspensions were plated out, harvested and the results evaluated as described in Chapters 2.6.1.4 to 2.6.1.8.

From the eight dose-response curves, eight IC_{50} values were calculated (Figures E1 to E4 in Appendix E), and in turn the IC_{50} values of the other drug were calculated using direct proportion. The drug ratio values were calculated by assigning the IC_{50} values of Plates A and H equal to the value of one (Table E1 in Appendix E). Then by using direct proportion, the other drug ratio values were calculated. For a worked example, see Table E.1 in Appendix E. These drug ratio values were then used to construct the isobologram, from which the nature of the interaction between the two drugs could be determined as seen in Figure 2.9 (Berenbaum, 1989).

2.7 STATISTICAL ANALYSIS

All values were expressed as means $\pm$ standard deviation, which was graphically

illustrated by the following symbol: Φ. Statistical analysis comparison between groups was carried out using the Student's *t*-test for difference of means (for paired samples). To test for correlation between two variables, linear regression analysis was performed and the squared correlation coefficient (r^2) and probability (p) values were calculated. A *p* value of less than 0,05 was taken as significant.

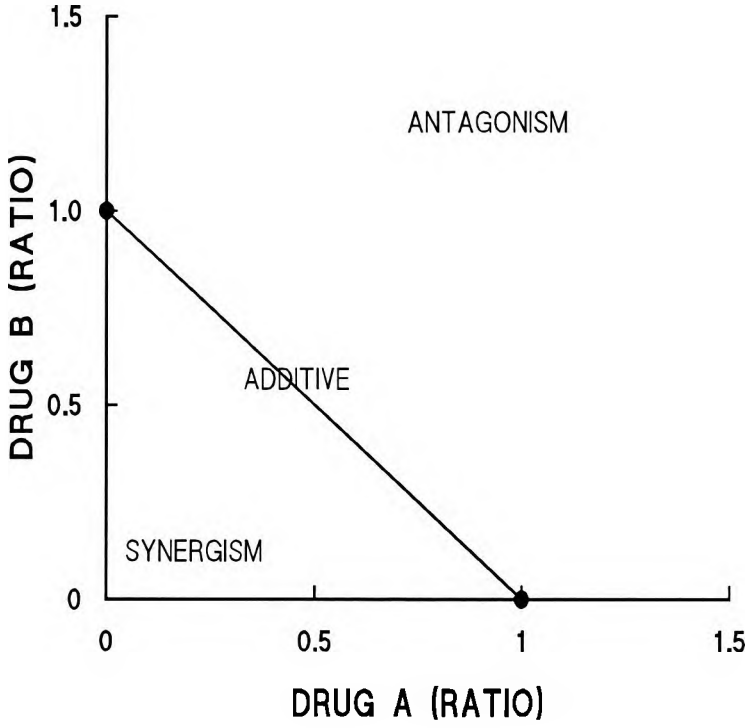


Figure 2.9: An isobologram indicating different drug interactions. Points below the zero interactive line (solid line), indicated synergism. Points above the interactive line indicated an antagonistic interaction between the two drugs. Whilst any points on or in the very near vicinity of the zero interactive line indicated an additive interaction.

CHAPTER THREE

PASSAGE OF IRON INTO P. FALCIPARUM-INFECTED ERYTHROCYTES

3.1 INTRODUCTION

The young red blood cells, with their high metabolic activity and ATP levels, are preferentially invaded by *P. falciparum* parasites. However, reticulocytes only make-up 2-3% of the red blood cell volume of the human host (Pasvol *et al.*, 1980), thus mature erythrocytes, with their low metabolic activity, are invaded by the merozoites. After merozoite invasion, the parasite becomes concentrically surrounded by the erythrocyte and the parasitophorous vacuole membranes (Figure 3.1) (Gero and Kirk, 1994). Thus, in order for nutrients to be acquired from the external milieu and for catabolites to be expeditiously disposed of, they have to cross the latter series of membranes and its own parasite plasma membrane.

However, the mature red blood cell does not contain any functional DNA and thus has very limited activity. In addition, the rigidity of the membrane can not support the exchange of solutes necessary for parasite growth. Thus, without major alterations in structure and function of the host membrane, the malarial parasite can not proliferate. One of the first alterations induced after invasion, involves the increase in membrane permeability without compromise of cell integrity. This is accomplished by depleting the erythrocyte membrane of cholesterol with consequent fluidization and the insertion of polypeptides into the erythrocyte membrane (Sherman and Greenan, 1984; Elmendorf and Haldar, 1993). The changes in permeation are cumulative and concomitant with parasite growth (Cabantchik, 1989).

For about ten hours post-invasion, the early ring stage remains relatively metabolically quiescent. Surface morphology of the infected erythrocyte changes dramatically from about 10 to 30 hours post-invasion. The characteristic smooth biconcave disc is transformed into a pleomorphic, irregularly shaped parasitized erythrocyte, with "knob-like" protrusions (Aikawa and Miller, 1983).

During schizogony of *P. falciparum*, a single intraerythrocytic parasite can asexually produce 16 offspring within 48 hours. Although the rate of multiplication is relatively slow compared to other prokaryotes, it nevertheless requires considerable traffic of solutes in

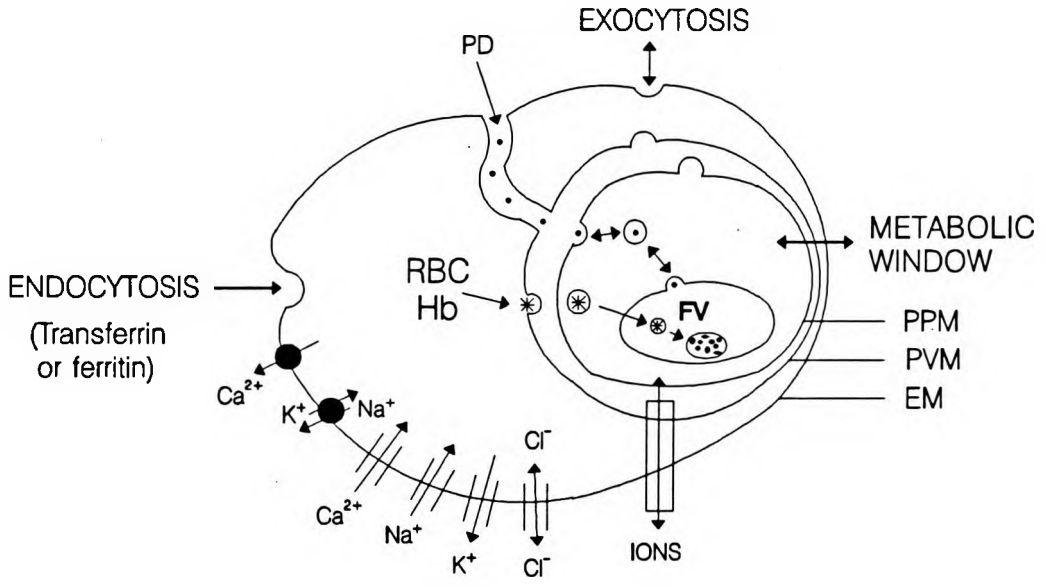


Figure 3.1: Possible mechanisms of iron acquisition by the malaria parasite. Uptake could be via the parasitophorous duct (PD), the metabolic window (i.e. directly through the erythrocyte membrane (EM), parasite plasma membrane (PPM) and the parasitophorous vacuole membrane (PVM)), endocytosis, ion channels/pumps or by digestion of host haemoglobin (Hb) in the parasite food vacuole (FV) to release the iron. Adapted from Lytton *et al.* (1994).

and out of the parasite and host cell. During the later stages of development, a multitude of metabolic and biosynthetic activities are initiated. The parasite overcomes the limitations of its host cell by activating and accelerating the pathways present, and inducing new permeable pathways in the erythrocyte membrane (Figure 3.1). The parasite utilizes pre-existing endogenous transporters present in the erythrocyte to handle substrates such as glucose, phosphate, lactate, certain amino acids and nucleosides (Cabantchik, 1990). Neo-transporters, i.e. parasite-induced pathways which display pore- or channel-like properties are also used to acquire substrates, such as amino acids (glutamine and cysteine), phospholipids, fatty acids, lactates and perhaps iron and other trace metals (Cabantchik, 1989).

3.1.1 ACQUISITION OF IRON

Malaria-infected cells are more permeable to cations, for example potassium and calcium, where the content of both increase substantially as the parasite matures (Bookchin *et al.*, 1981). Uptake is facilitated via Na^+-K^+- and Ca^{2+}-ATPase pumps or K^+- and Ca^{2+}-channels (Krishna and Ng, 1989). Divalent zinc and magnesium are also taken up by the parasite and utilized in many biochemical processes.

Iron is essential for DNA synthesis during the explosive growth and proliferative phase of *P. falciparum*. Many other metabolic processes of the parasite are also dependant on iron, including pyrimidine synthesis (dihydroorate dehydrogenase), glycolysis, the pentose phosphate shunt, carbon dioxide fixation (phosphoenol pyruvate carboxykinase), proteolysis of haemoglobin and mitochondrial electron transport (cytochrome oxidase) (Gordeuk *et al.*, 1994). How and from where the intraerythrocytic parasite acquires iron for its metabolism and proliferation has not yet been determined. Proposed sources include iron derived from plasma transferrin, non-transferrin-bound iron, the catabolism of ingested haemoglobin, a labile intraerythrocytic iron pool and iron derived from red cell ferritin (Figure 3.1).

3.1.1.1 Plasma diferric transferrin

Raventos-Suarez *et al.* (1982) first reported that malaria parasites depend on non-haem iron for survival. This was supported by Pollack and Fleming (1984), who showed that the iron is acquired extracellularly from the host plasma transferrin (see Chapter 1.4). However, normal mature erythrocytes are incapable of iron uptake, since this terminally differentiated cell lacks the transferrin-receptor.

It is postulated that the parasite synthesises its own transferrin-receptors, enabling it to take up iron from transferrin by receptor-mediated endocytosis (Figure 3.2). Two groups have detected these neo-transferrin receptors, with relative molecular weights of 93 and 102 kilodaltons, respectively (Rodriguez and Jungery, 1986; Haldar *et al.*, 1986). The latter receptor was analysed to be a single polypeptide acylated by 1,2-diacyl-*sn*-glycerol. This contrasts the human transferrin receptor which is an acylated glycoprotein disulphide-

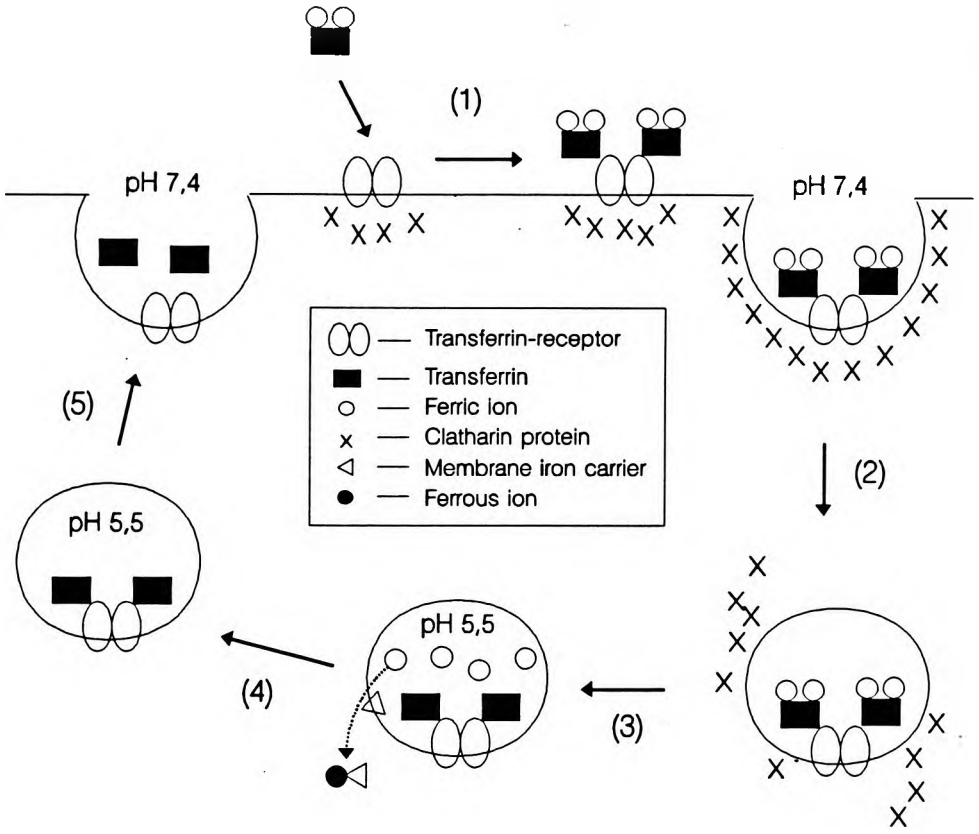


Figure 3.2: Transferrin-receptor mediated endocytosis. After binding specifically to the transferrin receptor (1), diferric transferrin is internalized by receptor mediated endocytosis (2). The lysosome becomes acidified and the ferric ions are released from transferrin (3). The apotransferrin receptor complex is exocytosed to the cell surface and released into the extracellular milieu (5). The receptor is then recycled. The ferric ions are reduced and transferred by carrier proteins to the cytosol (4). The ferrous ions are then either stored, utilized or used to regulate iron metabolism (Adapted from Klausner, 1988).

linked dimer composed of two 95 kilodalton subunits, which can bind two diferric transferrin molecules (see Chapter 1.4.2.4) (Pollack, 1992).

Transferrin-receptor-mediated uptake of iron by the parasitized erythrocytes is further substantiated by Fry (1989). He reported the presence of a membrane-associated diferric

transferrin reductase enzyme, which is proposed to reduce the ferric ions bound to the transferrin-transferrin-receptor complex. This facilitated the transfer of the more membrane permeable ferrous ions to the cytosol (Figure 3.3). This redox pathway of iron uptake is described for several other cell lines, for example, HeLa and hepatocytes (Low *et al.*, 1987; Thorstensen and Romslo, 1988; Toole-Simms *et al.*, 1990). The process only occurs once diferric transferrin is bound to the transferrin-receptor, thus the presence of a parasite transferrin-receptor is indirectly shown to exist. However, Pollack and Schnelle (1988) contest the presence of transferrin-receptors. Instead they suggest that transferrin is non-specifically bound to the membrane surface since it was found that both lactoferrin and bovine serum albumin could bind to the parasitized erythrocyte. The iron and proteins are then endocytosed, with the protein being degraded and the iron selectively retained.

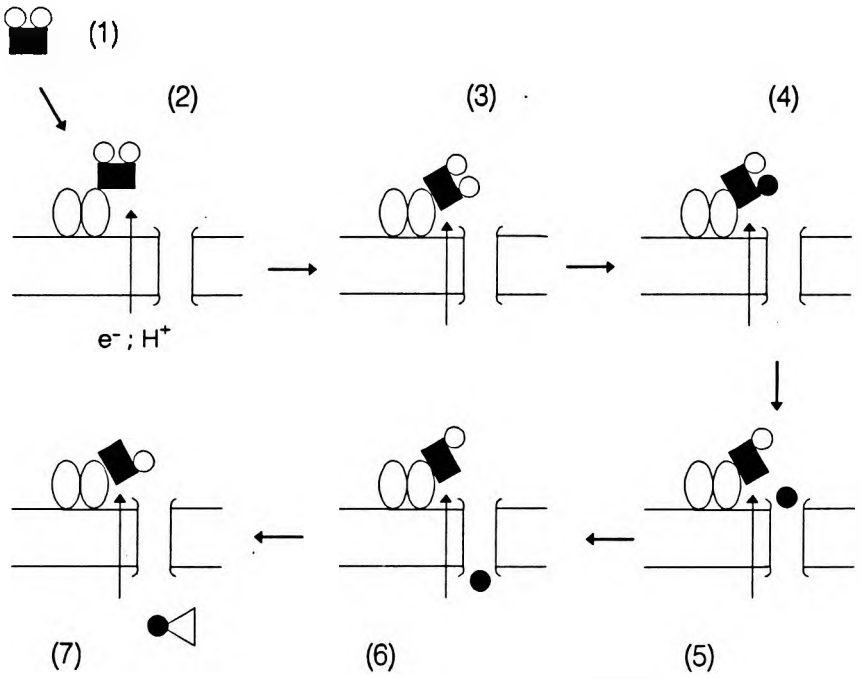


Figure 3.3: The redox mediated process for iron uptake from the transferrin-transferrin-receptor complex. Transferrin binds to the transferrin-receptor (1), resulting in a release of protons and reducing equivalents (2) by the reductase enzyme to destabilize the transferrin-Fe^{3+} bond (3). The ferric ions are reduced (4) and the Fe^{2+} ions bound to a membrane carrier (5) was then translocated across the membrane to a cytosolic carrier (7). Key as in Figure 3.2. (Thorstensen and Romslo, 1990).

An alternative mechanism by which the parasite could incorporate diferric transferrin is by the recently discovered parasitophorous duct (Figure 3.1). The latter is described to be a membranous extension of the parasitophorous vacuole membrane that interacts with the erythrocyte membrane, to provide a stable aqueous duct between the latter two membranes. The development of the duct is proposed to be at the early trophozoite stage (20-25 hours post-invasion) in the cytoplasm of the infected erythrocyte. This energy and temperature-dependant pathway could allow for serum macromolecules (e.g. transferrin) to passively diffuse into the parasitophorous space, from where they could be endocytosed through the parasite plasma membrane into the parasite (Pouvelle *et al.*, 1991). But, it is contended that the manifestation of the duct may be an experimental artifact and that the membranous extensions from the parasitophorous vacuole membrane do not fuse with the erythrocyte membrane to form the duct (Fujioka and Aikawa, 1994; Elford *et al.*, 1995).

3.1.1.2 Non-transferrin-bound iron

Initially it was thought that receptor-mediated endocytosis was the only pathway by which proliferating cells could acquire iron. However, several reports now suggest that iron can be incorporated in the form of non-transferrin plasma iron into HeLa, perfused rat liver cells and fibroblasts (Wright *et al.*, 1988; Sturrock *et al.*, 1990; Kaplan *et al.* 1991). Complete saturation of transferrin results in the accumulation of non-transferrin bound iron. This conditions occurs in iron overload patients (see Chapter 1.4.2.2.1) or if there is excessive haemolysis in for example haemolytic anaemia or patients infected with high malaria parasitaemias (Hershko and Peto, 1987; Bridges and Seligman, 1995).

Reticulocytes are also characterized to transport non-transferrin bound iron across the plasma membrane into the cytosol by an active, carrier-mediated process (Qian and Morgan, 1991). Recently, it has been reported that in iron-overload mice, the hepatic development of *P. yoelii* is increased by the presence of non-transferrin-bound iron (Gama *et al.*, 1996). It is therefore possible that the malaria parasites accumulate iron via a similar process as the HeLa and liver cells.

3.1.1.3 Erythrocytic haemoglobin

The intraerythrocytic parasite proliferates in an iron rich environment, consisting mainly

of haemoglobin (Zarchin *et al.*, 1986). The host haemoglobin is ingested by the parasite via a complex endocytotic process, and then delivered into the acidic plasmodial food vacuole (Figure 3.1). The haemoglobin is rapidly proteolysed into its constituent amino acids, which are subsequently utilized for protein synthesis (Rosenthal, 1995). However, the haem released from this process is not degraded as in other mammalian cells, since the enzyme responsible for the breakdown, haem oxygenase, is not detectable in *Plasmodia* (Eckman *et al.*, 1977). Thus, iron is not liberated from the haem molecule, instead the haem is sequestered as malaria pigment/haemozoin via an unique process (see Chapter 4.1).

It is possible that at the acidic pH of the plasmodial food vacuole, haemoglobin spontaneously denatures, and releases its iron as an intermediatory, reactive ferryl (Fe^{4+}) radical species. This radical could then attack another haem molecule, producing a porphyrin radical, which destabilizes the haem molecule to release the iron (Gabay and Ginsburg, 1993). The release of iron can be inhibited by histidine and imidazole, which scavenge the ferryl radical. Quinoline-containing antimalarials (chloroquine, quinine and mefloquine) also inhibit iron release by interacting with the porphyrin ring, thereby preventing the formation of porphyrin radicals (Gabay *et al.*, 1994). At present, the possibility that a small amount of haem iron is released in a controlled manner, represents a plausible explanation for the source of iron for the intraerythrocytic parasite.

3.1.1.4 Intraerythrocytic iron pool

In many cells, including the reticulocytes, the rate of iron uptake normally exceeds the rate of its utilization and excretion (Bridges and Seligman, 1995). This differential between uptake and utilization could account for the non-haem, non-ferritin, non-transferrin-bound iron detected in the cell cytosol.

This transit iron pool functions as a focal point of intracellular iron metabolism where it maintains an equilibrium of the iron between the cells of different organs in the body and exchanges iron between transferrin, macromolecules, ferritin, haem and non-haem compounds. It also supplies iron for enzyme activation involved in DNA synthesis, globin chain synthesis, tyrosine and proline hydrolase activity (Jacobs, 1975).

The exact chemical nature of the transit iron pool is unknown, although many attempts have been made to reveal its composition. Rothman *et al.* (1992) proposes that the autophagic degradation of ferritin contributes largely to the physiologic origin of this intracellular transit iron pool. Attempts to characterize the low molecular weight transport proteins which are proposed to complex the "free" iron, have only been partially successful and somewhat contradictory. It has been proposed that the iron bound in low molecular weight compounds are composed of amino acids, ascorbate, glucose, riboflavin, glycine, lactose, AMP, UTP, GTP and CTP; with citrate and ATP being the most cited ligands to bind the iron (Bates *et al.*, 1967; Miller and Liebman, 1969; Pollack, 1974; Wright *et al.*, 1988). However, it has also been reported that the low molecular weight iron-binding fractions contain no amino acids, nucleotides or sugars (Pollack *et al.*, 1985). Pollack (1994) recently proposed that the major ligand for iron in the low molecular weight pool of reticulocytes is ATP (a strong iron chelating agent). The iron pool was analyzed to consist mainly of ATP-iron together with a 13800 molecular weight polypeptide, which together form high molecular weight polynuclear iron aggregates. The formation of these polynuclear iron aggregates are proposed to protect the cell from hydroxyl radical formation, by removing the iron from the reactive mononuclear pool (Weaver *et al.*, 1993).

Vyoral *et al.* (1992) do not support the concept of the cytosolic low molecular weight iron pool as being a kinetic intermediate between transferrin and ferritin iron. It is however proposed that there are high molecular weight iron containing compounds which serve as ferritin iron precursors. Nunez *et al.* (1993) also propose that high molecular weight compounds namely, cytosolic ferritin, transferrin and an uncharacterized iron-binding protein are the cytosol intermediates involved in the transport of iron from the plasma membrane to the mitochondria. But the general consensus is that the transit iron pool consists of low molecular weight compounds complexed to iron.

There is no reason why the transit iron pool should consist of a single type of complex and probably does consist of various types of ligands in different cells/organisms. Although all the candidate ligands should share some properties, such that an equilibrium between ferric and ferrous compounds be maintained (Jacobs, 1975).

The oxidative state in which iron exists in the transit iron pool is also undetermined. Under anaerobic conditions, which predominate in the cell, more ferrous iron was isolated; suggesting that the iron in reticulocytes is predominantly in the ferrous oxidation state (Pollack *et al.*, 1985). Similarly, with the use of a calcein fluorescent probe, Breuer *et al.* (1995) found that the transit iron in the cytosol of K562 cells is maintained as iron (II), which was easily chelated by 2,2'-bipyridyl. The obvious absence of chelatable ferric iron for desferrioxamine, indicated the presence of vigorous reductive mechanisms in the cytoplasm. This is in total contrast to that reported by Jacobs (1975), White *et al.* (1976) and Rothman *et al.*, (1992); who observed that the intracellular iron was easily chelated by ferric chelating agents, such as desferrioxamine. Thus, it is probable that the oxidation state is determined by the redox potential within the cell or possibly at different sites. This lack of agreement on the chemical nature of the transit iron pool may persist until new characterization techniques become available.

Studies on red blood cell lysates parasitized with *P. berghei* revealed a labile iron pool (Hershko and Peto, 1988). It is possible that the uptake of extracellular iron supplements the labile iron pool in the infected erythrocyte before being utilized by the parasite. Furthermore, because it has been well characterized that the iron pool is easily chelatable by desferrioxamine, it is proposed that desferrioxamine inhibits parasite growth by chelating the iron from this intraerythrocytic iron pool (Raventos-Suarez *et al.*, 1982; Hershko and Peto, 1988). However, the introduction of a high molecular weight desferrioxamine-dextran derivative into the erythrocyte cytosol, does not inhibit parasite growth. Loyevsky *et al.* (1993b) reported a similar finding using a more lipophilic desferrioxamine derivative (N-methylanthranilate-desferrioxamine), which was encapsulated into uninfected erythrocytes. These erythrocytes were found to fully support parasite invasion and growth. Thus, showing that the non-haem iron in the erythrocytic cytosol is not necessary for parasite proliferation, and that the iron source is more likely to be present in the parasite compartment (Scott *et al.*, 1990).

3.1.1.5 Erythrocytic ferritin

The levels of non-haem iron in mature red blood cells are presumably too low to provide iron for all the needs of parasite metabolism. The iron storage protein, ferritin which is

found in most tissues, including red blood cells could be another source of iron for the parasite (see Chapter 1.4.2.4.2). Although the mature erythrocyte does not synthesize ferritin, it does contain measurable amounts of high-chain ferritin, which are remnants from the reticulocyte stage of development (Cazzola *et al.*, 1983; Pippard and Hoffbrand, 1989). It is possible that during endocytosis of the host cytosol, ferritin is also taken up into the parasite food vacuole, where at the acidic pH, the iron is reductively released from the spherical structure (Gabay and Ginsburg, 1993). A saturated ferritin molecule can accommodate over 4000 ferric ions (Klausner, 1988). However, Cazzola *et al.* (1983) reported that most of the erythrocytic ferritin is in an acidic isoform and has a relatively lower iron-binding capacity, thus resulting in less iron being supplied to the parasite. Ferritin, still remains a possible unexamined source of parasite iron.

3.1.2 IRON CHELATING AGENTS AND IRON UPTAKE

The inclusion of iron chelating agents into studies involving iron metabolism, enables researchers to distinguish between possible pathways involved in iron uptake (Morgan, 1983; Bridges and Cudkowicz, 1984; Qian and Morgan, 1991). Agents which possess the physical properties to permit access either to the membrane and cytosol are used to determine the primary site of iron release from transferrin to the cell. The most utilized agent is 2,2'-bipyridyl, a hydrophobic ferrous chelating agent (Morgan, 1983). The iron-free form of 2,2'-bipyridyl distributes into the apolar phase of the membrane and then blocks the iron uptake by chelating the iron during its transfer across the membrane into the cytosol (Figure 3.4).

Due to the ability of desferrioxamine to chelate extracellular as well as intracellular iron, it is widely used to contrast the effects of lipophilic iron chelating agents. In the classic model of diferric transferrin uptake (i.e. by receptor-mediated endocytosis), desferrioxamine has virtually no effect on iron uptake and a very limited effect on transferrin uptake (Baynes *et al.*, 1988). Nunez *et al.* (1983) reported that the inability of desferrioxamine to effectively block iron uptake is because the membrane site where iron becomes available for chelation, is inaccessible to desferrioxamine. Unlike other hydrophilic chelating agents,

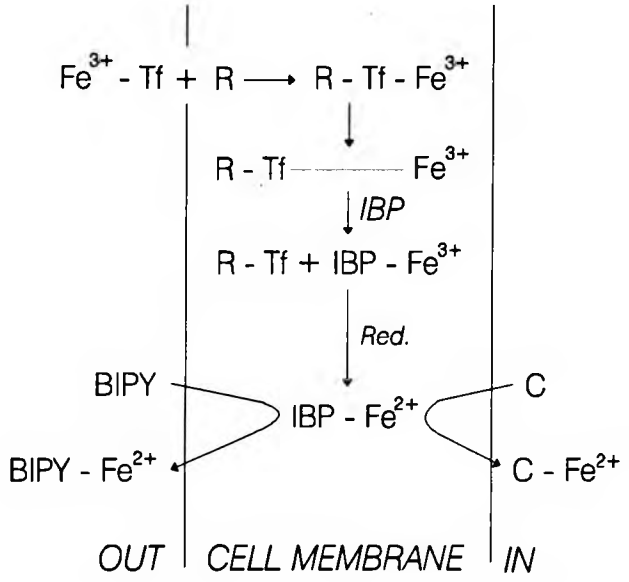


Figure 3.4: Possible mechanism by which 2,2'-bipyridyl (BIPY) inhibits the uptake of diferric transferrin. After the transferrin-Fe^{3+} complex (Tf-Fe^{3+}) binds to the transferrin receptor (R), a conformational change in transferrin results in a decreased affinity for iron. The free Fe^{3+} then binds to an iron-binding protein (IBP). The reduced Fe^{2+}, from the IBP-Fe^{2+} complex, is then transferred by a membrane carrier (C) into the cytosol. BIPY could inhibit iron uptake by chelating the IBP-bound ferrous ions (Nunez *et al.*, 1983).

desferrioxamine and desferrithiocin can enter the cell and chelate the intracellular pool of iron (Jin *et al.*, 1989). The decrease in intracellular iron induced by desferrioxamine results in an increase in biosynthesis of new transferrin receptors; whilst a decrease in extracellular iron enhances the release of previously internalized transferrin and synthesis of transferrin-receptors (see Chapter 1.4.2.4.3) (Bridges and Cudkowicz, 1984). The depletion of iron from proliferating cells results in the inhibition of metabolism and replication and eventually cell death (Lederman *et al.*, 1984).

The source and mechanism by which the intraerythrocytic parasite acquires iron has yet to be determined, however with the aid of iron chelating agents, the mechanism of uptake can possibly be verified.

3.2 AIMS

To determine the source of iron that is essential for the growth of the intraerythrocytic parasite; and if the source is extracellular, to identify the pathway(s) of iron uptake. To examine the effects of ferric and ferrous iron chelating agents on iron uptake.

3.3 EXPERIMENTAL DESIGN

Diferric transferrin was double labelled with ^{125}I and ^{59}Fe, as described in Chapter 2.2.1 and 2.2.2. The concentration and purity were tested via the immunodiffusion assay and urea polyacrylamide gel electrophoresis as detailed in Chapter 2.2.3 and 2.2.4, respectively. The uptake of diferric transferrin was subjected to varying conditions, i.e. stage, concentration and time. The uptake of non-transferrin bound iron, i.e. ferric citrate, was as described in Chapter 2.3.2 and the conditions of uptake were subject to change (stage, concentration, temperature and time). The single and combined effects of iron chelating agents, desferrioxamine and 2,2'-bipyridyl on the uptake of diferric transferrin and iron citrate, were also examined. Each experiment was duplicated with consistent results.

3.4 RESULTS

3.4.1 UPTAKE OF IRON

3.4.1.1 Uptake of diferric transferrin

The uptake of labelled diferric transferrin was monitored in ring- and trophozoite-infected and control erythrocytes to establish whether the malaria parasite utilized serum transferrin iron. At 37°C, there was a steady accumulation of iron in both the ring- and trophozoite-infected erythrocytes and this was associated with a similar rise in the molar ratio of iron to transferrin (Figures 3.5 and 3.6). After two hours of incubation, more iron had been accumulated by the trophozoites than the rings and more transferrin was associated with the trophozoites. In Figure 3.5, at time 0, the rings are very early into

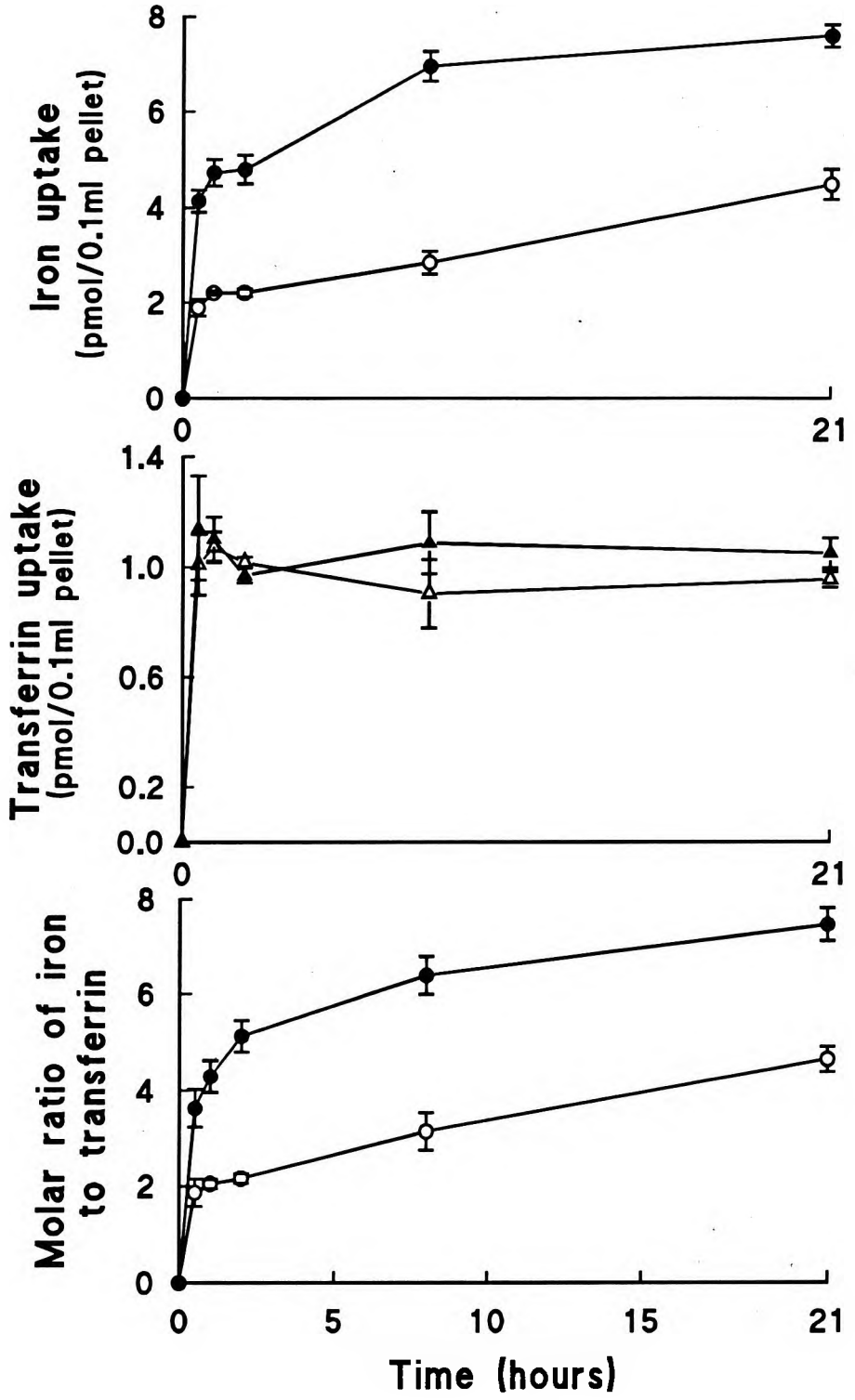


Figure 3.5: The time-dependant uptake of iron (top) and transferrin (middle) by ring-infected (11,51% parasitaemia: solid) and control (open) erythrocytes. The concentration of diferric transferrin added was 33,75 nM.

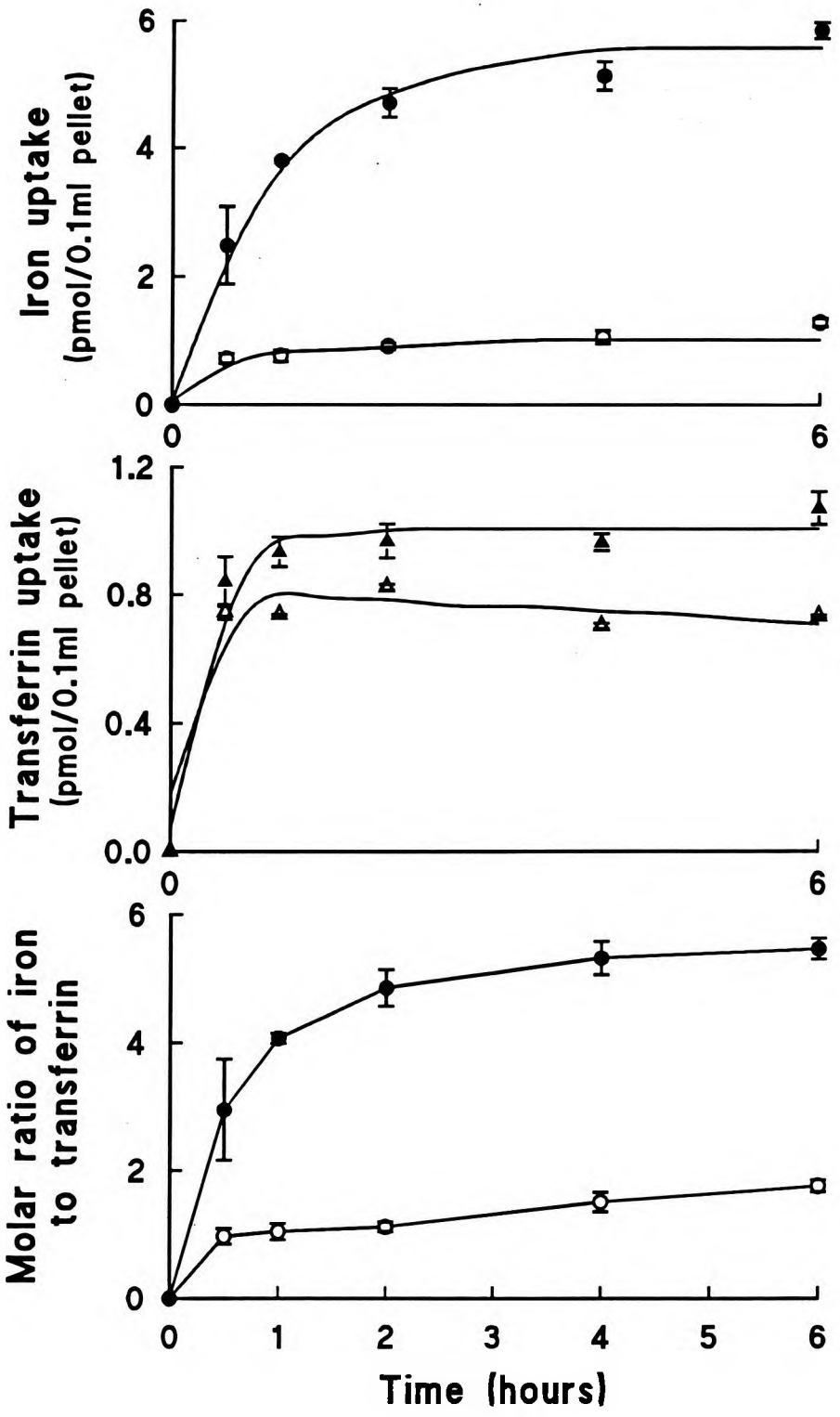


Figure 3.6: The time-dependant uptake of iron (top) and transferrin (middle) by trophozoite-infected (10,46% parasitaemia: solid) and control (open) erythrocytes. The concentration of diferric transferrin added was 33,75 nM.

their cycle and by the 21st hour, they had developed into early-mid trophozoites.

Diferric transferrin was taken up into the trophozoite-infected erythrocyte in an unsaturable concentration dependant manner (Figure 3.7). There was also a concentration dependant association of iron and transferrin with the control erythrocytes; which was possibly due to non-specific binding or association of the diferric transferrin to the erythrocytic membranes (Figure 3.7).

3.4.1.2 Uptake of ferric citrate

The possibility that parasitized erythrocytes accumulate non-transferrin bound iron, was investigated by using ferric citrate (Sturrock *et al.*, 1990). Iron uptake was found to be time dependant in the ring- and trophozoite-infected erythrocytes (Figure 3.8). Early trophozoite-infected erythrocytes accumulated approximately twice the amount of iron compared to rings. A concentration dependant uptake of non-transferrin bound iron was observed in the trophozoite-infected erythrocytes (Figure 3.7). The uptake of iron was found to be temperature dependant, with the pathway being sensitive to decreased temperature (4°C) after only 15 minutes of incubation (Figure 3.9). To determine which form of iron was preferentially accumulated by the parasites, trophozoite-infected erythrocytes were incubated in the presence of either diferric transferrin or ferric citrate at 37°C over a period of 6 hours.

It was observed that parasitized erythrocytes accumulated 4,27 $\pm$ 0,23 times more citrate-bound iron than transferrin-bound iron (Figure 3.10). In addition, it was noted that citrate-bound iron was associated with the control erythrocytes (Figures 3.7 to 3.10).

3.4.2 EFFECT OF IRON CHELATING AGENTS ON IRON UPTAKE

3.4.2.1 Diferric transferrin as the iron source

In studies evaluating the effect of desferrioxamine and 2,2'-bipyridyl on diferric transferrin uptake, it was found that the hydrophilic ferric chelating agent, desferrioxamine significantly inhibited iron uptake into the trophozoite-infected ($p < 0,005$) and control ($p <$

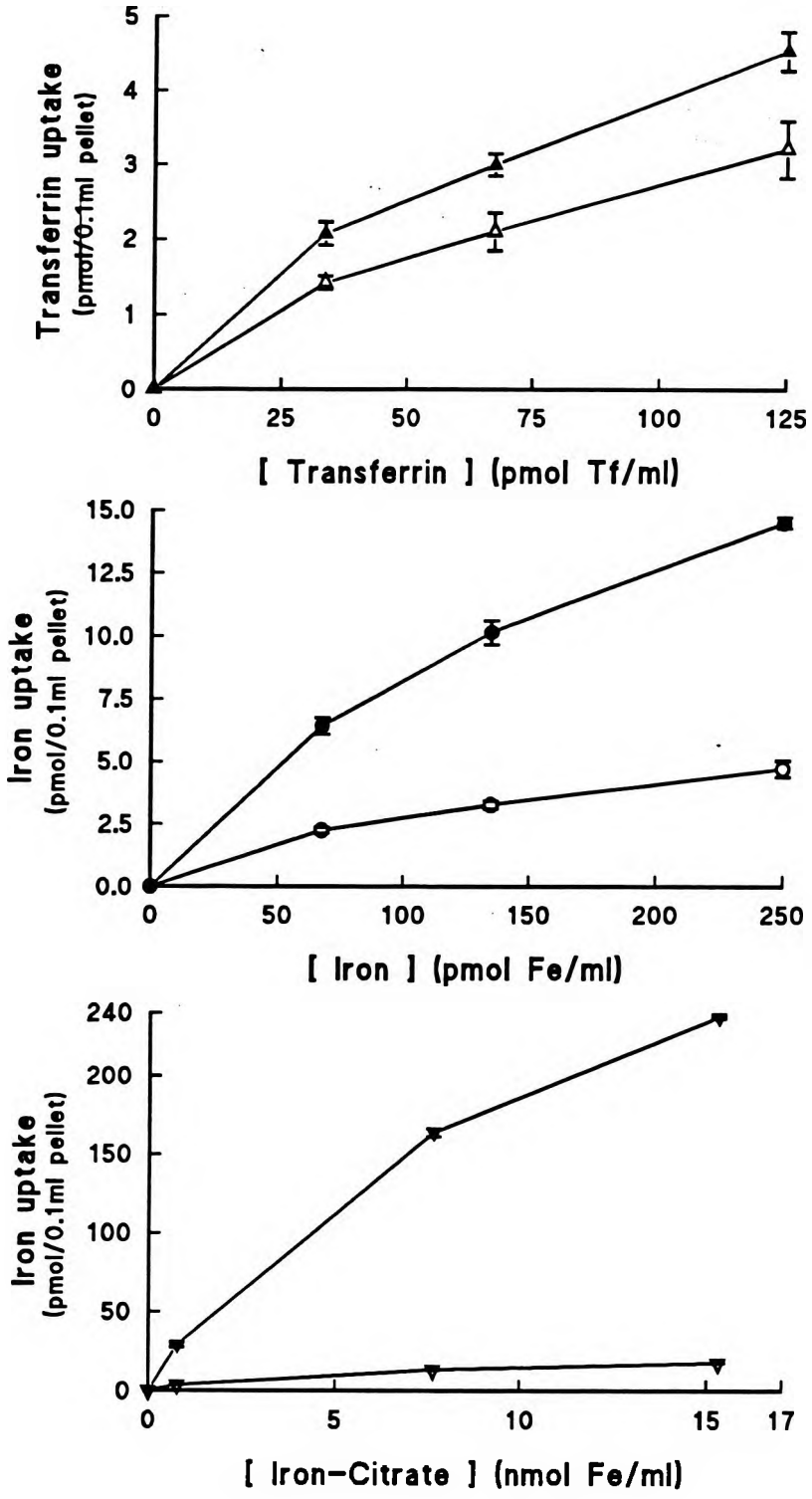


Figure 3.7: Concentration-dependant uptake of diferric transferrin (top, middle) and ferric citrate (bottom) after 4 hours by trophozoite-infected (11,83% parasitaemia: solid) and control (open) erythrocytes.

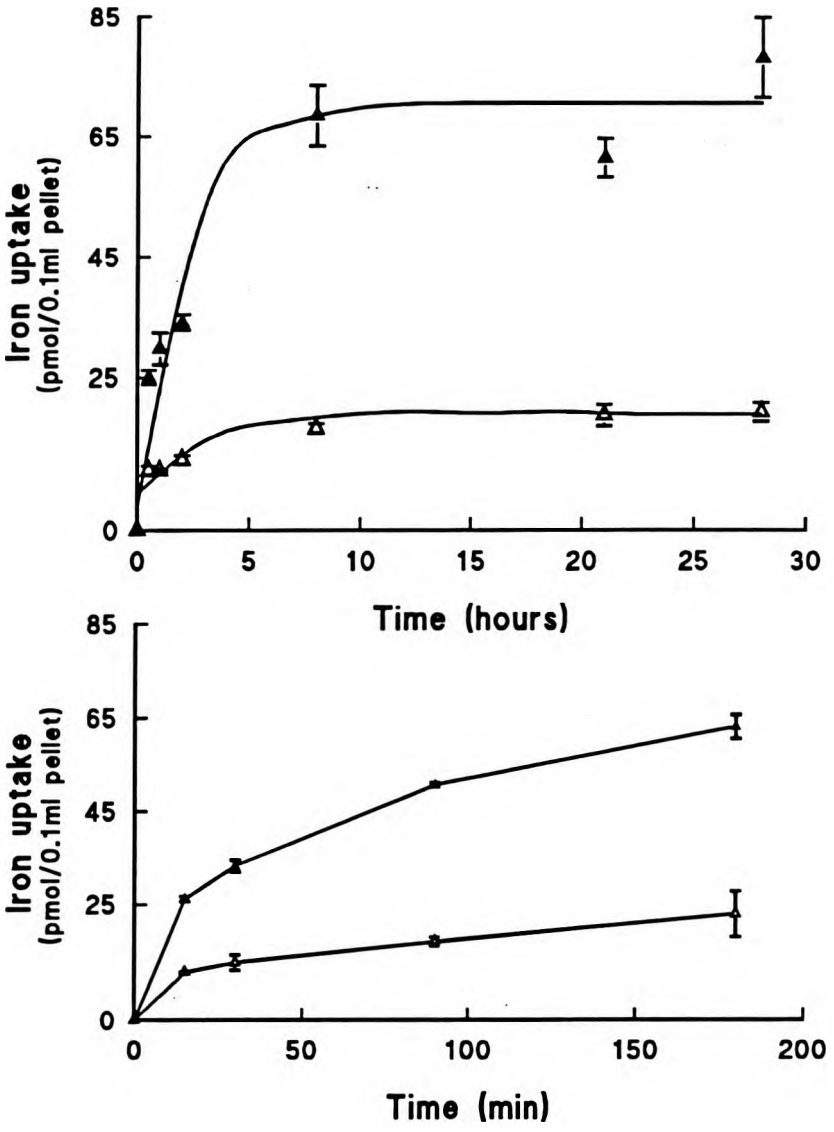


Figure 3.8: The time-dependant uptake of ferric citrate by the ring- (6,17% parasitaemia: ▲, top), trophozoite-infected (10,70% parasitaemia: ▲, bottom) and control (△) erythrocytes. The concentration of ferric iron added was 500,09 pM and 584,39 pM, respectively.

0,01) erythrocytes. While desferrioxamine did not significantly inhibit transferrin uptake into either the infected or control erythrocytes (Figure 3.11).

The lipophilic ferrous chelating agent, 2,2'-bipyridyl had a varying and unpredictable effect on transferrin uptake in the trophozoite-infected erythrocytes and no significant

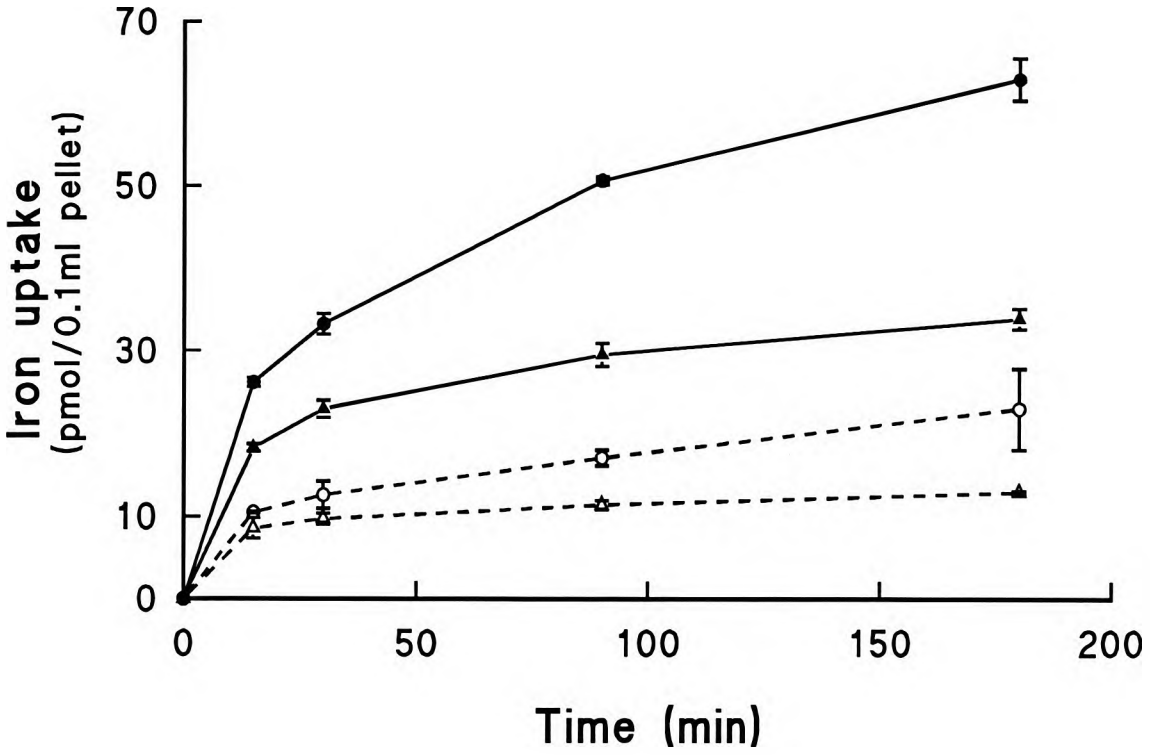


Figure 3.9: The temperature dependant uptake of ferric citrate by trophozoite-infected (10,70% parasitaemia: solid line) and control (dashed line) erythrocytes at 4°C (▲;△) and 37°C (●;○). The concentration of ferric iron added was 500,09 pM.

effect in the control erythrocytes. 2,2'-Bipyridyl significantly ($p < 0,02$) inhibited iron uptake into the trophozoite-infected erythrocytes, but no significant effect was observed in the control erythrocytes (Figure 3.12).

3.4.2.2 Combined effect of desferrioxamine and 2,2'-bipyridyl on diferric transferrin uptake

The combination of desferrioxamine and 2,2'-bipyridyl significantly ($p < 0,05$) affected iron uptake, but did not significantly affect transferrin uptake in the trophozoite- and control erythrocytes (Table 3.1). However, the combined effect of desferrioxamine and 2,2'-bipyridyl mimicked the inhibitory effect of the desferrioxamine concentration alone. A similar trend was observed with the addition of 50 μM of either chelating agent.

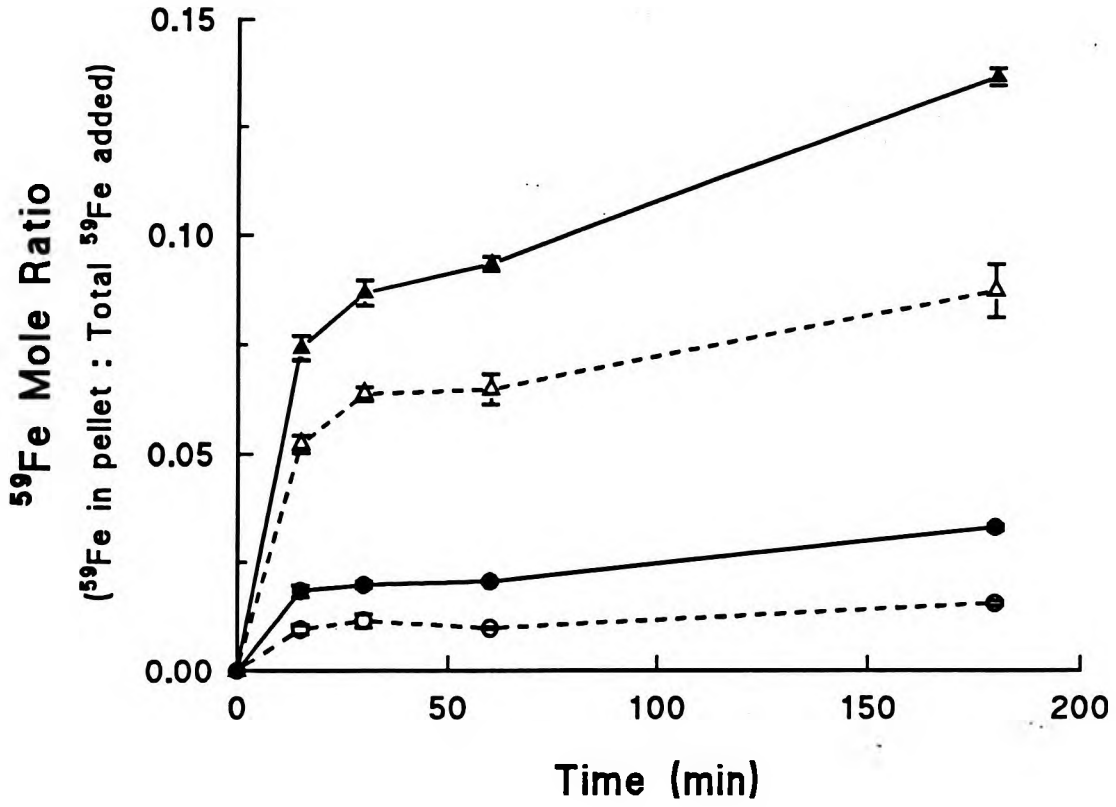


Figure 3.10: The time dependant uptake of diferric transferrin (●; ○) and ferric citrate (▲; △) by trophozoite-infected (8,48% parasitaemia: solid line and symbol) and control (dashed line and open symbol) erythrocytes at 37°C. The concentrations of transferrin- and citrate-bound ferric iron were 67,50 pM and 584,39 nM, respectively. The y-axis units are expressed as a ^{59}Fe mole ratio which was calculated from the ratio of pmol iron in the 0,1 ml pellet to total pmol of iron added.

3.4.2.3 Ferric citrate as the iron source

Both desferrioxamine and 2,2'-bipyridyl significantly ($p < 0,05$) inhibited non-transferrin bound iron uptake at concentrations similar to or greater than their respective IC_{50} values (Figure 3.13). Preincubation with 2,2'-bipyridyl did not completely block iron uptake, whilst desferrioxamine chelated 99% of the non-transferrin bound iron.

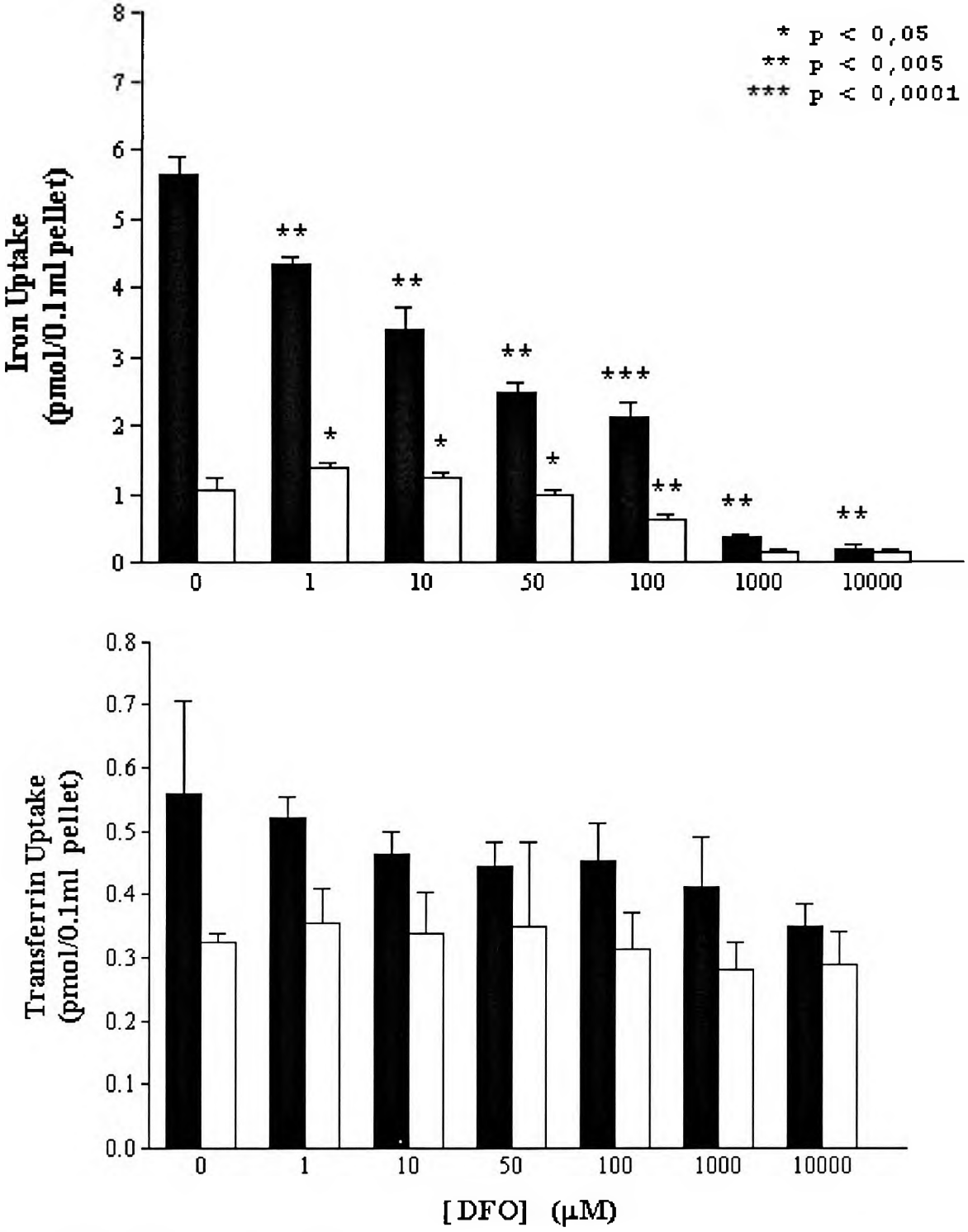


Figure 3.11: The dose dependant effect of desferrioxamine (DFO) on iron (top) and transferrin (bottom) uptake by trophozoite-infected (6,57% parasitaemia: solid) and control (open) erythrocytes at 37°C. The concentration of diferric transferrin added was 33,75 nM. Statistical differences were calculated between the untreated (0 μM) and treated samples.

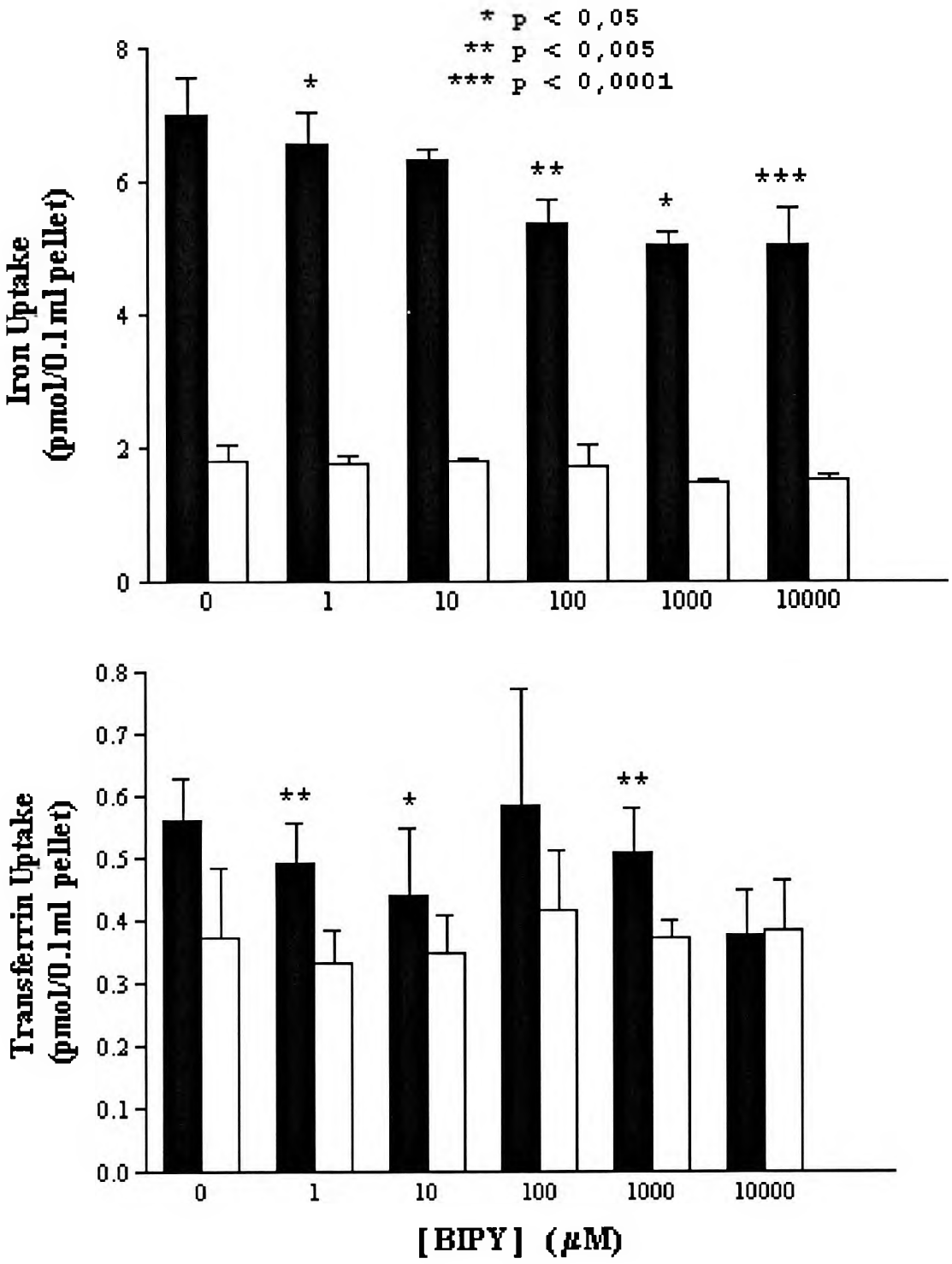


Figure 3.12: The dose dependant effect of 2,2'-bipyridyl (BIPY) on iron (top) and transferrin (bottom) uptake by trophozoite-infected (11,71% parasitaemia: solid) and control (open) erythrocytes at 37°C. The diferric transferrin concentration added was 33,75 nM. Statistical differences were calculated between the untreated (0 μM) and treated samples.

Table 3.1: The combined effect of desferrioxamine (DFO; 5 mM) and 2,2'-bipyridyl (BIPY; 5 mM) on the uptake of diferric transferrin by parasitized (8,97% parasitaemia) and control erythrocytes. The concentration of transferrin and ferric iron added was 33,75 nM and 67,50 nM, respectively. *: $p < 0,05$ and **: $p < 0,005$.

Iron chelating agents	^{125}I-Transferrin uptake (pmol/ 0,1 ml pellet)	^{59}Iron uptake (pmol/0,1 ml pellet)
PARASITIZED ERYTHROCYTES		
Control	0,54 ± 0,04	5,22 ± 0,22
DFO	0,42 ± 0.02*	0.20 ± 0,01**
BIPY	0,57 ± 0,12	3,71 ± 0,26**
DFO + BIPY	0,33 ± 0,07	0.21 ± 0,05**
CONTROL ERYTHROCYTES		
Control	0,46 ± 0,06	2,62 ± 0,27
DFO	0,37 ± 0,02	0,20 ± 0,01**
BIPY	0,53 ± 0,10	2,01 ± 0,11*
DFO + BIPY	0,42 ± 0,08	0,24 ± 0,13*

3.5 DISCUSSION

Conflicting opinions exist as to whether or not iron supplementation enhances host susceptibility to pathogenic microorganisms, or whether iron deficiency exerts a protective effect. Some reports suggest that iron supplementation does not exacerbate infections, such as malaria and it is beneficial to children and anaemic patients in malaria endemic areas (Cardoso *et al.*, 1996). However, the general consensus is that persons who have episodes of hyperferraemia or hypotransferrinaemia are more susceptible to bacteria, fungal or protozoal pathogens at those times than during periods when their iron saturation of

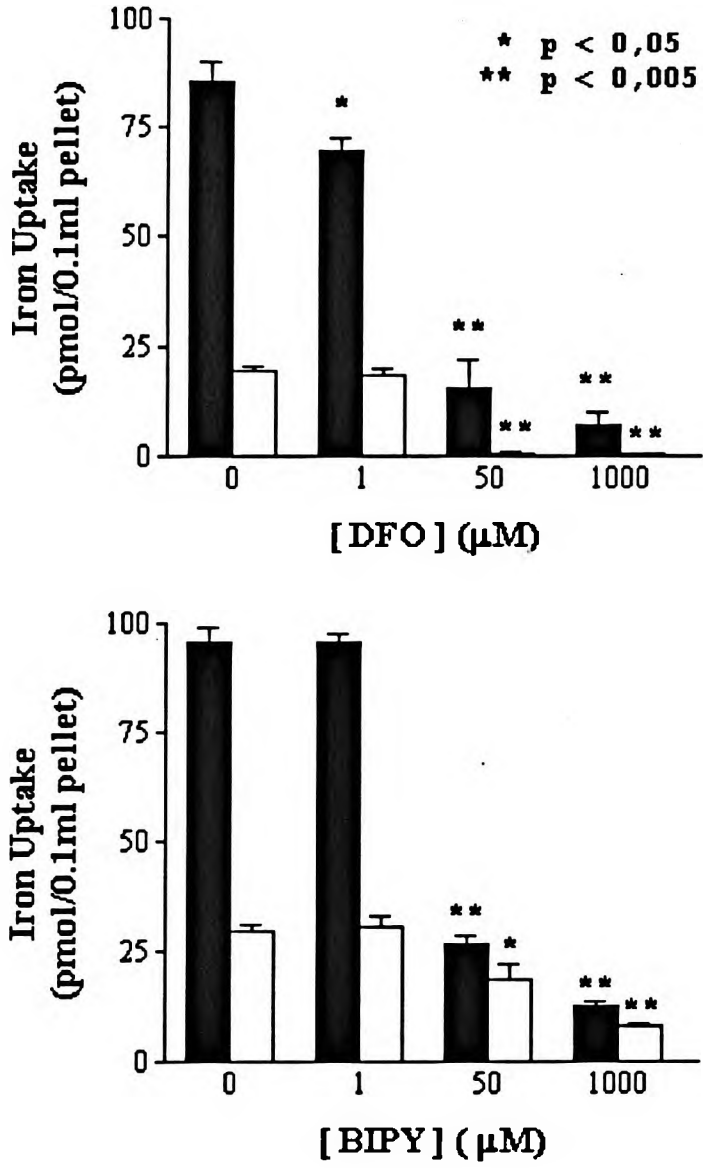


Figure 3.13: The effect of desferrioxamine (DFO; top) and 2,2'-bipyridyl (BIPY; bottom) on the uptake of ferric citrate into trophozoite-infected (solid) and control (open) erythrocytes. The parasitaemias used in these respective experiments were 7,73% and 5,96%. The concentration of ferric iron added was 784,88 nM.

transferrin is within normal limits (Weinberg, 1975; Oppenheimer, 1989). The latter suggests that the most likely source of iron for the intraerythrocytic parasite is found extracellularly. Thus, it seemed plausible to investigate whether the parasitized erythrocyte

acquires diferric transferrin or non-transferrin bound iron by similar pathways as exhibited in reticulocytes and other cell lines (Morgan, 1983; Nunez *et al.*, 1983; Qian and Morgan, 1991).

3.5.1 PLASMA DIFERRIC TRANSFERRIN

Extracellular iron, presented as iron saturated transferrin, was taken up by intraerythrocytic *P. falciparum* parasites, irrespective of the stage of development. Similar amounts of transferrin were associated with the ring-infected erythrocytes and controls, while a significantly greater amount of iron was incorporated into the ring-infected erythrocytes than in the controls (Figure 3.5). In contrast, there was a significant difference in the amount of transferrin and iron associated with the trophozoite-infected erythrocytes than the controls (Figure 3.6). This signifies that the parasite mainly incorporates its iron at the early-mid trophozoite stage, in preparation for the biosynthesis of iron-dependant enzymes.

According to Pollack (1989), the iron is incorporated into an insoluble pellet and into soluble components with molecular weights of about 1, 40 and 60 kilodaltons, with the 40 and 60 kilodalton components being parasite-derived iron products and the one kilodalton protein being the remnants of the degraded transferrin. The fact that the transferrin-molecule is degraded, suggests that the iron is not acquired by transferrin-receptor-mediated endocytosis, since transferrin is recycled and not degraded during such an endocytotic process. In addition, the concentration dependant experiments done in this study (Figure 3.7), and by Pollack and Schnelle (1989), showed that the pathway of uptake was not saturable or specific for transferrin. This argues against the existence of transferrin-receptors and indicates that another pathway is involved in iron uptake.

The parasite could have endocytosed the diferric transferrin from the host plasma, thereby acquiring its supply of iron and possibly other amino acids from the degraded plasma proteins (Figures 3.5 and 3.6). A similar endocytotic mechanism is described for the uptake of ferritin from the extracellular milieu (Burns and Pollack, 1988).

Alternatively, the uptake of diferric transferrin into the trophozoite-infected erythrocyte could be better explained if it was acquired by the parasitophorous duct, since the uptake of both iron and transferrin could be facilitated by this pathway (Figures 3.6 and 3.7). This pathway could allow the diferric transferrin to passively diffuse into the parasitophorous space, from where it could be endocytosed through the parasite plasma membrane into the parasite (Pouvelle *et al.*, 1991). The development of the parasitophorous duct is proposed to be at the early trophozoite stage (20-25 hours post-invasion), which eliminates the possibility that early ring-infected erythrocytes (0-8 hours post-invasion) accumulate iron and transferrin via this pathway (Figure 3.5). This tends to suggest that diferric transferrin is taken up into the early ring and trophozoite stages by two different pathways. The release of iron from the transferrin molecule at the erythrocyte membrane via the redox process (Figure 3.3), could possible account for the internalization of iron and exclusion of transferrin from the ring-infected erythrocytes (Figure 3.5). This mechanism of iron uptake is described for other cell lines, including the HeLa carcinoma cells and hepatocytes (Low *et al.*, 1987; Thorstensen and Romslo, 1988; Toole-Simms *et al.*, 1990). In the trophozoite-infected erythrocytes, both transferrin and iron are internalized into the parasite (Figures 3.6 and 3.7), which indicates that the diferric transferrin is taken up either by an endocytotic pathway or through the parasitophorous duct.

3.5.2 UPTAKE OF NON-TRANSFERRIN BOUND IRON

The malaria trophozoite-infected erythrocytes preferentially accumulated up to four times more non-transferrin bound iron than diferric transferrin (Figure 3.10). Peto and Thompson (1986), demonstrated that transferrin-bound iron is unimportant for parasite growth. The pathway for non-transferrin bound iron accumulation was determined to be concentration-, temperature- and time-dependant (Figures 3.7 and 3.9). The greater uptake of iron into the trophozoite stage, again demonstrates that it is at this stage that the parasite increases the uptake rate of iron in preparation for increased metabolism and DNA synthesis.

The fact that the accumulation of iron was temperature-dependant and a saturable process, suggests that it is the result of an active process, rather than an receptor-mediated endocytotic process which can be inhibited by low temperatures (Sanchez-Lopez and Haldar, 1992). The characteristics of the uptake pathway probably describes a facilitated diffusion system, mediated by a carrier. This system could be located in the erythrocyte membrane or parasite plasma membrane to facilitate iron uptake directly from the plasma or parasitophorous space (Figure 3.1). This pathway could be a remnant from the precursor erythroid stage, as Qian and Morgan (1991) have characterized a similar non-transferrin bound iron uptake process in the reticulocyte plasma membrane. The presence of a membrane carrier is further substantiated by the inability of citrate to permeate through the erythrocytic parasite. This is due to the molecular exclusion limit of the membrane, which prevents the citrate anion from permeating through the plasma bilayer (Elford *et al.*, 1995). Thus, in this study, citrate not only served to keep the ions in a soluble ferric state, but also to transport the ions to the erythrocyte membrane, where a particular mechanism facilitated the transport of the iron across the membranes into the parasite. Another mechanism besides the carrier-mediated pathway could be via the anion-selective channels located in the erythrocyte membrane (Haldar, 1994).

An unexpected observation was that the mature erythrocytes incorporated iron at 37°C and 4°C (Figure 3.9), since erythrocytes are reported to cease iron uptake upon maturation. The uptake at 37°C could be explained by the presence of an active, carrier mediated process, that is temperature dependent. This process could be a remnant of the precursor erythroid stage; as a similar process has been characterized to explain the uptake of non-transferrin-bound iron into reticulocytes (Morgan, 1988). The iron uptake at 4°C could be due to a passive diffusion system, which is not affected by temperature fluxes (Sanchez-Lopez and Haldar, 1992). Alternatively, it could be due to the tendency of iron ions to non-specifically adhere to plastic and cellular surfaces (Breuer *et al.*, 1995).

3.5.3 EFFECT OF 2,2'-BIPYRIDYL ON IRON UPTAKE

The mechanism by which 2,2'-bipyridyl inhibits iron uptake is routinely used to determine

whether a cell line incorporates iron via the transferrin receptor-mediated endocytotic pathway. 2,2'-Bipyridyl functions by chelating the reduced transferrin iron once the iron has bound to the membrane iron-binding protein (Figure 3.4) (Nunez *et al.*, 1993). This inhibitory action of 2,2'-bipyridyl normally completely blocks iron internalization, with little effect on transferrin uptake (Baynes *et al.*, 1988; Bridges and Cudkowicz, 1984). But, 2,2'-bipyridyl had no inhibitory effect on the uptake of either iron or transferrin (Figure 3.12), which suggests that the parasitized erythrocyte does not acquire iron by receptor-mediated endocytosis.

In contrast, 2,2'-bipyridyl had a profound effect on the uptake of non-transferrin bound iron (Figure 3.13; bottom). Uptake of non-transferrin bound iron has been characterized in many cell lines and a similar inhibitory effect is observed with the addition of ferrous ion chelating agents (Crane *et al.*, 1985). Therefore, in the presence of a transplasma membrane redox system in the erythrocyte membrane, the ferric ions could be reduced to the ferrous state, enabling 2,2'-bipyridyl to chelate the iron before it is transferred to a membrane carrier, thereby inhibiting its internalization and utilization by the parasite.

A transmembrane redox system is proposed to be the main mechanism by which *Saccharomyces cerevisiae* and the brush border epithelial cells, accumulate iron (Anderson *et al.*, 1995). Ferric reductase, a membrane-associated enzyme, is proposed to reduce the ferric ions to the ferrous state, which are then transported across the membrane via specific iron carriers.

The presence of such an enzyme on the membrane of the parasitized erythrocytes could explain the inhibitory effects of 2,2'-bipyridyl. Such that once the iron has been reduced to the ferrous state by the enzyme, 2,2'-bipyridyl which partitions itself into the erythrocytic and/or parasitic membranes could chelate the ferrous iron with a high affinity ($K_a = 10^{18}\ M^{-1}$). Once the hydrophilic 2,2'-bipyridyl-iron complex is formed, it moves from the lipid membrane to the hydrophilic extracellular medium. This movement allows for uncomplexed 2,2'-bipyridyl molecules to position themselves into the membranes, i.e. a concentration gradient is established. Thus, with a high enough concentration of 2,2'-bipyridyl, the uptake and accumulation of iron into the parasite can be rapidly and

effectively inhibited.

3.5.4 EFFECT OF DESFERRIOXAMINE ON IRON UPTAKE

In the *Plasmodium*-infected erythrocytes, desferrioxamine significantly inhibited iron uptake in a dose-dependant manner (Figure 3.11; top), whilst having a limited effect on transferrin uptake (Figure 3.11; top). This chelation of iron by desferrioxamine is in complete contrast to the effect observed in reticulocytes and other cell lines (Nunez *et al.*, 1983; Baynes *et al.*, 1988). These results suggest that the parasite acquires its iron by another pathway other than receptor-mediated endocytosis. One possibility being non-specific binding of transferrin to the erythrocyte membrane. It should be noted that non-specifically bound transferrin may still be functional and donate its iron to the cell (Cole and Glass, 1983). Thus, non-specifically-bound transferrin could still be of functional importance to the parasite.

The inhibitory effect of desferrioxamine on iron uptake possibly follows the pathway by which both desferrioxamine and diferric transferrin accumulate. Desferrioxamine may enter the parasite directly through the parasitophorous duct, thus bypassing the host cytoplasm (Pouvelle *et al.*, 1991 and Loyevsky *et al.*, 1993b). Once in the parasitophorous space, desferrioxamine probably diffuses through the parasite plasma membrane and parasite cytoplasm to the food vacuole along a concentration gradient, or by virtue of its weak base properties. Similarly, Pouvelle *et al.* (1991) proposed that the parasitophorous duct facilitates the uptake of serum transferrin into the parasite. Desferrioxamine did not seem to competitively inhibit diferric transferrin uptake by this pathway, since the uptake of transferrin was not significantly affected (Figure 3.11; bottom). Thus, the inhibitory action of desferrioxamine must be directed at another uptake pathway.

When non-transferrin-bound iron, in the form of ferric citrate, was presented to the parasitized erythrocyte, desferrioxamine inhibited its uptake in a dose-dependant manner (Figure 3.13; top). This inhibitory effect occurred regardless of whether desferrioxamine or the iron source was added 4 hours before the other. This indicates a dual mechanism

by which desferrioxamine could have acted. Firstly, the extracellular desferrioxamine could have chelated the citrate-bound iron, as citrate is an effective mediator in transferring iron to desferrioxamine (Bates *et al.*, 1967; Pollack *et al.*, 1976); and secondly, the desferrioxamine that penetrated into the parasitized erythrocytes, could have avidly chelated the intracellular iron. Thus, the potent antimalarial action of desferrioxamine in various *P. falciparum* strains (Table 5.1), can be partly explained by its effective inhibitory action of iron uptake and its ability to chelate iron from the parasite's intracellular transit iron pool.

In conclusion, the various experimental conditions used to establish the pathway of iron uptake, seem to indicate that *Plasmodium*-infected erythrocytes preferentially accumulated non-transferrin bound iron over transferrin-bound iron. In addition, diferric transferrin is probably not incorporated by receptor-mediated-endocytosis, but rather by a non-specific pathway, such as pinocytosis, the parasitophorous duct or a parasite-induced transporter. Alternatively, if transferrin binds non-specifically to the erythrocyte membrane, the iron along with non-transferrin bound iron could be transported into the parasitized erythrocyte by a transplasma membrane redox system. The uptake and incorporation of iron into the parasites food vacuole via endocytosis, raises questions as to whether this iron could become associated with the malaria pigment, since it has been characterized that haem can be exchanged between adjacent haemoglobin molecules (Bunn and Jandl, 1968).

CHAPTER FOUR

INVESTIGATION OF PARASITE HAEMOZOIN

4.1 INTRODUCTION

The deposition of a blackish-brown pigment in the patients tissue has long been identified as being one of the most conspicuous and unique features of a severe malaria infection (Sherman *et al.*, 1968). It has never been questioned that the pigment is a by-product of haemoglobin (Theakston *et al.*, 1970), however its structural composition and formation process is subject to debate.

4.1.1 DEGRADATION OF HAEMOGLOBIN

Rapid propagation of the parasite results in an increased demand for nutrients such as carbohydrates, phospholipids and protein. However, the parasite has a limited capacity for *de novo* synthesis or exogenous uptake of amino acids. These requirements are met in part by avidly ingesting and degrading the host haemoglobin in a specialized proteolytic food vacuole.

The host erythrocyte contains 18-20 mM of haemoglobin monomers, each of which is composed of 143 amino acid residues. It is estimated that approximately 25% of the haemoglobin in an infected erythrocyte can be degraded by a *P. falciparum* parasite during its life cycle (Roth *et al.*, 1986). Haemoglobin is ingested predominantly by the trophozoite stage, via the cytostome, a mouth-like structure that engulfs the erythrocyte cytosol into the parasite by pinocytosis. The vesicles containing the haemoglobin then fuse with a specialized proteolytic vacuole called the food or digestive vacuole.

In the food vacuole, catabolism appears to be an ordered process with the haemoglobin being split into its globin and haem components by haemoglobinases, which include both aspartic and cysteine proteinases (Rosenthal, 1995). Further proteolysis of globin involves a concerted action of parasitic serine, metallo-proteases and peptidases (Figure 4.1). The degradation process occurs optimally at a pH of 5,0 to 5,5 and the resulting amino acids are then diverted from the vacuole and principally used in protein synthesis (Goldberg *et al.*, 1990).

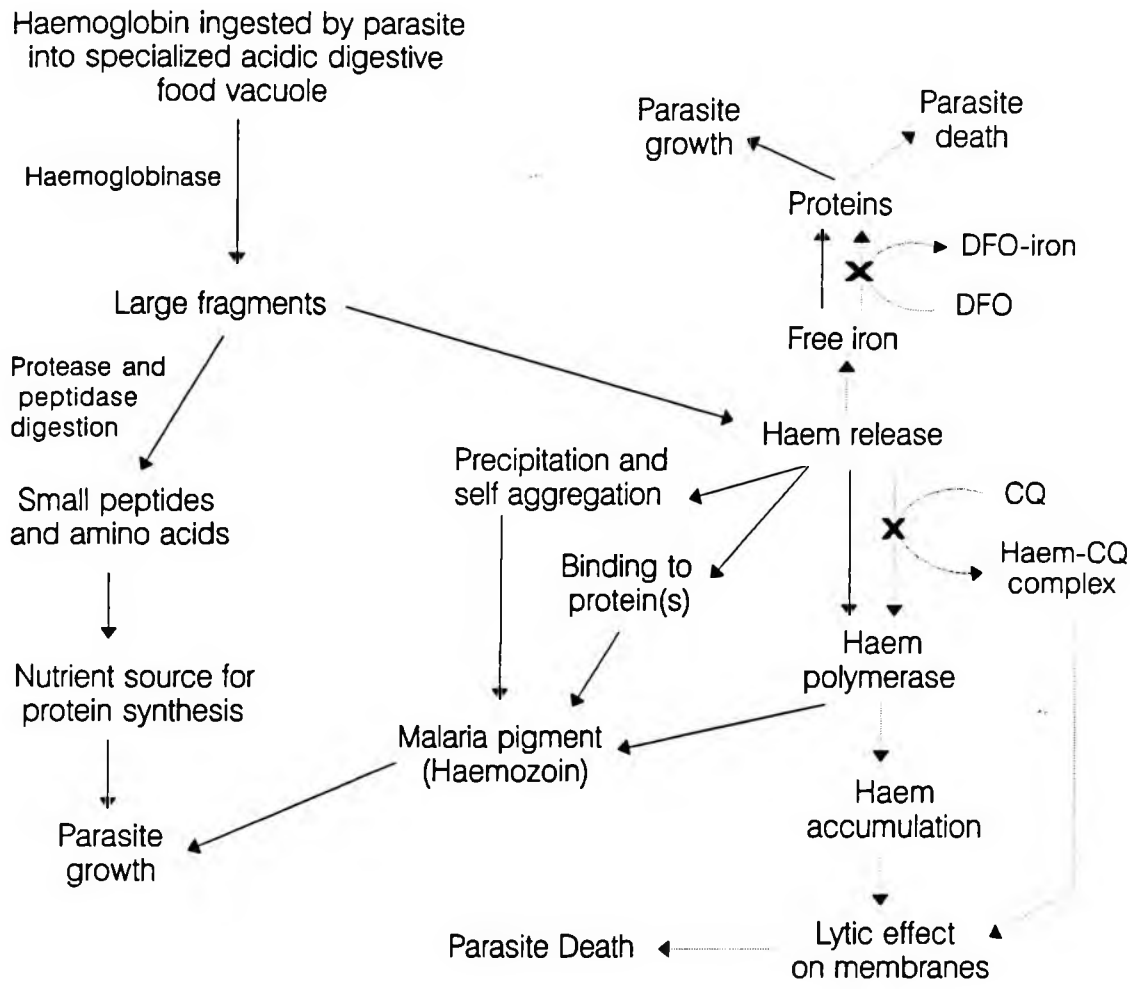


Figure 4.1: Pathway of haemoglobin degradation and haemozoin formation, with possible mechanisms by which chloroquine (CQ) and iron chelating agents, such as desferrioxamine (DFO) could inhibit parasite growth.

Under normal conditions, the haem ring that is released from degraded haemoglobin is split open by haem oxygenase and thereby excreted in the form of bilirubin (Figure 1.4). However, the latter enzyme has not been found in *P. falciparum* malaria, although it has been described in chloroquine-resistant *P. berghei* (Pandey and Tekwani, 1996). The haem moiety is not incorporated into any functional haem-containing proteins, such as cytochromes. Instead, it has been demonstrated that the parasite is capable of *de novo* biosynthesis of haem; since it contains a functional δ-amino-levulinate synthase gene

homologue (Surolia and Padmanaban, 1992; Wilson *et al.*, 1996). But the degree to which the parasite relies on this *de novo* biosynthetic pathway for its haem-containing molecules, is yet unknown.

Thus, when the ferrous haem is released from the globin, it undergoes oxidation into a toxic ferric form, i.e. haem or otherwise known as haemin or ferriprotoporphyrin IX. This molecule promotes membrane damage via lipid peroxidation and inhibits a variety of enzymes, including proteases. The parasite does not excrete haem nor does it possess the enzymatic activity (i.e. the haem oxygenase enzyme) to open the porphyrin ring and thereby form less toxic bile pigments (Eckman *et al.*, 1977). Instead, the parasite has developed an unique biochemical process to detoxify the haem by sequestering these molecules into an insoluble, inert crystalline material called malaria pigment or haemozoin.

Slater and Cerami (1992) suggested that the polymerization of haem to form the β-haematin component of haemozoin is catalysed by a novel haem polymerase enzyme. Specific malaria components such as phospholipids (Bendrat *et al.*, 1995) and histidine-rich proteins II (Sullivan *et al.*, 1996), have also been proposed to be involved in the haem polymerization process, and may be instrumental in initiating the oligomerization of the haem molecules. However, it has recently been reported that the "haem polymerase" activity observed in the parasite lysate may be due to an autocatalytic chemical process and not due to enzyme catalysis. This chemical reaction has also been described for the spontaneous *in vitro* formation of the β-haematin polymer from haem in a protein-free acidic solution (Egan *et al.*, 1994) and may induce the spontaneous aggregation of dimeric haem at a pH of 12 (Yamada and Sherman, 1979).

The composition of haemozoin has yet to be established as controversy exists as to whether the residual haem is stored in a protein-sequestered form or not.

4.1.2 PROTEIN COMPONENT OF HAEMOZOIN

Brown (1911) first proposed that the haemozoin structure is identical to crystalline

haematin (i.e. ferric haem with a hydroxide axial ligand). However, Deegan and Maegraith (1956) noted that the solubilities of these two compounds are different, thus it was proposed that haem is non-covalently bound to a protein. This protein possibly has a high affinity for haem and is either denatured or partially degraded globin (Sherman *et al.*, 1968), or a parasite-derived polypeptide with a molecular weight of about 14 to 21 kilodaltons (Yamada and Sherman, 1979; Ashong *et al.*, 1989). In addition to protein being associated with the haem molecules, Goldie *et al.* (1990) detected carbohydrate and trace amounts of lipids and nucleic acids associated with the haem molecules.

4.1.3 HAEM MOIETY OF HAEMOZOIN

Several researchers maintain that haemozoin consists only of haem (Homewood *et al.*, 1975; Fitch and Kanjananggulon, 1987; Slater *et al.*, 1991). Homewood *et al.* (1975) suggest that the haemozoin preparations are heavily contaminated with membranes and parasite cytosol, and due to the tendency of haemozoin to bind specifically to the hydrophilic sites of protein, the analysis of such preparations has lead to erroneous results. After obtaining protein-free haemozoin it was found that neither the crystalline structure nor solubility of the pigment changed in any way. Elemental analysis of the pure haemozoin, indicates that it is nearly indistinguishable from haem. The haem groups are hypothesized to be rearranged in a specific pattern which decreases their solubilities. Slater *et al.* (1991) proposed that the crystal is composed of a polymer of haem units linked between the central ferric ion of one haem unit and a carboxylate side group oxygen of another (Figure 4.2).

The exact number of haem units in each polymer is not known, but it has been calculated that approximately 15 to 18 iron porphyrin molecules are associated with each haemozoin crystal; and that each crystal contains approximately 1% ferric iron which is accounted for in terms of haem (Ashong *et al.*, 1989; Homewood *et al.*, 1975). High-resolution electron microscopy shows that within the crystalline structure, electron-dense iron atoms are rearranged to form a regular lattice with one nanometre spacing (Moore and Boothroyd, 1974).

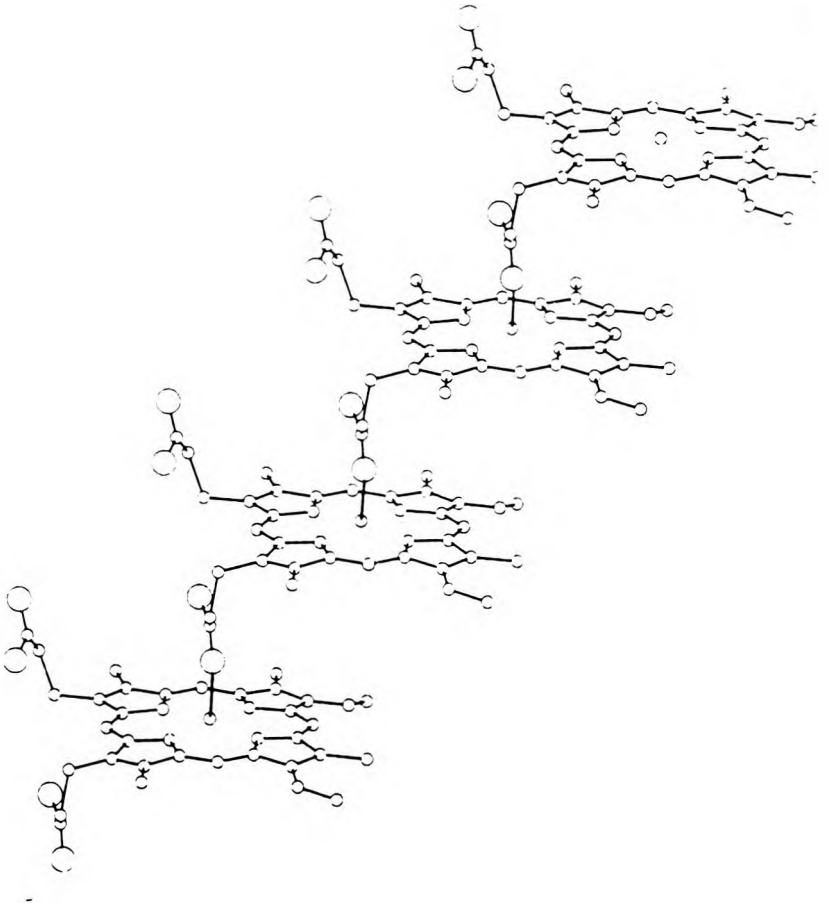


Figure 4.2: The structure of haemozoin as proposed by Slater *et al.* (1991).

By using non-invasive techniques, Bremard *et al.* (1993) eliminated any possible inference from the accompanying membrane and proteinaceous material and reported the haem iron to be paramagnetic, ferric in nature, in a high-spin state and engaged in square pyramidal coordination. Yayon *et al.* (1984a) substantiated these results using Mossbäuer spectroscopy. The findings suggest that haemozoin is in fact not a β-haematin polymer with μ-oxo bridges (Fitch and Kanjananggulpan, 1987), but rather a pure hydroxo-monomeric compound (Bremard *et al.*, 1993) (Figure 4.3). The absence of a μ-oxo haem dimer in haemozoin is confirmed by the inability to detect its characteristic visible band using spectral analysis (Hempelmann and Marques, 1994). Thus, polymerization of the

hydroxo-monomeric haem molecules is prevented by it being associated with biological residues, possibly proteins with high affinity for haem. This implies that the isolated polymeric structure is possibly an artefact which developed during the removal of the associated proteins (Bremard *et al.*, 1993). The polymer could have spontaneously formed from the monomer as previously described (Egan *et al.*, 1994 and Dorn *et al.*, 1995).

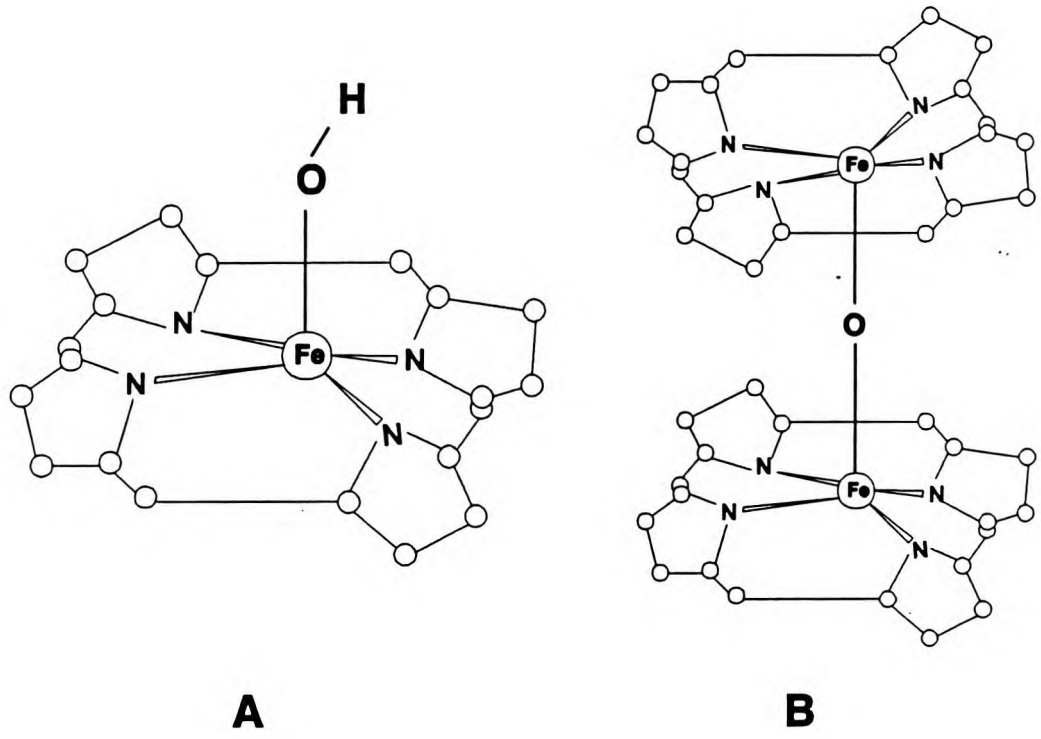


Figure 4.3: Molecular structure of the iron (III) ferriprotoporphyrin-IX complexes: (A) monomeric hydroxo complex and (B) dimeric μ-oxo complex. Adapted from Bremard *et al.* (1993).

It seems as if we have come full circle, back to the initial proposal of haemozoin being composed of both haem and protein. Thus, the question as to whether haemozoin is composed of protein or not, is still unanswered.

4.1.4 HAEM AS A HAEMOLYTIC AGENT

Under normal physiological conditions, the bond between haem and globin is very stable. However in aged or pathological (i.e. malaria infected) cells, some haemoglobin is oxidized and denatured. The released haem molecules are extremely hazardous when detached from their natural anchor, the globin moiety. The major biochemical hazard posed by haem and its chloride form, haemin is the potential for oxidation of cellular constituents. Such harmful effects include oxidation of proteins, peroxidation of phospholipids, destabilization of the membrane cytoskeleton, enzyme inhibition and cation leakage. All of which have been proposed to be the cause of haemin induced haemolysis of mouse and human erythrocytes (Chou and Fitch, 1980) and malaria infected erythrocytes (Orjih *et al.*, 1981).

4.1.4.1 Oxidation and peroxidation

Haemin can induce haemolysis by oxidizing the sulfhydral groups of the red blood cell membrane proteins (Sullivan *et al.*, 1992). Alternatively, haemin could modify the membrane phospholipids by lipid peroxidation, and thereby generate lipid radicals and reactive byproducts, such as malondialdehyde (Chiu and Lubin, 1989). Haemin is well suited to catalyse the peroxidative process, since the hydrophobic haemin molecules readily partition into the lipid bilayer and its iron content could promote the formation of hydroxyl radicals. The peroxidation of biological membranes results in a decline in the unsaturated to saturated fatty acid ratio. This leads to increased membrane rigidity, increased permeability to various ions and finally membrane rupture (Taraschi *et al.*, 1986).

4.1.4.2 Cytoskeletal stability

The erythroid membrane consists of a permeability barrier (lipid bilayer) in which are embedded certain proteins that are attached to an underlying cytoskeletal network (spectrins, actin and band 4.1). The latter components provide the membrane with both its strength and flexibility, so that any disruption of this complex protein network would be potentially harmful (Pasvol *et al.*, 1992). It is proposed that membrane destabilization is initiated by the release of band 4.1, which exposes the spectrin to dimerization by haemin. Haemin then depolymerizes the actin molecules, before the entire cytoskeleton

becomes dissociated and the erythrocyte lyses (Shaklai *et al.*, 1986). Thus, micromolar concentrations of haemin can alter the conformation of protein 4.1 and weaken the spectrin dimer-dimer association, as well as the spectrin-protein stability of the membrane cytoskeleton (Lui *et al.*, 1985).

4.1.4.3 Enzyme inhibition

By inhibiting the red blood cell cytosolic enzymes (pyruvate kinase, glucose-6-phosphate dehydrogenase, glutathione reductase and glutathione-S-transferase), haemin could cause haemolysis (Harvey and Beutler, 1982). The most significant effect of haemin on enzymes is its ability to inhibit proteases, which could inhibit haemoglobin degradation and cause parasite death by starvation (Chui and Lubin, 1989; Zarchin *et al.*, 1986). Haemin can also inhibit the erythrocytic membrane Ca^{2+}/Mg^{2+} ATPase enzyme by its peroxidative properties. This could be relevant to the parasitized erythrocytes, since an ATPase pump is functional in the erythrocyte membrane (Krishna *et al.*, 1994). Inhibition of this pump would unbalance the cationic homeostasis within the erythrocyte and influence membrane stability (Leclerc *et al.*, 1988).

4.1.4.4 Cation leakage

Micromolar concentrations of haemin cause haemolysis by a colloid-osmotic effect, with the following sequence of events. The depletion of glutathione and ATP from haemin treated cells, impairs the ability of the red blood cell membrane to maintain ion gradients, which leads to potassium ion efflux. The efflux, along with the osmotic gradient created by the haemoglobin and other molecules trapped inside, results in the entry of water and the red blood cell swells. The increase in cell size, destabilizes the membrane integrity and eventually leads to haemolysis (Chou and Fitch, 1981).

4.1.5 EFFECT OF ANTIMALARIALS ON HAEMIN INDUCED HAEMOLYSIS

With the recent discovery of the haem polymerase enzyme, there has been a resurgence of interest in the ferriprotoporphyrin IX / haemin hypothesis which proposes to explain the mechanism of action of chloroquine. Haemin is proposed to concentrate chloroquine in the

food vacuole, such that the haemin-chloroquine complex could lyse the parasite membrane (Figure 4.1) (Fitch, 1989). Other membrane-active agents, e.g. quinine, mefloquine and calcium can also potentiate the haemolytic response to haemin (Dutta and Fitch, 1983).

Thus, because haemin may be involved in the pathogenesis of certain haemolytic anaemias, a more complete understanding of haemin toxicity in uninfected and parasitized erythrocytes is needed. Due to the possibility of haemin iron being involved in lipid peroxidation, the effects of iron chelating agents (desferrioxamine and 2,2'-bipyridyl) on haemin induced haemolysis were studied.

4.2 AIMS

To establish whether transferrin-bound iron taken up by the parasitized erythrocyte is associated with the haemozoin found in the food vacuole. To determine the effects of iron chelating agents on pigmented parasites, haemozoin and on haemin induced haemolysis of uninfected and parasitized erythrocytes.

4.3 EXPERIMENTAL DESIGN

Infected erythrocytes were exposed to the $^{59}Fe_2$-transferrin from the early ring until the mid-late trophozoite stage. Whether the uptake of extracellular iron and the formation of haemozoin were interrelated, was determined as in Chapter 2.4.1. The effects of iron chelating agents on the latter were also investigated as in Chapter 2.4.2. The effects of desferrioxamine and 2,2'-bipyridyl on the structure of haemozoin and haemin were studied, along with the effects of these iron chelating agents on haemin induced haemolysis of uninfected and parasitized erythrocytes (Chapter 2.4.3 and 2.5, respectively).

4.4 RESULTS

4.4.1 INCORPORATION OF TRANSFERRIN BOUND IRON INTO MALARIA PARASITES

To verify that the isolation procedure had not altered the crystalline structure of haemozoin, a thin smear was prepared, Giemsa stained and examined under normal light microscopy (1000x magnification) (Figure 2.5). The comparison between Figure 2.5.A and 2.5.C, indicated that the isolated haemozoin crystals retained their morphological shape and colour, as found in the intact parasite.

There was significant uptake of ^{59}Fe into the isolated parasites (13,19%) compared to the erythrocyte control (0,17%). Approximately 41,90% of the total ^{59}Fe added, was associated with the haemozoin after 10 washes with SDS-PBS buffer (Figure 4.4). The incorporation of the ^{59}Fe into haemozoin was confirmed by gel electrophoresis. As shown in Figure 4.5, the major radioactive peak corresponds to the position of the haemozoin band. The Coomassie blue stained gel did not detect any protein associated with the haemozoin band, but did stain the globin and membrane impurities.

When non-labelled haemozoin was isolated and incubated in the presence of $^{59}FeCl_3$ at a pH of 5,0, 1,81% and 5,44% radio-activity was associated with the haemozoin pellets after 30 minutes and 24 hours, respectively.

4.4.2 *IN VITRO* EFFECT OF DESFERRIOXAMINE ON PARASITE HAEMOZOIN

The IC_{50} of desferrioxamine was determined to be 15,11 $\pm$ 3,00 μM (Table 5.2). Incubation of radiolabelled parasites with increasing concentrations of desferrioxamine showed decreased radioactivity in the isolated haemozoin (Figure 4.6). Decreases in radioactivity for all desferrioxamine concentrations were significantly ($p < 0,02$) different from the control. The construction of a linear regression line through this data indicated that there was a significant decrease in ^{59}Fe-associated with the parasite haemozoin as the

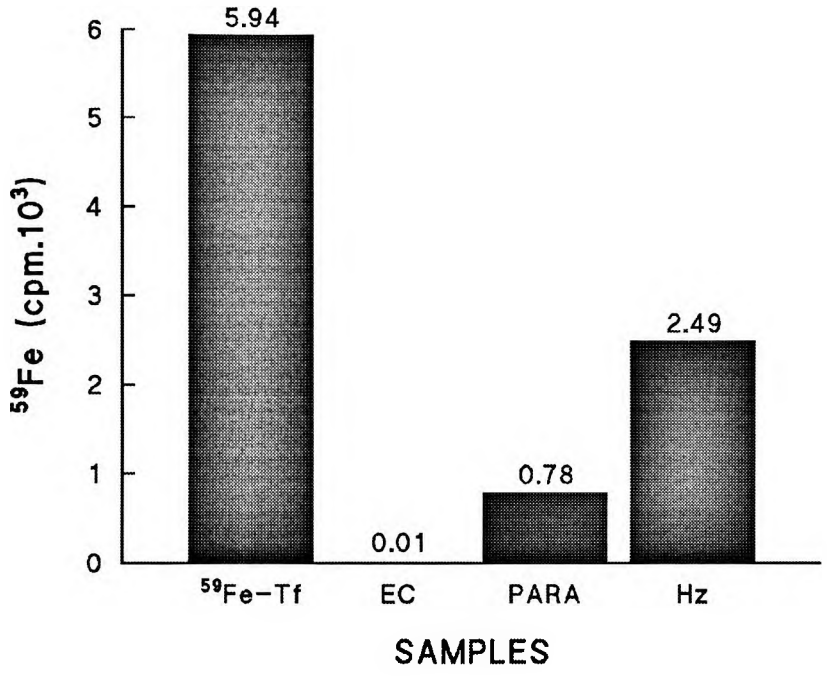


Figure 4.4: The distribution of ^{59}Fe in trophozoite-infected erythrocytes. ^{59}Fe-Tf was the initial $^{59}Fe_2$-transferrin added to the media; EC the erythrocyte control; PARA the isolated parasites and Hz the isolated haemozoin.

concentration of desferrioxamine increased (Figure 4.6). The final parasitaemia for each desferrioxamine concentration did not vary significantly from the control after the two hour incubation period.

4.4.3 EFFECT OF DESFERRIOXAMINE AND 2,2'-BIPYRIDYL ON ISOLATED LABELLED HAEMOZOIN

Labelled haemozoin incubated at the pH of the food vacuole (pH 5,0), and in the presence of various desferrioxamine concentrations resulted in the removal of the ^{59}Fe into the desferrioxamine supernatant (Figure 4.7; top). The presence of 2,2'-bipyridyl, even at concentrations up to three times its IC_{50} (25,33 $\pm$ 8,14 μM) did not remove ^{59}Fe from the haemozoin pellet (Figure 4.7; bottom).

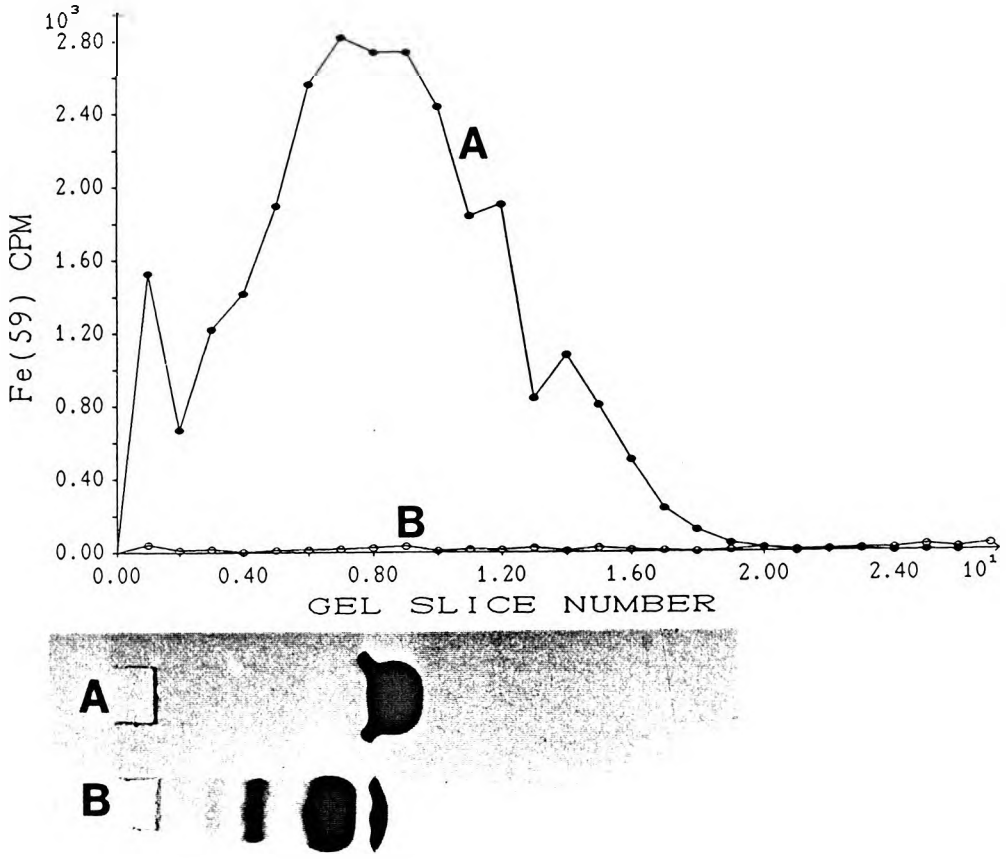


Figure 4.5: A 6-20% gradient SDS electrophoretic gel (bottom) of haemozoin (A) and haemoglobin (B) obtained from ^{59}Fe-labelled trophozoite-infected and control erythrocytes, with corresponding one minute gamma counts (top).

4.4.4 UV-VIS SPECTROPHOTOMETRIC ANALYSIS OF THE EFFECTS OF DESFERRIOXAMINE ON ISOLATED HAEMOZOIN AND HAEMIN

4.4.4.1 Effects of desferrioxamine on isolated labelled-haemozoin

The addition of purified haemozoin to the buffer (pH 5,15) did not produce any characteristic absorbance pattern, due to the insolubility of the crystal at this pH. Over a period of 45 minutes, 30 μM desferrioxamine did not produce any spectral changes, neither did 125 μM desferrioxamine over a period of 10,5 hours. For both concentrations of desferrioxamine, the spectra consisted of straight lines overlaying each other with no

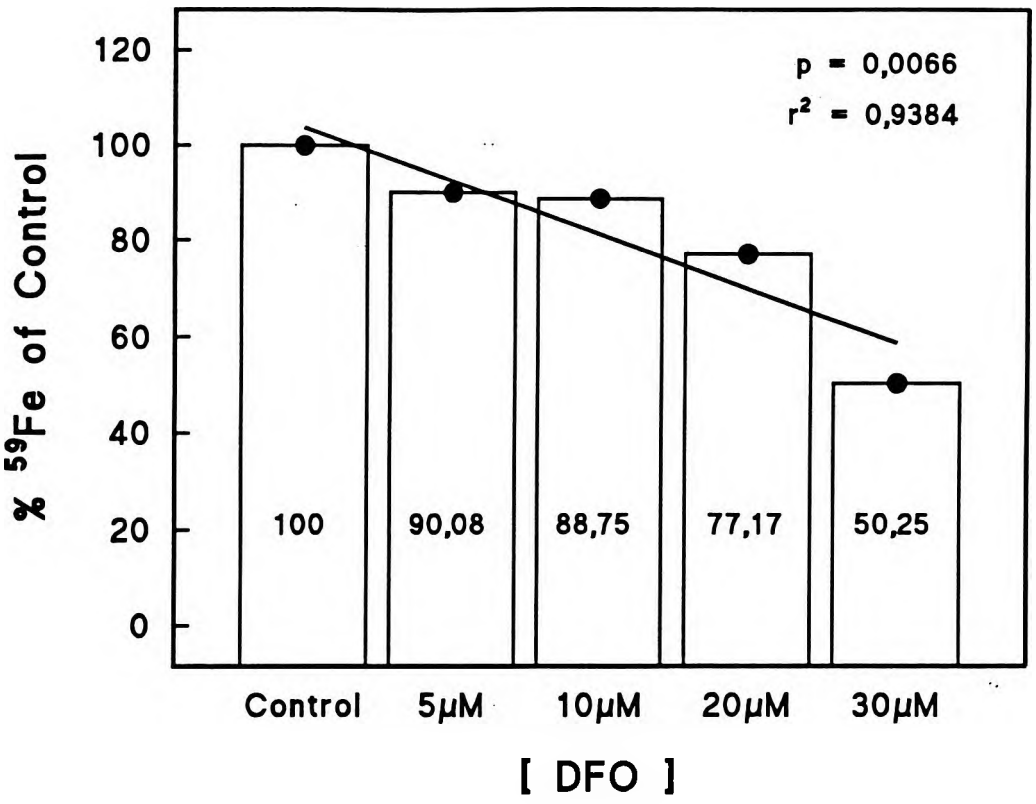


Figure 4.6: The *in vitro* effects of desferrioxamine (DFO) on the haemozoin ^{59}Fe content. The radioactive counts are expressed as a percentage of the control haemozoin.

peaks being formed. An increase in buffer pH to 12,77, solubilized the crystal to form a yellow-brown colour, which produced a split Soret peak at 396,0 nm. The addition of desferrioxamine (125 μM to 312,5 μM) to the solubilized crystals did not shift the haemozoin spectrum at all.

4.4.4.2 Effects of desferrioxamine on haemin

The absorbance spectrum produced by the solubilized haemozoin crystals closely resembled that of solubilized dimeric haemin at pH 12,77, with the split Soret peak being produced at 386,9 nm. The addition of 2,68 mM desferrioxamine to the solubilized haemin crystals (2,11 μM) did not alter the initial spectrum.

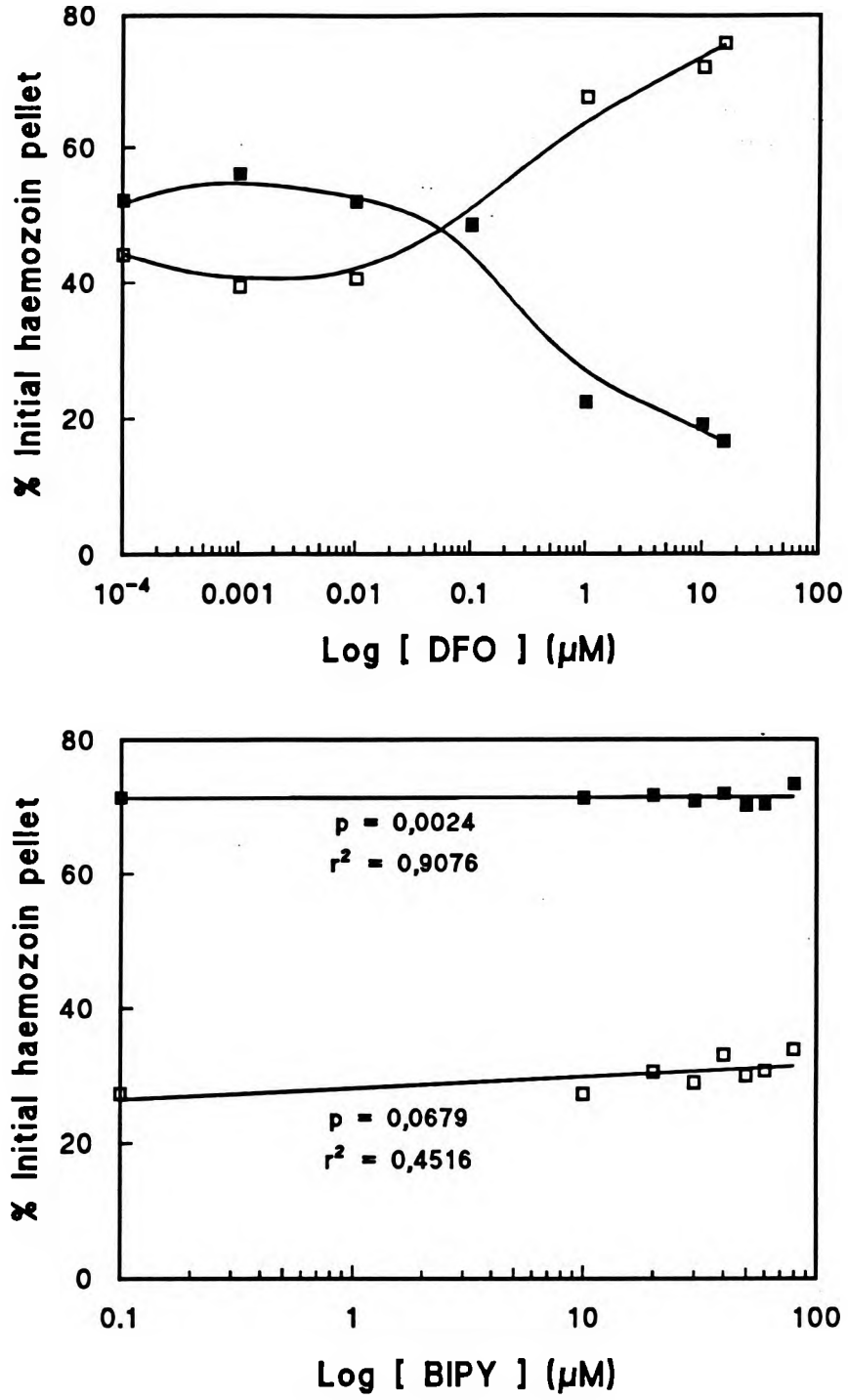


Figure 4.7: The effects of various concentrations of desferrioxamine (DFO; top) and 2,2'-bipyridyl (BIPY; bottom) on isolated ^{59}Fe-labelled haemozoin. The results are expressed as a percentage of the initial radioactivity associated with the pellet for each concentration. Where ■ represents the pellet and □ the supernatant.

4.4.5 HAEMIN INDUCED HAEMOLYSIS

4.4.5.1 Haemin induced haemolysis

The haemolytic effect of haemin, tested against FCR-3 infected and uninfected erythrocytes, was found to be concentration dependant. The parasitized erythrocyte membranes were approximately three times more susceptible when subjected to 25 μM haemin (Figure 4.8). Concentration (5 to 25 μM haemin), time and temperature contributed significantly ($p < 0,002$) to the haemolysis of the parasitized erythrocyte membranes (Table 4.1). The rate of haemolysis was greatest at higher concentrations of haemin, whilst temperature had little effect on the haemolytic rate after one or two hours of incubation. Further experiments were conducted at 37°C to facilitate normal parasite maturation, and for two hours to ensure that membrane stabilization or destabilization could take place.

4.4.5.2 Effect of chloroquine and haemin on haemolysis

4.4.5.2.1 Chloroquine alone

The addition of chloroquine for two hours to the uninfected erythrocytes resulted in slight but significant stabilization of the membranes ($p = 0,01$; $r^2 = 0,98$); whilst haemolysis was not significantly induced in the parasitized erythrocytes ($p = 0,45$; $0,58$) (Figure 4.9). As shown by the slope of the linear regression line in Figure 4.11, stabilization of the uninfected and parasitized erythrocytic membranes was achieved by pre-treating the erythrocytes with chloroquine for 30 minutes before the addition of the haemin. When chloroquine was added to the uninfected erythrocytes the calculated r^2 and p values from the linear regression curve were 0,46 and 0,06. While the r^2 and p values for the parasitized erythrocytes were 0,72 and less than 0,01, respectively (Figure 4.10).

4.4.5.2.2 Chloroquine and haemin combined

When the uninfected and parasitized erythrocytes were incubated for two hours in the presence of varying concentrations of chloroquine and haemin, a synergistic interaction occurred, resulting in a significant amount of haemolysis (Figure 4.9). The haemolysis occurred in a dose-dependant manner.

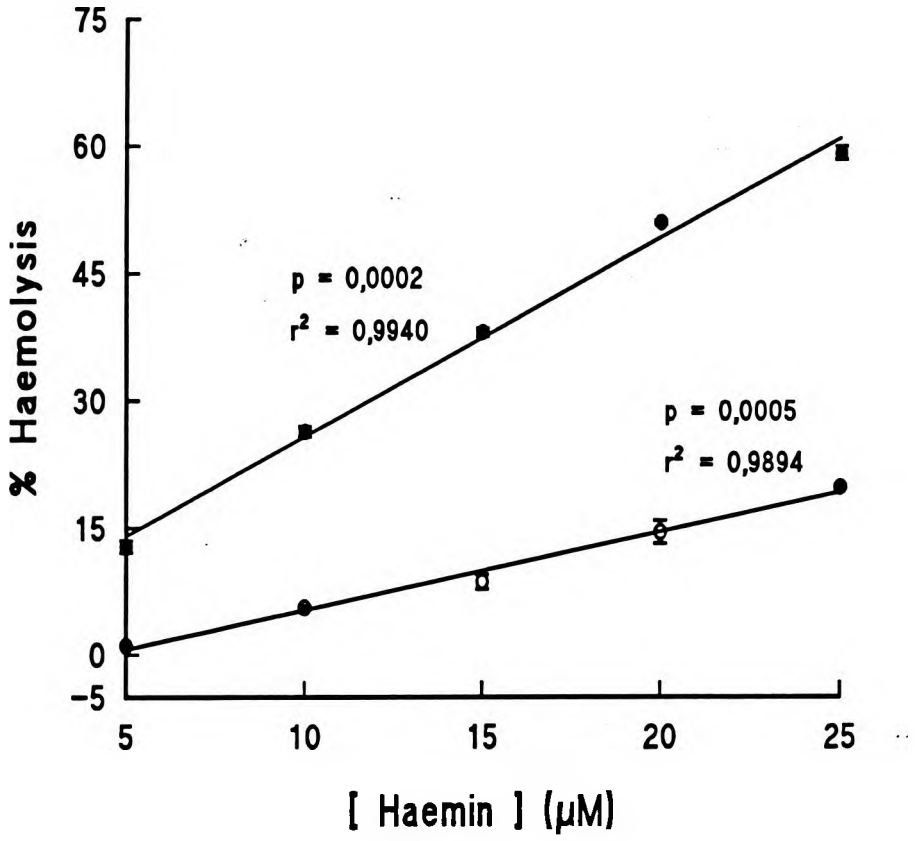


Figure 4.8: Concentration dependent effect of haemin induced haemolysis against the FCR-3 parasitized (●) and uninfected (○) erythrocytes, which were incubated at 37°C for 2 hours in the dark.

Table 4.1: The effect of time and temperature on haemin induced haemolysis of FCR-3 parasitized erythrocytes.

TEMPERATURE (°C)	TIME (Hour)	% HAEMIN INDUCED HAEMOLYSIS (± s.d.)	
		5 μM	25 μM
23	1	10,12 ± 0,78	52,45 ± 3,65
	2	11,12 ± 0,63	53,73 ± 0,50
37	1	8,04 ± 1,14	52,63 ± 0,32
	2	12,79 ± 0,72	59,31 ± 0,78

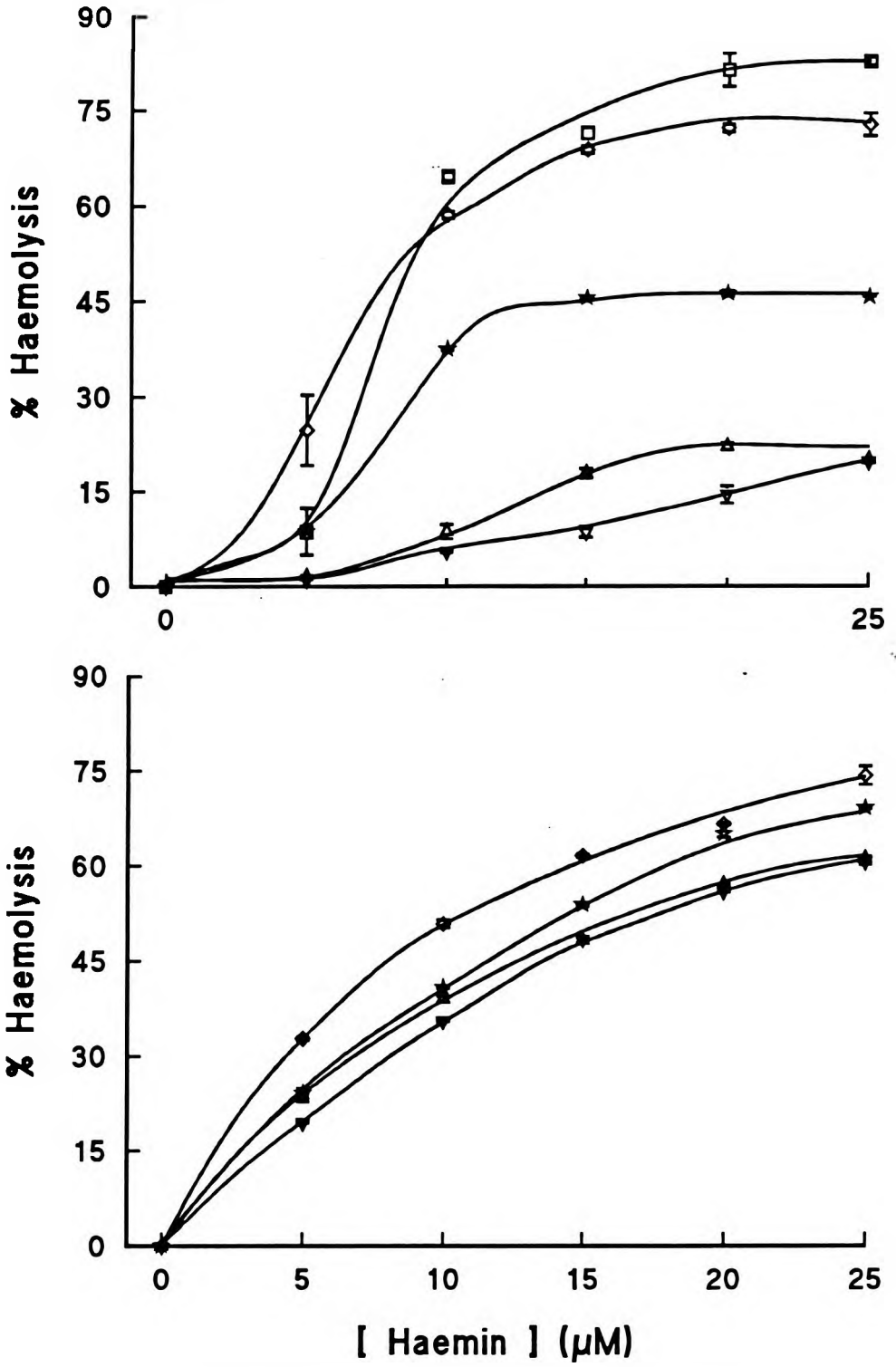


Figure 4.9: The haemolytic effect of chloroquine and haemin on the uninfected (top) and parasitized (bottom) erythrocytes after 2 hours of incubation. ▽: Haemin alone and haemin added to various concentrations of chloroquine: △: 1 μM; ★: 5 μM; ◇: 10 μM; □: 20 μM.

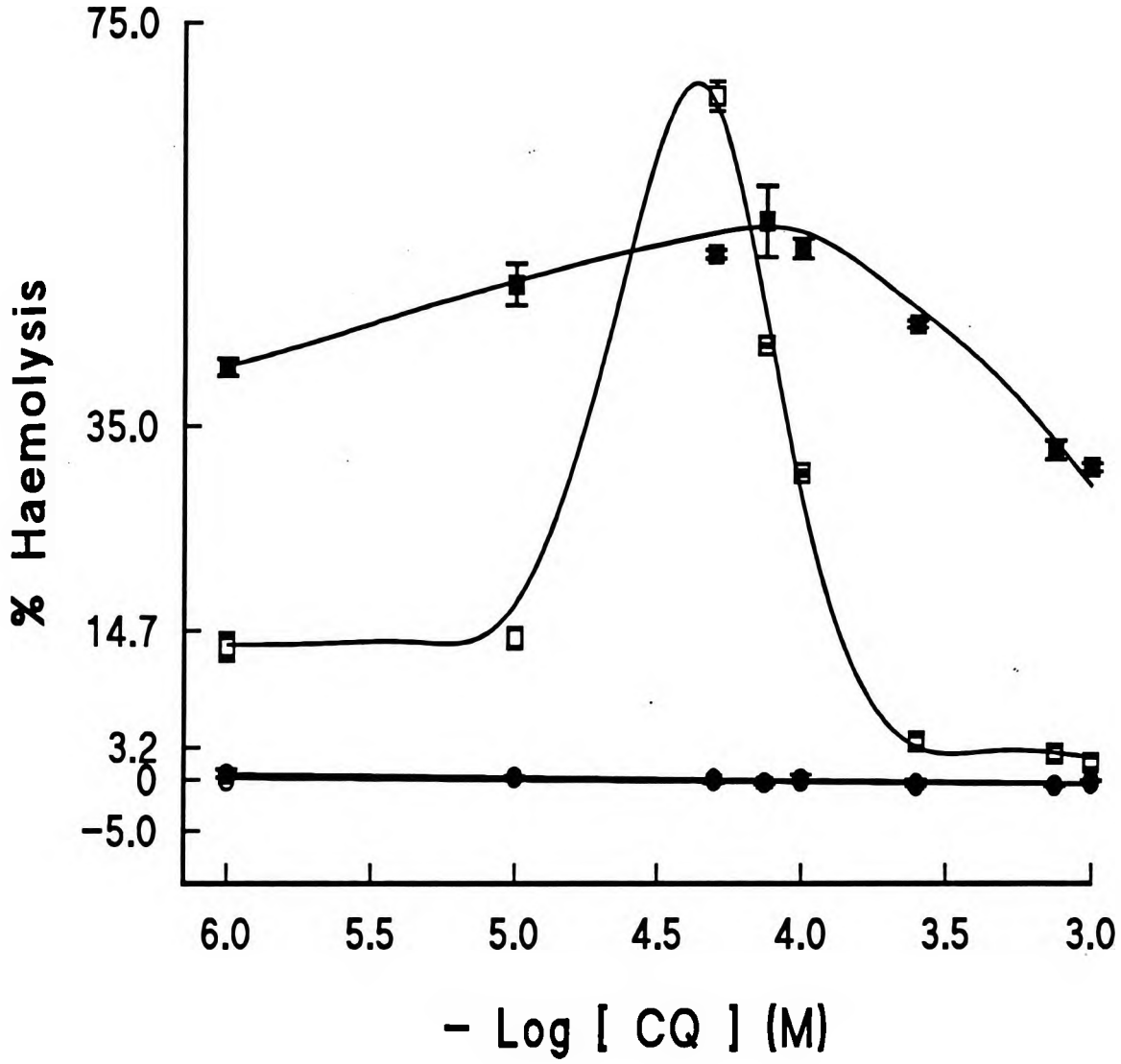


Figure 4.10: The effect of pre-treating erythrocytic membranes with chloroquine (CQ) for 30 minutes before the addition of haemin (2 hours). The parasitized (solid) and uninfected (open) erythrocytes were incubated with (■;□) or without (●;○) haemin. Haemin (5 μM) resulted in 3,19 ± 0,18% and 14,66 ± 0,19% lysis in uninfected and parasitized erythrocytes, respectively.

As seen in Figure 4.10, the effect of pre-treating the parasitized and uninfected erythrocytes with chloroquine was very different to the dose-response curves observed in

Figure 4.9. The dose-response curve for the uninfected erythrocytes was bell-shaped, i.e. high concentrations of chloroquine inhibited its own potentiating effect. This effect was not as pronounced in the parasitized erythrocytes. The maximum point of haemolysis, extrapolated from the curves of the uninfected and parasitized erythrocytes correspond to chloroquine concentrations of approximately 43 and 75 μM, respectively.

4.4.5.3 Effect of desferrioxamine and haemin on haemolysis

4.4.5.3.1 Desferrioxamine and haemin alone

A dose-dependant increase in haemolysis occurred in the uninfected and parasitized erythrocytes when desferrioxamine was added for up to two and half hours. The linear regression correlation values for desferrioxamine alone in the uninfected and parasitized erythrocytes were: $p = 0,29$, $r^2 = 0,81$; and $p = 0,01$, $r^2 = 0,81$, respectively (Figure 4.11; top). Haemin (5 μM) resulted in $0,89 \pm 0,41\%$ and $14,30 \pm 0,38\%$ haemolysis in the uninfected and parasitized erythrocytes, respectively. When desferrioxamine was added alone to the uninfected and parasitized erythrocytes it was calculated that their respective linear regression curves had p values of 0,04 and 0,07 and r^2 values of 0,67 and 0,60 (Figure 4.11; bottom). Haemin (5 μM) resulted in $6,10 \pm 0,86\%$ and $18,33 \pm 0,28\%$ lysis in uninfected and parasitized erythrocytes, respectively.

4.4.5.3.2 Desferrioxamine and haemin combined

Desferrioxamine significantly protected the erythrocytes from haemin induced haemolysis in both experimental situations shown in Figure 4.11. Pre-treatment of the parasitized erythrocytes resulted in slightly greater protection against lysis; such that 1 mM desferrioxamine and 5 μM haemin conferred 14,21% protection, contrasting with the 9,63% when desferrioxamine and haemin were added simultaneously. Linear regression curves were obtained when desferrioxamine and haemin were added to uninfected erythrocytes, with p and r^2 values of 0,68 and 0,23 (Figure 4.11; top) and 0,06 and 0,63 (Figure 4.11; bottom).

4.4.5.4 Effect of 2,2'-bipyridyl on haemin induced haemolysis

4.4.5.4.1 2,2'-Bipyridyl and haemin alone

A dose dependent increase in haemolysis occurred when 2,2'-bipyridyl was added to both

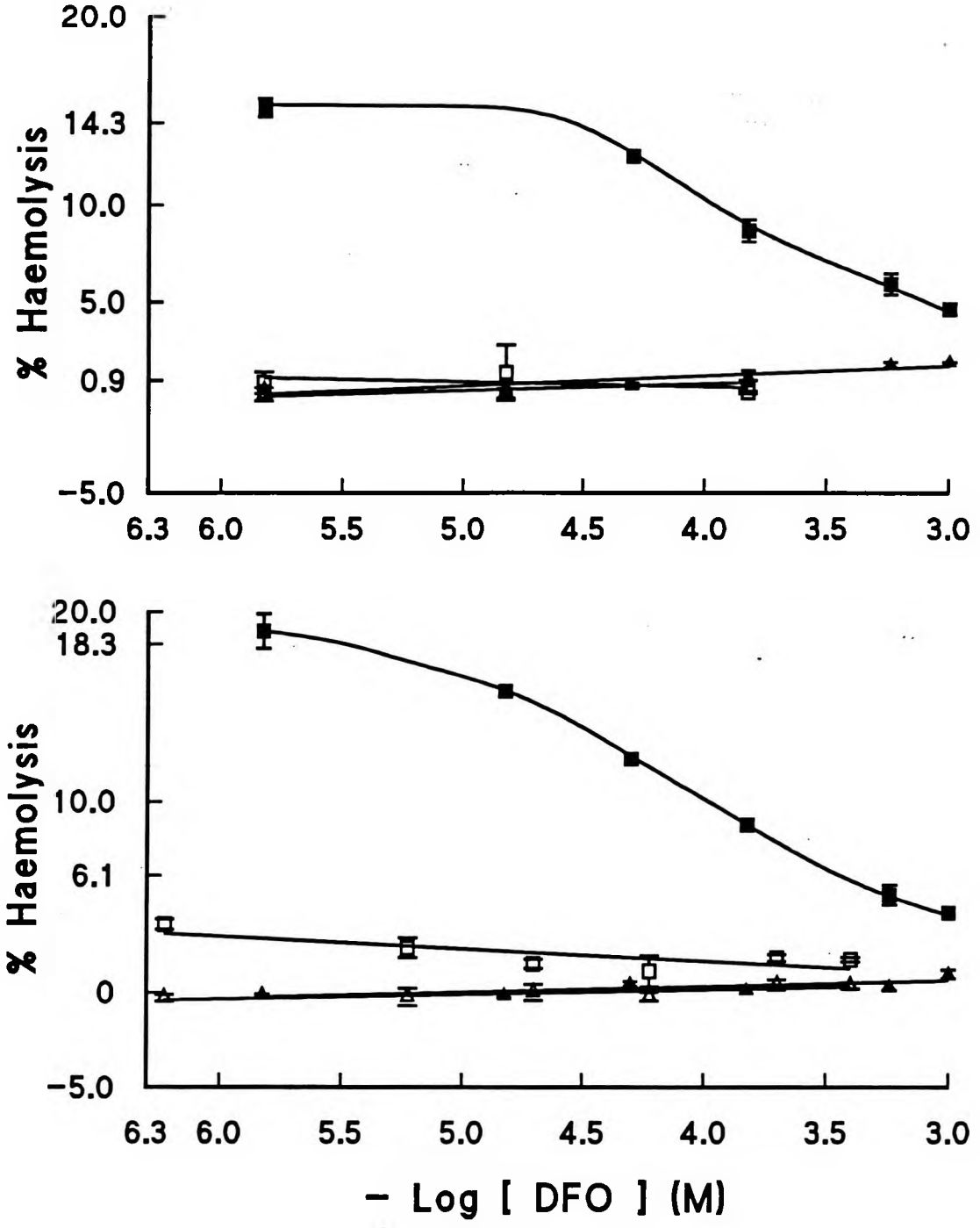


Figure 4.11: Effect of desferrioxamine (DFO) on haemin induced haemolysis. Top: DFO and haemin incubated for 2 hours. Bottom: Pre-treatment with DFO for 30 minutes before the addition of haemin (2 hours). The parasitized (solid) and uninfected (open) erythrocytes were incubated with DFO, either in the presence (■;□) or absence (▲;△) of 5 μM haemin.

the uninfected and parasitized erythrocytes under both experimental conditions (Figure 4.12). From Figure 4.12 (top), the linear regression correlation values for p and r^2 obtained for the uninfected erythrocytes were 0,51 and 0,15; and for the parasitized erythrocytes 0,01 and 0,83. Haemin (5 μM) resulted in 0,74 $\pm$ 0,62% and 14,30 $\pm$ 0,38% haemolysis in the uninfected and parasitized erythrocytes, respectively. The linear regression correlation p and r^2 values obtained for the uninfected erythrocytes were 0,09 and 0,56 and for the parasitized erythrocytes 0,02 and 0,77, respectively (Figure 4.12; bottom). Haemin (5 μM) resulted in 5,13 $\pm$ 0,61% and 14,66 $\pm$ 0,19% lysis in uninfected and parasitized erythrocytes, respectively.

4.4.5.4.2 2.2'-Bipyridyl and haemin combined

The simultaneous addition of 2,2'-bipyridyl and haemin for 2 hours protected the uninfected erythrocytes, but destabilized the parasitized erythrocyte membranes. From Figure 4.12 (top), the linear regression correlation p and r^2 values obtained for the uninfected and parasitized erythrocytes were 0,31; 0,33 and 0,001; 0,98, respectively.

Potentiation of haemolysis occurred when the uninfected erythrocytes were pre-treated with 2,2'-bipyridyl for 30 minutes; where the linear regression curve was calculated to have a p and r^2 value of 0,18 and 0,39. In contrast, the pre-treatment of the parasitized erythrocytes with 2,2'-bipyridyl, resulted in a small amount of protection against haemolysis (such that 1 mM 2,2'-bipyridyl reduced the haemin-induced haemolysis by 1,56%). The r^2 and p values calculated for the linear regression curve for the parasitized erythrocytes were 0,96 and much less than 0,001, respectively (Figure 4.12; bottom).

4.5 DISCUSSION

4.5.1 INCORPORATION OF TRANSFERRIN BOUND IRON INTO MALARIA PARASITES

The formation of haemozoin enables malaria parasites to continue digesting haemoglobin without having to contend with the toxic ferric form of haem and the resultant production

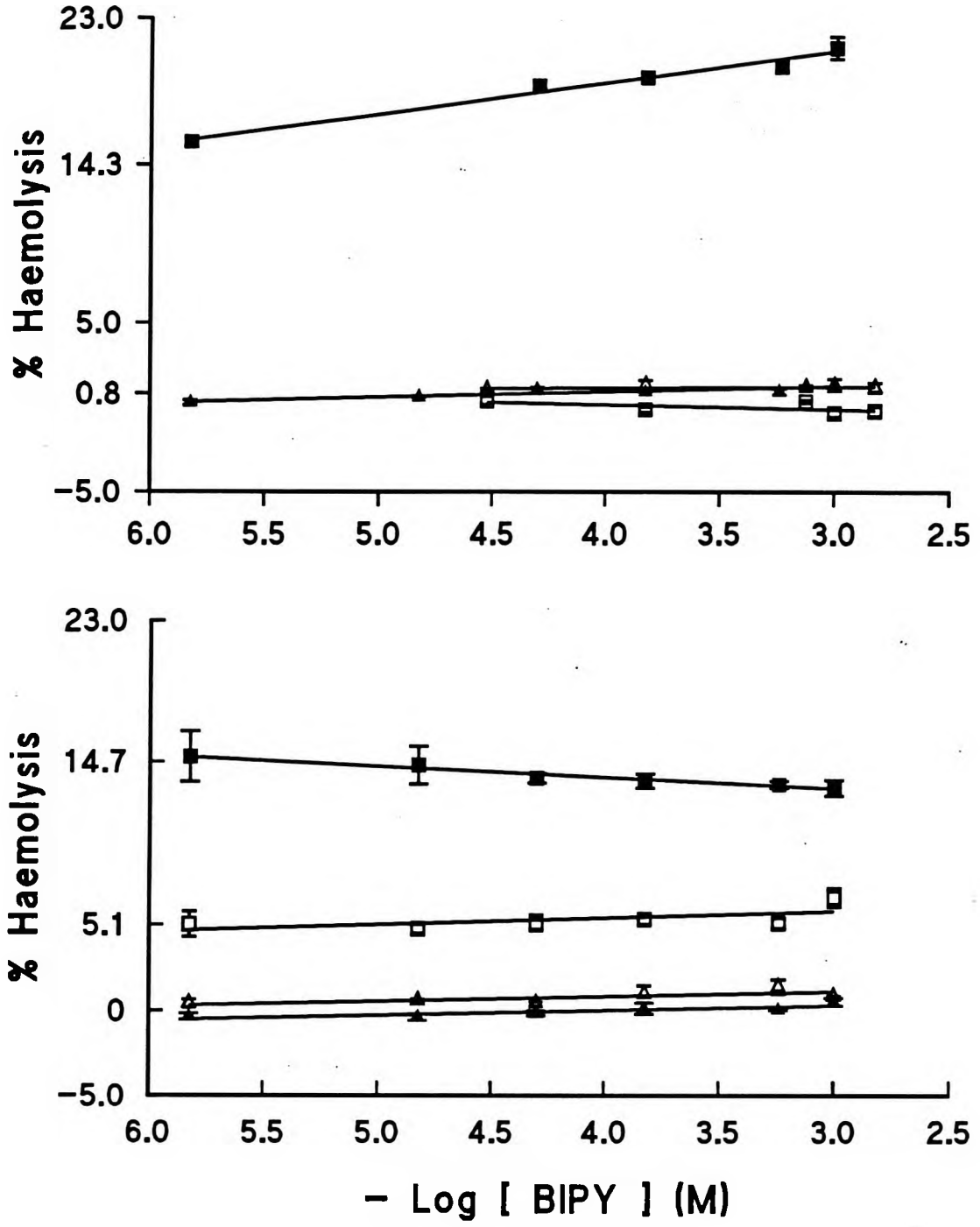


Figure 4.12: Effect of 2,2'-bipyridyl (BIPY) on haemin induced haemolysis. Top: BIPY and haemin incubated for 2 hours. Bottom: Pre-treatment with BIPY for 30 minutes before the addition of haemin (2 hours). The parasitized (solid) and uninfected (open) erythrocytes were incubated with BIPY, either in the presence (■;□) or absence (▲;△) of 5 μM haemin.

of superoxide. To determine whether the uptake of extracellular iron and the formation of haemozoin are interrelated; parasites were incubated in the presence of diferric radio-labelled transferrin from merozoite, through early ring until the mid-late trophozoite stage. As seen in Figures 4.4 and 4.5, there was significant incorporation of the extracellular ferric iron into the haemozoin crystals, (detected electrophoretically and by gamma counting the pure haemozoin crystal). The radioactivity associated with the haemozoin was present even after ten washes with SDS buffer, indicating that its presence was not due to non-specific binding of the labelled transferrin molecule to the haemozoin crystal.

Incorporation of iron into the haemozoin only occurred in viable parasites. When isolated haemozoin was incubated in the presence of radioactive iron at the food vacuole pH of 5,0, no significant amount of radioactivity was associated with the haemozoin. The radioactive iron remained in the supernatant, even after a 24 hour incubation period. In order for the extracellular iron to be incorporated into the haemozoin, the presence of an active parasitic metabolism was indicated and possibly would require one or several specific enzymes.

The presence of a ferric ion in the haemozoin structure, as detected in this study, is in accordance with the proposed structure that the crystal consists of a polymer of haem units linked between the central ferric ion of one haem and a carboxylate side-group oxygen of another (Slater *et al.*, 1991). However, Slater's proposed structure cannot account for the extracellular iron found to be associated with the crystal or how desferrioxamine could chelate the iron, since desferrioxamine can not chelate haem-associated iron (Keberle, 1964) (Figure 4.2). To account for the incorporation of extracellular iron into the haemozoin structure, I propose the following. After the haem units are released from the endocytosed haemoglobin molecules, the methyl groups situated around the haem structures are oxidized to carboxyl groups, which in turn bind extracellular iron to form the complex structure of the haemozoin crystal (Figure 4.13). This polymerization reaction may be similar to that proposed by Dorn *et al.* (1995), where the β-haematin in haemozoin is formed spontaneously or may be initiated and catalysed by a specific enzyme.

However, if Bremard's proposed structure for haemozoin is examined, it too could account for the inclusion of extracellular iron into the isolated crystal (Bremard *et al.*, 1993).

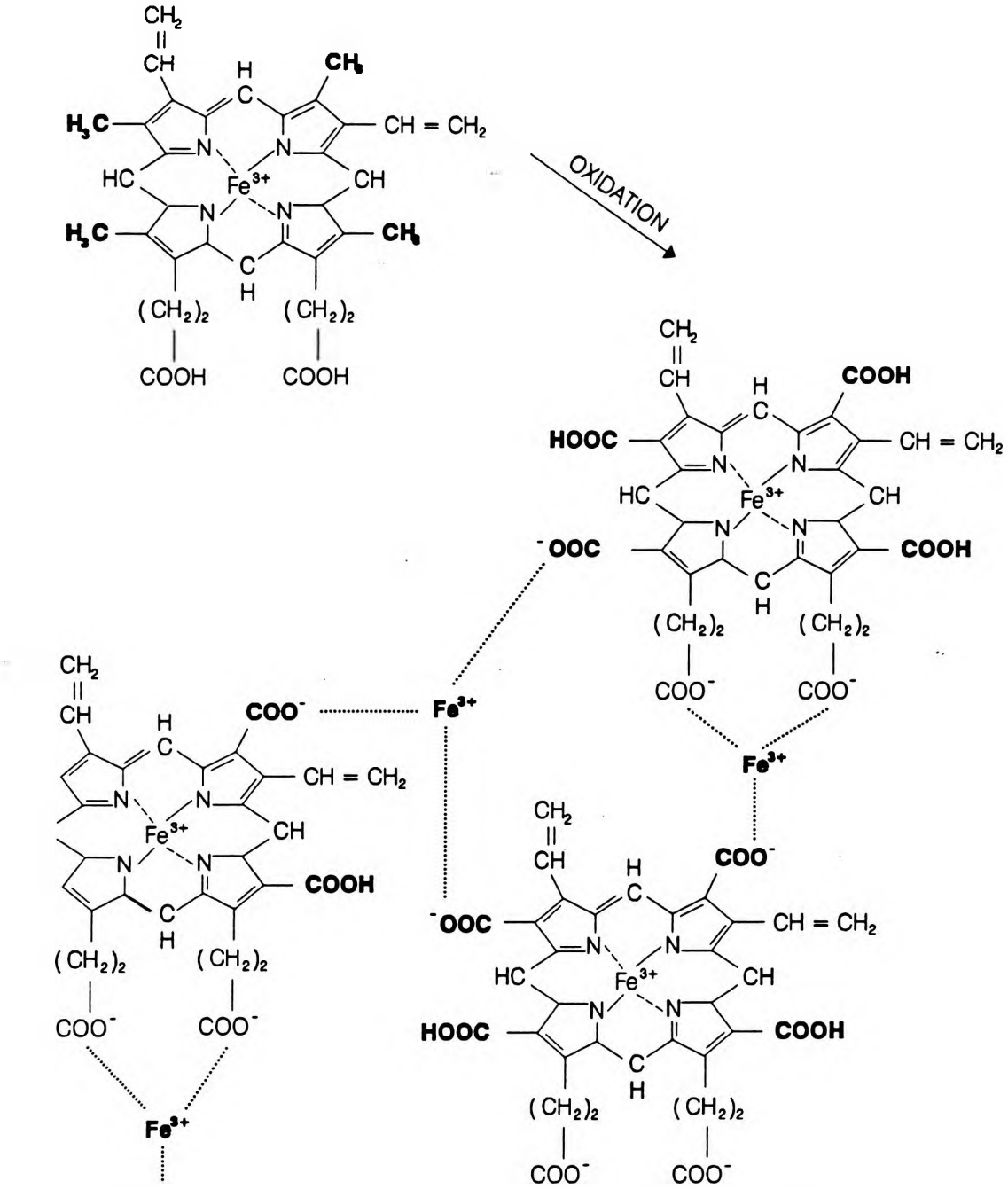


Figure 4.13: Proposed structure of the haemozoin crystal as determined from this study.

During the isolation procedure, the monomeric hydroxo complex (Figure 4.3) can be oxidized, with the result that the parasite synthesized protein is released. This oxidized complex could then bind the extracellular iron to form a more complex haemozoin structure.

The fact that the extracellular iron is incorporated into the crystal is unexpected, but possibly explains why the parasite acquires such a large amount of extracellular iron. It is possible that the iron is not only necessary for the formation and stabilization of the crystal, but the crystal in turn could act as a sink to prevent the iron from catalysing any radical-generating reactions. Thus, preventing cellular damage and parasite death.

4.5.2 EFFECT OF IRON CHELATING AGENTS ON HAEMOZOIN

4.5.2.1 Effect of desferrioxamine

Stage-dependent effects of desferrioxamine on the malaria parasite show that desferrioxamine is cytostatic to the ring and non-pigmented trophozoite stages, whilst cytocidal to the pigmented trophozoites and early schizonts (Figure 6.6 to 6.9; Whitehead and Peto, 1990). In addition to only affecting the haemozoin-containing stages, increasing concentrations of desferrioxamine were found to decrease the amount of radioactivity associated with the *in vitro* haemozoin structure (Figure 4.6). Desferrioxamine also directly chelated the iron from isolated radiolabelled haemozoin, where at concentrations greater than 0,06 μM desferrioxamine, the amount of radioactivity associated with the chelating agent substantially increased (Figure 4.7). These *in vitro* results seem to indicate that the presence of haemozoin is required for the antimalarial activity of desferrioxamine.

This possible disruption of the haemozoin crystal by desferrioxamine could release toxic haemin molecules, which are lytic to the parasite (Orjih *et al.*, 1981). The excess ferric iron released from the haemozoin could result in the production of free radicals, which could in turn promote enzyme and DNA damage, as well as membrane damage via lipid peroxidation (Aruoma *et al.*, 1989). Thus, the production of these free radicals and the release of a small proportion of haemin, could be enough to be cytocidal to the parasite.

Desferrioxamine cannot chelate haem-associated iron (Keberle, 1964), thus desferrioxamine most probably chelates the iron which is situated between the haem units in the haemozoin structure (see Figure 4.13). However, according to light and electron microscopic observations, the desferrioxamine-treated haemozoin structure does not seem

to be disrupted or differ from the crystalline structure of the control (Figure 6.12; Atkinson *et al.*, 1991). It is possible that due to the relatively high concentrations of other di- and trivalent cations present in the immediate environment, the iron could be substituted by these metals, in order to stabilize the crystal. In cases of iron deficiency, there is a tendency to incorporate zinc, instead of iron into the porphyrin structure and this could have taken place in these experiments (Labbe and Rettmer, 1989). Zinc has been shown to be sequestered along with iron into the haemozoin structure (Ginsburg *et al.*, 1986). Even though the structure remained intact, the release of iron from the crystal could promote lipid peroxidation. This possibility was supported by the observation that when the isolated haemozoin was incubated with desferrioxamine in Na^+/K^+-phosphate buffer, the supernatant was slightly brown in colour. Thus, in the absence of another cation, the crystal is disrupted to its monomeric form. In addition, the depletion of zinc from the parasite cytosol and membranes could have potentiated the haemolytic effects of the free iron and haemin, since zinc is an efficient membrane stabilizer.

4.5.2.2 Effect of 2,2'-bipyridyl

The inability of the ferrous iron chelating agent, 2,2'-bipyridyl, to affect the haemozoin crystal illustrates once again that the iron associated with the crystal is ferric in nature. From the antagonistic effect between 2,2'-bipyridyl and desferrioxamine, it was previously concluded that the antimalarial mechanism of action of iron chelating agents is not solely dependent on iron deprivation (Figure 5.13; Jairam *et al.*, 1991). The experiments done here tend to indicate that 2,2'-bipyridyl does not have any direct association with the haemozoin crystal (Figure 4.12). But rather, the lipophilicity of this ferrous iron chelating agent enables it to partition into the food vacuole membrane, chelating the iron as it exits the food vacuole and thereby inhibiting iron-dependant biochemical reactions.

4.5.3 THE DELETERIOUS EFFECTS OF HAEMIN ON ERYTHROCYTIC MEMBRANES

Haemin efficiently induced haemolysis in a time and temperature dependant manner in both the uninfected and parasitized erythrocytes, with the latter membranes being more

susceptible to lysis (Figure 4.8). This could be attributed to the difference in their respective membrane compositions, with the parasitized erythrocytic membrane consisting of less cholesterol and more unsaturated phospholipids (Shaklai *et al.*, 1986).

The mechanism by which haemin induces lysis, has been proposed to correlate with the concentration of haemin present (Schmitt *et al.*, 1993) In the present study, the concentration ranged from 5 to 25 μM, with the majority of the experiments using 5 μM. At such low concentrations, the haemin molecules are usually monomeric in nature, with the haemin iron being accessible for reaction. The resultant membrane damage is thus due to protein oxidation and/or lipid peroxidation. Probable targets for haemin in the erythrocytic membrane are the cytoskeletal protein, spectrin or the phospholipids. In these experiments, the more abundant phospholipids were more accessible to haemin than spectrin, since haemin was added extracellularly and spectrin is located on the inner surface of the membrane. These results once again show that haemin is extremely toxic and compounds should be sought to neutralize the cellular effects of haemin.

4.5.4 EFFECT OF CHLOROQUINE ON HAEMIN INDUCED HAEMOLYSIS

Quinoline-containing antimalarials are cationic amphiphiles, which accumulate to high levels in the food vacuole and are known to interact with membrane phospholipids (Ginsburg and Krugliak, 1988). In this study, it was found that at physiological pH and in an isotonic buffer, chloroquine stabilized the parasitized and uninfected erythrocytic membranes (Figure 4.9), which is similar to that reported by Ginsburg and Krugliak (1988). However, the small degree by which chloroquine stabilized the membrane, possibly implies that this is not an important factor in the antimalarial action of chloroquine.

Micromolar concentrations of chloroquine potentiated the haemolysis induced by haemin in both the uninfected and parasitized erythrocytes, which concurs with the idea that chloroquine enhances the intercalation of haemin between the membrane phospholipids (Figure 4.9 and 4.10). The greater susceptibility of the uninfected erythrocytes to haemin

toxicity in the presence of chloroquine, is compatible with the larger content of cholesterol and saturated phospholipids in the erythrocytic membranes. A lower cholesterol content in the parasite membrane would have failed to inhibit the partitioning of the haemin-chloroquine complex into the phospholipid bilayer, thus increasing the tendency for haemin to initiate peroxidation of the unsaturated phospholipids (Figures 4.9 and 4.10) (Taraschi *et al.*, 1986). However, pre-incubation with chloroquine resulted in the higher concentrations of chloroquine potentiating its own effect (Figure 4.10). It is possible that during the pre-incubation period, that chloroquine interacted with the phospholipids and thereby prevented haemin from intercalating between the phospholipids, and inducing haemolysis.

All experiments in support of the haemin-chloroquine complex hypothesis, including those done in this study, were carried out in the absence of plasma proteins. Zhang and Hempelmann (1987), however showed that this haemolytic haemin-chloroquine complex is neutralized in the presence of plasma proteins. Thus, the antimalarial action of chloroquine cannot be fully explained by the haemin-chloroquine hypothesis.

4.5.5 INHIBITION OF HAEMIN INDUCED HAEMOLYSIS BY DESFERRIOXAMINE

In view of the therapeutic use of desferrioxamine in haemoglobinopathies, associated with iron overload, Heinz body formation in thalassaemia and in malaria; it was important to investigate the possible *in vitro* role of desferrioxamine in haemin induced haemolysis.

The addition of desferrioxamine to both uninfected and parasitized-erythrocytes surprisingly resulted in slight haemolysis (Figure 4.11). The observed haemolysis could be induced by the desferrioxamine-ferrous ion complex, which is known to act as an oxygen radical generating system (Klebanoff *et al.*, 1989).

The most potent inhibitors of lipid peroxidation are those chelating agents forming the weakest ferrous ion complexes, for example, desferrioxamine (Braughler *et al.*, 1988).

This was shown to be the case in this study, when desferrioxamine protected both the uninfected and parasitized erythrocytic membranes from haemin induced haemolysis (Figure 4.11). Through its interaction with the iron moiety of haemin, desferrioxamine could either have prevented haemin from binding to the membrane or have extracted previously bound haemin from the membranes (Baysal *et al.*, 1990). Alternatively, desferrioxamine could have inhibited cell damage by acting as an electron donor, which would have prevented the peroxidative cleavage of the unsaturated phospholipid membranes by haemin (Braughler *et al.*, 1988).

The ability of desferrioxamine to reduce the haemolytic capacity of haemin at the membrane level and in the plasma could be therapeutically beneficial in the treatment of anaemia found in severe malaria-infected patients. This could be the mechanism by which desferrioxamine significantly decreases the recovery time of comatose cerebral malaria patients (Gordeuk *et al.*, 1992a). Desferrioxamine, not only decreases the plasma iron concentrations, but can also bind the toxic haemin molecules, thus preventing further cellular damage.

4.5.6 EFFECT OF 2,2'-BIPYRIDYL ON HAEMIN INDUCED HAEMOLYSIS

2,2'-Bipyridyl induced haemolysis in both the uninfected and parasitized erythrocytes (Figure 4.12), through its high affinity for ferrous ions, which stimulated lipid peroxidation of erythrocytic membranes (Braughler *et al.*, 1988). However, haemin and 2,2'-bipyridyl could have acted independently through their haemolytic properties, to potentiate the lysis of the parasitized erythrocytes. Whilst, parasitized erythrocytes, pre-treated with 2,2'-bipyridyl, were less sensitive to haemin induced haemolysis (Figure 4.12; bottom). This is possibly as a result of 2,2'-bipyridyl chelating the iron at or near the membrane, and thereby preventing haemin from inducing lipid peroxidation.

In conclusion, the uptake of extracellular iron is not only essential as a nutrient for parasite survival, but possibly also for the stabilization of the haemozoin crystal. The chelation of iron from haemozoin by desferrioxamine and not 2,2'-bipyridyl, tends to verify that the

iron is present in a ferric state. It seems unlikely that the induction of haemolysis is the primary antimalarial action of chloroquine, desferrioxamine and 2,2'-bipyridyl. However, it is apparent that the presence of "free" haemin in the parasitic food vacuole or in plasma could be potentially damaging to the host. However, in the presence of binding proteins or desferrioxamine treatment, haemolysis could effectively be prevented. Here, desferrioxamine did not only prevent haemolysis but also inhibited parasite growth through iron chelation. Thus, other iron chelating agents being designed and tested should not only include these properties of desferrioxamine, but also possibly improve upon them.

CHAPTER FIVE

THE INDIVIDUAL AND COMBINED EFFECT OF CHELATING AGENTS AND CLASSICAL ANTIMALARIALS ON THE IN VITRO GROWTH OF P. FALCIPARUM

5.1 INTRODUCTION

Chloroquine-resistance has appeared in nearly every site endemic for malaria, with varying patterns of spread of the resistant phenotype. The resistant parasites can be naturally selected for by exposure to the drug which eliminates the sensitive majority of the population and allows overgrowth of the minority of resistant parasites. In the clinical setting, mutational resistance occurs more frequently due to drug pressure from prolonged therapy or overuse of a single drug (Cabantchik, 1989). These two mechanisms of developing resistance could no doubt account for different types and levels of drug resistance found worldwide.

The expansion and resurgence of drug resistance has prompted the demand for novel chemotherapeutic strategies. By observing infected host immune systems and the biochemistry of proliferating organisms, an unique target has been identified. It involves the sequestration of plasma cations, which are essential for biochemical reactions (Oppenheimer, 1989; Murray *et al.*, 1978). Iron chelating therapy is successfully applied to iron overload disease states and is potentially useful in cancer chemotherapy, where the healthy tissue withstands temporary iron depletion, and the rapidly dividing tumour cells are inhibited (Hileti *et al.*, 1995).

By using chelating agents to mimic this nutritional immunity status, it may be possible to use these compounds as effective antimalarials.

5.1.1 Human plasma

Human plasma has naturally occurring cation chelating agents, such as citrate, ATP, ascorbate, glutathione, pyrophosphates, ceruloplasmin and apotransferrin. Apotransferrin has a high affinity for ferric ions ($K_a = 10^{26}\ M^{-1}$) and sequestration keeps the ions soluble for essential biochemical reactions (Bridges and Seligman, 1995). This sequestration also successfully withholds iron from any invading pathogen, such as malaria parasites. Clinical studies show that transferrin concentrations are elevated in malaria infections, in order to

decrease the concentration of free redox iron released from the haemolysed erythrocytes (Aremu, 1989). Apotransferrin and ceruloplasmin function as chain-breaking antioxidants, by chelating free plasma iron and copper, respectively, and thereby protect the host from oxidative stress. Reduced glutathione also prevents autooxidation by chelating cupric ions (Navas *et al.*, 1994).

Citrate can be described as a primitive low molecular weight chelating agent, which acts as a mediator in promoting a rapid exchange of ferric ions between transferrin molecules and from transferrin to ferritin (Aisen and Leibman, 1968). The iron can then be utilized for haem synthesis or be stored with ferritin (Bates *et al.*, 1967). The pyrophosphates and ascorbate are also reported to chelate transferrin-bound iron and facilitate iron transfer to ferritin (Konopka *et al.*, 1981).

Ascorbate (vitamin C) is needed for different physiological processes of living organisms. Through its reducing capacity, it can function as an antioxidant by scavenging reactive oxygen species (Navas *et al.*, 1994). However, ascorbate can also act as a pro-oxidant in the presence of trace amounts of ferrous and cupric ions, which can promote metal-dependent oxidative damage via the Haber-Weiss reaction (Figure 5.1).

In addition, ascorbate is involved in the maintenance of the cellular immune system. A deficiency in this vitamin is accompanied by decreased resistance to microbial infections, as in malaria infections (Das *et al.*, 1993).

$$Fe^{3+}\text{- complex} + O_2^{\cdot-} \longrightarrow Fe^{2+}\text{- complex} + O_2$$

$$Fe^{2+}\text{- complex} + H_2O_2 \longrightarrow OH^{\cdot} + OH^{-} + Fe^{3+}\text{- complex} \quad (A)$$

$$\text{Net: } O_2^{\cdot-} + H_2O_2 \xrightarrow[\text{catalyst}]{\text{metal}} O_2 + OH^{\cdot} + OH^{-}$$

Figure 5.1: The iron-catalysed Haber-Weiss reaction, where equation A is the Fenton reaction.

5.1.2 PHARMACOLOGICAL CHELATING AGENTS

The pharmacological chelating agents used in toxicology include amongst others, desferrioxamine, diethylene triamino pentaacetic acid and ethylene diamino tetraacetic acid. For over twenty years, iron overload therapy has relied on the use of desferrioxamine, where desferrioxamine is the drug of choice. Many other chelating agents with higher lipid solubilities or iron stability constants are being tested.

5.1.2.1 Desferrioxamine B, a hydroxamate chelating agent

5.1.2.1.1 The chemistry of desferrioxamine

Desferrioxamine B is a naturally occurring siderophore isolated from *Streptomyces pilosus* and is produced by fermentation under iron-limiting conditions. It is a simple aliphatic chain composed of a molecule of acetic acid, two molecules of succinic acid and three molecules of 1-amino-5-hydroxylamino-pentane (Figure 5.2) (Waxman and Brown, 1969). In the chain, there are three hydroxamine groups inside and one free amino group at the end, the latter accounts for the basic character of the compound (Keberle, 1964). When ferric ions are added, the long desferrioxamine chain coils around the ion to form an octahedral-iron complex, ferrioxamine. The hexadentate chelating agent binds iron in a 1:1 ratio (Waxman and Brown, 1969).

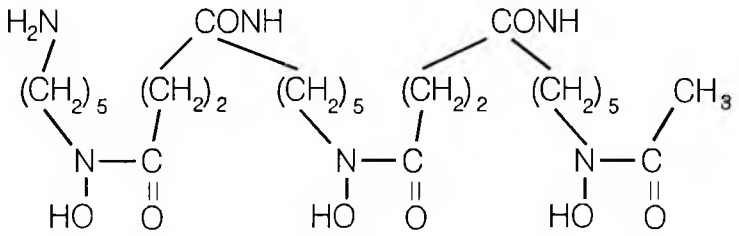


Figure 5.2: The chemical structure of desferrioxamine.

Desferrioxamine has a remarkably high affinity for ferric iron ($K_a = 10^{31}\ M^{-1}$), which favours selective iron starvation without hypocalcaemia being a side effect (K_a for Ca^{2+}

= 10^2 M^{-1}). Desferrioxamine can also bind Al^{3+}, Zn^{2+} and Mg^{2+} with binding affinities of 10^{21}, 10^{11} and 10^4 M^{-1}, respectively (Waxman and Brown, 1969; Swartz, 1985).

Desferrioxamine has been shown to mobilize iron from the storage proteins, ferritin and haemosiderin, however this probably involves an indirect transfer of iron. Iron cannot be chelated from the porphyrin system in haemoglobin or haem-containing enzymes, e.g. the cytochromes (Keberle, 1964). Desferrioxamine binds iron so tightly that it should quantitatively remove iron from transferrin, but *in vitro* and *in vivo* studies fail to demonstrate significant depletion of transferrin-bound iron by a stoichiometric excess of desferrioxamine at physiological pH (Pollack *et al.*, 1976).

5.1.2.1.2 Pharmacology of desferrioxamine

Desferrioxamine is used in the management of acute iron poisoning as well as in the long-term treatment of pathological iron overload, e.g. idiopathic haemochromatosis and transfusion haemosiderosis. It is also used in aluminium-related encephalopathy and in aluminium-related bone disease in chromic dialysis patients (Gibson and Swanepoel, 1995).

Desferrioxamine is poorly absorbed from the gastrointestinal tract and once in the bloodstream, renal filtration of the drug is rapid. The desferrioxamine-iron complex, ferrioxamine, that is formed is hydrophilic in nature and is responsible for the characteristic reddish colour of the urine (Keberle, 1964). Eighty percent of the ferrioxamine is excreted in the urine, with the remaining 20% leaving by the biliary route.

Following intravenous administration, the half-life of desferrioxamine is approximately 10 to 15 minutes, since it is metabolised by plasma enzymes (Bridges and Seligman, 1995). During this short half-life, desferrioxamine binds little iron, thus requiring multiple intramuscular injections every 24 hours for acute iron poisoning or pathological iron overload (Gibson and Swanepoel, 1995). Ideally, the drug should be used daily for periods of greater than 12 hours if tolerated by the patient (Bridges and Seligman, 1995).

This property of desferrioxamine places severe constraints on its clinical use. Contributing to the latter are the numerous, but infrequent adverse side-effects that have been reported;

namely, hypersensitivity reactions, as well as pain and inflammation at the injection site. Desferrioxamine is reported to be teratogenic in animals (Gibson and Swanepoel, 1995).

5.1.2.1.3 *In vitro* and *in vivo* malaria and desferrioxamine

In vitro studies indicate that desferrioxamine cannot easily permeate into ring-infected erythrocytes, but can slowly enter into the mature stages (Fritsch and Jung, 1986), to specifically chelate the intraparasitic iron (Scott *et al.*, 1990). Desferrioxamine exhibits cytostatic activity against the ring- and non-pigmented trophozoite-infected erythrocytes, whilst it is cytocidal towards the pigmented mature parasites (Whitehead and Peto, 1990). Desferrioxamine is known to act as a S-phase inhibitor, by blocking DNA synthesis through the central, iron-dependent ribonucleotide reductase enzyme (Hoffbrand *et al.*, 1976; Lederman *et al.*, 1984). However has little effect on RNA and protein synthesis in the parasite (Lytton *et al.*, 1994).

In vivo studies have found desferrioxamine to promote iron excretion and to suppress the manifestations of the infectious process (Fritsch *et al.*, 1985). It has also been reported that a constant infusion of desferrioxamine, either intravenously or subcutaneously, is required to suppress the infections (Fritsch *et al.*, 1985; Pollack *et al.*, 1987b).

5.1.2.1.4 Clinical studies of desferrioxamine in malaria

Encouraged by *in vitro* and *in vivo* studies, several investigators proceeded to test the antimalarial effect of desferrioxamine in malaria infected humans. By administrating continuous intravenous desferrioxamine, the parasite growth was inhibited, but within at least three weeks recrudescence was observed (Bunnag *et al.* 1992; Gordeuk *et al.*, 1992b). It is thus evident that desferrioxamine should be administered as an adjunctive treatment with classical antimalarials to achieve complete inhibition of the infection. This was shown to be the case when Traore *et al.* (1991) used chloroquine and desferrioxamine against chloroquine-resistant *P. falciparum*, and the combination decreased the parasitaemia more rapidly than the patients treated with chloroquine alone. Gordeuk *et al.* (1992a) reported a similar observation in children with cerebral *P. falciparum* malaria, who were continuously infused with desferrioxamine and the standard cerebral malaria treatment, quinine and sulfadoxine-pyrimethamine. Desferrioxamine decreased the median

recovery time and increased the rate of parasite clearance. However, in uncomplicated and severe malaria-infected patients, the combination of desferrioxamine and the artemisinin derivative, artesunate did not significantly (p = 0,3) enhance parasite clearance compared to treatment with artesunate alone (Looareesuwan *et al.*, 1996). Thus, the drug(s) used in combination with desferrioxamine, need to be carefully selected before being used in clinical trials.

5.1.2.2 Desferrithiocin

Desferrithiocin is a novel sulphur containing-siderophore isolated from *Streptomyces antibioticus* (strain DSM #1865) and belongs neither to the hydroxamate nor the cathecholate type of natural chelators (Wolfe, 1990). This tridentate molecule forms a hypothetical 2:1 diastereomeric complex with ferric iron (Figure 5.3). The three ligating centres in both diastereomers are the carboxyl group, the thiazoline nitrogen and the aromatic hydroxyl, where the latter two groups are critical for activity and any alterations can compromise the ability of these functional groups to coordinate with iron and can significantly reduce the iron-clearing properties of the compound. Of the non-chelating functionalities, the aromatic nitrogen and the thiazoline are not necessary, while the sulphur atom is required (Bergeron *et al.*, 1994).

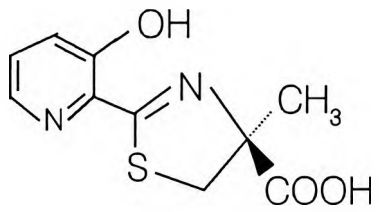


Figure 5.3: The chemical structure of desferrithiocin.

Desferrithiocin is structurally unrelated to desferrioxamine (see Figure 5.2) and has a different iron-binding stoichiometry of FeL_2 compared to the 1:1 ratio of the iron-desferrioxamine complex. Desferrithiocin has a similarly high selectivity and affinity for ferric iron as desferrioxamine, where their respective K_a values for ferric iron are 10^{30} and 10^{31} M^{-1}, respectively; with both being greater than apotransferrin (K_a = 10^{26} M^{-1}).

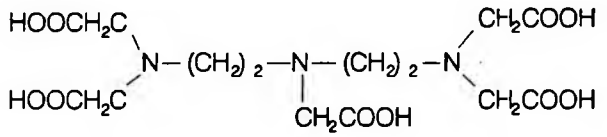
Desferrithiocin not only binds iron, but also Al^{3+} ($K_a = 10^{23}\ M^{-1}$), Zn^{2+} ($K_a = 10^{15}\ M^{-1}$) and Mg^{2+} ($K_a = 10^{8}\ M^{-1}$) (Wolfe, 1990).

Desferrithiocin is an efficient iron chelator and has been found to increase iron excretion *in vitro* and when administered orally or subcutaneously to iron-loaded rats. This suggests its potential in iron chelation therapy and possibly as an anti-malarial agent. Desferrithiocin has been found to be more effective than desferrioxamine, hydroxypyridone analogues (L1) and pyridoxal isonicontinyl hydrazone analogues in reducing hepatic iron *in vitro* (Baker *et al.*, 1992).

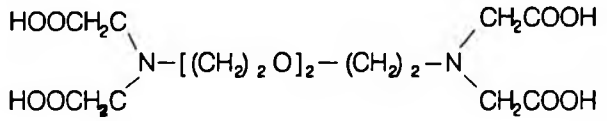
5.1.2.3 Aminocarboxylate compounds

This class of drugs includes derivatives of the basic aminocarboxylate structure, such as diethylene triamino pentaacetic acid (DTPA), ethylene diamino tetraacetic acid (EDTA) and ethylene bis (oxy-ethylene nitrilo) tetraacetic acid (EGTA) (Figures 5.4 and 5.5).

5.1.2.3.1 DTPA and EGTA



A



B

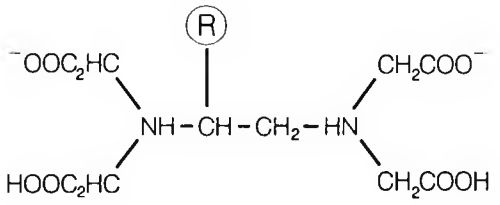
Figure 5.4: The chemical structures of diethylene triamino pentaacetic acid (DTPA; A) and ethylene bis (oxy-ethylene nitrilo) tetraacetic acid (EGTA; B).

DTPA is effective in promoting iron excretion, and the calcium derivative of DTPA can be used in iron overload patients (Singh and Hider, 1994). As with EDTA and EGTA, it is a hydrophilic molecule that is unable to penetrate into cells and directly interact with the

iron stores. Since transferrin-bound iron is unavailable for chelation, the iron source of DTPA is located in the non-transferrin-iron compartment of the plasma (Hershko and Peto, 1987). DTPA not only chelates Fe^{3+} ions ($K_a = 10^{29}\ M^{-1}$), but also a wide spectrum of other cations, such as Fe^{2+} ($K_a = 10^{16}\ M^{-1}$), Zn^{2+} ($K_a = 10^{18}\ M^{-1}$) and Cu^{2+} ($K_a = 10^{21}\ M^{-1}$) (Waxman and Brown, 1969). DTPA is also known to inhibit all protein synthesis as well as ferritin synthesis at a concentration of 2 mM (White *et al.*, 1976).

EGTA is commonly used in the laboratory to form a hexadentate ligand with a wide spectrum of cations, such as Fe^{2+} ($K_a = 10^{12}\ M^{-1}$), Zn^{2+} ($K_a = 10^{13}\ M^{-1}$), Cu^{2+} ($K_a = 10^{18}\ M^{-1}$) and Fe^{3+} ($K_a = 10^{21}\ M^{-1}$)(Auld, 1988).

5.1.2.3.2 EDTA



DERIVATIVE	Ⓡ
EDTA	H
DOTA	C_8H_{13}
DDDTA	$C_{10}H_{21}$
DHDTA	$C_{14}H_{29}$

Figure 5.5: The chemical structures of ethylene diamino tetraacetic acid (EDTA) and the alkyl derivatives, 1,2-diaminooctyl tetraacetic acid (DOTA), 1,2-diaminododecyl tetraacetic acid (DDDTA) and 1,2-diaminohexadecyl tetraacetic acid (DHDTA).

The usefulness of EDTA in treating lead poisoning led to its trial in iron mobilization in iron overload patients and as a possible antimalarial. The synthetic chelating agent, EDTA has an affinity for many cations, such as Mg^{2+} ($K_a = 10^{9}\ M^{-1}$), Fe^{2+} ($K_a = 10^{14}\ M^{-1}$), Zn^{2+} ($K_a = 10^{17}\ M^{-1}$), Cu^{2+} ($K_a = 10^{19}\ M^{-1}$) and Fe^{3+} ($K_a = 10^{25}\ M^{-1}$) (Waxman and Brown, 1969). For optimal clinical efficacy, EDTA is either administered subcutaneously or intravenously, to chelate the extracellular cations. Porter *et al.* (1988) reported that the efficacy of a chelating agent can be improved if its lipophilicity is increased. Thus, in

order to increase the efficacy and possible antimalarial activity of EDTA, the chemical structure could be chemically altered by increasing the length of a side chain of the agent as seen in Figure 5.5 (Porter *et al.*, 1990).

5.1.2.4 Nitrilotriacetic acid

As seen in Figure 5.6, nitrilotriacetic acid is a water soluble synthetic chelating agent, which is widely employed in laboratories as a means of loading ferric ions onto transferrin (Aroma *et al.*, 1989). However, nitrilotriacetic acid is a powerful carcinogen, causing acute nephrotoxicity, DNA damage and lipid peroxidation.

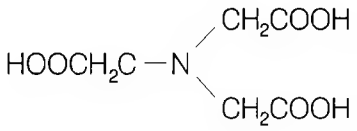


Figure 5.6: The chemical structure of nitrilotriacetic acid.

5.1.2.5 Ferrous iron chelating agents

Bathophenanthroline sulphonate (Figure 5.6; left) and 2,2'-bipyridyl (Figure 5.6; right) are two ferrous chelating agents, which are often used to investigate the pathway of transferrin-mediated iron uptake into reticulocytes and other cell lines. Both agents bind iron in a 1:3 ratio to form a bidentate ligand (Morgan, 1983).

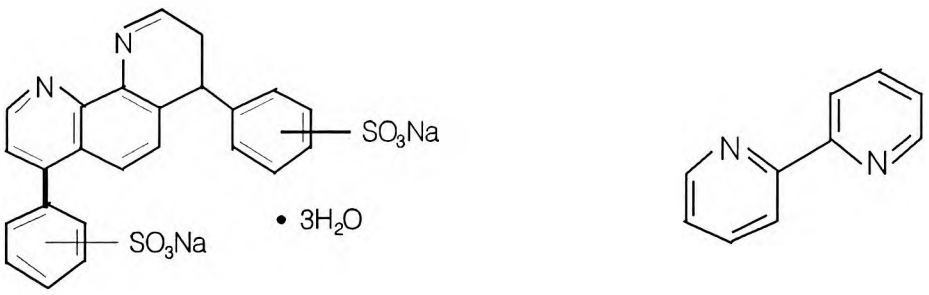


Figure 5.7: The chemical structure of bathophenanthroline sulphonate (left) and 2,2'-bipyridyl (right).

5.1.2.5.1 Bathophenanthroline sulphonate

Bathophenanthroline is known to inhibit the uptake of transferrin-bound iron, by interfering with the transplasma membrane electron transport mechanism (Figure 3.4) (Low *et al.*, 1987). The hydrophilic property of bathophenanthroline enables it to chelate ferrous ions before they are taken up into the erythrocytes. The reported presence of a diferric transferrin reductase enzyme in the plasma membrane of mature infected-erythrocytes could provide some support for this mechanism of action (Fry, 1989). There are no reports on the antimalarial activity of bathophenanthroline, but its iron chelating abilities make it a possible candidate.

5.1.2.5.2 2,2'-Bipyridyl

2,2'-Bipyridyl is an aromatic amine, which possesses a high affinity for ferrous ions ($K_a = 10^{18}\ M^{-1}$) and other cations such as Zn^{2+} ($K_a = 10^{14}\ M^{-1}$) and Cu^{2+} ($K_a = 10^{17}\ M^{-1}$) (Auld, 1988). *In vivo* investigations of 2,2'-bipyridyl reveal that it possesses sympathetic and possibly serotonergic properties, as well as inhibiting ferritin and haemoglobin synthesis (Primosigh and Thomas, 1968; Bass *et al.*, 1966). The lipophilicity of this compound, allows it to distribute in the apolar phase of the plasma membrane and uncouple the normal iron uptake process by reticulocytes (Nunez *et al.*, 1983). 2,2'-Bipyridyl functions by chelating the membrane-associated ferrous ions, and the water soluble chelate then moves from the membrane into the extracellular milieu (Figure 3.5). Thus, 2,2'-bipyridyl prevents iron from being incorporated into the iron-dependent enzymes in the parasite. In addition, 2,2'-bipyridyl is able to inhibit the metalloenzyme, diamine oxidase, by chelating its two Cu^{2+} ions (Bradsley *et al.*, 1974). This chelating action could enable 2,2'-bipyridyl to inhibit parasite growth, since iron and copper are essential for the survival of the protozoa.

5.1.3 CLASSICAL ANTIMALARIALS

Two major classes of antimalarials are used to treat malaria infections. They are the antifolates, including pyrimethamine (Figure 5.8.C) and the quinoline-containing drugs and their derivatives, quinine and chloroquine (Figure 5.8; A and B). But with the spread of

drug resistance to the traditional therapies, improvements in malaria chemotherapy should result from better understanding of the mechanisms that govern drug action and resistance.

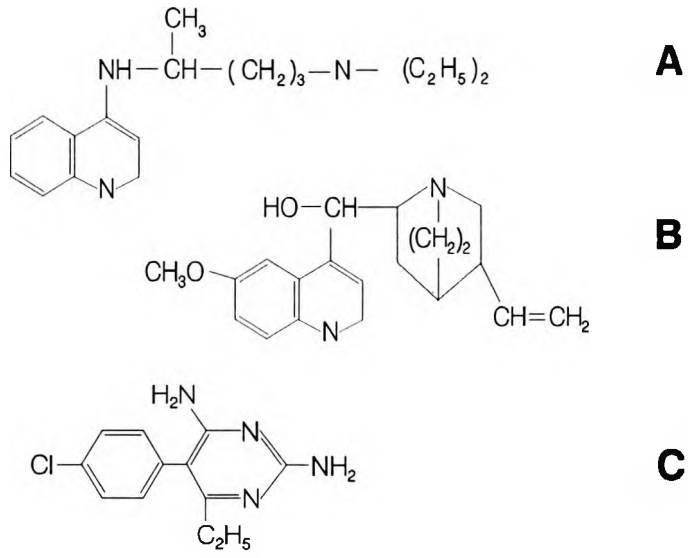


Figure 5.8: Chemical structure of chloroquine (A), quinine (B) and pyrimethamine (C).

5.1.3.1 Pyrimethamine

5.1.3.1.1 Mechanism of action

Parasites are unable to scavenge pyrimidines from their host, so are reliant on *de novo* folate synthesis (Figure 5.9) (Krungkrai *et al.*, 1990). Pyrimethamine selectively inhibits the dihydrofolate reductase enzyme, which exists in *P. falciparum* as a bifunctional protein with thymidylate synthase (Figure 5.9). Depletion of folate and pyrimidines, eventually result in cell cycle arrest and parasite death (Cowman and Foote, 1990).

5.1.3.1.2 Mechanism of resistance

Resistance to dihydrofolate reductase inhibitors can be mediated by amplification of the dihydrofolate reductase gene, resulting in an overproduction of dihydrofolate reductase, which overcomes the inhibitory effects of pyrimethamine (Inselburg *et al.*, 1987). Alternatively, specific point mutations in the dihydrofolate reductase gene could confer different degrees of resistance to pyrimethamine, depending on the positions of the

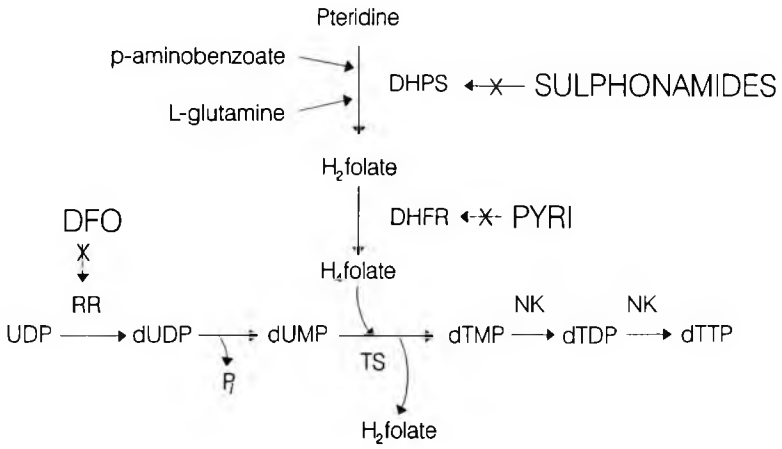


Figure 5.9: The *de novo* synthesis of folate in *P. falciparum* and the potential sites of inhibition of pyrimethamine (PYRI), sulphonamides and desferrioxamine (DFO). DHFR: dihydrofolate reductase; DHPS: dihydropteroate synthetase; RR: ribonucleotide reductase; NK: nucleotide kinase and TS: thymidylate synthase (Adapted from Bohinski, 1987; Krungkrai *et al.*, 1990).

mutations and the residues involved (Zolg *et al.*, 1993). Available evidence indicates that dihydrofolate reductase point mutations act by inhibiting pyrimethamine from binding to the enzyme (Zolg *et al.*, 1989). The precise effects produced by the point mutations suggest it may be possible to find alternative dihydrofolate reductase inhibitors that would act against pyrimethamine-resistant malaria (Canfield *et al.*, 1993).

5.1.3.2 Quinoline containing antimalarials

Much controversy still exists over the exact mechanism of action of chloroquine and quinine (Figure 5.8) and their related mechanism of resistance. Some of the possibilities are detailed below.

5.1.3.2.1 Ferriprotoporphyrin IX/haem hypothesis

Mechanism of action

During the digestion of host haemoglobin, the released haem molecules are normally sequestered in the inert haemozoin crystal (Slater and Cerami, 1992). Fitch (1989)

proposed that in the presence of chloroquine, haem bypasses the formation of the nontoxic aggregate, to form a complex with chloroquine (Figure 4.1); thereby retaining its haemolytic activity to disrupt erythrocytes and plasmodia (Chou and Fitch, 1981; Orijh *et al.*, 1981), and to inhibit the cysteine protease enzyme, which is involved in haemoglobin digestion (Vander Jaght *et al.*, 1986). In addition, the quinolines could inhibit haemozoin formation by inhibiting the putative haem polymerase enzyme (Chapter 4.1.1) (Slater and Cerami, 1992).

Mechanism of resistance

One of the possible mechanisms of chloroquine resistance could be due to the lack of haem to which the chloroquine could bind. It is possible that the chloroquine-resistant parasites possess a mechanism by which substantial amounts of haem are released from the parasitized erythrocytes (Wood *et al.*, 1984). Alternatively, the presence of a high-affinity binder or an acceleration of the biochemical processing of haem into haemozoin, could both account for the deficiency of haem in resistant parasites (Orjih and Fitch, 1993); although no experimental data is available to verify these proposals (Fitch, 1989).

5.1.3.2.2 Effect on the food vacuole

Mechanism of action

The weak base property of chloroquine suggests that it can be accumulated into the acidic food vacuole, i.e. the drug diffuses from the extracellular medium (pH 7,4) to the erythrocyte cytoplasm (pH 7,0 - 7,2) to the parasite cytoplasm (pH 6,8 - 7,0), and finally to the food vacuole (pH 4,8 - 5,0) (Aikawa, 1972; Ferrari and Cutler, 1990; Ginsburg and Stein, 1991).

Alternatively, chloroquine could be accumulated by a permease pump in the parasite plasma membrane. Warhurst (1988) proposes that the parasite cytoplasm has a higher pH than the erythrocyte cytoplasm and the pump facilitates this energetically unfavourable accumulation of chloroquine into the parasite. The pH difference between the erythrocyte and parasite cytoplasm is maintained by an ATP dependant pump (Mikkelson *et al.*, 1982). The quinoline then accumulates in the acidic food vacuole by simple diffusion.

High chloroquine concentrations greatly increase the food vacuole pH, and thereby inhibit acidic hydrolytic enzymes, which are required for haemoglobin degradation and by doing so inhibit parasite growth (Yayon *et al.*, 1984b; Ginsburg and Geary, 1987). Additionally, chloroquine could create a charge imbalance, cause the vacuoles to swell and the erythrocytes to haemolyse (Jacobs *et al.*, 1988).

Mechanism of resistance

The only consistent feature which distinguishes sensitive from resistant parasites, is the level of chloroquine accumulation within the trophozoite-infected erythrocytes (Homewood *et al.*, 1972; Geary *et al.*, 1986). If resistance is related to a decrease in drug concentration, then either less drug is accumulated or the drug is expelled from the acid food vacuole and parasite.

Ginsburg and Krugliak (1992) reported the pH of the food vacuole in the chloroquine-resistant parasites to be more alkaline, due to an elevated proton leak and/or a lower pump activity; with the resultant effect that less chloroquine is accumulated and pre-accumulated chloroquine exits the food vacuole and accumulates in the parasite cytoplasm.

Increased expulsion and modulators of resistance could be facilitated by the presence of a permease pump in the food vacuole membrane (Warhurst, 1988). Or multi-drug resistant glycoproteins could pump out the quinolines from the parasitized erythrocytes. Two P-glycoprotein homologues, termed "*P. falciparum* multi-drug resistant 1 and 2", have been isolated from the parasitized erythrocyte membrane. Amplification of the "*P. falciparum* multi-drug resistant 1" gene has been observed in some chloroquine-resistant strains (Foote *et al.*, 1989).

5.1.4 THE COMBINED EFFECT OF IRON CHELATING AGENTS AND CLASSICAL ANTIMALARIALS ON THE *IN VITRO* GROWTH OF *P. FALCIPARUM*

The emergence of chloroquine-resistant *P. falciparum* has initiated a considerable effort

to identify new antimalarials or combinations of such drugs. All the standard regimens, normally used to treat a *P. falciparum* infection, are now relatively ineffective. Recent studies report on the beneficial effects of combining the classical antimalarials with drugs such as antibiotics, antivirals and polysaccharides (Havlik *et al.*, 1993; Evans and Havlik, 1994 and Havlik *et al.*, 1994).

5.2 AIMS

To determine the sensitivities of various *P. falciparum* isolates to iron chelating agents and classical antimalarials. To use a wide spectrum of chelating agents against the strain, exhibiting the highest degree of chloroquine resistance. To determine the feasibility of using chelating agents as future antimalarials. From the latter, select two chelating agents, with high antimalarial activity and combine them with classical antimalarials and other chelating agents.

5.3 EXPERIMENTAL DESIGN

The tritiated hypoxanthine incorporation assay (Chapter 2.6) was used to determine the individual and combined effects of chelating agents and classical antimalarials on parasite growth.

5.4 RESULTS

5.4.1 EFFECT OF DESFERRIOXAMINE, 2,2'-BIPYRIDYL AND CLASSICAL ANTIMALARIALS ON *P. FALCIPARUM* ISOLATES

Various classical antimalarials (chloroquine, quinine and pyrimethamine) and iron chelating agents (desferrioxamine and 2,2'-bipyridyl) were tested against parasite strains showing varying degrees of drug resistance (Table 5.1). It should be noted that concentrations

greater than 100 μM of desferrioxamine or 2,2'-bipyridyl are required to achieve 100% inhibition of parasite growth. The IC_{50} values of desferrioxamine and 2,2'-bipyridyl for all the strains did not significantly vary from the FCR-3 IC_{50} values, except for desferrioxamine in the RSA-2 isolate ($p < 0,05$) (Table 5.1).

Table 5.1: Effect of various iron chelating agents and classical antimalarials on the *P. falciparum* isolates.

STRAIN	DRUG	IC_{50} ± s.d. (M)
3D7-A	Chloroquine	1,99 ± 0,12 n
	Desferrioxamine	12,92 ± 0,85 μ
	2,2'-Bipyridyl	18,54 ± 7,35 μ
RSA-2	Chloroquine	26,50 ± 5,09 n
	Quinine	14,36 ± 3,42 n
	Pyrimethamine	0,114 ± 0,01 μ
	Desferrioxamine	5,35 ± 0,47 μ
	2,2'-Bipyridyl	18,11 ± 1,80 μ
7G8	Chloroquine	85,15 ± 22,83 n
	Quinine	0,124 ± 0,022 μ
	Desferrioxamine	12,31 ± 1,25 μ
	2,2'-Bipyridyl	24,42 ± 5.73 μ
FAB-6	Desferrioxamine	13,63 ± 0,78 μ
	2,2'-Bipyridyl	39,49 ± 1,19 μ
FCR-3	Chloroquine	0,12 ± 0,01 μ
	Quinine	0,20 ± 0,16 μ
	Pyrimethamine	0,06 ± 0,02 μ
	Desferrioxamine	15,11 ± 3,00 μ
	2,2'-Bipyridyl	25,33 ± 8,14 μ

5.4.2 EFFECT OF VARIOUS CHELATING AGENTS ON THE *IN VITRO* GROWTH OF THE CHLOROQUINE-RESISTANT FCR-3 STRAIN

The parasites dependence on trace metals is exploited by the invaded host, by withholding essential nutrients such as iron, calcium and copper from the parasite. This effect of nutritional immunity was mimicked by using chelating agents, which have a wide degree of variability in their chemical structures and properties (Figures 5.2 to 5.7). These variabilities are reflected in their potency as antimalarials, with the potency decreasing from top to bottom of Table 5.2.

Table 5.2: The effect of chelating agents on the growth of the FCR-3 strain.

DRUG	IC_{50} ± s.d. (M)
Desferrioxamine	15,11 ± 3,00 μ
Desferrithiocin	22,11 ± 3,33 μ
Bathophenanthroline	23,58 ± 0,11 μ
2,2'-Bipyridyl	25,33 ± 8,14 μ
DHDTA	77,22 ± 13,38 μ
DDDTA	92,51 ± 9,32 μ
DOTA	116,51 ± 10,10 μ
EDTA	151,81 ± 15,22 μ
EGTA	182,82 ± 0,90 μ
DTPA	558,28 ± 48,92 μ
Nitrilotriacetic acid	1,74 ± 4,50 μ
Ascorbate	1,99 ± 0,33 m
Citrate	7,80 ± 1,04 m

There was a significant correlation ($p = 0,004$) between the efficacy of the EDTA class and the number of carbon atoms in the R-side group (Figure 5.10). Due to the insolubility

of DHDTA in culture medium, DMSO and concentrated HCl, all the aminocarboxylate derivatives were dissolved in 5% $NaHCO_3$ to maintain consistency. When hydrophilic EDTA, EGTA and DTPA were dissolved in culture medium, their IC_{50} values were 436,40 ± 25,21 μM, 414,46 ± 6,48 μM and 822,94 ± 29,08 μM, respectively. The 5% $NaHCO_3$ did not significantly effect parasite growth. High concentrations of citrate yielded severe haemolysis and methaemoglobin formation. An apotransferrin concentration of 12,55 ± 0,53 g/l was required to inhibit 50% of parasite growth.

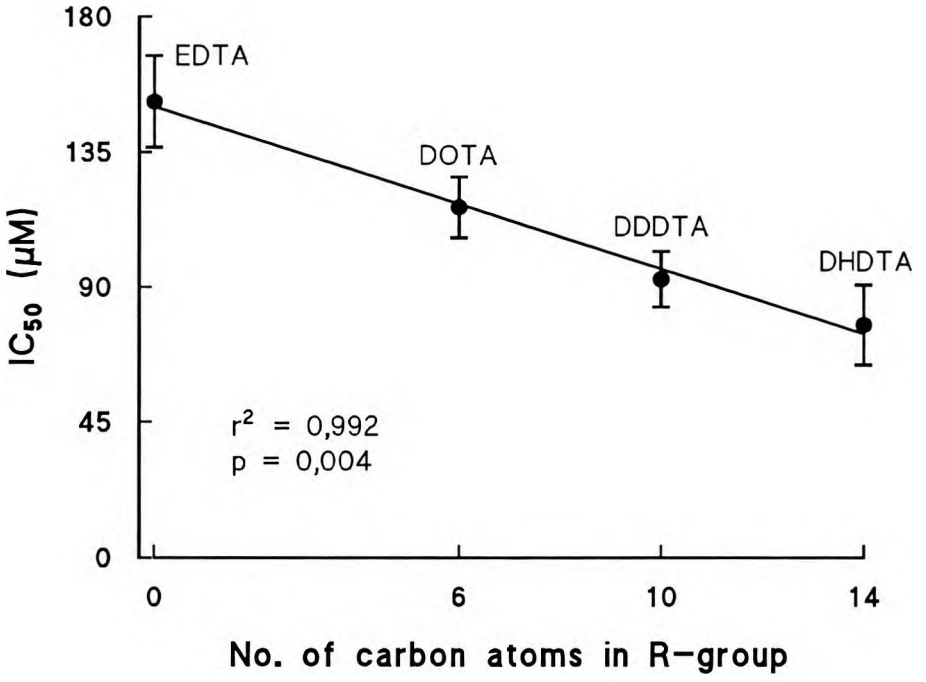


Figure 5.10: The correlation between the number of carbon atoms in the R-group and the antimalarial activity of the EDTA alkyl derivatives. (See Figure 5.5 for chemical structures).

5.4.3 COMBINED EFFECT OF IRON CHELATING AGENTS AND CLASSICAL ANTIMALARIALS ON THE GROWTH OF THE FCR-3 STRAIN

The additive interaction between iron chelating agents and the classical antimalarials (Figure 5.11 to 5.13) was determined using the type A method with fixed concentrations

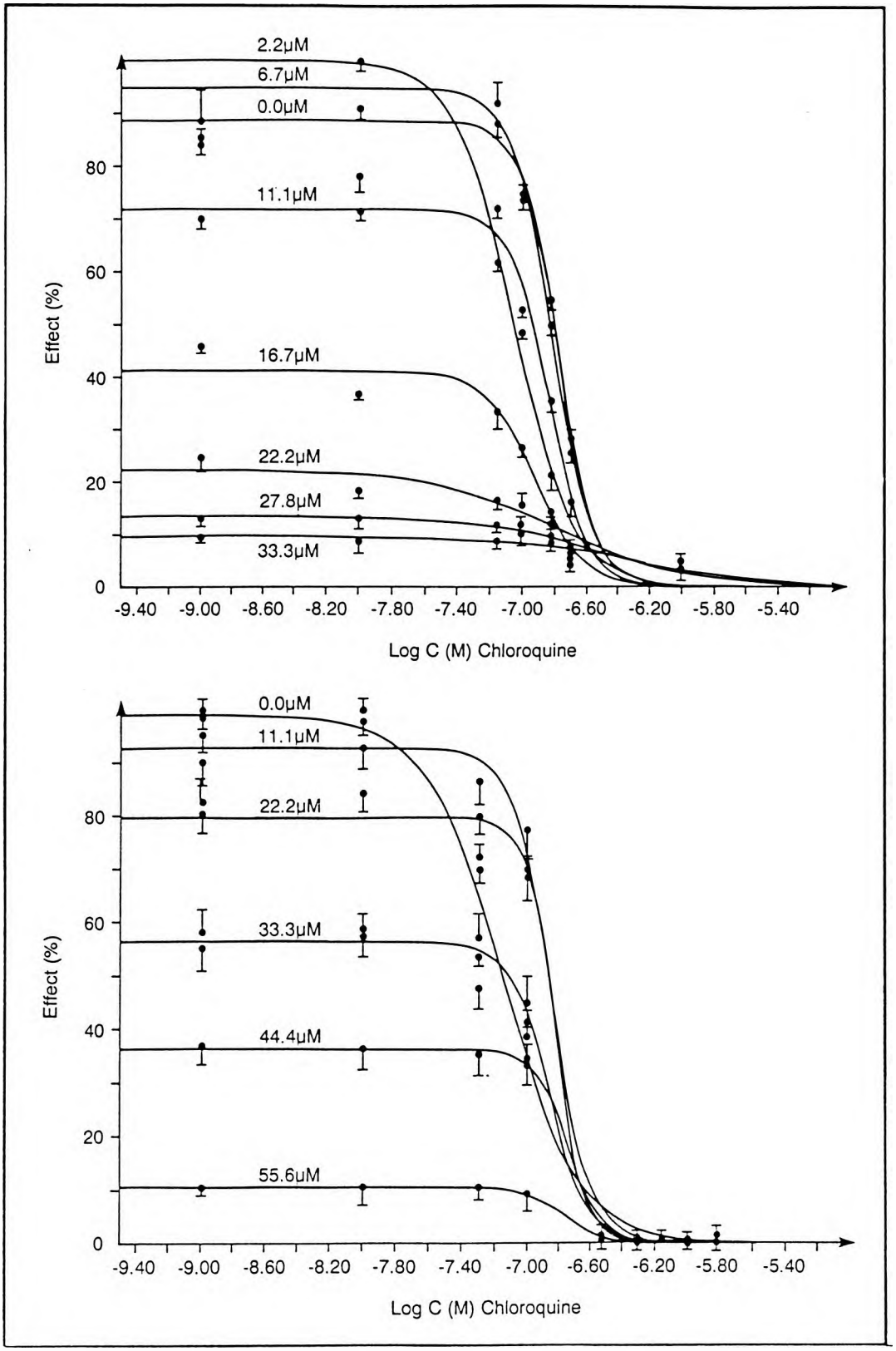


Figure 5.11: Dose-response curves showing the combined effects of chloroquine with desferrioxamine (top) and 2,2'-bipyridyl (bottom) on the growth of *P. falciparum* FCR-3 strain.

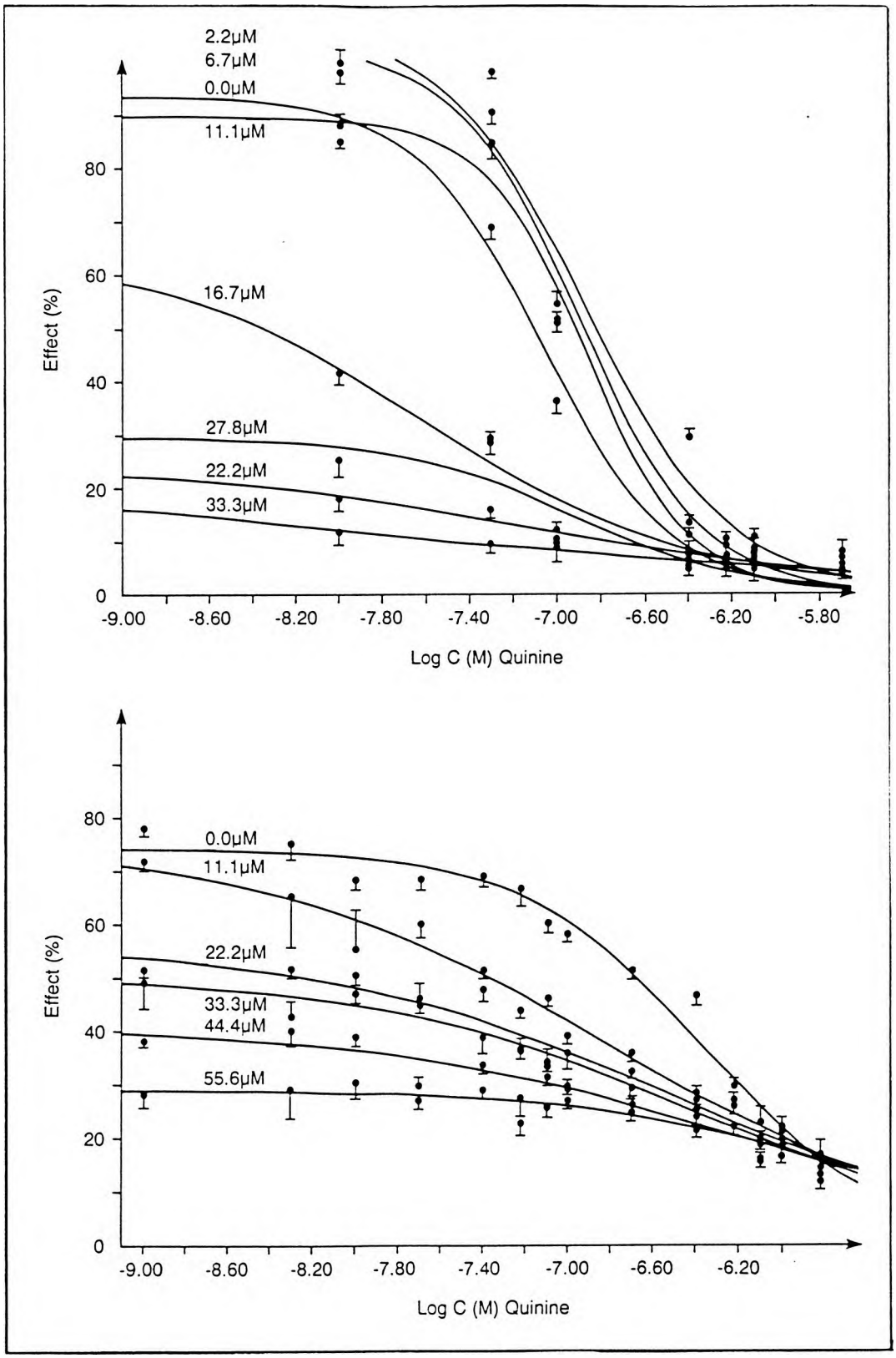


Figure 5.12: Dose-response curves showing the combined effects of quinine with desferrioxamine (top) and 2,2'-bipyridyl (bottom) on the growth of *P. falciparum* FCR-3 strain.

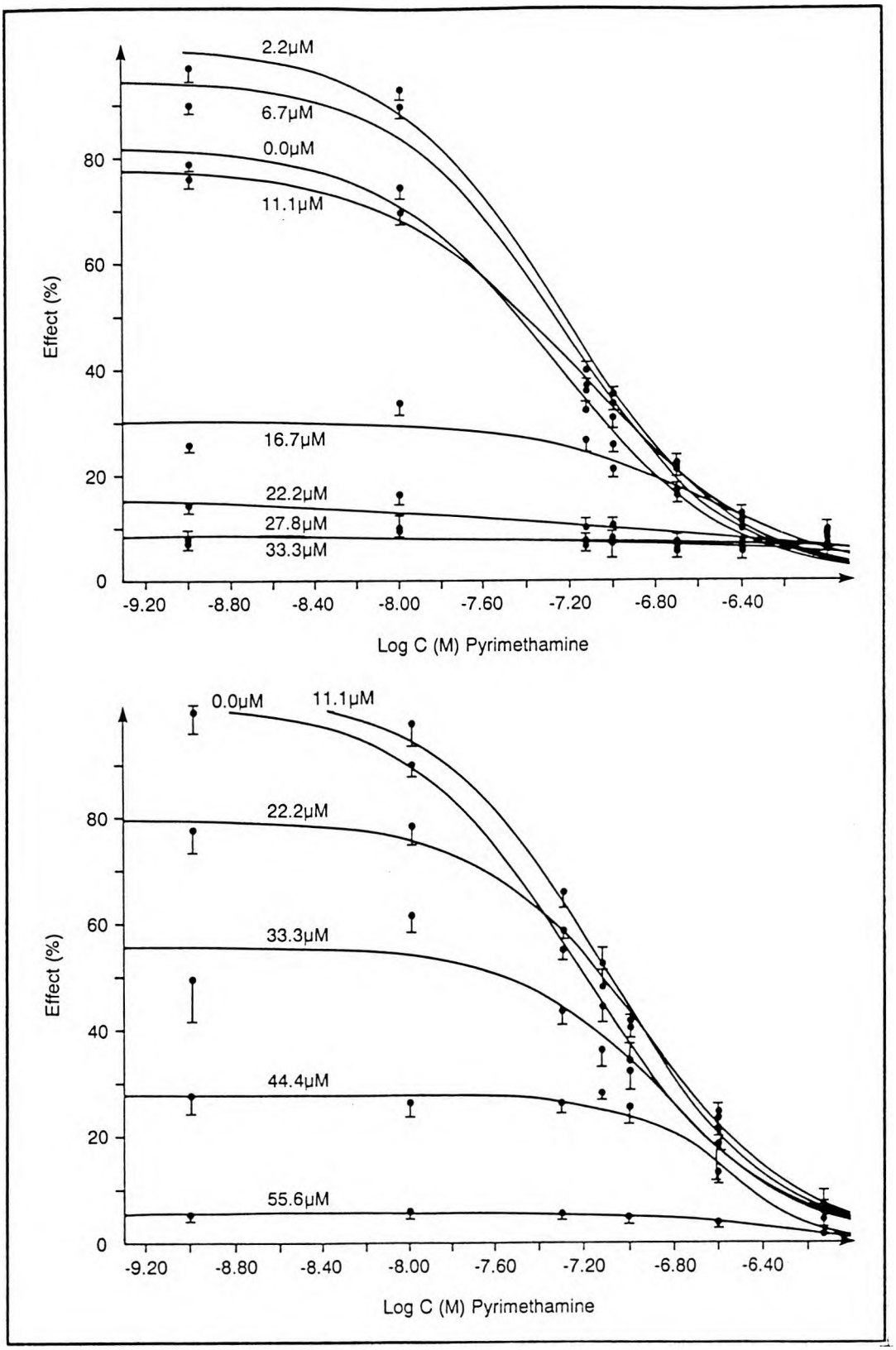


Figure 5.13: Dose-response curves showing the combined effects of pyrimethamine with desferrioxamine (top) and 2,2'-bipyridyl (bottom) on the growth of *P. falciparum* FCR-3 strain.

(Chapter 2.6.2.1.1). The presence of the iron chelating agents was indicated by the downward shift of the dose response curves of the classical antimalarials, as the concentration of iron chelating agents increased.

5.4.4 COMBINED EFFECT OF FERRIC AND/OR FERROUS IRON CHELATING AGENTS ON PARASITE GROWTH

The interaction between the ferric and ferrous iron chelating agents were tested using the type B method with fixed concentration ratios (Chapter 2.6.2.1.2). Two ferric chelating agents, namely desferrioxamine and desferrithiocin were combined and an additive interaction was observed (Figure 5.14); whilst a synergistic effect was observed when the two ferrous chelating agents, 2,2'-bipyridyl and bathophenanthroline were combined (Figure 5.15).

When a ferric and ferrous iron chelating agent were combined, variable interactions resulted. The combinations of bathophenanthroline, a hydrophilic ferrous chelating agent, with either desferrioxamine or desferrithiocin, ferric chelating agents, resulted in synergistic interactions (Figure 5.15; bottom). However, antagonism occurred when 2,2'-bipyridyl, a lipophilic ferrous chelating agent was combined with the latter ferric chelating agents (Figure 5.15; bottom). This antagonistic interaction between desferrioxamine and 2,2'-bipyridyl was present in both the chloroquine-sensitive, 3D7-A and -resistant FCR-3 strains (Figure 5.16).

To determine whether the latter antagonistic interaction was as a result of either drug affecting the accumulation of the other into the parasitized erythrocyte, a time interval of 9 hours was introduced between the addition of each chelating agent (Figure 5.17). The addition of desferrioxamine 9 hours before 2,2'-bipyridyl still resulted in an antagonistic interaction, however it was not as pronounced as when desferrioxamine and 2,2'-bipyridyl were simultaneously added at time 0. The addition of 2,2'-bipyridyl 9 hours before desferrioxamine, potentiated the antagonistic interaction, such that greater concentrations of the iron chelating agents were required to inhibit parasite growth.

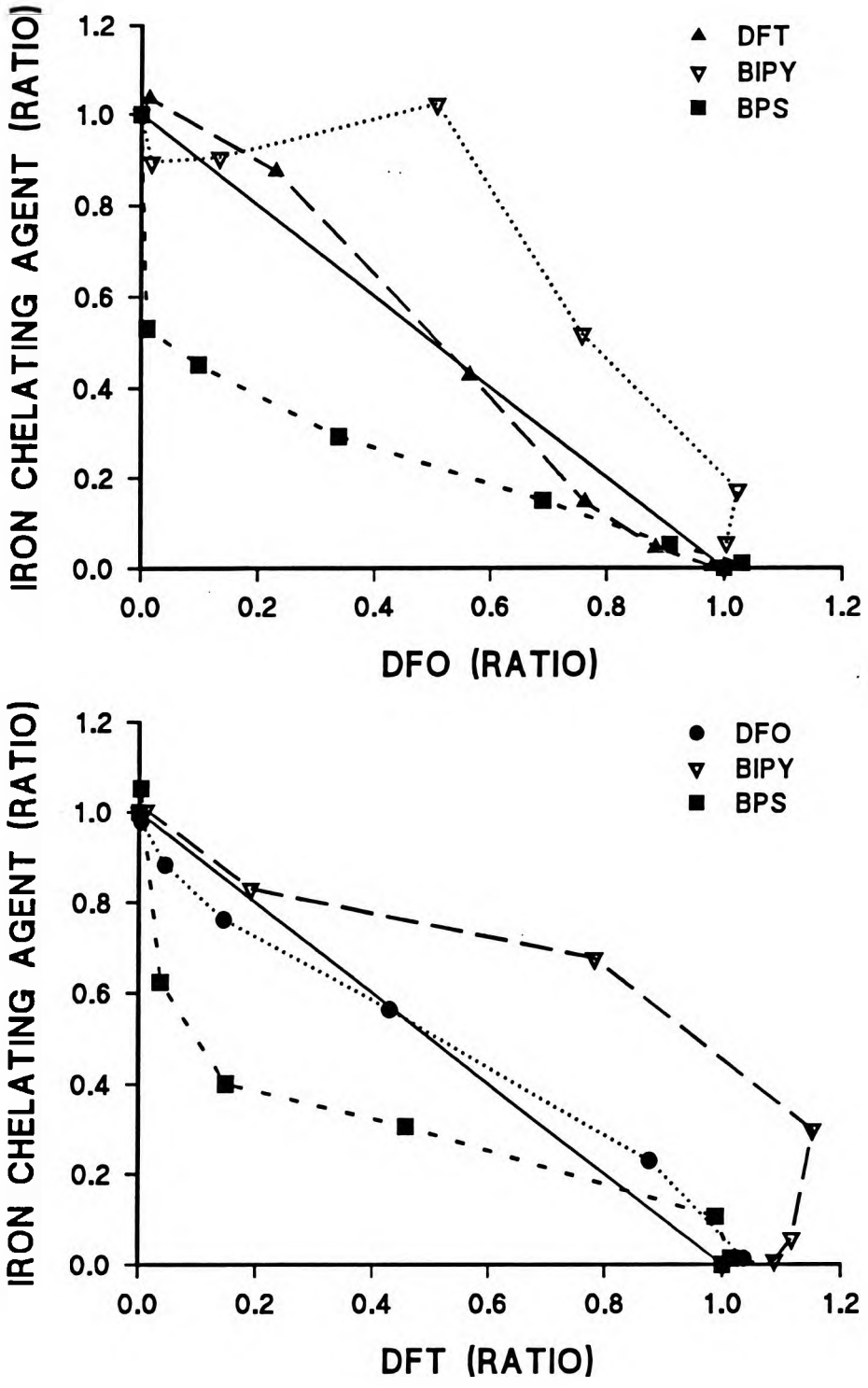


Figure 5.14: The isobolograms of the ferric iron chelating agents desferrioxamine (DFO; top) and desferrithiocin (DFT; bottom) against other iron chelating agents. Where BIPY is 2,2'-bipyridyl and BPS is bathophenanthroline.

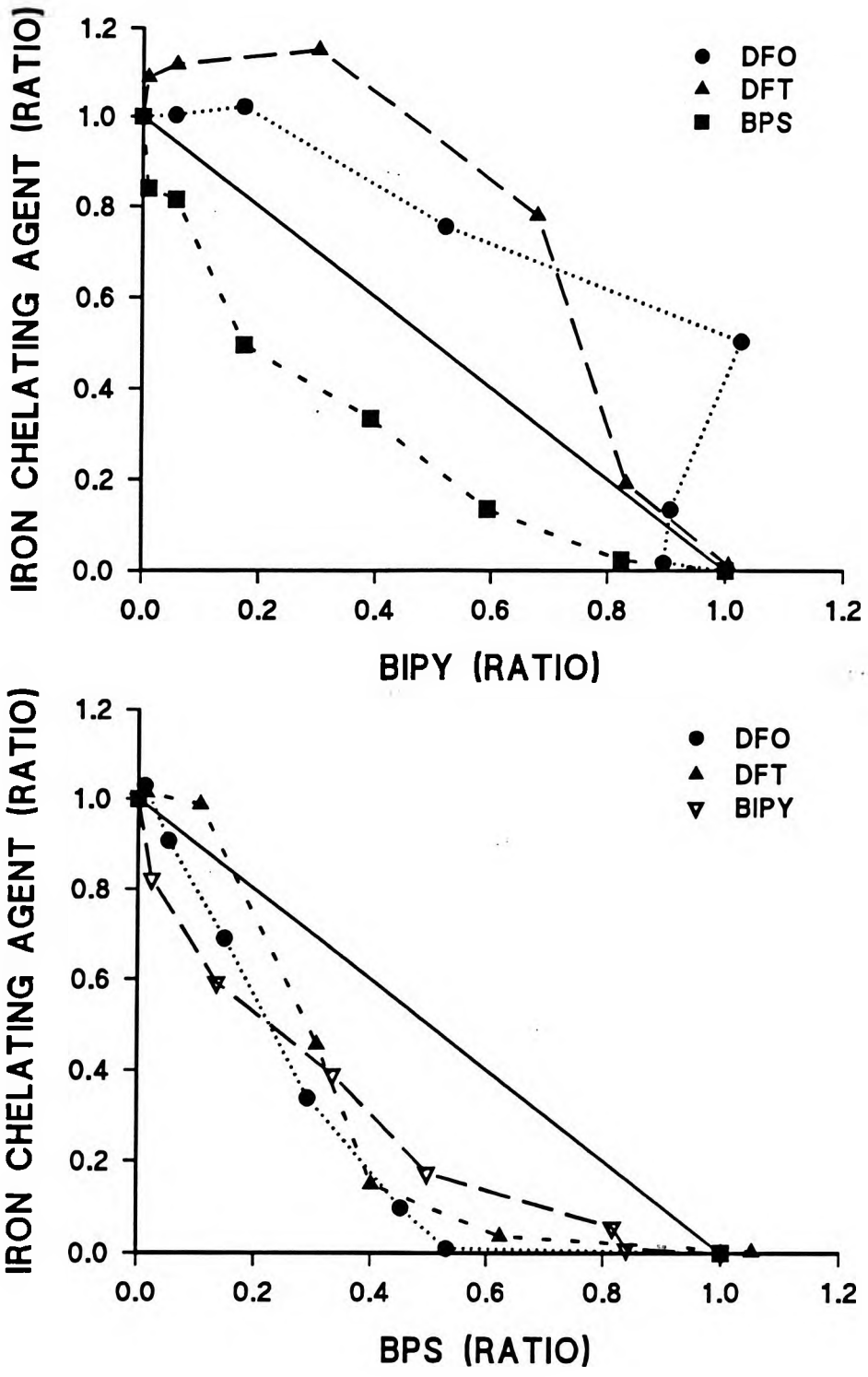


Figure 5.15: The isobolograms of the ferrous iron chelating agents 2,2'-bipyridyl (BIPY; top) and bathophenanthroline (BPS; bottom) against other iron chelating agents. Where DFO is desferrioxamine and DFT is desferrithiocin.

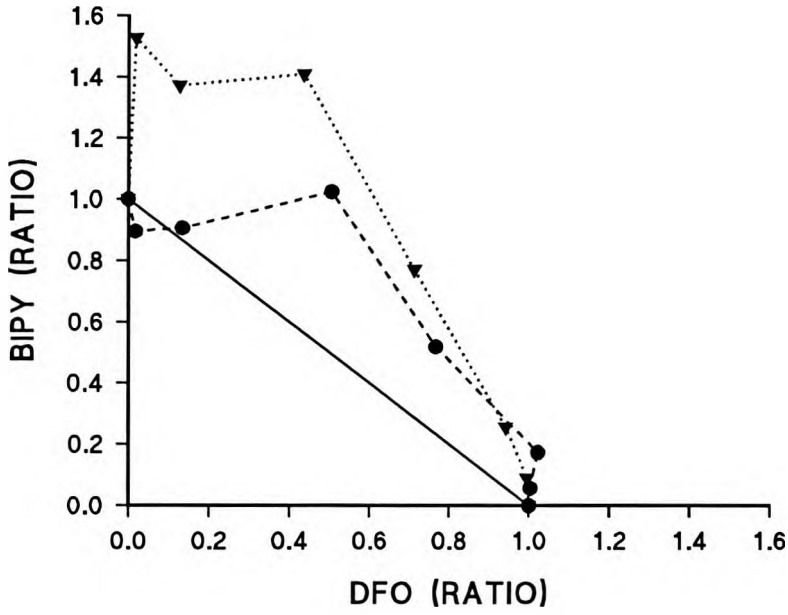


Figure 5.16: The isobologram showing antagonistic drug interactions between desferrioxamine and 2,2'-bipyridyl in both the chloroquine-sensitive 3D7-A (●) and chloroquine-resistant FCR-3 strains (▼).

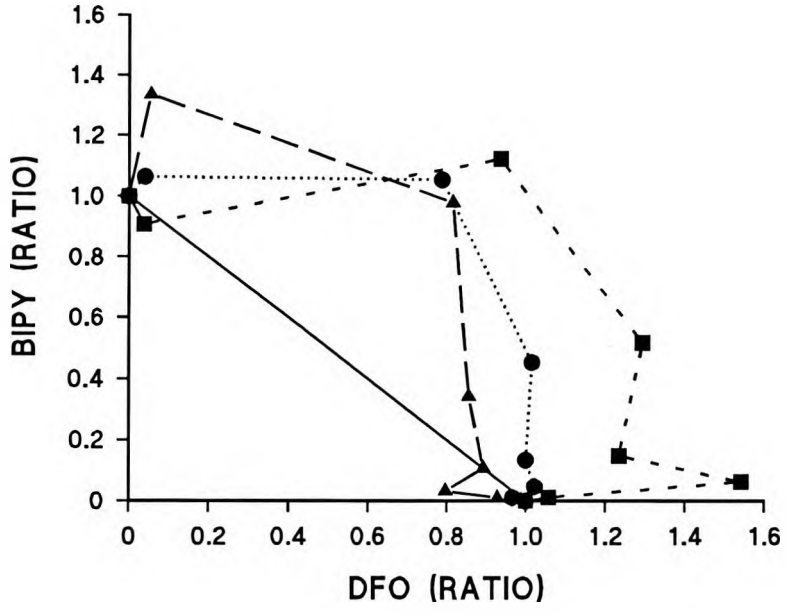


Figure 5.17: The effect of a time interval between the addition of desferrioxamine (DFO) and 2,2'-bipyridyl (BIPY). ●: DFO and BIPY added simultaneously at time 0 hour; ▲: DFO added 9 hours before BIPY and ■: BIPY added 9 hours before DFO.

5.5 DISCUSSION

5.5.1 EFFECT OF DESFERRIOXAMINE, 2,2'-BIPYRIDYL AND CLASSICAL ANTIMALARIALS ON THE GROWTH OF *P. FALCIPARUM* ISOLATES

In nature the parasites regularly undergo passage through mosquitoes, during which the sexual stages of the life cycle occur. Hence under natural conditions, genetic recombination inevitably occurs following meiosis, leading to diversification of such characteristics as antigens and drug susceptibility in the progeny (Sinden, 1991). The latter is well illustrated in Table 5.1, where the *in vitro* isolates display very different drug sensitivities. The resistant trait follows a Mendelian inheritance pattern with the progeny displaying various levels of resistance. Drug resistance may be due to a variety of mechanisms including natural selection or genetic or metabolic changes (Sinden, 1991). Ward *et al.* (1995) believes in the existence of more than one phenotypically distinct, resistance mechanism in the highly chloroquine-resistant parasites; such that one or more of the previously hypothesised mechanisms of resistance (Chapter 5.1.3.2) could account for the increased chloroquine-resistance in the FCR-3 strain. Alternatively, quinoline resistance could result from an increased rate of cytochrome P450 enzyme activity to form less active metabolites (Salganik *et al.*, 1987; Ndifor *et al.*, 1990).

The variations in IC_{50} values for the iron chelating agents in the different strains are more difficult to explain. Possibly the iron concentrations of the host plasma and erythrocyte affected the antimalarial activity of the agents. The plasma from three individuals were pooled, so theoretically the iron concentrations should be similar, whilst the erythrocytes were obtained from healthy individuals with no apparent iron abnormalities, as noted by the South African Blood Transfusion Services. The differences in sensitivities to the chelating agents could be due to genetic changes, as in chloroquine resistance, and slight biochemical changes. By altering biochemical processes, the parasites need for iron may be reduced or rendered unobtainable for chelation. In all the isolates the ferric iron chelator, desferrioxamine, had a greater antimalarial activity than the ferrous iron chelator, 2,2'-bipyridyl (Table 5.1). The greater efficacy of desferrioxamine over 2,2'-bipyridyl could be due to desferrioxamine being more efficient at low concentrations, because of its

greater binding affinity and low dissociation constant (Singh and Hider, 1994).

5.5.2 EFFECT OF VARIOUS CHELATING AGENTS ON THE *IN VITRO* GROWTH OF THE CHLOROQUINE-RESISTANT FCR-3 STRAIN

5.5.2.1 Citrate

Citrate is known to sequester trace metals such as Ca^{2+}, Mg^{2+} and Fe^{3+}. Thus, due to the non-selectivity of citrate, a high concentration was required to render a nutritional immunity status. The physiological concentration of citrate in adult whole blood is reported to be about 0,1 mM. The IC_{50} of 7,80 $\pm$ 1,04 mM (Table 5.2) would result in citrate toxicity and Ca^{2+} deficiency. In addition, the resultant acidity at this high concentration could cause acidosis and haemolysis (White and Warrell, 1988). The ferric-citrate complex acts as a poor catalyst for the production of hydroxyl radicals via the Fenton reaction (Figure 5.1), but this is unlikely to be the mechanism of antimalarial activity (Prabhu and Krishnamurthy, 1993). The most probable mechanism of action would be the sequestration of essential cationic nutrients. However, due to the toxic concentrations required to inhibit parasite growth, citrate can be eliminated as a possible antimalarial.

5.5.2.2 Ascorbate

Ascorbate inhibited the parasite in a dose dependent manner, with an IC_{50} of 1,99 $\pm$ 0,33 mM (Table 5.2). A healthy individual only contains up to 200 μM ascorbate in the plasma, which is definitely insufficient to have any antimalarial effect (Das *et al.*, 1993). Golenser *et al.* (1991) reported that the pro-oxidant actions of ascorbate prevent the development of the trophozoite-infected erythrocytes to the late schizont stage.

Ascorbate can maintain the metals in their reduced state, thus depriving the parasite of metals (Marva *et al.*, 1989). However, high concentrations of vitamin C do not eliminate *P. berghei* infections in mice (Levander and Ager, 1993), thus, ascorbate can be disregarded as a possible antimalarial.

5.5.2.3 Apotransferrin

The plasma of healthy and malaria-infected individuals contain approximately 1,96 ± 0,42 g/l and 2,64 ± 0,56 g/l of transferrin, respectively (Aremu, 1989). This is significantly less than the concentration (12,55 ± 0,53 g/l) required to inhibit an *in vitro* infection with a 0,5% parasitaemia. Apotransferrin probably functions by chelating the plasma iron ($K_a = 10^{26}\ M^{-1}$), thereby inhibiting the iron dependent processes of the parasite (Bridges and Seligman, 1995).

However, the parasitaemias in malaria infections are rarely so low, thus much higher concentrations of apotransferrin would be required. But it may be potentially harmful to therapeutically administer high concentrations of apotransferrin, due to its involvement in the intricately balanced immune system. Thus, the addition of apotransferrin cannot be considered as a practical solution in eliminating a malarial infection.

5.5.2.4 Aminocarboxylate compounds

5.5.2.4.1 DTPA

The hydrophilic nature of DTPA inhibits the drug from penetrating into parasitized erythrocytes (Figure 5.4) and this probably accounts for it being an ineffective antimalarial (IC_{50} = 558,28 ± 48,92 μM; Table 5.2). Thus, DTPA chelates and deprives the parasite of extracellular cations, such as iron, zinc and copper. However, due to the high concentrations of cations in human plasma, very high concentrations of DTPA would have to be administered in order to achieve a deficient status. In addition, since DTPA does not selectively chelate iron, it can result in hypocalcaemia (Gibson and Swanepoel, 1995). Therefore, DTPA is not practical as a therapeutic agent in the treatment of malaria.

5.5.2.4.2 EDTA

The high concentration of EDTA (IC_{50} = 151,81 ± 15,22 μM) required to inhibit parasite growth could be accounted for by its hydrophilic nature (Table 5.2). This property prevents the agent from permeating into the parasitized erythrocytes, and instead the extracellular cations are chelated. At these high concentrations, there was sufficient EDTA to chelate the majority of the cations in the culture medium, causing a deficiency of essential nutrients, which adversely affected parasite growth. The disodium form of EDTA

was used in these experiments to enable EDTA to chelate cations with higher stability constants than sodium. Calcium deficiency caused by Na_2EDTA is known to inhibit merozoite reinvasion, thus it is possible that the malaria infection could be inhibited over a double life cycle (Klaasen, 1985). However, as for DTPA, the use of Na_2EDTA would be contraindicated in clinical practice.

5.5.2.4.3 Alkyl derivatives of EDTA

In order to increase the lipophilicity of EDTA, Dr. Leseticky (Charles University, Prague) modified the R-group of EDTA by altering the length of the attached alkyl groups (Figure 5.5). This was proven to be the case and as seen in Figure 5.10, there is a significant correlation ($p = 0,004$) between the lipophilicity of the drug and the number of alkyl groups added to the EDTA structure. This modification effectively increased the antimalarial activity of the EDTA class with the IC_{50} value decreasing from $151,81 \pm 15,22$ μM for EDTA (R = H) to $77,22 \pm 13,38$ μM for DHDTA ($R = C_{14}H_{29}$) (Table 5.2). But the increase in lipid solubility could be potentially hazardous in a clinical setting, as this property could allow the chelating agent to cross the blood brain barrier, resulting in central nervous system toxicity (Porter *et al.*, 1990).

5.5.2.4.4 EGTA

EGTA was nearly one and a half times less effective as an antimalarial than EDTA . The hydrophilic nature of EGTA dictates that it acts extracellularly and chelates, with decreasing affinity, calcium, iron and magnesium (Baker *et al.*, 1985). It is unlikely that under the relatively anaerobic conditions of malaria cultivation, that this aminocarboxylate ligand acts as a free radical generator, but primarily by starving the parasite of essential cations (Aruoma *et al.*, 1989).

5.5.2.4.5 Effect of $NaHCO_3$ on aminocarboxylate activity

The use of different solvents, such as culture medium or 5% $NaHCO_3$ (125 μM in the highest concentration) resulted in significant differences in antimalarial activities of the aminocarboxylates (Chapter 5.4.2). This can be attributed to the fact that these weak acids can displace CO_2 from carbonates and react with the metals and form hydrogen. The sodium-chelate complex is then able to chelate cations for which it has greater affinity

(Klaassen, 1985). Although it should be noted that the culture medium, which is used to prepare the parasite suspension, already contains 25 mM $NaHCO_3$. The addition of a further 125 μM did not significantly increase the pH or affect parasite growth. Another possibility for the variability observed is that the chelating agent is saturated with the cations from the culture medium, before the dilutions are added to the parasitized suspension. This is possible since the plasma-supplemented culture medium contains 0,1 g/l of $MgSO_4.7H_2O$ and $CaNO_3.4H_2O$, and trace amounts of iron and copper (Freshney, 1987).

5.5.2.5 Nitrilotriacetic acid

Nitrilotriacetic acid (Figure 5.6) is often used to load cells with iron, but it has been reported that nitrilotriacetic acid is ineffective in blocking iron uptake into reticulocytes, since its hydrophilicity prevents it from reaching the site in the plasma membrane, where the iron becomes available for chelation (Nunez *et al.*, 1983). However, nitrilotriacetic acid is proposed to inhibit cell growth through its ability to free radicals, which can result in the lipid peroxidation of membranes (Aruoma *et al.*, 1989). Thus, it is possible that nitrilotriacetic acid induces haemolysis of the parasitized erythrocytes. However with the antioxidant properties of the plasma constituents, the latter seems unlikely to be the mechanism by which nitrilotriacetic acid inhibits parasite growth. The ineffectiveness of nitrilotriacetic acid as an antimalarial (IC_{50} of 1,74 $\pm$ 0,004 mM) and its reported carcinogenicity, warrants that it be disregarded as a possible antimalarial.

5.5.2.6 Desferrioxamine

Desferrioxamine was the most potent of the tested chelating agents, with an IC_{50} of 15,11 $\pm$ 3,00 μM (Table 5.2). The antimalarial activity of desferrioxamine on the *in vitro* growth of *P. falciparum* is also documented by Raventos-Suarez *et al.* (1982) and Pollack and Fleming (1984). It is proposed that desferrioxamine specifically chelates essential intraparasitic iron, rather than the extracellular plasma or intraerythrocytic iron (Figure 3.11) (Peto and Thompson, 1986; Scott *et al.*, 1990).

Desferrioxamine is also reported to increase free radical formation in the presence of oxygen and may contribute to the antimalarial activity of desferrioxamine. This is possible

since malaria parasites are particularly sensitive to oxidative stress, as the host-derived antioxidant defense system does not provide much protection from the deleterious effects of free radicals (Buffington *et al.*, 1986). However, free radical damage is not regarded as the primary mechanism of action for desferrioxamine. Instead, its mode of antimalarial action resides in its potential to induce a deficiency in bioavailable iron. This would greatly affect the metabolism of plasmodia, which are strongly dependent on iron-dependent reductases, oxidases and hydrolases (Raventos-Suarez *et al.*, 1982).

Although, desferrioxamine is the most potent antimalarial of the iron chelating agents tested, it does not completely inhibit the malarial infection even at 100 μM, thus it should be used in conjunction with another antimalarial agent (Figure 5.11 to 5.13).

5.5.2.7 Desferrithiocin

Desferrithiocin was effective in inhibiting the *in vitro* growth of the malaria parasite, with an IC_{50} value of 22,11 $\pm$ 3,33 μM. Fritsch *et al.* (1987) has also reported that desferriferrithiocin has antimalarial properties against the *P. falciparum* KCB strain with an IC_{50} value of between 25 to 30 μM. Despite the usual loss of iron binding affinity of bidentate ligands, desferrithiocin affects *in vitro* parasite growth at concentrations comparable to desferrioxamine (IC_{50} value of 15,11 $\pm$ 3,00 μM), bathophenanthroline (IC_{50} value of 23,58 $\pm$ 0,11 μM) and 2,2'-bipyridyl (IC_{50} value of 25,33 $\pm$ 8,14 μM).

Desferrithiocin is proposed to cross the cell membrane by a diffusion controlled process and to accumulate mainly in the cytosol and to a lesser degree in the mitochondria (Jin *et al.*, 1989). Thus, it is possible that desferrithiocin has access to the intracellular iron pools and mitochondria in parasitized erythrocytes and thereby inhibit the iron-dependent biochemical processes in the parasite (Feagin *et al.*, 1991; Pollack, 1994).

The availability of iron for incorporation into iron-dependant enzymes (ribonucleotide reductase and dihydroorate dehydrogenase enzyme) may further be decreased if desferrithiocin mobilizes and chelates the iron from the parasitized erythrocyte ferritin (Chapter 3.1.1.5) (Longueville and Crichton, 1986).

The release of the desferrithiocin-iron complex from the cell is much slower than for uncomplexed desferrithiocin, possibly due to the increased size of the chelate complex, which consists of 2 molecules of desferrithiocin and an iron atom (Jin *et al.*, 1989). As a result of the slow efflux of the chelate complex, its toxic properties possibly also contribute to the inhibitory action of the drug. However, its toxic properties are not confined to the parasitized erythrocytes. The chelate complex is reported to affect T-cell function, increase the oxidative damage of haemoglobin and disrupt the structural integrity of membranes (Bierer and Nathan, 1989; Rice-Evans *et al.*, 1987). *In vivo* studies reveal a variety of toxic signs such as decreased body weight, anorexia, dysfunction and neurological symptoms (Wolfe, 1990).

Therefore, the sodium salt analogue of desferrithiocin (used in these experiments) does not appear to be a viable option. Although, small structural modifications to the chemical structure of desferrithiocin have been shown to profoundly reduce the compounds observed toxic side effects, while still maintaining its affinity for ferric iron and its iron clearing properties. This was achieved by the removal of the methyl group from the desferrithiocin backbone (Figure 5.3). Thus, the latter analogue may be beneficial as an antimalarial chemotherapeutic agent (Bergeron *et al.*, 1994).

5.5.2.8 Bathophenanthroline and 2,2'-bipyridyl, ferrous iron chelating agents

The chelating agents, bathophenanthroline and 2,2'-bipyridyl were found to be the next most potent of the antimalarials tested (Table 5.2), with their activities being attributed to their high specificity for the ferrous iron (Morgan, 1983).

Bathophenanthroline does not inhibit parasite growth through free radical generation, but possibly chelates the extracellular or membrane-associated iron or copper, and thereby inhibits the iron/copper dependent metabolism of the parasite.

As initially proposed 2,2'-bipyridyl did inhibit the uptake of both transferrin and non-transferrin-bound iron into parasitized erythrocytes (Figures 3.12 and 3.13, respectively). 2,2'-Bipyridyl possibly also inhibits the metalloenzymes in the parasite by depleting the intraparasitic iron and copper pools. The toxicity of the copper-2,2'-bipyridyl chelate is

possibly due to the formation of hydroxyl radicals by the copper-catalysed Fenton reaction (Figure 5.1), which can induce single-stranded DNA breaks and subsequent cell death (Chevion, 1988).

5.5.3 COMBINED EFFECT OF IRON CHELATING AGENTS AND CLASSICAL ANTIMALARIALS ON THE GROWTH OF THE FCR-3 STRAIN

Overall the drug combinations resulted in additive effects on the *in vitro* growth of *P. falciparum* (Figure 5.11 to 5.13). When combined, chloroquine and desferrioxamine acted independently of one another (Figure 5.11). The latter result was clinically substantiated by Traore *et al.* (1991); who showed that the combination of desferrioxamine and chloroquine increased the rate of parasite clearance in *P. falciparum*-infected patients. However, when low concentrations of desferrioxamine and the antimalarials were combined, a slight antagonistic interaction was observed (Figures 5.11 to 5.13). The antagonist interaction between desferrioxamine and chloroquine was also observed by Jambou *et al.* (1992). Similarly, an antagonistic interaction was observed between low concentrations of 2,2'-bipyridyl and pyrimethamine (Figure 5.13).

Chloroquine may exert its antimalarial effect through its interaction with haem (Chapter 5.1.3.2.1) or its lysosomotropic properties (Chapter 5.1.3.2.2), or by its ability to produce free radicals via the Fenton reaction (Figure 5.1) (Barraviera, 1989). Alternatively, chloroquine could increase the pH of the food vacuole and thereby, either inhibit the release of iron from internalized transferrin or from digested haemoglobin (Lestas, 1976; Gabay and Ginsburg, 1992). The presence of a transmembrane enzyme, NADH diferric transferrin-reductase, enables iron to be transported through the plasma membrane (Fry, 1989). Recently, Toole-Simms *et al.* (1990) reported that chloroquine can inhibit this reductase enzyme, and thereby influence endosome acidification and iron metabolism.

The antimalarial effect of desferrioxamine may be through its ability to produce free radicals in the presence of ferrous irons (Jin *et al.*, 1989). Conversely, desferrioxamine is also reported to be an effective inhibitor of iron-stimulated lipid peroxidation, implying

that the primary mechanism of chloroquine may not be through its ability to induce oxidative stress (Halliwell and Gutteridge, 1989). Gordeuk *et al.*, (1995) also proposed that the presence of the free radical scavenger, desferrioxamine could possibly protect cerebral capillaries from iron-catalysed free radical damage. However, the primary mechanism of action of desferrioxamine is still thought to be the chelation of the intraparasitic iron, which could interfere with metabolic processes, such as cytochrome activity and DNA synthesis. The cytocidal effect of desferrioxamine on the pigmented trophozoite-infected erythrocytes may be as a result of the chelation of the iron from the iron-containing enzymes involved in DNA synthesis, ribonucleotide reductase (Figure 5.2), dihydroorate dehydrogenase and DNA polymerase (Cabantchik, 1995).

High concentrations of desferrioxamine (33,3 μM) masked the effects of chloroquine, such that no additive effect on parasite growth was observed (Figure 5.11). This could indicate that at such high concentrations of desferrioxamine, the primary mechanism by which the parasites were killed was by the capacity of desferrioxamine to chelate cations, such as copper, zinc, cobalt, magnesium and calcium, that are present in the extra- and intracellular fluids (Waxman and Brown, 1969).

Additive effects were observed when desferrioxamine was combined with quinine or pyrimethamine (Figures 5.12 and 5.13). Thus, desferrioxamine did not interfere with the suggested lysosomotropic actions of quinine or vice versa. Both desferrioxamine and pyrimethamine inhibit DNA synthesis, by affecting the levels of deoxyribonucleotide triphosphates (Figure 5.2). By inhibiting the dihydrofolate reductase and thymidylate synthetase enzymes, pyrimethamine prevents the formation of tetrahydrofolate and the conversion of dUMP to dTMP, respectively. Desferrioxamine inhibits the ribonucleotide reductase enzyme by chelating the intraparasitic iron, thus inhibiting the regeneration of the iron-radical centre in the enzyme (Figure 5.2). The resultant effects are that desferrioxamine decreases dUDP and dUMP synthesis and with the inhibition of H_4-folate production by pyrimethamine, no dTTP is synthesised. With the net result that an additive effect was observed on the inhibition of ^{3}H-hypoxanthine incorporation into parasite DNA (Figure 5.13). The results from a clinical trial on children with cerebral malaria, supported the finding that desferrioxamine can be effectively used in combination with the standard

therapy for cerebral malaria, i.e. quinine and sulfadoxine-pyrimethamine (Gordeuk *et al.*, 1992a).

When the ferrous iron chelating agent, 2,2'-bipyridyl, was combined with chloroquine, pyrimethamine and quinine (Figures 5.11 to 5.13), additive effects were observed on the inhibition of parasite growth. This indicated that the ferrous iron-chelating agent, which works at the membrane level, does not interfere with the accumulation or the effects of these antimalarials. It also shows that the primary mechanism of action for these classical antimalarials is not by the production of iron-catalysed free radicals, as the addition of 2,2'-bipyridyl would have inhibited their formation. Conversely, the classical antimalarials do not interfere with the iron chelating abilities or free radical activities of 2,2'-bipyridyl.

5.5.4 COMBINED EFFECT OF FERROUS AND/OR FERRIC IRON CHELATING AGENTS ON PARASITE GROWTH

5.5.4.1 Combined effect of two ferric chelating agents on parasite growth

Desferrioxamine and desferrithiocin, the two most efficient of the tested chelating agents with IC_{50} values of 15,11 $\pm$ 3,00 and 22,11 $\pm$ 3,33 μM, respectively, are hydrophilic, ferric iron chelating agents (Table 5.2 and Figures 5.1 and 5.2). The additive interaction observed between these two agents, indicates that there is no interference with the pathway by which they accumulate into the parasitized erythrocyte (Figure 5.14). Desferrithiocin passively diffuses into the parasitized erythrocyte at a faster rate than desferrioxamine (Jin *et al.*, 1989), thus there is no delay in the inhibition of parasite growth. Desferrioxamine, on the other hand, accumulates slowly into the parasite as a function of the concentration gradient between the extra- and intracellular media. Desferrithiocin is reported to mobilize iron mainly from the cell cytosol and to a lesser extent from the mitochondria. In contrast desferrioxamine is reported to mobilize iron equally from the cytosol and lysosomes (Jin *et al.*, 1989). Thus, the combination of desferrioxamine and desferrithiocin could mobilize and chelate iron from the latter organelles in the parasitized erythrocytes, such that they complement each others antimalarials activities.

These agents both chelate the ferric state of iron, thus the equilibrium of the parasite iron will shift towards the formation of ferric iron and the concentration of ferrous iron will decrease (Figure 5.18). With the chelation of ferric iron and subsequent depletion of ferrous iron, essential biochemical reactions in the parasite will be inhibited and parasite death will eventually occur.

Both desferrioxamine and desferrithiocin form toxic iron-chelate complexes which are retained in the parasite for extended periods of time and this could contribute to their combined antimalarial action (Bierer and Nathan, 1989; Cabantchik, 1995).

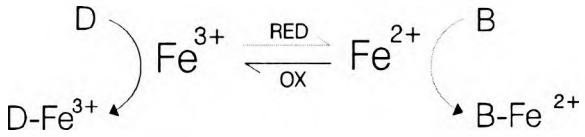


Figure 5.18: The influence of ferrous (B) and ferric (D) iron chelating agents on the equilibrium of iron.

An additive effect has also been reported to occur between the two hydrophilic ferric iron chelating agents, L1 (deferiprone) and desferrioxamine (Mabeza *et al.*, 1997). However, when hydrophobic ferric chelating agents, such as the hydroxamate-based agents (pyridoxal and salicylaldehyde isonicotinoyl hydrazone) and reversed siderophores were combined with desferrioxamine, an overadditive/synergistic interaction resulted (Tsafack *et al.*, 1995; Tsafack *et al.*, 1996). This interaction is proposed to involve the following: the lipophilic agent rapidly enters the parasite, chelates the iron and then transfers this iron to the extracellularly located, desferrioxamine. Thus, desferrioxamine can withhold both the intra- and extracellular iron from the parasite (Tsafack *et al.*, 1996).

5.5.4.2 The combined effect of two ferrous iron chelating agents on parasite growth

The combined effect of the hydrophilic ferrous chelating agent, bathophenanthroline and the lipophilic ferrous chelating agent, 2,2'-bipyridyl resulted in a synergistic interaction (Figure 5.15). Bathophenanthroline is able to chelate extracellular iron which is reduced

at the cell surface by the transplasma membrane electron transport system (Crane *et al.*, 1985; Low *et al.*, 1987). Whilst, once partitioned in the parasitized cell, 2,2'-bipyridyl can chelate the membrane associated iron (Nunez *et al.*, 1983). Thus, both chelating agents target the uptake of iron into the parasitized erythrocyte, thereby possibly inhibiting parasite growth.

Alternatively, it is possible that once the hydrophilic 2,2'-bipyridyl-iron complex is formed, it re-orientates itself to the membrane surface such that it can transfer the iron to the extracellularly located bathophenanthroline. The uncomplexed 2,2'-bipyridyl can then re-enter the parasitized erythrocyte to chelate additional iron. Iron predominantly exists in the ferrous state under the reducing anaerobic environment in the parasite. Thus, with the majority of the iron chelated, the remaining ferric iron would be intracellularly reduced to re-establish the ferric:ferrous iron equilibrium within the parasite (Figure 5.18). The combination of these two ferrous iron chelating agents could eventually result in the depletion of the parasite iron and thereby inhibit parasite metabolism.

5.5.4.3 The combined effect of bathophenanthroline, a ferrous iron chelating agent and a ferric chelating agent, desferrioxamine or desferrithiocin, on parasite growth

The combined interactions of bathophenanthroline with desferrioxamine or desferrithiocin, both resulted in synergistic effects on the parasite growth (Figure 5.15; bottom). All three of these chelating agents are hydrophilic in nature, however desferrioxamine and desferrithiocin can diffuse into the parasitized erythrocyte, while bathophenanthroline functions at the erythrocytic membrane surface (Jin *et al.*, 1989; Low *et al.*, 1987). In combination, whilst desferrioxamine and desferrithiocin chelate the intraparasitic iron, bathophenanthroline could prevent the uptake of iron into the parasitized erythrocytes. Thus, with depleted stores and possibly a major uptake pathway inhibited, the biochemical reactions which are catalysed by iron would eventually be inhibited. In addition, the build up of toxic iron-chelate complexes within the parasitized erythrocyte could also contribute to the parasites death (Cabantchik, 1995).

5.5.4.4 The combined effect of 2,2'-bipyridyl, a ferrous iron chelating agent and a ferric chelating agent, desferrioxamine or desferrithiocin, on parasite growth

In contrast to the synergistic interactions between the hydrophilic bathophenanthroline and ferric iron chelating agents, there was an antagonistic interaction when the lipophilic ferrous chelating agent, 2,2'-bipyridyl and the hydrophilic desferrioxamine or desferrithiocin were combined (Figure 5.15; top). The antagonistic effect between 2,2'-bipyridyl and desferrioxamine was observed in both chloroquine-sensitive and -resistant malaria strains (Figure 5.16); which possibly indicates that the iron metabolism in chloroquine-sensitive and -resistant parasites is unchanged regardless of their sensitivities to the classical antimalarials.

These chelating agents were selected as they differed in their sites and modes of action and effectively inhibited parasite growth. If they function by simply withholding iron, the combined effect should have been either additive or synergistic; however the interaction was antagonistic. Since desferrioxamine and desferrithiocin have similar chemical properties and abilities to inhibit parasite growth, the combination of 2,2'-bipyridyl and desferrioxamine was examined more closely to try and determine the reason for the antagonistic interactions between the lipophilic ferrous chelating agents and hydrophilic ferric chelating agents.

The antagonistic interaction was also observed by Jairam *et al.* (1991), who reported that this antagonism is abrogated when 2,2'-bipyridyl is saturated with ferrous ions, and that the resultant inhibition of parasite growth is due to the antimalarial activity of the desferrioxamine present. However, the converse is also possible, since the addition of iron saturated desferrioxamine has no antimalarial activity (Figure 6.3; left), the inhibition would be due to 2,2'-bipyridyl. 2,2'-Bipyridyl, a bidentate chelating agent, binds iron in a 3:1 ratio, while desferrioxamine, a hexadentate chelator, binds iron in a 1:1 ratio. Comparisons of activity on a molar basis will give desferrioxamine three times as many iron-binding equivalents as 2,2'-bipyridyl. Thus, approximately three times as much 2,2'-bipyridyl is required to chelate the same amount of iron as desferrioxamine (Singh and Hider, 1994). If the IC_{50} values of these two agents are compared (i.e. 15,11 $\pm$ 3,00 and

25,33 ± 8,14 μM for desferrioxamine and 2,2'-bipyridyl, respectively), 2,2'-bipyridyl is still efficient in inhibiting parasite growth and this could be attributed to its lipophilicity.

Under the anaerobic conditions in the parasitized erythrocyte, the iron should be predominantly in the ferrous state, which would be easily chelated by 2,2'-bipyridyl ($K_a = 10^{18} M^{-1}$), compared to desferrioxamine ($K_a = 10^2 M^{-1}$). However, desferrioxamine has a very high affinity for ferric iron ($K_a = 10^{31} M^{-1}$), whilst 2,2'-bipyridyl has a much lower affinity for this oxidised state (Waxman and Brown, 1969). Thus, the presence of both agents will shift the equilibrium between the ferric and ferrous states (Figure 5.18) and this competition for iron could be partially responsible for the observed antagonism (Yegorov *et al.*, 1993).

To investigate whether this antagonistic interaction was due to any interference with the agents uptake and accumulation, a 9 hour interval was introduced between the addition of the two iron chelating agents. When 2,2'-bipyridyl was added at time 0 and desferrioxamine 9 hours later, the antagonistic interaction was potentiated (Figure 5.17). Thus, 2,2'-bipyridyl was already partitioned into the erythrocytic and parasitic membrane, before desferrioxamine could start to passively diffuse into the parasitized erythrocyte. Desferrioxamine accumulates via the concentration gradient between the extracellular medium and the cell, and tends to mobilize iron from the cytosol and lysosomes in hepatocytes (Jin *et al.*, 1989). However, the antimalarial activity of desferrioxamine is localized to the parasite and possibly the food vacuole (Scott *et al.*, 1990). However, with 2,2'-bipyridyl partitioned into the lipophilic phase of the erythrocytic and parasitic membranes, 2,2'-bipyridyl could possibly block the diffusion of desferrioxamine across the membranes.

The possibility that 2,2'-bipyridyl interfered with the accumulation of desferrioxamine was further supported when desferrioxamine was added 9 hours before 2,2'-bipyridyl. An antagonistic interaction was still observed, however it was not as pronounced when desferrioxamine and 2,2'-bipyridyl were added simultaneously at time 0 or when 2,2'-bipyridyl was added before desferrioxamine (Figure 5.17). In this experiment, desferrioxamine had time to diffuse into the parasite and exert its antimalarial effects

before the addition of 2,2'-bipyridyl. It is possible that with higher concentrations desferrioxamine, that once the hydrophilic iron-2,2'-bipyridyl complex moves from the membrane into the extracellular medium, that desferrioxamine could permeate into the parasitized erythrocyte to inhibit parasite growth (Morgan, 1983).

In addition, desferrioxamine could scavenge the free radicals produced by 2,2'-bipyridyl (Hartley *et al.*, 1989), thereby preventing 2,2'-bipyridyl from inducing DNA damage and parasite death (Chevion, 1988). A similar antagonistic drug interaction has been reported between desferrioxamine and another ferrous-chelating agent, L2-9 (1[N-ethoxycarbonylmethyl-pyridoxy-lidenium]-2-[2'-pyridyl] hydrazine bromide) (Iheanacho *et al.*, 1990).

The antagonistic effect between desferrioxamine and 2,2'-bipyridyl can not only be accounted for by the interference of desferrioxamine accumulation by 2,2'-bipyridyl. The competition for iron and the inhibition of free radical generation possibly also contributes to the antagonistic interactions between lipophilic ferrous chelating agents and hydrophilic ferric chelating agents.

From the chelating agents tested, it can be concluded that both the lipophilicity of the compound and its affinity for iron, play an important role in determining its antimalarial potency. By examining such a wide spectrum of chelating agents, the data obtained in this chapter could contribute to the design of new iron chelating agents and antimalarial drugs. It is very likely that the iron chelating agents exert their antimalarial action by some other mechanisms, in addition to iron deprivation. It is also important to determine what variables affect the antimalarial activity of the iron chelating agents, to ensure successful treatment in a clinical setting.

CHAPTER SIX

THE EFFECT OF DIFFERENT VARIABLES ON THE ANTIMALARIAL ACTIVITY OF IRON CHELATING AGENTS

6.1 INTRODUCTION

Many factors affect the efficacy of a drug, e.g. the drug dose and pharmacokinetic variables such as bioavailability, volume of distribution, half-life and clearance rate. These factors are in turn affected by the health of the patient. For example, the volume of distribution of quinine in healthy patients is 1,5 to 3,5 l/kg. Whilst in uncomplicated malaria it is 1,7 l/kg, and in cerebral malaria, it is 1,2 l/kg. That is, the dose required to eliminate the infection is proportional to the severity of disease (Warrell *et al.*, 1990). In addition to the above, the following four variables may affect the efficacy of an antimalarial.

6.1.1 INOCULUM SIZE

Geary *et al.* (1988) reported that there is a direct relation (r = 0,987 to 0,998) between the IC_{50} of chloroquine and inoculum size, where the latter is the product of parasitaemia and haematocrit, reflecting the amount of parasites present in the culture. The theory behind this is that as the parasite accumulates the drug, the medium is depleted of the drug. Therefore, as the inoculum size increases, the initial drug concentration should be increased in order to maintain lethal intracellular concentrations. This results in a greater IC_{50} value, as the inoculum size increases.

In view of this, it is important to determine whether there is a correlation between the inoculum size and the concentration of the iron chelating agents required to inhibit 50% of parasite growth.

6.1.2 EXTRACELLULAR pH

Geary *et al.*, (1988) reported that due to the weak base property of chloroquine, its antimalarial activity is affected by the pH of the extracellular milieu. Similarly, desferrioxamine and 2,2'-bipyridyl are basic in nature. Thus, by altering the pH of the extracellular medium, it is possible to determine whether these two chelating agents

accumulate via a pH gradient.

Any alteration of the extracellular pH can also affect a number of other components, such as the erythrocytic membranes and the cytoadherence of parasitized erythrocytes in cerebral malaria. Any change in external pH could influence the charge density of the erythrocytic membrane, which in turn could affect the passage of drugs through the membrane or their incorporation into the membrane (Deamer and Nichols, 1989). Whilst, an acidic pH of 6,8 is associated with increased binding of malaria-infected erythrocytes to the cerebral endothelial cells (Marsh *et al.*, 1988). However, it seems unlikely that the serum pH in malaria patients would decrease below 7,2, even as a result of metabolic acidosis or lactic acid production by the parasites (Molyneux, 1990; Vander Jagt *et al.*, 1990; Marsh *et al.*, 1996). The presence of even modest concentrations of methaemoglobin, released from haemolysed infected erythrocytes, could exacerbate tissue hypoxia and metabolic acidosis (Anstey *et al.*, 1996). Although if the parasites are sequestered in the cerebral capillaries and venules, it may be possible that as a result of localised hypoxia and the production of lactic acid, the pH in the immediate surroundings of the parasitized erythrocytes may decrease (Molyneux, 1990; Marsh *et al.*, 1996). This pathological event could influence the chelating abilities of desferrioxamine.

6.1.3 TRANSITION METALS

The observed inhibitory effects of metal chelating agents on intraerythrocytic malaria parasites indicate that trace metals play a vital role in the biology of these organisms (Ginsburg *et al.*, 1986). Desferrioxamine and 2,2'-bipyridyl not only have high binding affinities for iron ($K_a = 10^{31}\ M^{-1}$ and $10^{18}\ M^{-1}$, respectively), but can also chelate other di- and trivalent cations, such as copper and aluminium (Waxman and Brown, 1969).

Cations play an important role in a variety of different biochemical processes, but can also catalyse potentially harmful reactions. The transition metals, iron and copper, have variable oxidation states, which enables them to be remarkably good promoters of free radical damage by the Fenton reaction (Figure 5.1), which could interfere with plasmodial

growth (Gulumian, 1994).

Approximately 80% of the absorbed Al^{3+} is transported in the plasma, bound to albumin or transferrin (K_a of 10^{21} M^{-1}) (Swartz, 1985). Al^{3+} is only required in some organisms as a trace element. In humans it is not considered to be essential for maintaining vital biochemical reactions. Desferrioxamine binds Al^{3+} with a affinity constant of 10^{21} M^{-1}, which facilitates treatment of Al^{3+} toxicity in chronic dialysis patients. Aluminium toxicity is also implicated as the underlying cause of Alzheimer disease (Swartz, 1985).

However, the formation of chelates such as Fe^{3+}-desferrioxamine, can adversely affect the antimalarial activity of the iron-chelating agent (Raventos-Suarez *et al.*, 1989). Thus, any concomitant medication such as mineral supplementation can possibly affect the efficacy of iron chelating agents as antimalarials (Oppenheimer, 1989).

In this study, iron, copper and aluminium were combined with desferrioxamine and 2,2'-bipyridyl to determine whether these cations are alternative targets for the antimalarial action of the chelating agents, and to determine whether the chelates are harmful to parasite growth.

6.1.4 STAGE DEPENDENCY AND RECRUDESCENCE

Malaria parasites exhibit a typical circadian rhythm, with the life cycle of the parasite being a multiple of 24 hours. Each of the parasite stages exhibit different metabolic rates and membrane permeabilities (Landau *et al.*, 1991). By identifying the stage of parasite development most susceptible to the drug, the drug efficacy, i.e. dosage and the duration of therapy, can be improved to achieve optimal therapeutic success. Such information concerning desferrioxamine and 2,2'-bipyridyl could improve our understanding of their possible mechanisms and sites of action.

6.1.4.1 Stage-dependency effects of iron chelating agents

Lederman *et al.* (1984) demonstrated that desferrioxamine can reversibly inhibit the S-

phase of the human lymphocyte proliferation cycle by chelating the essential iron required for the functioning of the replication process. The following three enzymes are required for nuclear division, and are potential targets for desferrioxamine: DNA polymerase (the central enzyme involved in the copy synthesis of DNA strands), dihydroorate dehydrogenase (involved in pyrimidine synthesis) and ribonucleotide reductase (catalyses the reduction of ribonucleotide triphosphates) (Lytton *et al.*, 1994).

The *P. falciparum*-synthesized ribonucleotide reductase enzyme consists of two subunits, a large subunit, which contains the substrate and redox active sulphydryl groups, and a small subunit, which contains a dinuclear iron centre and tyrosyl radical cation (Rubin *et al.*, 1993). The tyrosyl radical promotes the reduction of the ribonucleotide triphosphate, and the oxidized enzyme is then returned to the active form through a series of reactions, with NADPH serving as the ultimate reducing agent (Reichard and Ehrenberg, 1983). However, after the reduction process, the ferrous ion centre becomes loosely bound to the protein and is easily chelated by desferrioxamine, 2,2'-bipyridyl, bathophenanthroline sulphonate or EDTA. This results in the formation of aporibonucleotide reductase, which can no longer be reactivated by oxygen (Fontecave *et al.*, 1990).

Ultrastructural changes induced by desferrioxamine are primarily associated with the nucleus (Atkinson *et al.*, 1989). The observed morphological changes include primary lesions associated with fragmentation, expansion and breakdown of the nuclear envelope into membranous sections, and subsequent vacuolisation and swelling of the nucleoplasm. The latter desferrioxamine-induced effects contrast with the changes caused by pyrimethamine, where nuclear division is arrested at metaphase, after the formation of mitotic spindle fibres (Aikawa and Beaudoin, 1968). There are no apparent morphological effects on other plasmodial organelles, such as the mitochondria and food vacuole. Additionally, the ATP-energy supply in desferrioxamine-treated parasites is not substantially reduced, which implies that the iron-dependant mitochondrial enzymes required for electron transport and ATP formation, are not inhibited by desferrioxamine (Lytton *et al.*, 1994). Since mature erythrocytes do not contain the ribonucleotide reductase enzyme and with sufficient difference between the human and parasite ribonucleotide reductase enzymes (41%), the latter enzyme could be a potential target for

inhibition by iron chelating agents, such as desferrioxamine.

6.1.4.2 Recrudescence

Decreased chloroquine-sensitivity in *P. vivax*, along with high recrudescence rates are being reported (Marlar-Than *et al.*, 1995). Similarly, recrudescence has been reported in clinical trials, where desferrioxamine is used as the sole antimalarial agent to treat asymptomatic and symptomatic *P. falciparum*-infected patients. In the asymptomatic patients, the infection recurs on average four months after the completion of treatment, while in the symptomatic patients, the parasitaemia recurs after only seven days (Gordeuk *et al.*, 1992b; Bannag *et al.*, 1992).

The phenomenon of recrudescence should be examined to try and adjust the duration and dosage of treatment, such as to improve the efficacy of iron chelating agents as antimalarial agents.

Additional information about the relation between variables such as inoculum size, pH, cation supplementation, stage dependency and recrudescence, and their effects on the antimalarial activity of desferrioxamine and 2,2'-bipyridyl, could lead to the synthesis and development of a more efficient antimalarial or iron chelating agent.

6.2 AIMS

To investigate the effects of different variables such as inoculum size, pH, cations, stage dependency and recrudescence on the antimalarial activity of iron chelating agents.

6.3 EXPERIMENTAL PLAN

6.3.1 EFFECT OF INOCULUM SIZE ON DRUG EFFICACY

The hypoxanthine incorporation assay (Chapter 2.6) was used to determine whether the

IC_{50} of the iron chelating agents, desferrioxamine and 2,2'-bipyridyl are dependant on inoculum size. Pre-determined concentrations of desferrioxamine, 2,2'-bipyridyl and chloroquine were plated out into 96-well microculture plates. The parasitized erythrocytes were added in pre-determined inoculum sizes, with the haematocrit percentage being kept constant at 1%, and the parasitaemia adjusted to 0,5%, 6,0% and 10,0%. A 1% haematocrit of control erythrocytes was also plated out (Geary *et al.*, 1990). The addition of [G-^{3}H]-hypoxanthine, extraction of parasite DNA and data evaluation were performed as described in Chapter 2.6.

6.3.2 EFFECT OF pH ON DRUG EFFICACY

To change the pH gradient between the extracellular medium and the parasite, the following modifications to the basic ^{3}H-hypoxanthine technique (Chapter 2.6) were made. The pH of the culture medium was adjusted to 6,6, 7,1, 7,4 and 7,8 with NaOH/HCl, before the uninfected and parasitized erythrocyte suspensions were prepared (Geary *et al.*, 1990). Sodium bicarbonate was omitted from the 10% plasma-supplemented culture medium, to prevent further alterations in the medium pH. The various dilutions of iron chelating agents were added to the microculture plates and the rest of the experiment concluded as previously described in Chapter 2.6.

6.3.3 EFFECT OF CATION-CHELATES ON PARASITE GROWTH

The basic ^{3}H-hypoxanthine incorporation assay (Chapter 2.6) was used to determine whether mineral supplementation could interfere with the antimalarial properties of the chelating agents. The stock solutions of desferrioxamine, 2,2'-bipyridyl, copper sulphate and iron chloride were prepared in culture medium, while the aluminium sulphate stock solution was dissolved in blood-PBS (Chapter 2.1.3.2). The following concentrations of each chelating agent and cation were prepared in incomplete culture medium: 1, 5, 10, 25, 35, 50 and 100 μM. The only adjustment to the standard technique was that 12,5 μl of each chelating agent and cation were added in equimolar concentrations. The plates were

left to stand in the dark for approximately one hour to allow the cation-chelates to form. The rest of the experiment was performed as described in Chapter 2.6.

6.3.4 STAGE-SPECIFICITY OF IRON CHELATING AGENTS, DESFERRIOXAMINE AND 2,2'-BIPYRIDYL

6.3.4.1 Microscopic examination of the stage-specificities of desferrioxamine and 2,2'-bipyridyl

A highly synchronous culture consisting of ring-infected erythrocytes was adjusted to a 2% parasitaemia and 5% haematocrit in gentamycin-free, complete culture medium. The suspension was aliquoted out into 6-well plates, for desferrioxamine (33,3 μM), 2,2'-bipyridyl (50 μM) and drug-free control, and incubated at 37°C in a candle jar. The chelating agents were added at time 0 (the early ring stage), at 24 hours (the trophozoite stage) and at 32 hours (the schizont stage) (Figure 1.1). Thin blood smears were prepared at 8 hourly intervals for 84 hours, Giemsa-stained and microscopically examined under oil immersion (1000x magnification). The number of ring-, trophozoite- and schizont-infected erythrocytes were counted in a minimum of 2000 erythrocytes, to determine the effect of the chelating agents on parasite growth.

6.3.4.2 Rate of inhibition of parasite growth by desferrioxamine and 2,2'-bipyridyl

The rate of inhibition was determined by the amount of ^{3}H-hypoxanthine incorporated into the developing parasite DNA. A well synchronized culture, consisting of ring-infected erythrocytes was adjusted to a 2% parasitaemia and 1% haematocrit with CO_2-gassed, gentamycin-free complete culture medium, which was supplemented with tritiated hypoxanthine (final concentration of 13 μCi). Concentrations of 50 and 100 μM desferrioxamine and 2,2'-bipyridyl were prepared and then combined in the following desferrioxamine:2,2'-bipyridyl ratios, 50:100, 100:100 and 100:50. The parasitized-erythrocyte suspension and the latter drug concentrations were added to the appropriate flasks and incubated at 37°C. At times 1,5, 6, 10, 20, 24, 29, 32, 42 and 48 hours, 200 μl of the parasite suspension was removed from the flask and pipetted into a well of a 96-

well microculture plate and immediately harvested (Chapter 2.6). Six readings of each concentration were made at each time interval.

6.3.4.3 Morphological examination

At the specific time intervals detailed in Chapter 6.3.4.2, 50 μl of parasite suspension was removed from each flask to determine the stage and morphology of the parasites. The morphological effects of 50 μM desferrioxamine and 50 μM 2,2'-bipyridyl on day four were photographed under oil immersion (1000x magnification).

6.3.4.4 Recrudescence of desferrioxamine-treated parasites

The phenomenon of recrudescence was examined *in vitro*, by using highly synchronous FCR-3 ring-infected erythrocytes, which had been adjusted to a 3% parasitaemia and 14,5% haematocrit. Desferrioxamine (150 μM) was added to the culture for eight days and Giemsa stained blood smears were examined for sixteen consecutive days to monitor any change in morphology and parasitaemia. On day 5, the parasitaemia of the control was halved by the addition of blood.

6.4 RESULTS

6.4.1 EFFECT OF INOCULUM SIZE ON THE EFFICACY OF CHLOROQUINE AND IRON CHELATING AGENTS

As the inoculum size increased, the dose-response curves for desferrioxamine and 2,2'-bipyridyl shifted to the right, indicating that the concentration required to inhibit 50% of parasite growth, also increased. When the IC_{50} values were graphed against inoculum size, the trend indicated that an increase in inoculum size correlated with an increase in the inhibitory concentrations of both chelating agents (Figure 6.1).

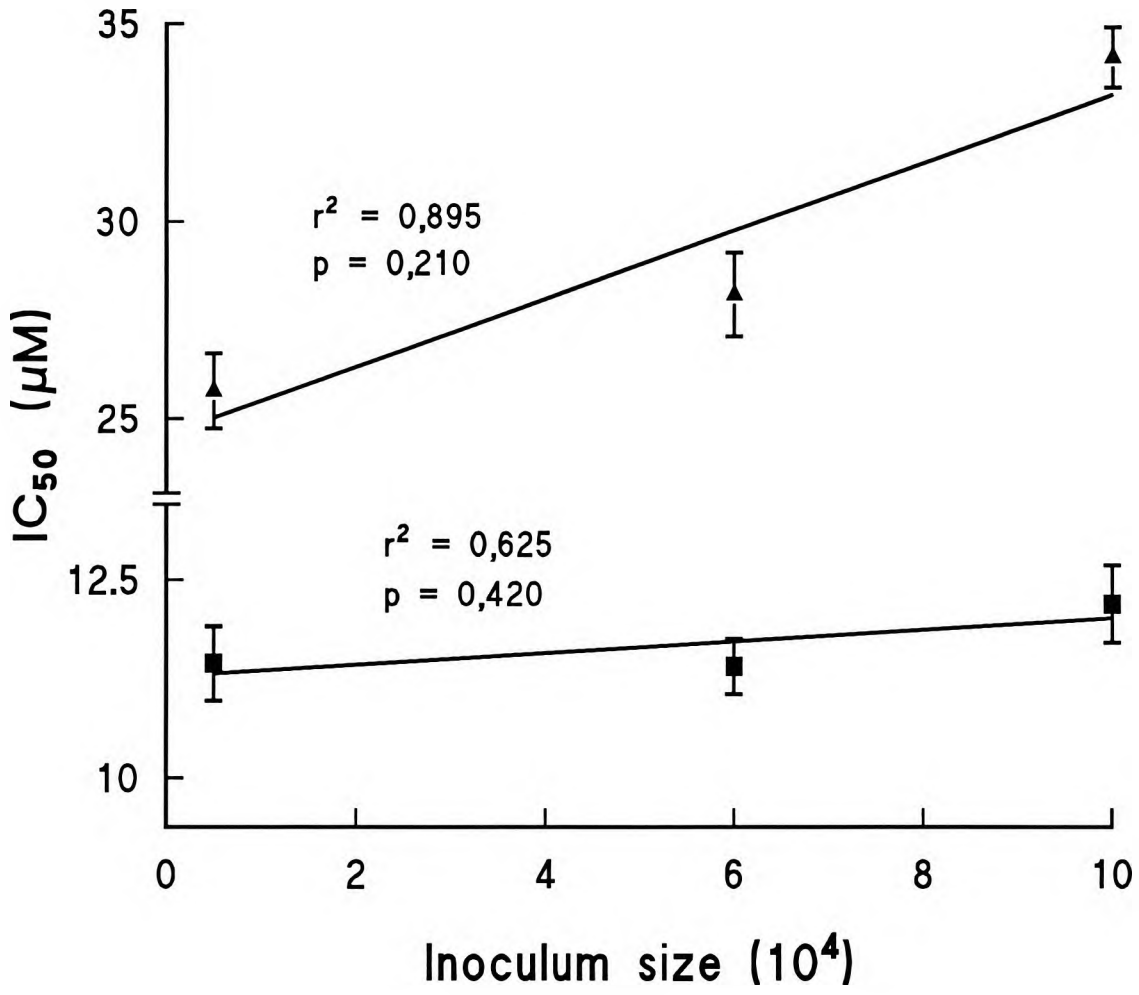


Figure 6.1: The dependence of the IC_{50} of desferrioxamine (■) and 2,2'-bipyridyl (▲) on inoculum size.

6.4.2 EFFECT OF pH ON THE EFFICACY OF THE IRON CHELATING AGENTS, DESFERRIOXAMINE AND 2,2'-BIPYRIDYL

The extracellular medium pH influenced the susceptibility of the parasites to both iron chelating agents. As the pH increased, the concentration of desferrioxamine required to inhibit 50% of parasite growth decreased, whilst for 2,2'-bipyridyl, the IC_{50} increased (Figure 6.2).

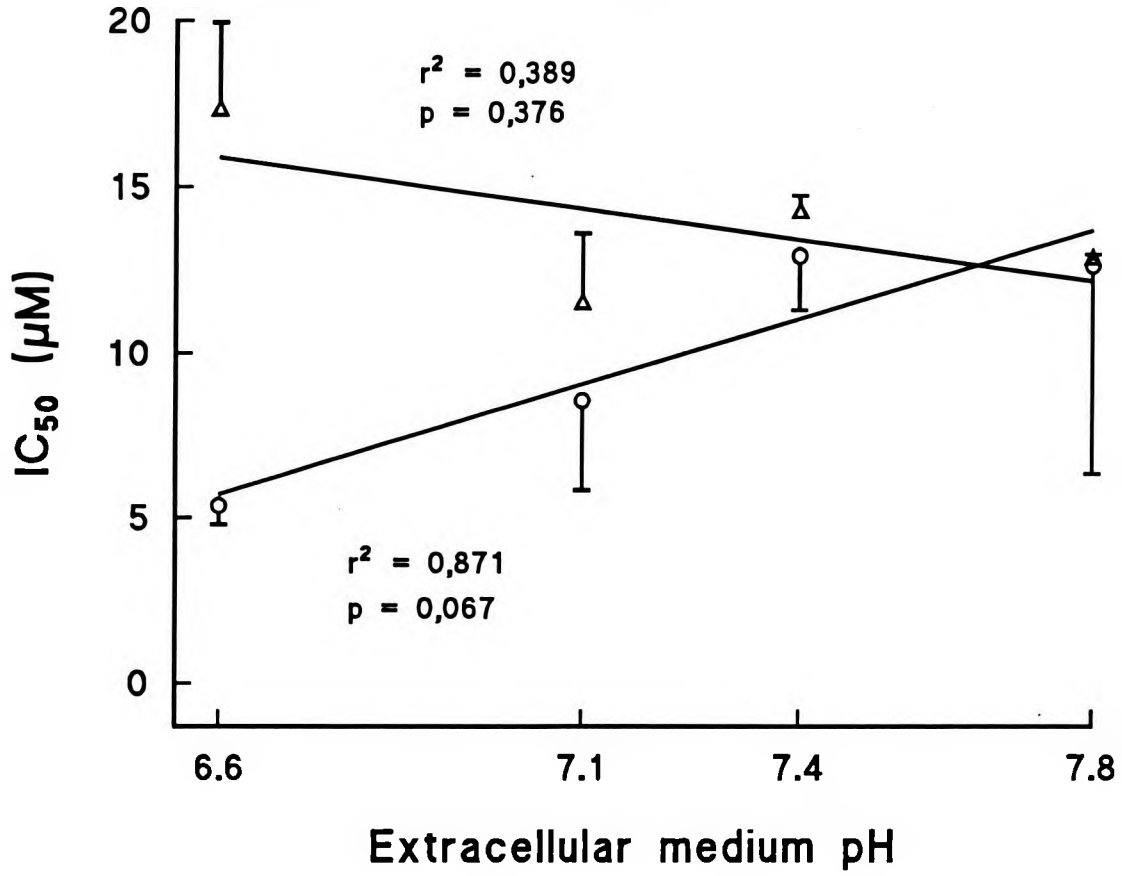


Figure 6.2: Dependence of the IC_{50} of desferrioxamine (△) and 2,2'-bipyridyl (○) on the extracellular medium pH. IC_{50} values were derived from 2 experiments and the bars represent standard deviations of the means.

6.4.3 EFFECT OF CATION-CHELATES ON PARASITE GROWTH

The antimalarial activities of desferrioxamine and 2,2'-bipyridyl are probably due to their iron chelating properties, although they do have the capacity to chelate other metals. To examine this possibility, equimolar amounts of different di- and trivalent metals were added alone, or with desferrioxamine and 2,2'-bipyridyl to the parasite suspension. Table 6.1 shows the IC_{50} values obtained from the individual dose-response curves for desferrioxamine, 2,2'-bipyridyl and copper. Whilst for iron and aluminium only linear curves could be generated; where 100 μM of the respective cations resulted in 99,84 $\pm$ 3,92% and 107,23 $\pm$ 0,66% parasite survival. The r^2 and p values calculated from the

linear regression curve for Fe^{3+} were 0,07 and 0,57, respectively, and for Al^{3+}, 0,27 and 0,22, respectively.

The inhibitory action of desferrioxamine was greatly decreased when chelated to Fe^{3+} - there was 82,72 ± 9,34 % parasite growth when 100 μM of Fe^{3+}-desferrioxamine was added in a 1:1 ratio (Figure 6.3; top). The Al^{3+}-desferrioxamine chelate (100 μM) resulted in a 20% decrease in the linear response compared to Al^{3+} alone and there was 86,83 ± 9,89 % parasite growth with the addition of 100 μM of the Al^{3+}-desferrioxamine chelate (Figure 6.3; top). There was no significant change to the dose-response curve when desferrioxamine was chelated to copper; where the IC_{50} values of desferrioxamine decreased from 13,59 ± 1,09 to 10,09 ± 0,40 μM when chelated to Cu^{2+} (Table 6.1 and Figure 6.3; top). The inhibitory action of 2,2'-bipyridyl was not inhibited by any of these three metals (Figure 6.3; bottom). As a result there was no significant change to the dose-response curve when 2,2'-bipyridyl was chelated to Fe^{3+}. Although both the Al^{3+}-2,2'-bipyridyl and Cu^{2+}-2,2'-bipyridyl chelates resulted in synergistic interactions, with their respective IC_{50} values being four- and five-fold lower than the IC_{50} of 2,2'-bipyridyl alone (Table 6.1).

Table 6.1: The IC_{50} of the iron chelating agents and cations alone and combined in equimolar concentrations. The hyphens denote that linear curves were generated and no IC_{50} values could be determined (Figure 6.3).

	ALONE IC_{50} ± s.d. (μM)	**Desferrioxamine** IC_{50} ± s.d. (μM)	**2,2'-Bipyridyl** IC_{50} ± s.d. (μM)
		13,59 ± 1,09	20,74 ± 1,16
Cu^{2+}	7,65 ± 1,56	10,09 ± 0,40	4,10 ± 0,99
Fe^{3+}	-	-	18,28 ± 1,05
Al^{3+}	-	-	5,40 ± 0,94

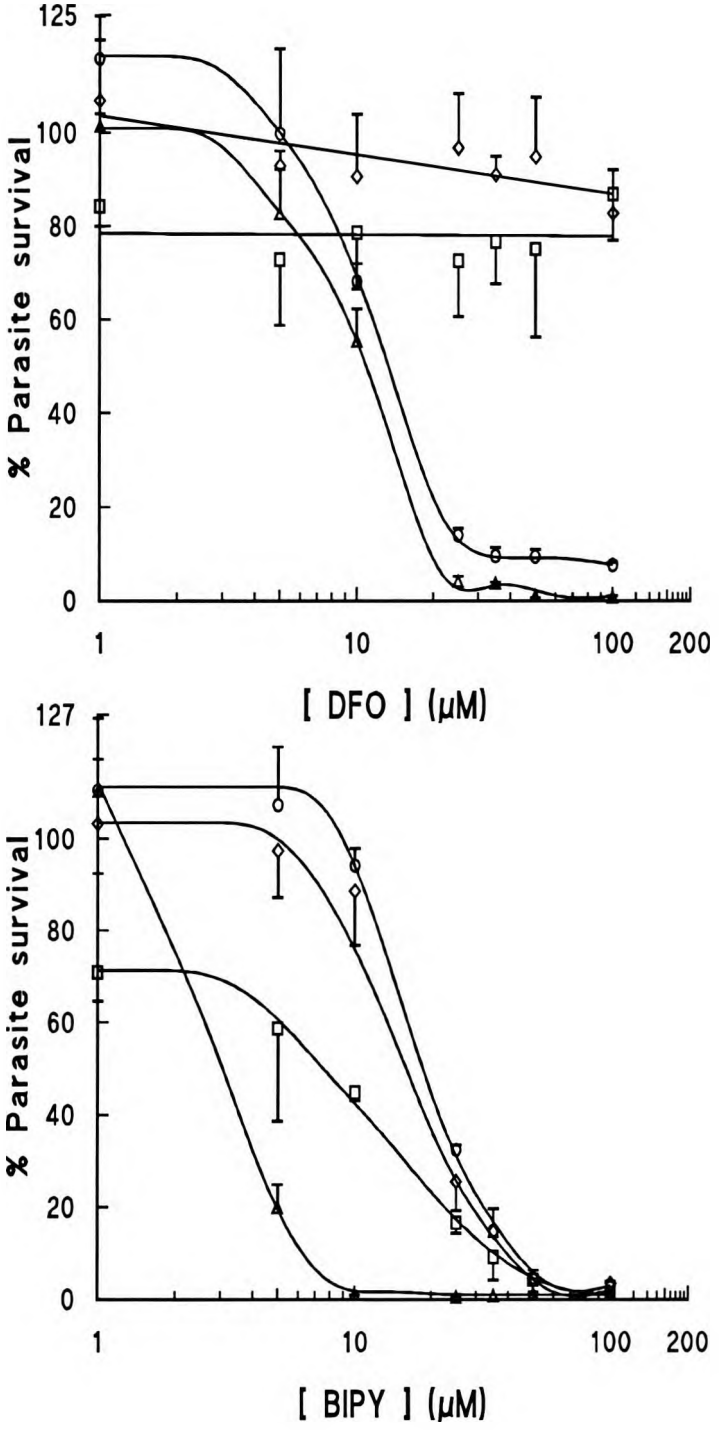


Figure 6.3: The *in vitro* effect of cation-chelates on parasite growth. Symbols represent ○: desferrioxamine (DFO) and 2,2'-bipyridyl (BIPY) alone; △: + Cu^{2+}; ◇: + Fe^{3+} and □: + Al^{3+}. Where the r^2 and p values for the Fe^{3+}-desferrioxamine linear graph are 0,61 and 0,04, respectively; and for the Al^{3+}-desferrioxamine linear graph, 0,94 and 0,0014, respectively.

6.4.4 STAGE-SPECIFICITY OF DESFERRIOXAMINE AND 2,2'-BIPYRIDYL ON THE INTRAERYTHROCYTIC LIFE CYCLE OF MALARIA

6.4.4.1 Microscopic examination of the stage-specificities of desferrioxamine and 2,2'-bipyridyl

The life cycle of the parasitized erythrocytes have distinct time periods where each stage is most prevalent. The complete cycle takes approximately 42 hours.

6.4.4.1.1 Drug addition at the ring stage

Desferrioxamine did not affect the first cycle of rings or the development of early trophozoite-infected erythrocytes (Figure 6.4). As the trophozoite stage matured, the percentage parasitaemia decreased, when compared with the control. These mature trophozoite-infected erythrocytes persisted in culture for longer periods than in the control experiments, resulting in a delayed formation of the schizont-infected erythrocytes, as well as decreased numbers. This trend subsequently carried through to the next ring stage.

2,2'-Bipyridyl induced the ring stage to persist for a longer period in culture, resulting in a decreased percentage of trophozoite-infected erythrocytes being formed. Although the persistence of the trophozoite stage in culture reduced the percentage of schizonts formed, it did not delay the formation of this stage. However, the schizont stage also persisted in culture and resulted in delayed formation of the second cycle of ring-infected erythrocytes.

6.4.4.1.2 Drug addition at the trophozoite stage

After 24 hours, the parasites had developed into haemozoin-containing trophozoites. Addition of desferrioxamine decreased the percentage trophozoite-infected erythrocytes, but the mid-late trophozoite stage persisted in culture until the second cycle, where the percentage parasitaemia increased in parallel with the control (Figure 6.5). The persistence of the trophozoite stage in culture, resulted in a 30% decrease in the percentage of schizont-infected erythrocytes formed, and the subsequent cycle of ring-infected erythrocytes was also affected.

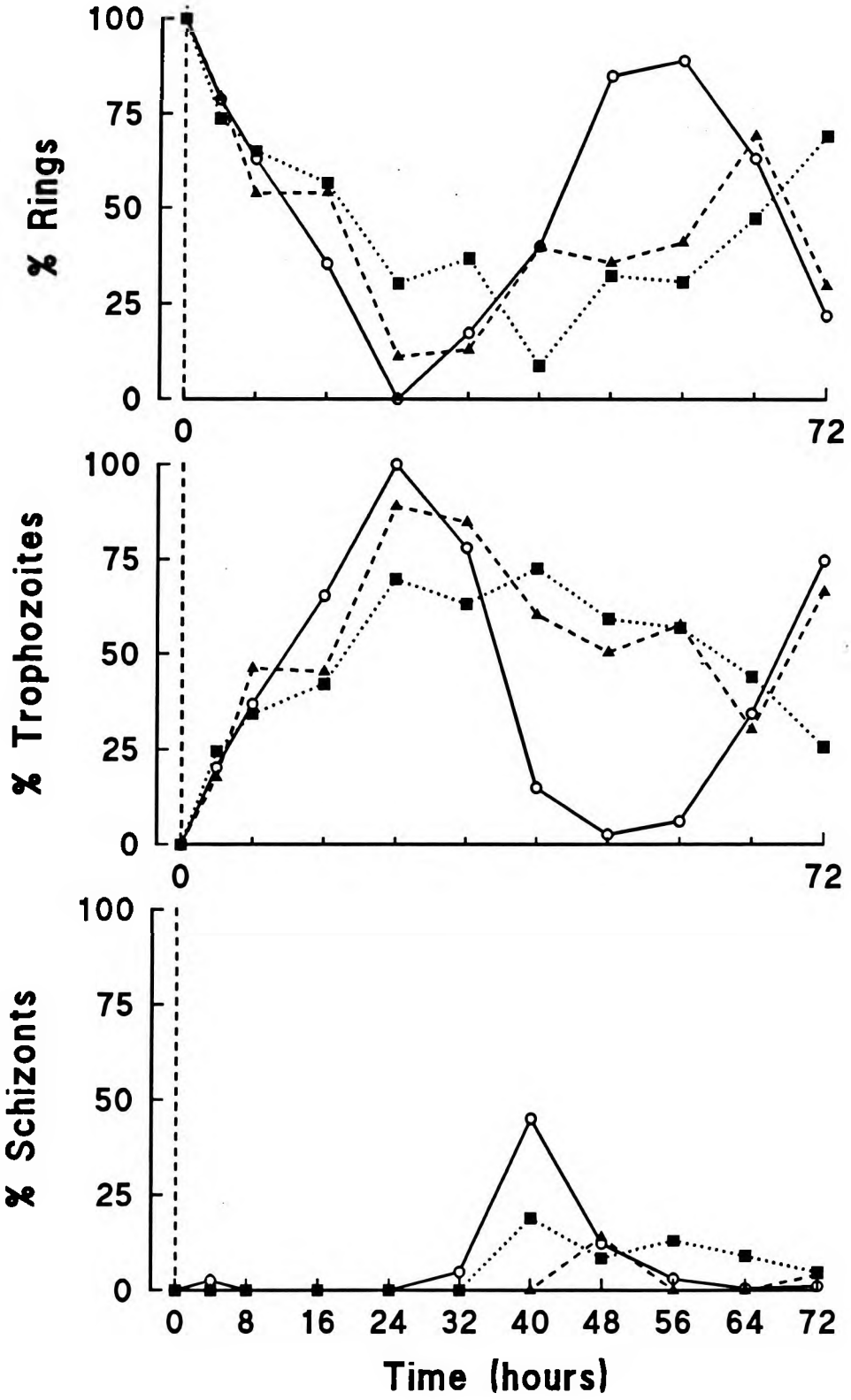


Figure 6.4: Morphological changes occurring through-out the life cycle of the parasite, with drugs added at time 0 (ring stage). ○: Control; ■/dot: 2,2'-bipyridyl and ▲/dash: desferrioxamine.

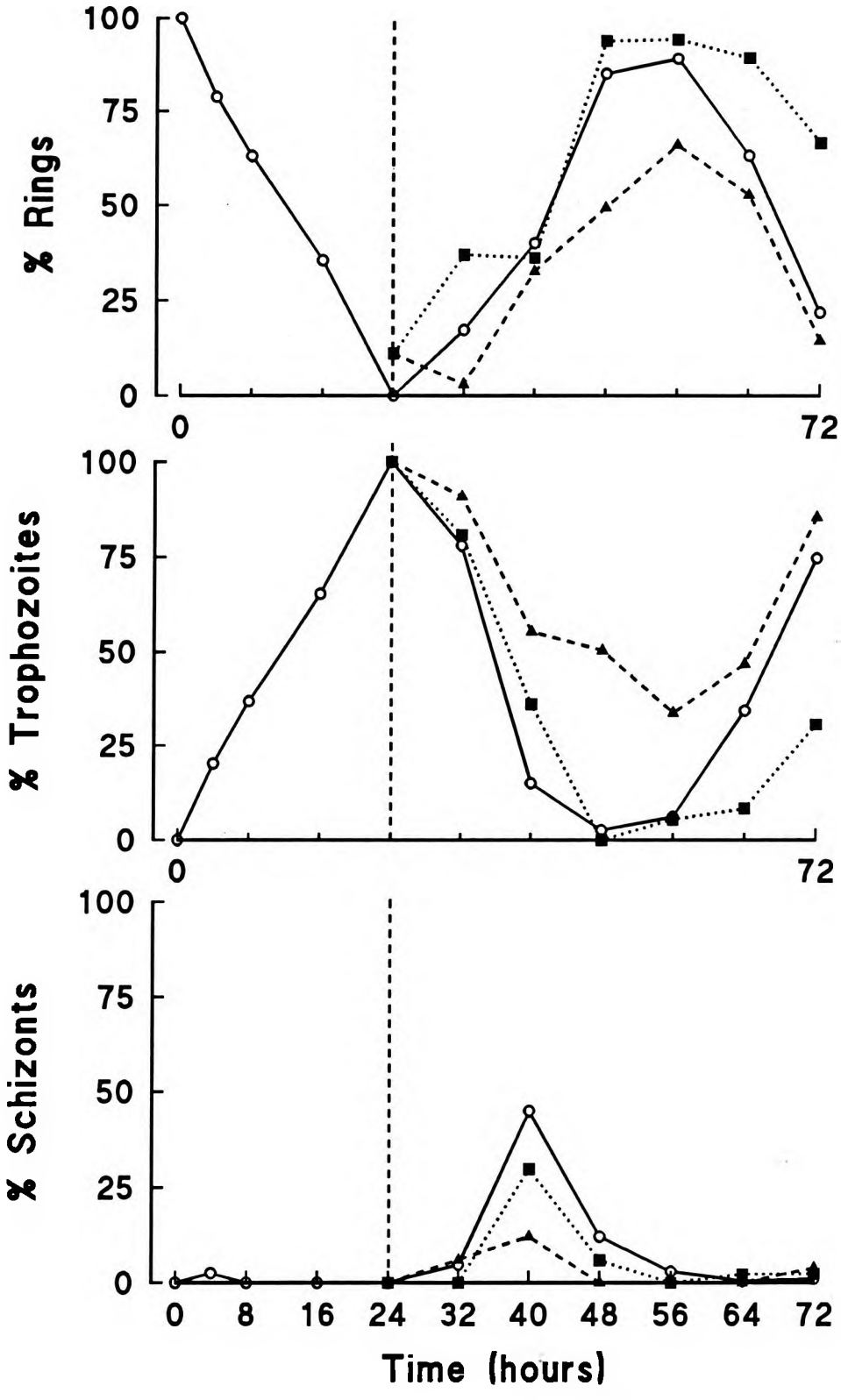


Figure 6.5: Morphological changes occurring through- out the life cycle of the parasite, with drugs added at time 24 hours (trophozoite stage). ○: Control; ■/dot: 2,2'-bipyridyl and ▲/dash: desferrioxamine.

2,2'-Bipyridyl did not significantly affect the development of the trophozoite-infected erythrocyte to the schizont stage, although there was a slight reduction in the percentage schizont-infected erythrocytes formed. Development of the schizont-infected erythrocytes to the ring stage was not affected. But, as in Figure 6.4, these ring-infected erythrocytes persisted for a longer period in culture and the development of the second cycle of trophozoite-infected erythrocytes was delayed.

6.4.4.1.3 Drug addition at the schizont stage

After 32 hours, the trophozoite-infected erythrocytes had developed to the schizont stage, with the start of segmentation. Eight hours after the addition of desferrioxamine, there was a decrease in the percentage schizont-infected erythrocytes, but the second cycle of the ring- and trophozoite-infected erythrocytes developed normally. 2,2'-Bipyridyl did not affect the schizont-infected erythrocytes, but did prolong the second cycle of the ring-infected erythrocytes, and had a profound inhibitory effect on the development of the second cycle of trophozoite-infected erythrocytes (Figure 6.6).

6.4.4.2 Inhibition of ^{3}H-hypoxanthine incorporation into parasite DNA by desferrioxamine and 2,2'-bipyridyl

In the untreated control the hypoxanthine was incorporated in a time-dependent manner, with a rapid increase in incorporation occurring at the mid trophozoite stage in preparation for DNA synthesis. From the radioactive counts in Figure 6.7, it was evident that 50 μM 2,2'-bipyridyl was more effective than 50 μM desferrioxamine in preventing ^{3}H-hypoxanthine incorporation. When expressed as a percentage of the control, desferrioxamine had no effect on the rate of ^{3}H-hypoxanthine incorporation during the first 10 hours of exposure. Subsequently, desferrioxamine inhibited the rapid increase in ^{3}H-hypoxanthine incorporation found in the control culture (Figure 6.7). 2,2'-Bipyridyl initiated its effect immediately on the ring stage, as shown by the lower amount of ^{3}H-hypoxanthine associated with the mature parasites. The incorporation of hypoxanthine into the parasite DNA was not significantly different when treated with either 50 μM or 100 μM of either chelating agent.

When desferrioxamine and 2,2'-bipyridyl were added in combination (Figure 6.7), the

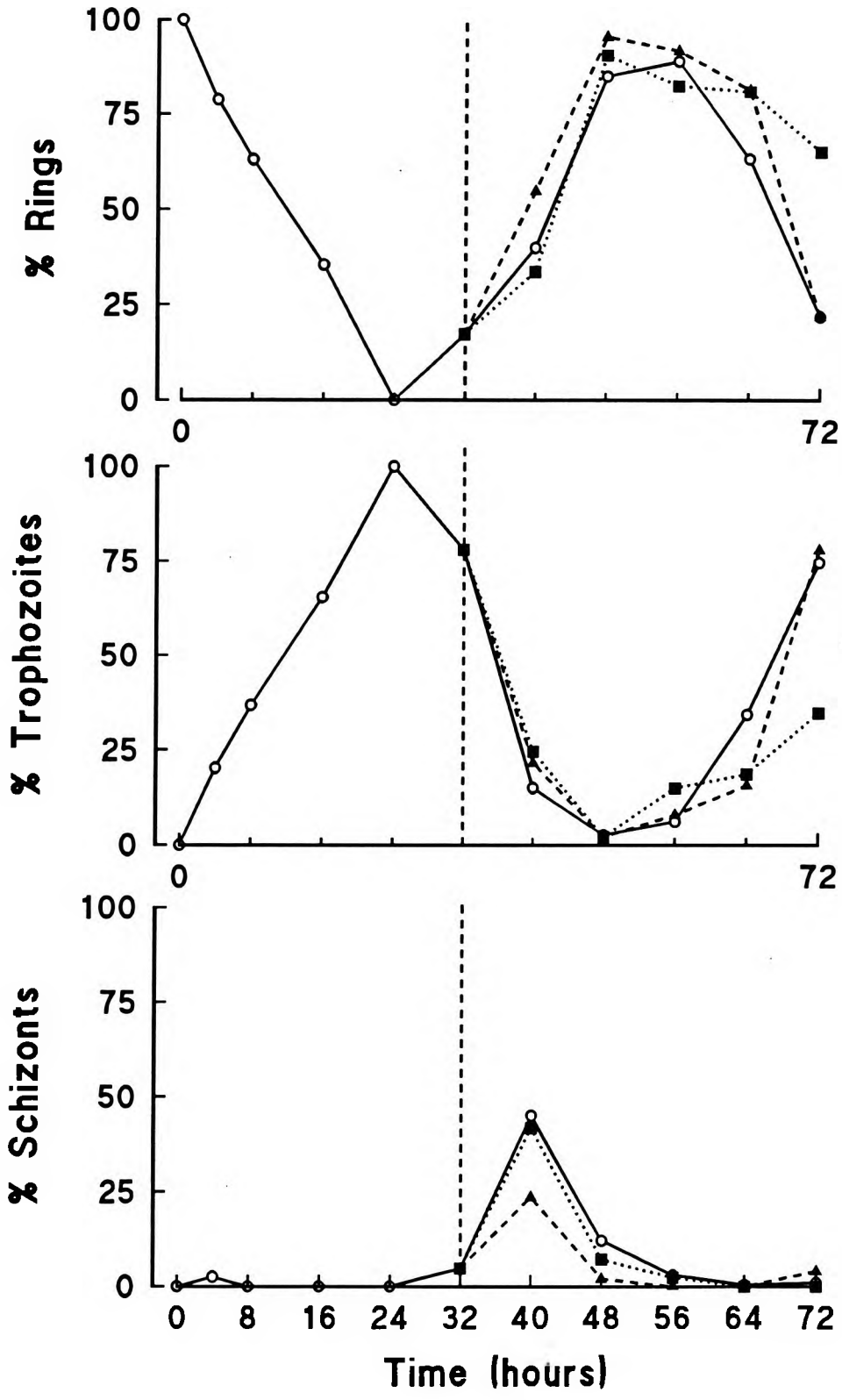


Figure 6.6: Morphological changes occurring through-out the life cycle of the parasite, with drugs added at time 32 hours (schizont stage). ○: Control; ■/dot: 2,2'-bipyridyl and ▲/dash: desferrioxamine.

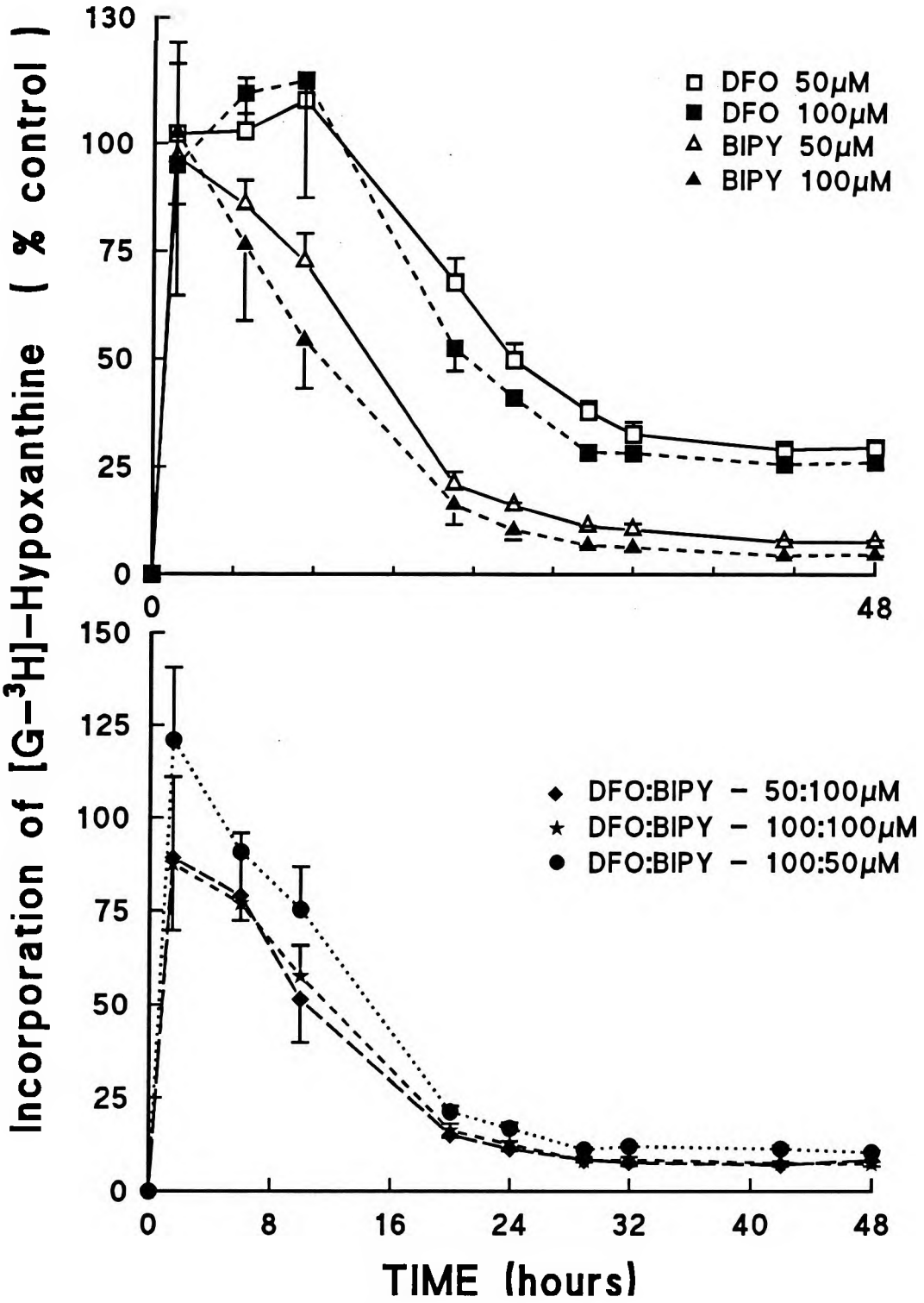


Figure 6.7: ^{3}H-hypoxanthine incorporation into desferrioxamine (DFO) and 2,2'-bipyridyl (BIPY) treated cultures. Each measurement was the mean of six readings. The data and standard deviations are taken from a single experiment.

100:100 μM or 50:100 μM ratios inhibited approximately the same amount of ^{3}H-hypoxanthine incorporation as 100 μM 2,2'-bipyridyl. The addition of desferrioxamine and 2,2'-bipyridyl in a 2:1 ratio, resulted in slight antagonism occurring at the early ring- to early trophozoite-stages (i.e. from 1,5 to 10 hours after the initiation of treatment).

6.4.4.3 Morphological changes induced by desferrioxamine and 2,2'-bipyridyl

Morphological examination of the slides prepared in conjunction with the readings in Chapter 6.4.4.1 and 6.4.4.2, showed that desferrioxamine (50 μM and 100 μM) and 2,2'-bipyridyl (50 μM and 100 μM) did not induce any apparent effect on the early ring- to early trophozoite-stages (Figure 6.8). After 29 hours of treatment with 2,2'-bipyridyl, late ring-infected erythrocytes still persisted in culture with late trophozoite-infected erythrocytes; whilst the control culture had developed into early schizont-infected erythrocytes. The early trophozoite stage was relatively unaffected by desferrioxamine and 2,2'-bipyridyl, however the mature trophozoite-infected erythrocytes, in an arrested state of development, persisted in culture for the duration of the experiment. They became abnormally vacuolated with no evidence of nuclear division, while untreated parasites developed into recognizable pigmented trophozoite-infected erythrocytes and segmented schizont-infected erythrocytes (Figure 6.8.A). The cytoplasm of the desferrioxamine treated parasites appeared very disrupted and after 32 hours there was no apparent cellular organization (Figure 6.8.B). The degree of vacuolation induced by the iron chelating agents was concentration dependent. The parasite cytoplasm of the 2,2'-bipyridyl treated parasites started to contract and become more dense in appearance after 4 days (Figure 6.8.C). The formation and structure of the haemozoin did not appear to be affected by desferrioxamine or 2,2'-bipyridyl. The combination of desferrioxamine and 2,2'-bipyridyl resulted in fewer ring-infected erythrocytes persisting in the culture, less vacuolation of the trophozoite-infected erythrocytes and after 42 hours, segmented schizont-infected erythrocytes were observed, as in the control.

6.4.4.4 Recrudescence of desferrioxamine pre-treated parasites

From slide examinations, it was observed that by day 7, desferrioxamine had caused extensive vacuolation and death in the majority of trophozoite-infected erythrocytes. The parasitaemia was 1,25% compared to 4,48% in the control. On day 8, desferrioxamine

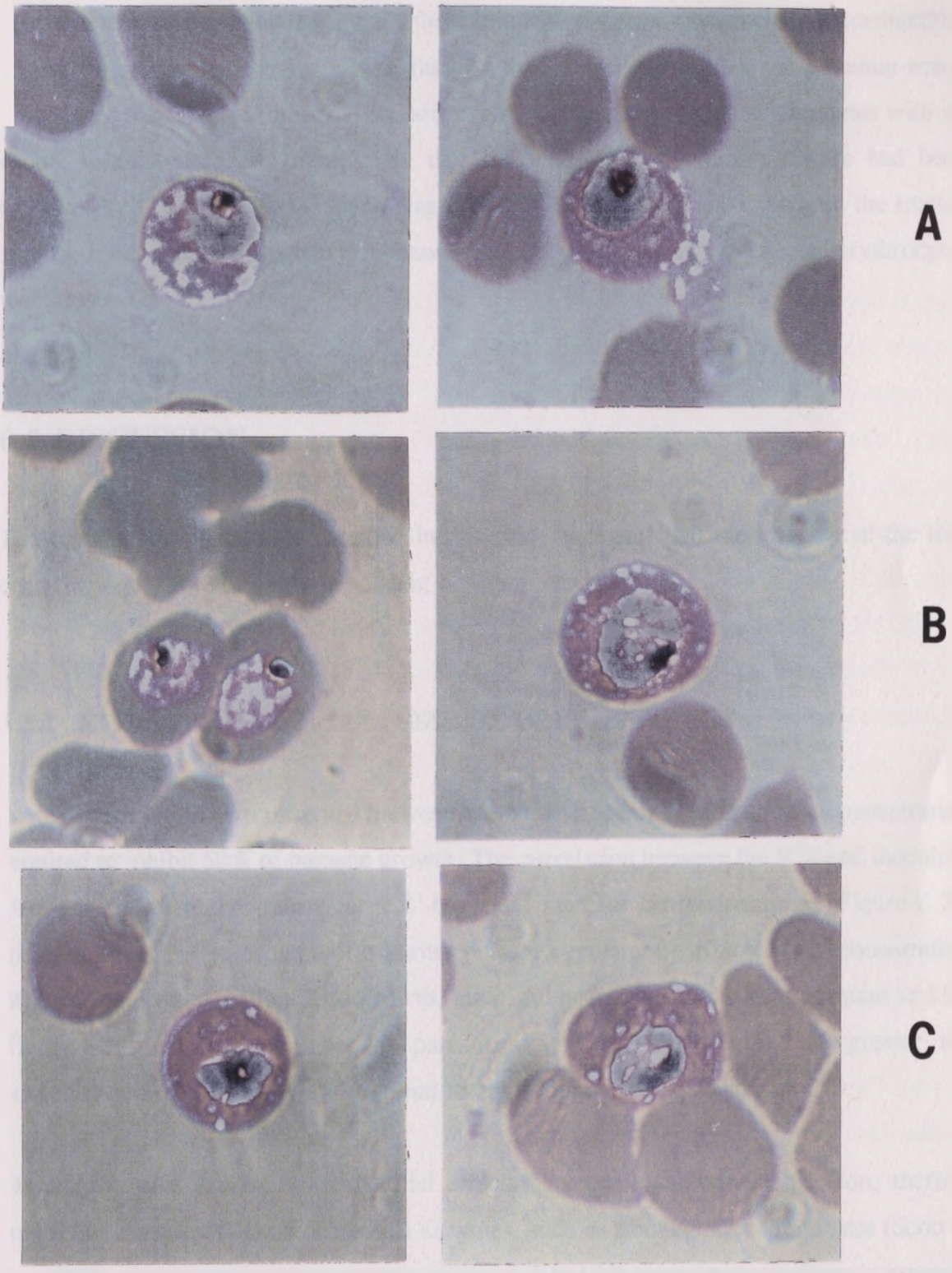


Figure 6.8: Morphological changes induced after 4 days of treatment. Drug-free control (A), 50 μM desferrioxamine (B), 50 μM 2,2'-bipyridyl (C). Giemsa-stained smears photographed under oil immersion (1000x magnification).

treatment was stopped and by day 10, the trophozoite-infected erythrocytes (parasitaemia: 0,39%) were slightly less vacuolated than on day 7, even though the parasitaemia was a third lower than day 7. By day 14, healthy mid-trophozoite-infected erythrocytes with no visible vacuolation were present. By day 16, the synchrony of the culture had been disrupted and the total parasitaemia was 10,69% in the control and 0,46% in the treated culture. By day 16, healthy late trophozoite- and segmenting schizont-infected erythrocytes were observed.

6.5 DISCUSSION

The consistency of the data obtained in this study indicates that the efficacy of the iron chelating agents are strongly dependent on many variables.

6.5.1 EFFECT OF INOCULUM SIZE ON DRUG EFFICACY

A weak correlation was observed between haematocrit, parasitaemia and the concentration required to inhibit 50% of parasite growth. The correlation between the IC_{50} and inoculum size was significantly greater for 2,2'-bipyridyl than for desferrioxamine (Figure 6.2), indicating that the percentage of parasites present significantly affected the concentration of drug required to inhibit 50% growth, since the haematocrit was kept constant at 1%. Thus, the greater the number of parasitized erythrocytes present, the greater the concentration of 2,2'-bipyridyl required to achieve a cytotoxic effect.

Desferrioxamine exerts its antimalarial effects by chelating intraparasitic iron, thereby inhibiting iron-dependent biochemical enzymes, such as ribonucleotide reductase (Scott *et al.*, 1990). An increase in parasitaemia from 0,5% to 10% would not significantly increase the intraparasitic iron concentration available for chelation, thus accounting for the fact that the IC_{50} of desferrioxamine was not significantly ($p = 0,42$) affected by the change in inoculum size (Figure 6.2.B).

The dependence of the IC_{50} values on inoculum size can possibly explain the variations in IC_{50} values obtained in different experiments (Figure 5.1 and 5.2).

6.5.2 EFFECT OF pH ON DRUG EFFICACY

The extracellular pH of the medium affected the inhibitory effect of desferrioxamine, such that as the pH increased, the IC_{50} decreased (Figure 6.2). A similar trend was observed with chloroquine (Geary *et al.*, 1990). Jin *et al.* (1989) found that desferrioxamine is evenly distributed between the acidic lysosome and cytosol in rat hepatocytes. Thus, desferrioxamine could accumulate in the food vacuole via the transvacuolar pH gradient. At the lower pHs (e.g. 6,8), a higher concentration of desferrioxamine was required to inhibit parasite growth. This is possibly due to the fact that at an acid pH, the transferrin-iron bond is weakened and the iron is easily released from the transferrin molecule (Octave *et al.*, 1982), thus resulting in an increase in the concentration of "free" iron available for desferrioxamine to chelate. In addition, the existing pH gradient between the parasite and extracellular medium is not as great as when the medium is more alkaline. Thus, desferrioxamine would have had to accumulate via a concentration gradient, and higher concentrations of desferrioxamine would be required to achieve parasite death.

This hydrophilic chelating agent could also have chelated the extracellular iron, before entering into the parasitized erythrocyte. Therefore, a higher concentration of desferrioxamine is required to chelate the extracellular, as well as intraparasitic iron. Desferrioxamine could protect the cerebral capillaries by chelating any "free" iron or acting as a free radical scavenger. This protective effect has been noted in cerebral malaria patients, treated with desferrioxamine, who emerged from their coma approximately 23 hours earlier than those receiving placebo (Gordeuk *et al.*, 1992a).

When 2,2'-bipyridyl was used the IC_{50} increased as the pH increased (Figure 6.2). It is possible that as the pH increases, the titration of protons alter the polarity of the hydrophilic head, thereby affecting the orientation or position (e.g. depth) of the 2,2'-bipyridyl molecule in the apolar phase of the membrane (Brasseur and Ruysscharet, 1986;

Deamer and Nichols, 1989). This alteration in polarity possibly altered the chelating ability of 2,2'-bipyridyl, thereby increasing the concentration of drug required to inhibit parasite growth.

Clinically the plasma pH does not vary as greatly as in these experiments, although it does demonstrate that the antimalarial activity of iron chelating agents can be influenced by any pH change induced by the pathology of malaria.

6.5.3 EFFECT OF CATION-CHELATES ON PARASITE GROWTH

6.5.3.1 Cation supplementation

The *in vitro* inhibitory effect of desferrioxamine and 2,2'-bipyridyl on the growth of *P. falciparum* was found to occur within a single parasite cycle (Figures 5.1 and 6.3). This finding argues against the gradual depletion of iron stores in the parasite. Instead, the rapid onset of action suggests a more direct effect on parasite growth, specifically targeted towards certain metabolic activities of the parasite.

Under normal conditions, the concentration of plasma transferrin-bound iron is less than 160 μg/dl, i.e. approximately 60 μM iron, which represents approximately 30% saturation of transferrin. Whilst, in iron-overload patients with haemochromatosis the percentage transferrin saturation increases from 61 to 100 %, with the serum iron increasing from 160 to 307 μg/dl (Bridges and Seligman, 1995). In these experiments the maximum concentration of Fe^{3+} added was 100 μM, which falls just outside the normal transferrin saturation level. However, the presence of additional iron in the plasma could mimic the release of iron from haemolysed malaria-infected erythrocytes (Aremu, 1989). The addition of 25 and 100 μM Fe^{3+} resulted in 120, 36 $\pm$ 8,78 % and 99,84 $\pm$ 3,92 % parasite growth, respectively. Thus, it is possible that the majority of the Fe^{3+} was chelated and rendered inactive by the plasma transferrin and once bound to transferrin, the complex could be incorporated and utilized by the parasite (Figures 3.5 and 3.6). This could account for the slight stimulation of growth. It is also possible that the excess iron was rendered inert by being hydrolysed at the neutral pH of the culture medium, to form

extremely insoluble ferric hydroxide (Bullen, 1981).

Transferrin is also a potent ligand for the trace amounts of Al^{3+} circulating in the plasma ($K_a = 10^{19}\ M^{-1}$) and binds Al^{3+} in a 1:2 mole ratio (Cochran *et al.*, 1984; Swartz, 1985). Serum Al^{3+} concentrations are reported to increase to a maximum concentration of approximately 20 μM in dialysis patients (Cochran *et al.*, 1984). The highest concentration of Al^{3+} used in these experiments was 100 μM, which resulted in 107,23 $\pm$ 0,66 % parasite growth; whilst 10 μM resulted in 96,35 $\pm$ 12,36 % growth. It is thus possible that the Al^{3+} was chelated and rendered inactive by the plasma transferrin, since a competitive equilibrium exists between Al^{3+} and Fe^{2+} for transferrin binding sites (Cochran *et al.*, 1984).

Copper on the other hand, exhibited a significant toxic effect on parasite growth with an IC^{50} value of 7,65 $\pm$ 1,65 μM (Table 6.1). Copper *per se* is known to act as an oxidant on erythrocytes (Marva *et al.*, 1989), and in the presence of the H_2O_2 released from the parasitized erythrocytes, copper could possibly catalyse the production of free radicals via the Fenton reaction (Golenser *et al.*, 1991). The free radicals could severely affect parasite biochemistry, as well as cause double stranded DNA breaks, which would eventually lead to a loss of genetic information and death (Chevion, 1988).

6.5.3.2 Effect of cation-desferrioxamine chelates

The addition of equimolar concentrations of Fe^{3+} ions significantly decreased the antimalarial activity of desferrioxamine by producing non-toxic chelates (Figure 6.3). This confirms that one of the main mechanisms by which desferrioxamine acts as an antimalarial is by iron deprivation, and that it is a pre-requisite for desferrioxamine to enter the parasitized erythrocyte to exert its antimalarial actions. Scott *et al.* (1990) substantiated this finding by using a membrane impermeable desferrioxamine-dextran derivative to demonstrate that desferrioxamine functions by chelating the intraparasitic iron and not the extra- or intra-erythrocytic iron.

Desferrioxamine binds Cu^{2+} with an affinity constant of $10^{14}\ M^{-1}$, which is significantly less than for Fe^{3+}, $10^{31}\ M^{-1}$ (Waxman and Brown, 1969). The Cu^{2+}-desferrioxamine

complexes significantly ($p < 0,02$) decreased the concentration of desferrioxamine required to inhibit 50% of parasite growth. It is possible that due to the higher affinity of desferrioxamine for Fe^{3+} over Cu^{2+}, some of the Cu^{2+} ions are displaced from Cu^{2+}-desferrioxamine complex. The chelation of iron probably induces a deficient state, while the free copper catalyses the Fenton reaction and exerts oxidative stress on the parasitized erythrocytes (Golenser *et al.*, 1991). Alternatively, if the Cu^{2+}-desferrioxamine chelate could enter into the parasitized erythrocytes, the chelates could catalyse the formation of hydroxyl radicals, which could mediate an oxidative attack on the phosphodiester backbone to yield nicked DNA products (Joshi *et al.*, 1994). Ultra-structural observations have shown that desferrioxamine disrupts the nuclear apparatus of the parasite (Atkinson *et al.*, 1991).

The effect of the Al^{3+}-desferrioxamine chelates on the parasitized erythrocytes resulted in approximately 20% inhibition of parasite growth, regardless of the concentration of Al^{3+}-desferrioxamine added, i.e. 1 to 100 μM (Figure 6.3; top). Due to the octahedral conformation of the chelate, it is probably unlikely that the chelate could penetrate through the cell membrane to exert any antimalarial effects. At the higher concentrations of 15 to 100 μM, the antimalarial activity of desferrioxamine was greatly inhibited (Figure 6.3), again indicating that the cation-free form of desferrioxamine needs to penetrate the parasite to effectively inhibit parasite proliferation.

6.5.3.3 Effect of cation-2,2'-bipyridyl chelates

Aluminium forms a zerovalent complex with 2,2'-bipyridyl (BIPY), i.e. $[AlBIPY_3]^\circ$ (Cotton and Wilkinson, 1980), which according to the Nernst equation would pass freely in and out of the cell by simple diffusion (Hoyes and Porter, 1993). The latter complex resulted in a synergistic interaction, with a four fold decrease in the IC_{50} of 2,2'-bipyridyl (Table 6.1). This is probably due to the chelate acting as a catalyst of free radical production, due to its involvement in the redox series.

The concentration of 2,2'-bipyridyl required to inhibit 50% parasite growth, was significantly ($p < 0,0001$) decreased once complexed to Cu^{2+} (Figure 6.3). The chelates possibly generate hydroxyl radicals, which then initiate peroxidation of the membrane fatty

acids and affect membrane stability and parasite survival (Koppenol, 1994).

In contrast, there was no significant difference in the inhibition of parasite growth when 2,2'-bipyridyl was added alone or complexed to iron (Table 6.1 and Figure 6.3). The iron-2,2'-bipyridyl complex does not inhibit parasite growth via the Fenton reaction as the one-electron reduction of H_2O_2 by the Fe^{2+}-(2,2'-bipyridyl)$_3$ complex is thermodynamically unfavourable (Koppenol, 1994). In addition, the low organic/aqueous partition coefficient of this complex would prevent it from partitioning into the parasite membrane (Nunez *et al.*, 1983). It is also possible that the observed antimalarial effect is as a result of the iron being displaced from 2,2'-bipyridyl by other cations which are more readily bound by 2,2'-bipyridyl. Such that the uncomplexed 2,2'-bipyridyl molecule can partition itself into the erythrocytic and parasitic membranes and thereby inhibit the uptake of iron into the parasitized erythrocyte. 2,2'-Bipyridyl could also enter and chelate iron in mitochondria, however the iron-chelate complex is not released from this organelle or the cell (Ponka *et al.*, 1979). Thus, it is possible that the inhibition of parasite growth is as a result of this complex inhibiting mitochondrial activity.

6.5.4 STAGE-SPECIFIC EFFECTS AND RECRUDESCENCE

Both desferrioxamine and 2,2'-bipyridyl exhibited stage specific effects on parasite growth, as determined morphologically (Figures 6.4 to 6.6 and 6.8) and by the incorporation of tritiated hypoxanthine (Figures 5.4 and 6.7).

6.5.4.1 Stage dependent effects of desferrioxamine

6.5.4.1.1 Effects on the ring stage

Not all the developmental stages of the parasite were sensitive to desferrioxamine. Desferrioxamine was relatively ineffective against the ring stage, with no observable morphological changes nor inhibition of hypoxanthine uptake in the first ten hours of the life cycle. Although the parasitaemias of the second generation of ring-infected erythrocytes were decreased, this was due to the reduction in percentage of schizont-infected erythrocytes in the previous cycle.

Desferrioxamine is poorly permeant to ring-infected erythrocytes, where only 5% is taken up after 24 hours of exposure (Loyevsky *et al.*, 1993b). With such limited access to the parasite, the concentration of desferrioxamine retained is not able to chelate all the erythrocytic iron and inhibit parasite growth. At this early stage of development, the metabolic activity is considered to be low, with very few iron dependent enzymes present, thus desferrioxamine would have a very limited inhibitory effect on cellular metabolism. To rationalise why the ring-infected erythrocytes are resistant to desferrioxamine, Lytton *et al.* (1994) proposed that these parasites may not contain the enzymatic pathways required for the functional integration of the metal into iron-containing enzymes. Whitehead and Peto (1990) also demonstrated the cytostatic effects of desferrioxamine on the ring- and non-pigmented trophozoite-infected erythrocytes.

6.5.4.1.2 Effects on the trophozoite stage

The antimalarial effect of desferrioxamine is clearly shown to manifest exclusively in the advanced developmental stages, namely the late trophozoite, early schizont stages (Figures 6.5 and 6.6). The differential drug sensitivity of the ring- and trophozoite-infected erythrocytes could be attributed to the different permeation properties of their respective erythrocytic membranes (Lytton *et al.*, 1993). The increased fluidity of the trophozoite-infected erythrocyte membranes allow a greater variety of nutrients/drugs to pass through into the parasite.

The rate-limiting step in the antimalarial activity of desferrioxamine is the diffusion of desferrioxamine across three consecutive membranes and through the various aqueous compartments of the ring- and trophozoite-infected erythrocytes (Figure 3.1). It is proposed that in the advanced stages of the life cycle, desferrioxamine is taken up via a process referred to as fenestration, that is via the aqueous parasitophorous duct, which extends from the host erythrocytic membrane to the parasite plasma membrane (Figure 3.2) (Loyevsky and Cabantchik, 1993a). Although permeation via fenestration would still be rate-limiting to desferrioxamine, it would allow a higher concentration of the drug to accumulate in the parasite and have a more potent inhibitory effect on parasite growth. The parasitophorous duct only develops at the early trophozoite stage, thus resulting in desferrioxamine uptake and inhibition of the mature stages, but not the ring-infected

erythrocytes (Figures 6.4 and 6.5).

The antimalarial activity of desferrioxamine appears to affect the progression of trophozoite- to schizont-infected erythrocytes (Figure 6.5), which coincides with the period of maximal metabolic activity, especially DNA synthesis (Atkinson *et al.*, 1989). Similar phenomena have been reported in human lymphocytes, K562 cells and mouse mammary tumour cells, where iron chelating agents and iron deprivation inhibit cell proliferation by decreasing the ribonucleotide reductase activity (Lederman *et al.*, 1984; Ganeshaguru *et al.*, 1980; Furukawa *et al.*, 1992; Nyholm *et al.*, 1993a). Thus, desferrioxamine could have inhibited the *P. falciparum*-synthesized ribonucleotide reductase (Rubin *et al.*, 1993), and consequently inhibited the progression of trophozoite-infected erythrocytes to the schizont stage. It is possible that desferrioxamine inhibited the enzyme directly, by chelating the loosely bound ferrous ions from the reduced enzyme (Reichard and Ehrenberg, 1983). Alternatively, desferrioxamine could have depleted the intraparasitic iron pool, thereby preventing the regeneration of the iron-radical centre, which only has a half-life of about four hours, or by preventing the incorporation of iron into newly synthesized apo-ribonucleotide reductase (Nyholm *et al.*, 1993a).

Another mechanism by which desferrioxamine could inhibit the enzymatic process is through its ability to function as a free radical scavenger, and thereby prevent the tyrosyl radical from reducing the ribonucleotide triphosphates (Hartley *et al.*, 1989). This mechanism is similar to that reported for hydroxyurea (Nyholm *et al.*, 1993b). As a result of the non-functional ribonucleotide reductase enzyme, intracellular concentrations of dNTPs remain very low and this can directly affect DNA polymerase activity. The DNA polymerase enzyme depends on the presence of dNTP, and a deficiency of these substrates would reduce or inhibit DNA synthesis (Atkinson *et al.*, 1989). Lytton *et al.* (1994) also reported that treatment with desferrioxamine reduced DNA synthesis in trophozoite-infected erythrocytes to about 20% of the control. The observed decrease in hypoxanthine incorporation into parasite DNA (Figure 6.7) could also be due to the breakdown of the nuclear apparatus. Ultrastructural studies have confirmed that the plasmodial nucleus is a site for desferrioxamine action (Atkinson *et al.*, 1989).

Several lines of direct evidence suggest that the ribonucleotide reductase enzyme could be a potential, but not the sole molecular target for desferrioxamine action. Thus, the enzymes involved in the replication apparatus, along with other unidentified enzymes, could be targets for desferrioxamine inhibition.

6.5.4.1.3 Recrudescence

The removal of desferrioxamine from treated mammalian cells results in complete reversal of the inhibitory effects, allowing for normal DNA synthesis and cell proliferation (Lederman *et al.*, 1984). But the malaria-infected erythrocytes show a different pattern of susceptibility to iron chelation therapy. Lytton *et al.* (1994) reported that after twelve hours of *in vitro* drug exposure, the effects of desferrioxamine are irreversible since the addition of a permeating iron-complex (Fe^{3+}-nitrilotriacetic acid) did not reverse this inhibition. They concluded that the lack of recovery is probably due to the inability of the parasite to use iron. However, in the latter experiments, DNA synthesis was only monitored for a total of twelve hours, and according to the clinical trials, it took the parasite approximately seven days after a "zero" parasitaemia to return to its normal metabolic status in the presence of the patient's activated immune system (Bunnag *et al.*, 1992). Data from this study (Chapter 6.4.4.4) indicated that after one week of treatment with 150 μM desferrioxamine (i.e. ten times the IC_{50} value), it took approximately one drug-free week for the parasite to restore its normal metabolism, including DNA synthesis. This could be attributed to the limited efflux of desferrioxamine from the parasite, and could play an essential role in limiting the capacity of the parasite to recovery from treatment (Cabantchik, 1995). Thus, a much longer period is required to monitor parasite recovery from the exposure to desferrioxamine. The iron chelating effects of desferrioxamine are reversible and cytostatic; such that desferrioxamine suppresses the parasitaemia to barely undetectable numbers and with the restoration of the iron supply and the repair or synthesis of iron-dependant enzymes, the parasite can resume its normal replication cycle (Chapter 6.4.4.4).

6.5.4.2 Stage-dependant effects of 2,2'-bipyridyl

The morphological or ultrastructural effects induced by 2,2'-bipyridyl on the malaria parasite are undocumented. 2,2'-Bipyridyl, a bidentate ferrous ion chelating agent is an

effective antimalarial (Table 6.1 and Jairam *et al.*, 1991).

6.5.4.2.1 Effect on the ring stage

From the microscopic examination of the effects of 2,2'-bipyridyl on a synchronous culture, it can be concluded that 2,2'-bipyridyl affects the progression of the ring-infected erythrocytes to the trophozoite stage, as the ring-infected erythrocytes persisted in culture for a much longer period than in the control (Figure 6.4 and Chapter 6.4.4.3). The second generation of rings were similarly affected, but no morphological changes were observed. The inhibitory effect on the ring stage was also demonstrated by the significant decrease in hypoxanthine incorporation during the first ten hours of the cycle (Figure 6.7). The greater partition coefficient of 2,2'-bipyridyl enables the drug to permeate at a faster rate into the parasitized erythrocyte and inhibit parasite growth. The lipophilicity of 2,2'-bipyridyl enables it to enter the erythrocytic membrane, and its antimalarial activity could be due to the prevention of nutrients (e.g. iron and hypoxanthine) permeation into the parasitized erythrocyte.

6.5.4.2.2 Effect on the trophozoite stage

Due to the hydrophobic nature of 2,2'-bipyridyl, it partitions itself into the apolar phase of the erythrocytic membrane (Figure 3.5), which enables it to bind ferrous ions as they move into the erythrocyte (Nunez *et al.*, 1983). It is possible for 2,2'-bipyridyl to distribute throughout the pool of intracellular membranes, since there is constant movement between the intracellular and plasma membranes (Steinman *et al.*, 1983). Thus, 2,2'-bipyridyl could prevent the passage of iron into many organelles, including the mitochondria, food vacuole and nucleus (Ponka *et al.*, 1979). 2,2'-Bipyridyl could be acting by a similar mechanism to desferrioxamine (Chapter 6.1.4.1). This could account for the similarity in the morphological changes induced by 2,2'-bipyridyl and desferrioxamine, in the haemozoin-containing trophozoite-infected erythrocytes, which appeared vacuolated with a disrupted cytoplasm (Chapter 6.4.4.3). Additionally, no significant changes in parasitaemia (Figures 6.5 and 6.6) were observed when 2,2'-bipyridyl and desferrioxamine were added to the late trophozoite- and early schizont-infected erythrocytes. It is possible that 2,2'-bipyridyl causes chromosomal breaks possibly through free radical damage (Chevion, 1988), as well as affects the iron-dependent

enzymes involved in nuclear division. This nuclear damage could occur during mitosis, when the iron associated with the interphase nucleolus is transferred to the chromosomes (Robbins and Pederson, 1970). Thus, 2,2'-bipyridyl could chelate this iron and thereby inhibiting mitosis and parasite proliferation.

With respect to other possible targets, i.e. the mitochondria and food vacuole, iron deficiency induced by 2,2'-bipyridyl could result in the inhibition of mitochondrial enzymes, which are necessary for electron transport and ATP formation (Lytton *et al.*, 1994). In addition, if the parasite mobilises iron from digested haemoglobin in the acidic food vacuole (Gabay and Ginsburg, 1993), 2,2'-bipyridyl could inhibit the movement of iron from the food vacuole into the parasite cytosol. By inhibiting the functions of these organelles, the parasite metabolism would be disrupted and the cytoplasm would become contracted and dense in appearance (Chapter 6.4.4.3).

Thus, although 2,2'-bipyridyl primarily acts on the ring-infected erythrocytes, it is possible that 2,2'-bipyridyl also inhibits the iron-dependant metabolism of the trophozoite-infected erythrocytes.

6.5.4.3 Combined effect of desferrioxamine and 2,2'-bipyridyl

The combination of 2,2'-bipyridyl and desferrioxamine results in an antagonistic effect on the incorporation of hypoxanthine into parasite DNA (Figure 5.13). The antagonism primarily occurred at the ring stage (Figure 6.7), where 2,2'-bipyridyl is predominantly active. Morphologically, it was observed that the ring-infected erythrocytes did not persist in culture as long as those treated solely with 2,2'-bipyridyl and the mature stages were not as affected as those treated with individual drugs (Figure 6.8). During the ring stage, it is possible that these chelating agents complex with the non-transferrin-bound iron, and thereby prevent 2,2'-bipyridyl from inhibiting this early stage.

For the free radical generating Fenton reaction to be optimally efficient, a 1:1 ratio of Fe^{3+} and Fe^{2+} is required to drive the reaction in a forward direction to produce the toxic hydroxyl radical (Figure 5.1) (Braughler *et al.*, 1986). Thus, if 2,2'-bipyridyl exerts its antimalarial effects through free radical damage and desferrioxamine chelates the ferric

ions in the Fenton reaction, the production of free radicals would be greatly reduced and parasite growth would occur (Figure 5.16). Thus, the combination of a ferric and ferrous iron chelating agent would not be a feasible option.

It is concluded that the sensitivity of the malaria parasite to iron chelating agents is not only dependent on the stage of parasite development, but also on drug treatment (concentration and duration) and the solubility of the drugs (e.g. permeation, which could affect the capacity of the parasite to recover after drug removal). The antimalarial activity is also greatly influenced by any variation in inoculum size, change in extracellular pH and the presence of various cations.

CHAPTER SEVEN

CONCLUDING DISCUSSION

It has been shown that the parasitized erythrocytes preferentially accumulate non-transferrin bound iron from the extracellular milieu, along with a low concentration of diferric transferrin (Figure 3.9). Both forms were accumulated in a concentration- and time- dependant manner (Figures 3.5 to 3.8), with the uptake of non-transferrin-bound iron also being temperature-dependant (Figure 3.10). More iron was found to be associated with the trophozoite-infected erythrocytes than with the ring stage; which is possibly due to the many iron-dependant biochemical reactions which predominate in the later stages of parasite development (Figure 3.5 to 3.7). The non-transferrin bound iron was possibly accumulated by a facilitated diffusion system, mediated by a carrier protein or via the parasitophorous duct (Figure 3.1). The diferric transferrin was not internalized by the transferrin receptor-mediated endocytotic pathway, but by a non-specific endocytotic process, such as pinocytosis. Once internalized the transferrin is probably degraded, with the amino acids being incorporated into parasite proteins and the iron selectively retained (Pollack and Schnelle, 1988).

The parasite contains many iron-dependant metabolic enzymes, however the amount of iron taken up probably exceeds its rate of utilization. In reticulocytes and hepatocytes, the excess iron is usually stored in association with ferritin or haemosiderin (Pollack, 1994). The parasite however utilized a storage component that is unique to malaria parasites, the haemozoin crystal. A large percentage of the accumulated iron was found associated with the haemozoin, in the ferric state (Figures 4.4 and 4.5). The haemozoin crystals possibly acted as a sink to prevent the iron from catalysing any radical generating reactions, and in turn, the iron was necessary for the formation and stabilization of the haemozoin structure. From the data obtained in this thesis, it was proposed that the haemozoin crystal is formed as a result of the following: After the haem units are released from the endocytosed haemoglobin, the methyl groups situated around the haem units are oxidized to carboxyl groups which in turn bind the extracellular iron to form the complex haemozoin structure (Figure 4.13).

In the absence of trivalent cations, the haemozoin crystal dissociates into the monomeric form consisting of haem units, which are extremely toxic and haemolytic in nature (Figure 4.8; Table 4.1; Orijh *et al.*, 1981). The higher content of unsaturated phospholipids in the

parasitized erythrocytic membrane compared to the uninfected erythrocytes, resulted in the former erythrocytes being more susceptible to haemin induced lipid peroxidation (Figure 4.8). The haemin induced haemolysis was further potentiated by the presence of micromolar concentrations of chloroquine (Figures 4.9 and 4.10), which concurs with the possibility that chloroquine enhances the intercalation of haemin between the membrane phospholipids, to facilitate enhanced haemolysis. This latter haemolytic action is proposed to be a mechanism by which chloroquine inhibits parasite growth (Fitch, 1989). However, the haemin-chloroquine complex is neutralized by the addition of plasma proteins (Zhang and Hempelmann, 1987), thus the antimalarial action of chloroquine cannot be fully explained by the haemin-chloroquine haemolytic hypothesis.

The increased resistance to chloroquine has prompted the demand for novel chemotherapeutic strategies. One of which involves the sequestration of plasma cations, specifically iron, due to its unique involvement in the DNA synthesis enzyme, ribonucleotide reductase. The naturally occurring plasma chelating agents, such as citrate, ascorbate and apotransferrin are not effective in inhibiting parasite growth, however the pharmacological agents, desferrioxamine, EDTA, DTPA, and EGTA had varied success (Table 5.2). The hydrophilic chelating agents, EDTA, DTPA, and EGTA were relatively inefficient in inhibiting parasite growth, as they could only chelate the extracellular cations. This contrasted with the hydrophilic chelating agents, bathophenanthroline sulphonate and desferrithiocin. Bathophenanthroline sulphonate effectively inhibited parasite growth, through its ability to specifically prevent the uptake of ferrous ions into the parasitized erythrocyte; while desferrithiocin possibly depleted the parasite iron located in the infected erythrocyte and the parasitic transit iron pool (Table 5.2). The alkyl derivatives of EDTA were more potent than EDTA, where the length of the alkyl side group was directly related to the lipophilicity of the compound and its antimalarial activity (Table 5.2 and Figure 5.10). However, the increased lipophilicity of the derivatives could be potentially hazardous in the clinical setting, as this property could allow the agent to cross the blood brain barrier, resulting in central nervous system toxicity (Porter *et al.*, 1990).

To determine whether the parasite preferentially utilized ferric or ferrous ions in its

metabolism, ferric and ferrous iron chelating agents (desferrioxamine and 2,2'-bipyridyl, respectively) were used to contrast each others activity (Table 5.2). Both agents exhibited potent antimalarial activity against various chloroquine-sensitive and -resistant strains (Table 5.1). However due to the lipophilicity and central nervous system properties of 2,2'-bipyridyl, it should only be used in laboratory experiments (Bass *et al.*, 1966). Desferrioxamine has already been successfully used in clinical trials to treat uncomplicated to comatosed cerebral malaria infections (Gordeuk *et al.*, 1992b; Gordeuk *et al.*, 1995).

In summary, 2,2'-bipyridyl was found to have the following effects on parasitized erythrocytes. 2,2'-Bipyridyl affected the development of the ring-infected erythrocytes (Figures 6.4 and 6.7), although morphologically this stage did not appear to be affected. This is in contrast to the trophozoite- and schizont-infected erythrocytes, which became vacuolated and more dense in appearance (Figure 6.8). The inhibitory affect on the mature stages of development could be related to the dose-dependant manner in which the uptake of non-transferrin bound iron was inhibited (Figure 3.13; bottom); whilst the uptake of diferric transferrin was not inhibited. 2,2'-Bipyridyl effectively inhibits parasite growth (Table 5.1 and 5.2), possibly by chelating iron which catalyses essential biochemical reactions in the nucleus and mitochondria (Ponka *et al.*, 1979; Feagin *et al.*, 1991). The accumulation of the toxic iron-chelate complexes in the parasite may also have contributed towards the inhibition of parasite development (Table 6.1 and Figure 6.3) (Ponka *et al.*, 1979; Cabantchik, 1995). 2,2'-Bipyridyl did not affect the haemozoin crystalline structure (Figure 4.7), which indicates that the haemozoin-associated iron is in the ferric state and not readily accessible for chelation by 2,2'-bipyridyl. In addition, it was found that the presence of 2,2'-bipyridyl potentiated the haemolysis induced by haemin (Figure 4.12); however, this is unlikely to be the primary mechanism by which 2,2'-bipyridyl inhibits parasite growth.

The following can be used to form a more complete understanding of how desferrioxamine inhibits parasite growth. Desferrioxamine preferentially manifests its antimalarial activity against the mature developmental stages, i.e. the mid trophozoite to early schizont stages (Figures 6.5 to 6.7); with the development of the ring-infected erythrocytes being unaffected (Figure 6.4). Morphologically, the trophozoite-infected erythrocytes became

vacuolated, with the cytoplasm being disrupted; whilst the ring stage appeared unaffected (Figure 6.8). The observed effects could be due to desferrioxamine inhibiting the uptake of both transferrin and non-transferrin bound iron into the parasitized erythrocytes (Figures 3.11 and 3.13); as well as its abilities to permeate into and chelate the intra-parasitic iron (Scott *et al.*, 1990). The antimalarial activity of desferrioxamine was related to its ability to chelate ferric ions, since the action of desferrioxamine was abolished once the Fe^{3+}-desferrioxamine complex was formed (Figure 6.3 and Table 6.1). The cytocidal effects of desferrioxamine occurred during the mature stages of parasite development when haemozoin was being formed (Scott *et al.*, 1990). It is at these latter stages that desferrioxamine can passively diffuse through the concentric membranes around the parasite and decrease the iron content in the haemozoin crystal (Figure 4.6). By doing so, it was verified that the haemozoin iron exists in the ferric state (Figure 4.7) and that the extracellular iron is incorporated between the haem units in the haemozoin crystal (Figure 4.13), since desferrioxamine can not chelate the haem-associated iron (Bridges and Seligman, 1995). The haemozoin crystal may be disrupted by this chelating action but this would only be temporary as other trivalent cations could quickly replace the chelated iron and stabilize the structure. Thus, no haem molecules should be released from the crystal, although if a low concentration are released, desferrioxamine could protect the host cells from haem induced damage (Figure 4.11).

The effective antimalarial properties of desferrioxamine could be attributed to its avid iron chelating abilities, however its low permeation coefficient does decrease the possible efficacy of desferrioxamine. To increase the permeation coefficient and efficacy of desferrioxamine, it could be possible to increase its lipophilicity by modifying its chemical structure, which was achieved for EDTA (Figure 5.10) and the reversed siderophores (Cabantchik, 1995). Alternatively, desferrioxamine could be encapsulated in multilamellar liposomes (phospholipid bilayer vesicles), which would allow desferrioxamine to permeate into and inhibit all stages of parasite growth (Allen, 1994). Lysosomes are effective for targeted drug delivery and have been shown to be effective carriers of desferrioxamine to the lung tissue in rats and in potentiating the inhibitory actions of desferrioxamine against macrophages infected with *Leishmania* (Tabak *et al.*, 1994; Segovia *et al.*, 1989).

The administration of desferrioxamine alone, did not inhibit 100% of parasite growth, although the additive interaction between desferrioxamine and a classical antimalarial (chloroquine, quinine or pyrimethamine) completely eliminated the malaria infection (Figures 5.11 to 5.13). However, the antagonistic interaction between 2,2'-bipyridyl and desferrioxamine or desferrithiocin (Figure 5.15; top), indicate that hydrophilic ferric and lipophilic ferrous iron chelating agents, should not be combined. This antagonistic interaction may be due to either 2,2-bipyridyl inhibiting the diffusion and accumulation of desferrioxamine into the parasite or desferrioxamine inhibiting the formation of free radicals by 2,2'-bipyridyl or both possibly competing for the parasitic iron. This is in complete contrast to the synergistic interaction which occurs when 2,2'-bipyridyl and bathophenanthroline, two lipophilic ferrous iron chelating agents are combined. This synergistic interaction is also observed when bathophenanthroline is combined with desferrioxamine or desferrithiocin (hydrophilic ferric iron chelating agents) (Figure 5.15; bottom). The interaction is possibly due to bathophenanthroline working extracellularly at the membrane surface by inhibiting the uptake of ferrous ions; whilst the other agents chelate the intracellular iron. In addition, the formation and accumulation of the toxic iron-chelate complexes could contribute to the inhibition of parasite growth. The combination of two hydrophilic ferric iron chelating agents (desferrioxamine and desferrithiocin) complemented each others inhibitory actions and resulted in an additive interaction (Figures 5.14 and 5.15). Both these agents can sequester the intra-parasitic iron and the complexes are retained in the parasitized erythrocyte for an extended period. A combination of these two mechanisms could result in the inhibition of essential biochemical reactions and eventual parasite death.

Thus, it can be concluded that the unique pathways involved in the iron metabolism of *P. falciparum*-infected erythrocytes could be potential targets for new antimalarial drugs, which are membrane permeable and have a high affinity for iron. The efficacy of these agents could be increased by combining them with the classical antimalarials or other iron chelating agents.

APPENDICES

APPENDIX A

LIST OF CHEMICALS

Acetic acid	BDH
Acrylamide	Promega
Acrylogel 5 premix	BDH
Agarose	LKB
AGI-X8 chloride 200-400	Biorad
Al_2SO_4	BDH
Apotransferrin	South African Blood Transfusion Services
APS	Biorad
Ascorbate	Saarchem
Barbital	Merck
2,2'-Bipyridyl	Fluka
Bis	BDH
Bolton & Hunter ^{125}Iodine reagent	Amersham
Borate	Merck
Bromophenol blue	BDH
Calcium lactate	Saarchem
Chelex-100 sodium 200-400	Biorad
Chloroquine sulphate	Sigma
Citrate	BDH
Contrad	Merck
Coomassie Brilliant Blue R-250	BDH
Cupric sulphate	BDH
D-sorbitol	Saarchem
Desferrioxamine mesylate	Ciba-Geigy
DTPA	Fluka
EDTA	BDH/Saarchem

EGTA	Boehringer Mannheim
Ethanol	Saarchem
Gelatine	Sigma
Gentamycin sulphate	Sigma
Giemsa stain	BDH
Glucose	Merck
Glycerol	BDH
Glycine	Biorad
Haemin chloride	Sigma
HEPES	Boehringer Mannheim
Human transferrin antibody	Sigma
Hypoxanthine	Sigma
^{3}H-Hypoxanthine	Amersham
Iron (III) chloride	Sigma
^{59}Iron (III) chloride	Amersham
KH_2PO_4	Merck
Methanol	Merck
Mikroskopie Immersion Oil	Merck
$Na_2HPO_4.12H_2O$	Saarchem
$Na_2HPO_4.2H_2O$	Merck
NaCl	Saarchem
$NaHCO_3$	Saarchem
Nitrilotriacetic acid	Saarchem
PAGE Blue 83	BDH
Phenol red 2000x concentrate	Sigma
Pyrimethamine	Sigma
Quinine Sulphate	Fluka
RPMI-1640	Highveld Biological
Saline	SABAX
Saponin	Fluka
SDS	Biorad
Sodium acetate	BDH

Sucrose	BDH
TEMED	LKB
Trichloroacetic acid	Saarchem
Tris	Saarchem
Urea	Isolab/BDH
Xylene	Hopkins & Williams
Zinc chloride	Merck

APPENDIX B

B.1 CALCULATION FORMULA USED TO DETERMINE THE VOLUME OF FERRIC CHLORIDE REQUIRED TO PREPARE A DIFERRIC TRANSFERRIN SOLUTION

1 mmol transferrin = 80 000 mg

1 x 12 / 80 000 mmol transferrin = 12 mg transferrin

Therefore, 12 mg transferrin = 2 x 12 / 80 000 mmol Fe

But, 1 mmol transferrin = 2 mmol Fe as $FeCl_3$

Then 12 mg transferrin = 12 / 40 000 $FeCl_3$

1 mmol $FeCl_3$ = 162,4 mg

Therefore, 12 / 40 000 mmol $FeCl_3$ = 162,4 x 12 / 40 000 = 48,72 μg $FeCl_3$

There is 55,9 μg Fe in 162,4 μg $FeCl_3$

Therefore, 1 μg Fe = 162,4 / 55,9 = 2,905 μg $FeCl_3$

If the bottle contained 170 μg Fe/ml of $FeCl_3$ solution,

then 170 μg Fe = 2,905 x 170 = 493,88 μg $FeCl_3.ml^{-1}$

Therefore, 48,72 μg $FeCl_3$ = 48,72 μg / 493,88 $\mu g.ml^{-1}$

= 0,09865 ml $\equiv$ 98,65 μl $FeCl_3$

B.2 SOLUTIONS USED IN THE RADIAL IMMUNODIFFUSION TECHNIQUE

- **Barbiturate buffer:** 106,70 mM barbital, 365,69 mM Tris, 1,73 mM calcium lactate and 1,0 mM NaN_3 in distilled water. The solution was brought to pH 8,6 and stored at 4°C. The buffer was diluted 1:4 before use.

- **Agarose gel solution:** 1% (w/v) agarose in barbiturate buffer was heated to 90°C with constant stirring until dissolved. The solution was then aliquoted out into 10 ml iron-free glass tubes and stored at 4°C.
- **Staining solution:** 1 g Coomassie Brilliant Blue R-250 was dissolved in 90 ml ethanol, 20 ml acetate and 90 ml distilled water.
- **Destaining solution:** 90 ml ethanol, 20 ml acetate and 90 ml distilled water.

APPENDIX C

C.1 SOLUTIONS USED IN THE 6 M UREA POLYACRYLAMIDE GEL ELECTROPHORETIC TECHNIQUE

- **20x Tris/borate/EDTA buffer:** 2 M Tris, 0,2 M borate and 32 mM EDTA (pH 8,4) in distilled water. Chelex-100 was added to the solution and agitated for 2 hours to remove trace amounts of iron present in the buffer. The buffer was filtered into an iron-free glass container. Storage at 4°C.
- **Urea solution:** 10 M urea was prepared with Chelex-100, agitated for 2 hours before being filtered into an iron-free container and stored at 4°C.
- **Acrylamide stock solution:** A 36% stock solution of Acrylogel 5® (a 5% (w/w) premix of N,N'-methylene-bisacrylamide in acrylamide) was prepared and agitated for 6 hours with Chelex-100. The solution was filtered into a iron-free dark glass container and stored at 4°C for up to 1 month.
- **Ammonium persulfate solution:** 98,6 mM APS was prepared and stored at 4°C in an iron-free glass container.
- **Electrode buffer:** The 20x Tris/borate/EDTA buffer was diluted to a 1x buffer in ice cold Millipore water.
- **Casting solution:** 6% polyacrylamide gel prepared in an acid cleaned flask as follows: 30 ml 10 M urea, 2,5 ml 20x buffer, 8,4 ml acrylamide stock, 6,6 ml distilled water, 30 μl TEMED and 2 ml APS.
- **Sample diluting buffer:** 3 ml urea, 0,125 ml 20x Tris/borate/EDTA buffer, 0,75 ml distilled water and 0,75 mM sucrose were dissolved together with Chelex-100 added, and agitated for 1 hour. The solution was filtered into an iron-free glass container and stored at 4°C. Sucrose was used in preference to glycerol to increase the density of the buffer. Before use, a few drops of Bromophenol Blue was added.
- **Coomassie Blue Stain:** 1 g Coomassie Brilliant Blue R-250 dissolved in ethanol, acetic acid and distilled water in a ratio of 90:20:90.
- **Destain solution:** 20 ml Acetic acid, 90 ml ethanol and 90 ml distilled water.

APPENDIX D

D.1 SOLUTIONS USED IN THE 6-20% LINEAR GRADIENT SDS GEL ELECTROPHORETIC TECHNIQUE

- **Stock acrylamide solution:** 38,8 g acrylamide and 1,1 g bisacrylamide were in 100 ml of distilled water.
- **Phosphate buffer:** 300 mM Na_2HPO_4 solution, pH 11,2.
- **3% Casting gel:** 10 ml phosphate buffer, 1,5 ml acrylamide stock solution, 8,5 ml distilled water, 20 mg APS and 20 μl TEMED.
- **20% Casting gel:** 10 ml phosphate buffer, 10 ml acrylamide stock solution, 20 mg APS and 20 μl TEMED.
- **Electrode buffers:** A 3% (v/v) phosphate buffer was prepared for the anode (bottom) reservoir. 500 mg SDS was added to the 3% phosphate buffer for the cathode (top) reservoir.
- **Sample diluting buffer:** 1,2 g urea, 100 mg SDS, 900 μl phosphate buffer, 900 μl distilled water and a trace amount of phenol red.
- **Haemoglobin sample:** The haemoglobin control was prepared from the supernatant of the lysed uninfected erythrocytes. The supernatant was microcentrifuged at 1000 *g* for 10 minutes before being diluted in a 1:1 ratio with sample diluting buffer.
- **Haemozoin sample:** Haemozoin samples were prepared by mixing 30 μl of the pure isolated haemozoin with 30 μl sample diluting buffer.
- **Coomassie Blue Stain:** 0,75 g PAGE Blue 83 per 1l methanol and 150 g TCA per 1l distilled water, mixed in a 1:1 ratio.
- **Destain solution:** 5 ml glacial acetic acid, 30 ml methanol and 65 ml distilled water.

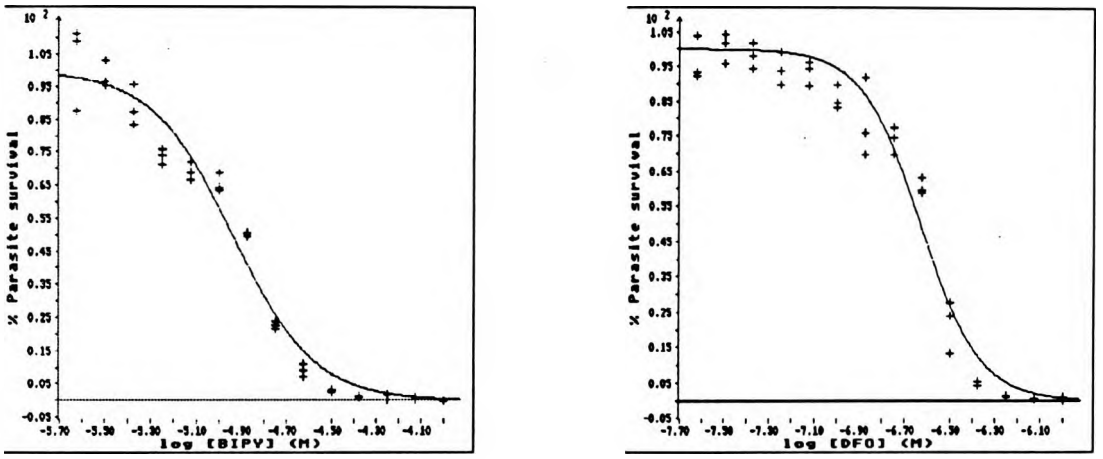


Figure E.1: The dose-response curves generated for plates A and B. Plate A (left) is 100 μM BIPY plated out alone, with an IC_{50} value of 11,46 $\pm$ 0,37 μM. Plate B (right) is 1 μM DFO and 75 μM BIPY combined, with an IC_{50} value of 0,23 $\pm$ 0,01μM.

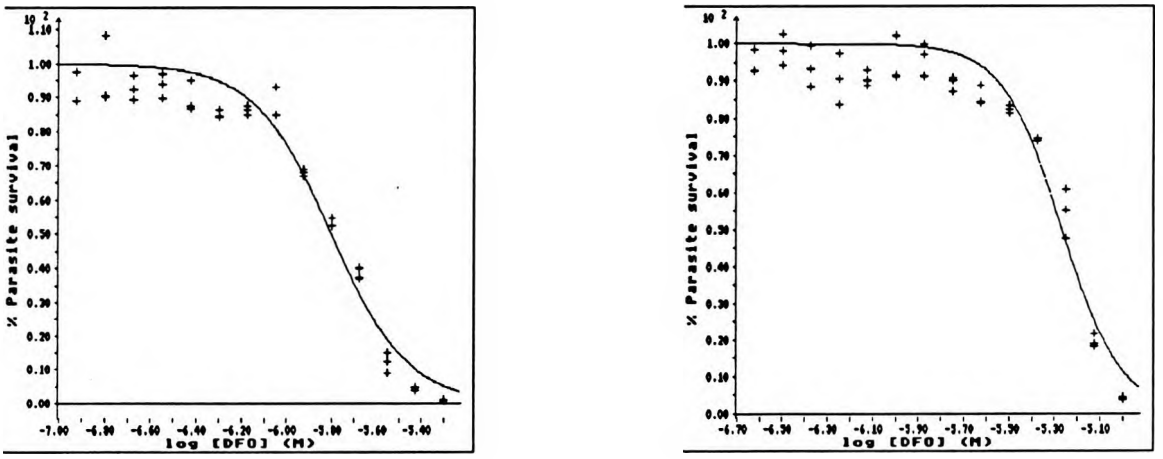


Figure E.2: The sigmoid dose-response curves generated for plates C and D. Plate C (left) is 5 μM DFO and 50 μM BIPY combined, with an IC_{50} value of 1,57 $\pm$ 0,06μM. Plate D (right) is 10 μM DFO and 30 μM BIPY combined, with an IC_{50} value of 5,39 $\pm$ 0,17 μM.

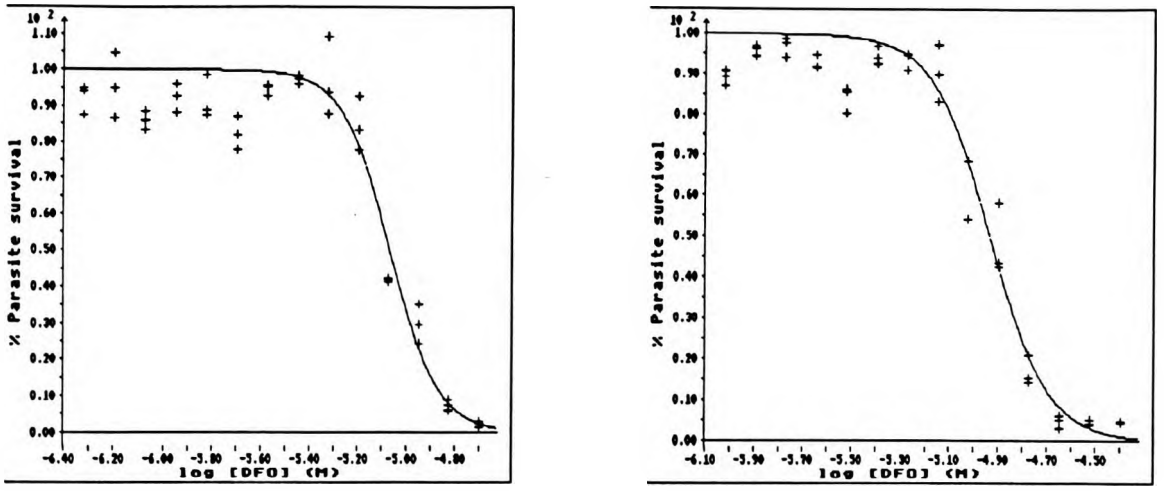


Figure E.3: The sigmoid dose-response curves generated for plates E and F. Plate E (left) is 20 μM DFO and 20 μM BIPY combined, with an IC_{50} value of 8,53 $\pm$ 0,30μM. Plate F (right) is 40 μM DFO and 10 μM BIPY combined, with an IC_{50} value of 11,67 $\pm$ 0,33μM.

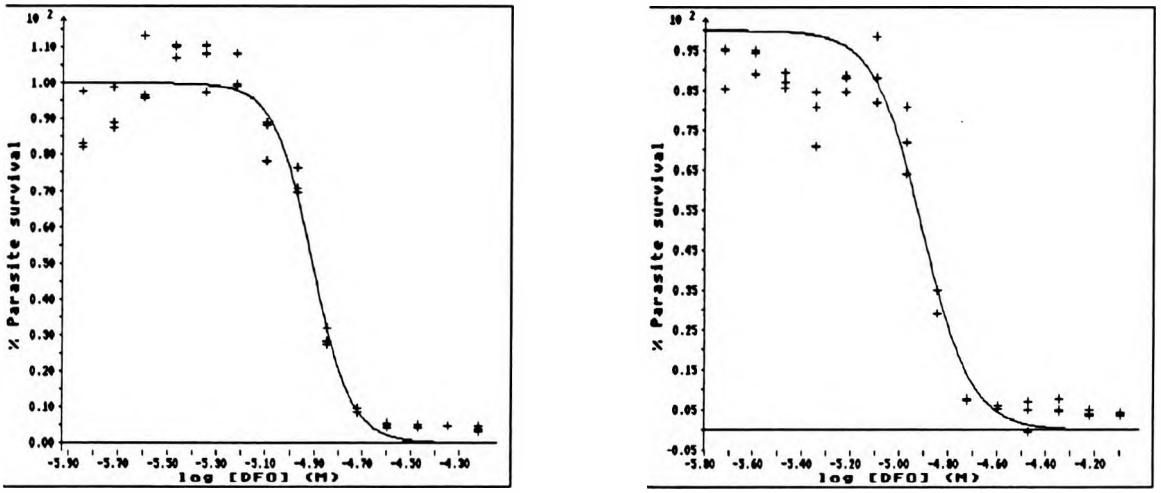


Figure E.4: The sigmoid dose-response curves generated for plates G and H. Plate G (left) is 60 μM DFO and 5 μM BIPY combined, with an IC_{50} value of 12,33 $\pm$ 0,29μM. Plate H (right) is 80 μM DFO plated out alone, with an IC_{50} value of 12,38 $\pm$ 0,45μM.

Table E.1. Data used to generate the isobolograms. Fixed ratios of drugs used in the combination experiments and the IC_{50} values obtained from Figures E1-E4, to generate the isobologram in Figure 5.16. Where DFO is desferrioxamine and BIPY is 2,2-bipyridyl.

PLATE	[ ] (μM)		IC_{50} (μM)		DRUG RATIO	
	DFO	BIPY	DFO	BIPY	DFO	BIPY
A	0	100	0,000	11,456	0,000	1,000
B	1	75	0,233	17,484	0,019	1,526
C	5	50	1,573	15,733	0,127	1,373
D	10	30	5,390	16,171	0,435	1,412
E	20	20	8,526	8,826	0,713	0,770
F	40	10	11,673	2,918	0,943	0,255
G	60	50	12,331	1,028	0,996	0,090
H	80	0	12,381	0,000	1,000	0,000

REFERENCES

Aikawa M. High resolution autoradiography of malaria parasites treated with ^{3}H-chloroquine. Am J Pathol 1972;67:277-280.

Aikawa M, Beaudoin RL. Studies on nuclear division of a malarial parasite under pyrimethamine treatment. J Cell Biol 1968;39:749-754.

Aikawa M, Miller LH. Structural alterations of the erythrocyte membrane during malarial parasite invasion and intraerythrocytic development. In: Evered D, Whelan J, editors. **Malaria and the Red Cell.** London: Pitman, 1983:45-63.

Aisen P. Some physiochemical aspects of iron metabolism. In: **Iron metabolism.** Ciba Foundation Symposium, New York: Elsevier, 1977;51:1-14.

Aisen P, Leibman A. Citrate-mediated exchange of Fe^{3+} among transferrin molecules. Biochem Biophys Res Comm 1968;32(Pt 2):220-226.

Allen TM. Long-circulating (sterically stabilized) liposomes for targeting drug delivery. TIPS 1994;15(7):215-220.

Anderson GJ, Dancis A, Roman DG, Klausner RD. Ferric iron reduction and iron uptake in eucaryotes: studies with the yeasts: *Saccharomyces cerevisiae* and *Schizosaccharomyces pombe*. Adv Exp Med Biol 1994;356:81-89.

Anstey NM, Hassanali MY, Mlalsi J, Manyenga D, Mwaikambo ED. Elevated levels of methaemoglobin in Tanzanian children with severe and uncomplicated malaria. Trans Royal Soc Trop Med Hyg 1996;90:147-151.

Aremu CY. Changes in serum transferrin and iron concentrations in humans suffering from malaria with parasitaemia. Ann Trop Med Parasitol 1989;83(Pt 5):517-520.

Arosio P, Levi S, Santambragio P, Cozzi A, Rovida E, Corsi B, Tamborini E, Spada S, Albertini A. Chemico-physical and functional differences between H and L chains of human ferritin. Adv Exp Med Biol 1994;356:13-22.

Aruoma OI, Halliwell B, Gajewski E, Dizalaroglu M. Damage to the bases in DNA induced by hydrogen peroxide and ferric ion chelates. J Biol Chem 1989;264(Pt 34):20509-20512.

Ashong JO, Blench IP, Warhurst DC. The composition of haemozoin from *Plasmodium falciparum*. Trans Royal Soc Trop Med Hyg 1989;83:167-172.

Atkinson CT, Bayne MT, Gordeuk VR, Brittenhan GM, Aikawa M. Stage-specific ultrastructural effects of desferrioxamine on *Plasmodium falciparum in vitro*. Am J Trop Med Hyg 1991;45(Pt 5):593-601.

Auld DS. Use of chelating agents to inhibit enzymes. Meth Enzymol 1988;158:110-114.

Babior BM, Stossel TP. Heme formation: The supply of iron: iron deficiency and iron excess. In: Babior BM, Stossel TP, editors. **Hematology: A Pathophysiological approach.** 3rd Ed. New York: Churchill Livingstone, 1994:43-61.

Baker E, Page M, Torrance J, Grady R. Effect of desferri-oxamine, rhodotorulic acid and cholythydroxamic acid on transferrin and iron exchange with hepatocytes in culture. Clin Physiol Biochem 1985;3:277-288.

Baker E, Wong A, Peter H, Jacobs A. Desferrithiocin is an effective iron chelator *in vivo* and *in vitro* but ferrithiocin is toxic. Br J Haematol 1992;81:424-431.

Barraviera B. Effects of antimalarial drugs and of clindamycin on erythrocyte metabolism. A review. Rev Inst Med Trop Sao Paulo 1989;31(Pt 3):200-205.

Bass P, Purdon RA, Patterson MA, Butler DE. Gastric anti-secretory and other pharmacologic studies on 2,2'-bipyridine. J Pharmacol Exp Ther 1966;152(Pt 1):104-115.

Bates GW, Billups C, Saltman P. The kinetics and mechanism of iron (III) exchange between chelates and transferrin. I. The complexes of citrate and nitrilotriacetic acid. J Biol Chem 1967;242(Pt 12):2810-2815.

Baynes R, Friedman B, McNamara L, Bothwell T, Bukofzer G, Macfarlane B. Transferrin iron interactions with cultured hepatocellular carcinoma cells (PLC/PRF/5). Eur J Cell Biol 1988;46:282-288.

Baysal E, Monteiro HP, Sullivan SG, Stern A. Desferrioxamine protects human red blood cells from hemin induced hemolysis. Free Rad Biol Med 1990;9:5-10.

Bendrat K, Berger BJ, Cerami A. Haem polymerization in malaria. Nature 1995;378:138.

Berenbaum MC. What is synergy? Pharmacol Rev 1989;1989(Pt 41):93-141.

Bergeron RJ, Liu CZ, McManis JS, Xis MXB, ALgee SE, Wiegand J. The desferrithiocin pharmcophore. J Med Chem 1994;37:1411-1417.

Bierer BE, Nathan DG. The effect of desferrithiocin, an oral iron chelator, on T-cell function. Blood 1990;76(Pt 10):2052-2059.

Bohinski RC. In: Bohinski RC. ed. **Modern Concepts in Biochemistry**, 5th Ed. Boston: Allyn and Bacon Inc., 1987:88, 89, 705.

Bolton AE, Hunter WM. The labelling of proteins to high specific radioactivities by conjugation to a 125I-containing acylating agent. Biochem J 1973;133:529-539.

Bookchin RM, Lew VL, Nagel RL, Raventos C. Increase in postassium and calcium transport in human red cells infected with *Plasmodium falciparum in vitro*. J Physiol 1981;312:65P.

Borg DC, Schaich KM. Iron and iron-derived radicals. In: **Oxygen radicals.** An Upjohn Symposium. 1987:20-33.

Bradsley WG, Childs RE, Crabbe MJC. Inhibition of enzymes by metal ion-chelating reagents. The action of copper-chelating reagents on diamine oxidase. Biochem J 1974;137:61-66.

Brasseur R, Ruysschaert JM. Conformation and mode of organization of amphiphilic membrane components: a conformational analysis. Biochem J 1986;238:1-11.

Braughler JM, Burton PS, Chase RL, Pregenzer JF, Jacobsen EJ, VanDoornik FJ, Tustin JM, Ayer DE, Bundy GL. Novel membrane localized iron chelators as inhibitors of iron-dependent lipid peroxidation. Biochem Pharmacol 1988;37(Pt 20):3853-3860.

Braughler JM, Duncan LA, Chase RL. The involvement of iron in lipid peroxidation importance of ferric to ferrous ratios in initiation. J Biol Chem 1986;261(Pt 22):10282-10289.

Bremard C, Girerd JJ, Kowalewski P, Merlin JC, Moreau S. Spectroscopic investigations of malaria pigment. Appl Spectrosc 1993;47(Pt 11):1837-1842.

Breuer W, Epsztejn S, Cabantchik ZI. Iron acquired from transferrin by K562 cells is delivered into a cytoplasmic pool of chelatable iron (II). J Biol Chem 1995;270(Pt 41):24209-24215.

Breuer W, Epsztejn S, Millgram P, Cabantchik IZ. Transport of iron and other transition metals into cells as revealed by a fluorescent probe. Am J Physiol 1995;268:CC1354-C1361.

Bridges KR, Cudkowicz A. Effect of iron chelators on the transferrin receptor in K562 cells. J Biol Chem 1984;259(Pt 21):12970-12977.

Bridges KR, Seligman PA. Disorders of iron metabolism. In: Handin RI, Lux SE, Stossel TP, editors. **Blood: Principles and Practice Hematology**. Philadelphia: JB Lippincott Company 1995:1433-1472.

Brown WH. Malarial pigment (so-called melanin): its nature and mode of production. J Exp Med 1911;13:290-300.

Buffington GD, Hunt NH, Cowden WB, Clark IA. Malaria: A role for reactive oxygen species in parasite killing and host pathology. In: Rice-Evans C, editor. **Free radicals, cell damage and disease.** London: Richelieu Press, 1986:201-219.

Bullen JJ. The significance of iron in infection. Rev Infect Dis 1981;3(Pt 4):1127-1138.

Bunn HF, Jandl JH. Exchange of heme among haemoglobins and between hemoglobin and albumin. J Biol Chem 1968;243(Pt 3):465-475.

Bunnag D, Poltera AA, Viravan C, Looareesuwan S, Harinasuta KT, Schindlery C. Plasmodial effect of desferrioxamine in human vivax or falciparum malaria from Thailand. Acta Trop 1992;52:59-67.

Burns ER, Pollack S. *P. falciparum* infected erythrocytes are capable of endocytosis. In Vitro Cell Dev Biol 1988;24(Pt 5):481-486.

Cabantchik ZI. Altered membrane transport of malaria-infected erythrocytes: A possible pharmacologic target. Blood 1989;74(Pt 5):1464-1471.

Cabantchik ZI. Properties of permeation pathways induced in the human red cell membrane by malaria parasites. Blood Cells 1990;16:421-432.

Cabantchik ZI. Iron chelators as antimalarials: the biochemical basis of selective cytotoxicity. Parasitol Today 1995;11(Pt 2):74-78.

Canfield CJ, Milhous WK, Ager Al, Rossan RN, Sweeney TR, Lewis TVJ, Jacobus DP. PS-15: A potent, orally active antimalarial from a new class of folic acid antagonists. Am J Trop Med Hyg 1993;49(Pt 1):121-126.

Cardoso MA, Ferreira MU, Ribeiro GS, Penteado MDVC, Andrade HF. Dietary iron supplementation does not aggravate experimental malaria in young rats. J Nutr 1996;126:467-475.

Cazzola M, Arosio P, Barosi G, Bergamaschi G, Dezza L, Ascari E. Ferritin in the red cells of normal subjects and patients with iron deficiency and iron overload. Br J Haematol 1983;53:659-665.

Chevion M. A site-specific mechanism for free radical induced biological damage: The essential role of redox-active transition metals. Free Rad Biol Med 1988;5:27-37.

Chiu D, Lubin B. Oxidative hemoglobin denaturation and RBC destruction: The effect of heme on red cell membranes. Semin Hematol 1989;26(Pt 2):128-135.

Chou AC, Fitch CD. Hemolysis of mouse erythrocytes by ferriprotoporphyrin IX and chloroquine. J Clin Invest 1980;66:856-858.

Chou AC, Fitch CD. Mechanism of hemolysis induced by ferriprotoporphyrin IX. J Clin Invest 1981;68:672-677.

Cochran M, Coates J, Neoh S. Competitive equilibrium between aluminium and ferric ions for the binding sites of transferrin. FEBS 1984;176(Pt 1):129-132.

Cole ES, Glass J. Transferrin binding and iron uptake in mouse hepatocytes. Biochim

Biophys Acta 1983;762:102-110.

Conrad ME, Umbreit JN. A concise review: Iron absorption - The mucin-mobilferrin-integrin pathway. A competitive pathway for metal absorption. Am J Hematol 1993;42:67-73.

Conrad ME, Umbreit JN, Peterson RDA, Moore EG, Harper KP. Function of integrin in duodenal mucosal uptake of iron. Blood 1993;81(Pt 2):517-521.

Cotton FA, Wilkinson G. In: Cotton FA, Wilkinson G, editors. **Advance inorganic chemistry: A comprehensive text**, 4th Edition. New York: John Wiley and Sons Inc, 1980:107-194, 326-351, 1310-1322.

Cowman AF, Foote SJ. Chemotherapy and drug resistance in malaria. Int J Parasitol 1990;20(Pt 4):503-513.

Crane FL, Sun IL, Clark MG, Grebing C, Low H. Transplasma-membrane redox systems in growth and development. Biochim Biophys Acta 1985;811:233-264.

Das BS, Patnaik JK, Mohanty S, Mishra SK, Mohanty D, Satpathy SK, Base TK. Plasma antioxidants and lipid peroxidation products in *falciparum* malaria. Am J Trop Med Hyg 1993;49(Pt 6):720-725.

Davies TME, Li G-Q, Guo X-B, Spencer JL, St John A. Serum ionized calcium, serum and intracellular phosphate and serum parathormone concentrations in acute malaria. Trans Royal Soc Trop Med Hyg 1993;87:49-53.

Deamer DW, Nichols JW. Proton flux mechanisms in model and biological membranes. J Membr Biol 1989;107:91-103.

Deegan T, Maegraith BG. Studies on the nature of malarial pigment (haemozoin). I. The pigment of the human species, *Plasmodium falciparum* and *P. malariae*. Ann Trop Med Parasitol 1956;50:212-222.

de Jong G, van Dijk JP, van Eijk HG. The biology of transferrin. Clin Chim Acta 1990;190:1-46.

Desjardin RE, Canfield CJ, Haynes JD, Chulay JD. Quantitative assessment of antimalarial activity *in vitro* by a semiautomated microdilution technique. Antimicrob Agents Chemother 1979;16(Pt 6):710-718.

Dorn A, Stoffel R, Matile H, Bubendorf A, Ridley RG. Malarial haemozoin/β-haematin supports haem polymerization in the absence of protein. Nature 1995;374:269-271.

Dutta P, Fitch CD. Diverse membrane-active agents modify the haemolytic response of FP-IX. J Pharmacol Exp Ther 1983;225(Pt 3):729-734.

Eckman JR, Modler S, Eaton JW, Berger E, Engle RR. Heme catabolism in drug-sensitive and drug-resistant malaria. J Lab Clin Invest 1977;90:767-770.

Egan TJ, Ross DC, Adams PA. Quinoline anti-malarial drugs inhibit spontaneous formation of β-haematin (Pt malaria pigment). FEBS lett 1994;352:54-57.

Elford BC, Cowman GM, Ferguson DJP. Parasite-regulated membrane transport processes and metabolic control in malaria-infected erythrocytes. Biochem J 1995;308:361-374.

Elmendorf HG, Haldar K. Secretory transport in *Plasmodium*. Parasitol Today 1993;9:98-102.

Evans SE, Havlik I. *In vitro* drug interaction between amantadine and classical antimalarial drugs in *Plasmodium falciparum* infections. Trans Royal Soc Trop Med 1994;88:683-686.

Feagin JE, Gardner MJ, Williamson DH, Wilson RJM. The putative mitochondrial genome of *Plasmodium falciparum*. J Protozool 1991;38(Pt 3):243-245.

Ferrari V, Cutler DJ. Uptake of chloroquine by human erythrocytes. Biochem Pharmacol 1990;39(Pt 4):753-762.

Fitch CD. Ferriprotoporphyrin IX: Role in chloroquine susceptibility and resistance in malaria. In: **Malaria and the Red Cell 2.** New York: Liss AR Inc., 1989:45-52.

Fitch CD, Chevli R, Banyal HS, Phillips G, Pfaller MA, Krogstad DJ. Lysis of *Plasmodium falciparum* by FPIX and a CQ-FPIX complex. Antimicrob Agents Chemother 1982;21(Pt 5):819-822.

Fitch CD, Kanjananggulpan P. The state of ferriprotoporphyrin IX in malaria. J Biol Chem 1987;262(Pt 32):15552-15555.

Fontecave M, Gerez C, Mansuy D, Reichard P. Reduction of the Fe(III)-tyrosyl radical centre of *Escherichia coli* ribonucleotide reductase by dithiothreitol. J Biol Chem 1990;265(Pt 19):10919-10924.

Foote SJ, Thompson JK, Cowman AF, Kemp DJ. Amplification of the multidrug resistance gene in some chloroquine-resistant isolates of *P. falciparum*. Cell 1989;57:921-930.

Freese JA, Sharp BL, Ridl FC, Markus MB. *In vitro* cultivation of southern African strains of *Plasmodium falciparum* and gametocytogenesis. SAMJ 1988;73:720-722.

Freshney RI. The culture environment: Substrate, gas phase, medium and temperature. In: Freshney RI, editor. **Culture of animal cells: a manual of basic technique**. 2nd Ed. New York: Alan Liss Inc., 1987:57-84.

Fritsh G, Jung A. ^{14}C-Desferrioxamine B: Uptake into erythrocytes infected with *Plasmodium falciparum*. Z Parasitenkd 1986;72:709-713.

Fritsch G, Treumer J, Spira DT, Jung A. *Plasmodium vinckei*: suppression of mouse infections with desferrioxamine B. Exp Parasitol 1985;60:171-174.

Fry M. Diferric transferrin reductase in *Plasmodium falciparum*-infected erythrocytes. Biochem Biophys Res Comm 1989;158(Pt 2):469-473.

Fujioka H, Aikawa M. There is no ducking the duct: reply. Parasitol Today 1994;10(Pt 6):223-224.

Furukawa T, Naitoh Y, Kohno H, Tokunaga R, Taketani S. Iron deprivation decreases ribonucleotide reductase activity and DNA synthesis. Life Sci 1992;50(Pt 26):2059-2065.

Gabay T, Ginsburg H. Hemoglobin denaturation and iron release in acidified red blood cell lysate - a possible source of iron for intraerythrocytic malaria parasites. Exp Parasitol 1993;77:261-272.

Gabay T, Krugliak M, Shalmiev G, Ginsburg H. Inhibition by anti-malarial drugs of haemoglobin denaturation and iron release in acidified red blood cell lysates - a possible mechanism of their anti-malarial effect? Parasitol 1994;108:371-381.

Ganeshaguru K, Hoffbrand AV, Grady RW, Cerami A. Effect of various iron chelating agents on DNA synthesis in human cells. Biochem Pharmacol 1980;29:1275-1279.

Geary TG, Divo AA, Jensen JB, Zangwill M, Ginsburg H. Kinetic modelling of the response of *Plasmodium falciparum* to CQ and its experimental testing *in vitro*. Biochem Pharmacol 1990;40(Pt 4):685-691.

Gero AM, Kirk K. Nutrient transport pathways in *Plasmodium*-infected erythrocytes: What and where are they? Parasitol Today 1994;10(Pt 10):395-399.

Ginsburg H, Geary TG. Current concepts and new ideas on the mechanism of action of quinoline-containing antimalarials. Biochem Pharmacol 1987;36(Pt 10):1567-1576.

Ginsburg H, Gorodetsky R, Krugliak M. The status of zinc in malaria (*Plasmodium falciparum*) infected human red blood cells: stage dependant accumulation, compartmentation and effect of dipicolinate. Biochim Biophys Acta 1986;886:337-344.

Ginsburg H, Krugliak M. Effects of quinoline-containing antimalarials on the erythrocyte membrane and their significance to drug action on *Plasmodium falciparum*. Biochem Pharmacol 1988;37(Pt 10):2013-2018.

Ginsburg H, Krugliak M. Quinoline-containing antimalarials - mode of action, drug resistance and its reversal. An uptake with unresolved puzzles. Biochem Pharmacol 1992;43(Pt 1):63-70.

Ginsburg H, Stein W.D. Kinetic modelling of chloroquine uptake by malaria-infected erythrocytes. Assessment of the factors that may determine drug resistance. Biochem Pharmacol 1991;41(Pt 10):1463-1470.

Goldberg DE, Slater AFG, Cerami A, Henderson GB. Hemoglobin degradation in the malaria parasite *Plasmodium falciparum*: An ordered process in a unique organelle. Proc Natl Acad Sci USA 1990;87:2931-2935.

Goldie P, Roth EF, Oppenheim J, Vanderberg JP. Biochemical characterization of

Plasmodium falciparum hemozoin. Am J Trop Med 1990;43(Pt 6):584-596.

Golenser J, Marva E, Kamil M, Hempelmann E, Cohen A, Har-El R, Chevion M. Free radicals and malaria. South Afr J Sci 1991;87:584-587.

Goma J, Renia L, Miltgen F, Mazier D. Iron overload increases hepatic development of *Plasmodium yoelii* in mice. Parasitol 1996;112:165-168.

Gordeuk VR, Thuma PE, Brittenham GM. Iron chelation therapy for malaria. Adv Exp Med Biol 1994;356:371-383.

Gordeuk VR, Thuma P, Brittenham GM, McLaren C, Parry D, Backenstose A. Effect of iron chelation therapy on recovery from deep coma in children with cerebral malaria. N Engl J Med 1992a;327:1473-1477.

Gordeuk VR, Thuma PE, Brittenham GM, Zulu S, Simwanza G, Mhangu A, Flesch G, Parry D. Iron chelation with desferrioxamine B in adults with asymptomatic *Plasmodium falciparum* parasitemia. Blood 1992b;79(Pt 2):308-312.

Gordeuk VR, Thuma PE, McLaren C, Biemba G, Zulu S, Poltera AA, Askin JE, Brittenham GM. Transferrin saturation and recovery for coma in cerebral malaria. Blood 1995;85(Pt 11):3297-3301.

Graninger W, Thalhammer F, Hollenstein U, Zotter GM, Dremsner PG. Serum protein concentrations in *Plasmodium falciparum* malaria. Acta Trop 1992;52:121-128.

Greenwood B, Marah K, Snow R. Why do some African children develop severe malaria? Parasitol Today 1991;7(Pt 10):277-281.

Haldar K. Ducts, channels and transporters in *Plasmodium*-infected erythrocytes. Parasitol Today 1994;10(Pt 10):393-395.

Haldar K, Henderson CL, Cross GAM. Identification of the parasite transferrin receptor of *Plasmodium falciparum*-infected erythrocytes and its acylation via 1,2-diacyl-sn-glycerol. Proc Natl Acad Sci USA 1986;83:8565-8569.

Halliday JW, Ramm GA, Moss D, Powell L. A new look at ferritin metabolism. Adv Exp

Med Biol 1994;356:149-156.

Halliwell B, Gutteridge JMC. Oxygen toxicity, oxygen radicals, transition metals and disease. Biochem J 1984;219:1-14.

Halliwell B, Gutteridge JMC. Protection against oxidants in biological systems: the superoxide theory of oxygen toxicity. In: Halliwell B, Gutteridge JMC, editors. **Free radicals in biology an medicine.** 2nd Ed. Oxford: Claredon Press, 1989:86-187.

Hartley A, Davies MJ, Rice-Evans C. Desferrioxamine and membrane oxidation: radical scavenger or iron chelator? Biochem Soc Trans 1989;17:1002-1003.

Harvey JW, Beutler E. Binding of heme by glutathione-S-transferase: a possible role of the erythrocyte enzyme. Blood 1982;60(Pt 5):1227-1230.

Havlik I, Pullinger H, Herweg B, van Zyl R, Butkow N. Combined effect of ciprofloxacin and tertracycline with quinine and chloroquine on the *in vitro* growth of *Plasmodium falciparum*. Rec Adv Chemother 1993;714-715.

Havlik I, Rovelli S, Kaneko Y. The effect of curdlan sulphate on *in vitro* growth of *Plasmodium falciparum*. Trans Royal Soc Trop Med 1994;88:686-687.

Hempelmann E. Analytical SDS polyacrylamide gel electrophoresis (SDS-PAGE). In: Peters JH and Baumgarten H, editors. **Monoclonal Antibodies.** Berlin: Springer-Verlag, 1984:430-434.

Hempelmann E, Marques HM. Analysis of malaria pigment from *Plasmodium falciparum*. J Pharmacol Toxicol Methods 1994;32(Pt 1):25-30.

Hershko C, Peto TEA. Non-transferrin plasma iron. Br J Haematol 1987;66:149-151.

Hershko C, Peto TEA. Deferoxamine inhibition of malaria is independant of host iron status. J Exp Med 1988;168:375-387.

Hess FI, Kilian A, Sollner W, Nothdurft HD, Proll S, Loscher T. *Plasmodium falciparum* and *Plasmodium berghei*: Effect of magnesium on the development of parasitemia. Exp Parasitol 1995;80:186-193.

Hileti D, Panayiotidis P, Hoffbrand AV. Iron chelators induce apoptosis in proliferating cells. Br J Haematol 1995;89:181-187.

Hoffbrand AV, Ganeshaguru K, Hooton JWL, Tatterall MHN. Effect of iron deficiency and desferrioxamine on DNA synthesis in human cells. Br J Haematol 1976;33:517-526.

Hofheinz W, Merkli B. Quinine and quinine analogues. In, Peters W and Richards WHG. ed. **Antimalarial drug II: Current antimalarials and new drug developments. Handbook of Experimental Pharmacology,** 1984;68(Pt 2):61-81.

Homewood CA, Moore GA, Warhurst DC, Atkinson EM. Purification and some properties of malarial pigment. Ann Trop Med Parasitol 1975;69(Pt 3):283-287.

Homewood CA, Warhurst DC, Peters W, Baggaley VC. Lysosomes, pH and the anti-malarial action of chloroquine. Nature 1972;235:50-52.

Howard RJ, Pasloske BL. Target antigens for asexual malaria vaccine development. Parasitol Today 1993;9(Pt 10):369-372.

Hoyes KP, Porter JB. Subcellular distribution of desferrioxamine and hydroxypyridin-4-one chelators in K562 cells affects chelation of intracellular iron pools. Br J Haematol 1993;85:393-400.

Iheanacho EN, Samuni A, Avramovici-Grisaru S, Sarel S, Spira DT. Inhibition of *Plasmodium falciparum* by a synthetic iron chelator. Trans Royal Soc Trop Med Hyg 1990;84:213-216.

Inselburg J, Bzik DJ, Harii T. Pyrimethamine resistant *Plasmodium falciparum*: overproduction of dihydrofolate reductase by a gene duplication. Molec Biochem Parasitol 1987;26:121-134.

Jacobs A. An intracellular transit iron pool. In: Brown EB, editor. **Progress in Hematology**. New York: Grune and Stratton 1975:91-100.

Jacobs GH, Oduola AM, Kyle DE, Milhous WK, Martin SK, Aikawa M. Ultrastructural study of the effects of chloroquine and verapamil on *Plasmodium falciparum*. Am J Trop Med Hyg 1988;39:15-20.

Jairam KT, Havlik I, Monteagudo FSE. Possible mechanisms of action of desferrioxamine and 2,2'-bipyridyl on inhibiting the *in vitro* growth of *Plasmodium falciparum* (FCR3 strain). Biochem Pharmacol 1991;42(Pt 8):1633-1634.

Jambou R, Ghogomu NA, Kouka-Bemba D, Hengy C. Activity of chloroquine and desferrioxamine *in vitro* against newly isolated *Plasmodium falciparum* and their antagonism in combination. Trans Royal Soc Trop Med Hyg 1992;86:11.

Jensen JB. Concentration from continuous culture of erythrocytes infected with trophozoites and schizont of *Plasmodium falciparum*. Am J Trop Med Hyg 1978;27:1274-1276.

Jensen JB, Trager W. *Plasmodium falciparum* in culture, use of outdated erythrocytes and description of the candle jar method. J Parasitol 1977;63(Pt 5):883-886.

Jin Y, Baquet A, Florence A, Crichton RR, Schneider Y-J. Desferrithiocin and desferrioxamine B. Cellular pharmacology and storage iron mobilization. Biochem Pharmacol 1989;38(Pt 19):3233-3240.

Joshi RR, Likhute SM, Kumar K, Ganesh KN. DNA cleavage by Cu(II)-desferal: identification of C1'-hydroxylation as the initial event for DNA damage. Biochim Biophys Acta 1994;1199:285-292.

Kaplan J, Jordan I, Sturrock A. Regulation of the transferrin-independent iron transport system in cultured cells. J Biol Chem 1991;266(Pt 5):2997-3004.

Keberle H. The biochemistry of desferrioxamine and its relation to iron metabolism. Ann NY Acad Sci 1964;119:758-768.

Klaasen OC. Heavy metals and heavy metal antagonists. In: Gilman AG, Goodman LS, Pall TW, Murad F, editors. **The Pharmacological basis of therapeutics**. New York: MacMillan Publishing Company, 1985:1308-1322.

Klausner RD. From receptors to genes - Insight from molecular iron metabolism. Clin Res 1988;36:494-500.

Klausner RD, Rouault TA, Harford JB. Regulating the fate of mRNA: The control of cellular iron metabolism. Cell 1993;72:19-28.

Klebanoff SJ, Waltersdorph AM, Michel BR, Rosen H. Oxygen-based free radical generation by ferrous ions and deferoxamine. J Biol Chem 1989;264(Pt 33):19763-19771.

Konopka K, Mareschal J-C, Crichton RR. Iron transfer from transferrin to ferritin mediated by polyphosphate compounds. Biochim Biophys Acta 1981;677:417-423.

Koppenol WH. Chemistry of iron and copper in radical reactions. In: Rice-Evans CA, Burdon RH, editors. **Free radical damage and its control.** New York: Elsevier Science, 1994;28:3-24.

Krishna S, Ng LL. Cation metabolism in malaria-infected red cells. Exp Parasitol 1989;69:402-406.

Krishna S, Cowan GM, Robson KJ, Meade JC. *Plasmodium falciparum*: Further characterization of putative cation ATPases. Exp Parasitol 1994;78:113-117.

Krungkrai J, Webster HK, Yuthanvang Y. Folate and cobalamin metabolism in *Plasmodium falciparum*. Parasitol Today 1990;6(Pt 12):388-391.

Kühn LC, Hirling H, Henderson B, Emery-Goodman A, Neupert B, Kaldy P. The structure and function of iron regulatory factor. Adv Exp Biol Med 1994;356:101-109.

Labbe RF, Rettmer RL. Zinc protoporphyrin: a product of iron-deficient erythropoiesis. Semin Hematol 1989;26(Pt 1):40-46.

Lambros C, Vanderberg JP. Synchronization of *Plasmodium falciparum* erythrocytic stages in culture. J Parasitol 1979;65(Pt 3):418-420.

Landau I, Chabaud A, Cambie G, Ginsburg H. Chronotherapy of malaria: An approach to malaria chemotherapy. Parasitol Today 1991;7(Pt 12):350-352.

Leclerc L, Vasseur C, Vursaux E, Marden M, Poyart C. Inhibition of membrane erythrocyte (Ca^{2+} + Mg^{2+})-ATPase by hemin. Biochem Biophys Acta 1988;946:49-56.

Lederman HM, Cohen A, Lee JWW, Freedman MH, Gelfand EW. Deferoxamine: A reversible S-phase inhibitor of human lymphocyte proliferation. Blood 1984;64(Pt 3):748-753.

Lestas AN. The effect of pH upon human transferrin: Selective labelling of the two iron-binding sites. Br J Haematol 1976;32:341-350.

Levander DA, Ager AL. Malarial parasites and antioxidant nutrients. Parasitol 1993;107:S95-S106.

Low H, Grebing C, Lindgren A, Tally M, Sun IL, Crane FL. Involvement of transferrin in the reduction of iron by the transplasma membrane electron transport system. J Bioener Biomembr 1987;19(Pt 5):535-549.

Loyevsky M, Cabantchik ZI. Antimalarial action of hydrophilic drugs: Involvement of aqueous access routes to intracellular parasites. Molec Pharmacol 1993a;45:446-452.

Loyevsky M, Lytton SD, Mester B, Libman J, Shanzer A, Cabantchik ZI. The antimalarial action of desferal involves a direct access route to erythrocytic (*Plasmodium falciparum*) parasites. J Clin Invest 1993b;91:218-224.

Lui S-C, Zhai S, Lawler J, Palek J. Hemin-mediated dissociation of erythrocyte membrane skeletal. J Biol Chem 1985;260(Pt 22):12234-12239.

Lytton SD, Mester B, Dayan I, Glickstein H, Libman J, Shanzer A, Cabantchik ZI. Mode of action of iron(III) chelators as antimalarials. I. Membrane permeation properties and cytotoxic activity. Blood 1993;81:214-221.

Lytton SD, Mester B, Libman J, Shanzer A, Cabantchik ZI. Mode of action of iron(III) chelators as antimalarials. II. Evidence for differential effects on parasite iron dependent nucleic acid synthesis. Blood 1994;84:910-915.

Mabeza GF, van Zyl RL, Havlik I, AP MacPhail, Gordeuk VR. The anti-malarial activity of L1, an orally active iron chelating agent. Trans Royal Soc Trop Med Hyg 1997;submitted.

Makey DG, Seal US. The detection of four molecular forms of human transferrin during the iron binding process. Biochim Biophys Acta 1976;453:250-256.

Marlar-Than, Myat-Phone-Kyaw, Aye-Yu-Soe, Khaing-Khaing-Gyi, Ma-Sabai, Myint-Oo. Development of resistance of chloroquine by *Plasmodium vivax* in Myanmat. Trans Royal Soc Trop Med Hyg 1995;89:307-308.

Marsh K, English M, Crawley J. The pathogenesis of severe malaria in African children. Ann Trop Med Parasitol 1996;90(Pt 4):395-402.

Marsh VM, Brown J, Whittle HC, Greenwood BM. *Plasmodium falciparum*: The behaviour of clinical isolates in an *in vitro* model of infected red blood cell sequestration. Exp Parasitol 1988;65:202-208.

Marva E, Cohen A, Saltman P, Chevion M, Golenser J. Deleterious synergistic effects of ascorbate and copper on the development of *Plasmodium falciparum*: an *in vitro* study in normal and in G6PD-deficient erythrocytes. Int J Parasitol 1989;19(Pt 7):779-785.

May PM, Williams DR. The inorganic chemistry of iron metabolism. In: Jacobs A, Worwood M, editors. **Iron in Biochemistry and Medicine II**. London: Academic Press, 1980:1-28.

McClelland A, Kühn LC, Ruddle FH. The human transferrin receptor gene: Genomic organisation, and the complete primary structure of the receptor deduced from a cDNA sequence. Cell 1984;39(Pt 1):267-274.

Medfile. Malaria prevention for the South African. Medfile 1991;5(Pt 9):73-79.

Mikkelson RB, Tananbe K, Wallach DFH. Membrane potential of *Plasmodium*-infected erythrocytes. J Cell Biol 1982;93:685-689.

Miller JPG, Perkins DJ. Model experiments for the study of iron transfer from transferrin to ferritin. Eur J Biochem 1969;10:146-151.

Milon G. Drugs or vaccines? Parasitol Today 1994;10(Pt 10):402-407.

Molyneux ME. Cerebral malaria in children: Clinical implicationsof cytoadherence. Am J Trop Med Hyg 1990;43(Pt 2):38-41.

Moore GA, Boothroyd B. Direct resolution of the lattice planes of malarial pigment. Ann Trop Med Parasitol 1974;68(Pt 4):489.

Morgan EH. Comparative iron metabolism. In: Jacobs A, Worwood M, editors. **Iron in Biochemistry and Medicine II**. London: Academic Press 1980:641-687.

Morgan EH. Chelator-mediated iron efflux from reticulocytes. Biochim Biophys Acta 1983;733:39-50.

Morgan EH. Membrane transport of non-transferrin-bound iron by reticulocytes. Biochim Biophys Acta 1988;943:428-439.

Murray MJ, Murray AB, Murray MB, Murray CJ. The adverse effect of iron replication on the course of certain infections. Br Med J 1978;2:1113-1115.

Navas P, Villalba JM, Cordoba F. Ascorbate function at the plasma membrane. Biochim Biophys Acta 1994;1197:1-13.

Ndifor AM, Ward SA, Howell RE. Cytochrome P-450 activity in malarial parasites and its possible relationship to chloroquine resistance. Molec Biochem Parasitol 1990;41:251-258.

Nunez M, Cole ES, Glass J. The reticulocyte plasma membrane pathway of iron uptake as determined by the mechanism of 2,2'-bipyridyl inhibition. J Biol Chem 1983;258(Pt 2):1146-1151.

Nurse GT. Iron, the thalassaemias and malaria. Lancet 1979;938-940.

Nyholm S, Mann GJ, Johansson AG, Bergeron RJ, Graslund A, Thelander L. Role of ribonucleotide reductase in inhibition of mammalian cell growth by potent iron chelators. J Biol Chem 1993;268(Pt 35):26200-26205.

Nyholm S, Thelander L, Graslund A. Reduction and loss of the iron center in the reaction of the small subunit of mouse ribonucleotide reductase with hydroxyure. Biochem 1993;32:11569-11574.

Octave J-N, Schneider Y-J, Hoffman P, Trouet, Crichton RR. Transferrin uptake by cultured rat embryo fibroblasts: The influence of lysosmotropic agents, iron chelators and colchicine on the uptake of iron and transferrin. Eur J Biochem 1982;123:235-240.

Oppenheimer SJ. Iron and malaria. Parasitol Today 1989;5(Pt 3):77-79.

Orjih AU, Banyal HS, Chevli R, Fitch CD. Hemin lyses malaria parasites. Science

1981;214:667-669.

Orjih AU, Fitch CD. Hemozoin production by *Plasmodium falciparum*: variation with strain and exposure to chloroquine. Biochim Biophys Acta 1993;1157:270-274.

Pandey AV, Tekwani BL. Identification and quantification of haemozoin: Some additional facts. Parasitol Today 1996;12 (9):370.

Pasvol G, Clough B, Carlsson J. Malaria and the red cell membrane. Blood Reviews 1992;6:183-192.

Pasvol G, Weatherall DJ, Wilson RJM. The increased susceptibility of young red cells to invasion by the malarial parasite *Plasmodium falciparum*. Br J Haematol 1980;45:285-295.

Peto TEA, Thompson JL. A reappraisal of the effects of iron and desferrioxamine on the growth of *Plasmodium falciparum in vitro*: the unimportance of serum iron. Br J Haematol 1986;63:273-280.

Pippard MJ, Hoffbrand AV. Iron. In: Hoffbrand AV, Lewis SM, editors. **Postgraduate Haemotology**, 3rd edition. Oxford: Heinemann Professional Publishing 1989:26-54.

Pollack S. Effects of iron and desferrioxamine on the growth of *Plasmodium falciparum in vitro*. Br J Haemtol 1987a;65:256-257.

Pollack S. *P. falciparum* iron metabolism. In: **Malaria and the Red Cell 2.** New York: Alan R. Liss Inc., 1989:151-161.

Pollack S. Receptor-mediated iron uptake and intracellular iron transport. Am J Hematol 1992;39:113-118.

Pollack S. Intracellular iron. Adv Exp Med Biol 1994;356:165-171.

Pollack S, Aisen P, Lasky FD, Vanderhoff G. Chelate mediated transfer of iron from transferrin to desferrioxamine. Br J Haematol 1976;34:231-235.

Pollack S, Campara T, Weaver J. Low molecular weight iron in guinea pig reticulocytes.

Am J Hematol 1985;19:75-7?.

Pollack S, Fleming J. *Plasmodium falciparum* takes up iron from transferrin. Br J Haematol 1984;58:289-293.

Pollack S, Rossan RN, Davidson DE, Escajadillo A. Desferrioxamine suppresses *Plasmodium falciparum* in Aotus monkeys. Proc Soc Exp Biol Med 1987b;184:162-164.

Pollack S, Schnelle V. Inability to detect transferrin receptors on *P. falciparum* parasitized red cells. Br J Haematol 1988;68:125-129.

Pollack S, Vanderhoff G, Lasky F. Iron removal from transferrin: An experimental study. Biochim Biophys Acta 1977;497:481-487.

Ponka P, Borova J, Neuwirit J, Fuchs O, Necas E. A study of intracellular iron metabolism using pyridoxal isonicotinoyl and other synthetic chelating agents. Biochim Biophys Acta 1979;586:278-297.

Porter JB, Gyparaki M, Burke LC, Huehns ER, Sarpong P, Saez V, Hilder RC. Iron mobilization from hepatocyte monolayer cultures by chelators: The importance of membrane permeability and the iron-binding constant. Blood 1988;72(Pt 5):1497-1503.

Porter JB, Hilder RC, Huehns ER. Uptake of the hydroxypyridinone oral iron-chelating agents. Semin Hematol 1990;27(Pt 2):95-100.

Pouvelle B, Spiegel R, Hsiao L, Howard RJ, Morris RL, Thomas AP, Taraschi TF. Direct access to serum macromolecules by intraerythrocytic malaria parasites. Nature 1991;353:73-75.

Prabhu HR, Krishnamurthy S. Ascorbate-dependant formation of hydroxyl radicals in the presence of iron chelates. Ind J Biochem Biophys 1993;30:289-292.

Primosigh JV, Thomas ED. Studies on the partition of iron in bone marrow cells. J Clin Invest 1968;57:1473-1482.

Qian ZM, Morgan EH. Effect of metabolic inhibitors on uptake of non-transferrin-bound iron by reticulocytes. Biochim Biophys Acta 1991;1073:456-462.

Raventos-Suarez C, Pollack S, Nagel RL. *Plasmodium falciparum*: Inhibition of *in vitro* growth by desferrioxamine. Am J Trop Med Hyg 1982;31(Pt 5):919-922.

Reichard P, Ehrenberg A. Ribonucleotide reductase - A radical enzyme. Science 1983;221:514-519.

Rice-Evans C, Baysal E, Peter H. Effects of desferrithiocin on erythrocytes under extracellular oxidant stress. 62nd Meeting. Biochem Soc Trans 1987;15:851-852.

Robbins E, Pederson T. Iron: Its intracellular locatization and possible role in cell division. Proc Natl Acad Sci USA 1970;66(Pt 4):1244-1251.

Rodrigeuz MH, Jungery M. A protein on *Plasmodium falciparum*-infected erthyrocytes fuctions as a transferrin receptor. Nature 1986;324:388-391.

Roitt I, Boshoff J, Male D. Immunity to protozoa and worms. In: Roitt I, Boshoff J, Male D, editors. **Immunology**. 2nd Ed. New York: Gower Medical Publishing, 1989:17.17.

Rosenthal PJ. *Plasmodium falciparum*: Effects of proteinase inhibitors on globin hydrolysis by cultured malaria parasites. Exp Parasitol 1995;80:272-281.

Roth EF, Brotman DS, Vanderberg JP, Schulman S. Malarial pigment-dependent error in the estimation of hemoglobin content in *P. falciparum*-infected red cells: implications for metabolic and biochemical studies of the erythrocytic phases of malaria. Am J Trop Med Hyg 1986;35(Pt 5):906-911.

Rubin H, Salem JS, Li L-S, Yang FD, Mama S, Wang Z-M, Fisher A, Hamann CS, Cooperman BS. Cloning, sequence determination, regulation of the ribonucleotide reductase subunits from *Plasmodium falciparum*: a target for antimalarial therapy. Proc Natl Acad Sci USA 1993;90:9280-9284.

Salganik RI, Pankora TG, Chekhonadskikh TV, Igonina TM. Chloroquine resistant *Plasmodium berghei*: biochemical basis and counter-measures. WHO Bulletin 1987;63(Pt 3):381-386.

Sanchez-Lopez R, Haldar K. A transferrin-independant iron uptake activity in *Plasmodium falciparum*-infected and uninfected erythrocytes. Molec Biochem Parasitol 1992;55:9-20.

Sayers MH, Lynch SR, Jacobs P, Charlton RW, Bothwell TH, Walker RB, Mayet F. The effects of ascorbic acid supplementation on the absorption of iron in maize, wheat and soya. Br J Haematol 1973;24:209-218.

Schmitt TH, Frezzatti WA and Schreier S. Hemin-induced lipid membrane disorder and increased permeability: a molecular model for the mechanism of cell lysis. Arch Biochem Biophys 1993;307(Pt 1):96-103.

Scott MD, Ranz A, Kuypers FA, Lubin BH, Meshnick SR. Parasite uptake of desferrioxamine: A prerequisite for antimalarial activity. Br J Haematol 1990;75:598-602.

Segovia M, Navarro A, Artero JM. The effect of liposome-entrapped desferrioxamine on *Leishmania donovani in vitro*. Ann Trop Med Parasitol 1989;83(Pt 4):357-360.

Shaklai N, Avissar N, Rabizadeh E, Shaklai M. Disintegration of red cell membrane cytoskeleton by hemin. Biochem Int 1986;13(Pt 3):467-477.

Sharp B, Freese J. Drug resistance in malaria. CME 1995;13(Pt 8):883-890.

Sherman IW, Greenan JRT. Altered red cell membrane fluidity during schizogonic development of malarial parasites (*Plasmodium falciparum* and *P. lophurae*). Trans Royal Soc Trop Med Hyg 1984;78:641-644.

Sherman IW, Ting IP, Rublr JA. Characterization of the malaria pigment (haemozoin) from the avian malaria parasite *Plasmodium lophurae*. J Protozool 1968;15(Pt 4):158-164.

Sinden RE. Mitosis and meiosis in malarial parasites. Acta Leiden 1991;60(Pt 1):19-27.

Singh S, Hider RC. Therapeutic iron-chelating agents. In: Rice-Evans CA, Burdon RH, editors. **Free radical damage and its control**. New York: Elsevier Science, 1994:189-216.

Slater AFG, Cerami A. Inhibition by chloroquine of a novel haem polymerase enzyme activity in malaria trophozoites. Nature 1992;355:167-169.

Slater AFG, Swiggard WJ, Orton BR, Flitter WD, Goldberg DE, Cerami A, Henderson GB. An iron-carboxylate bond links the heme units of malaria pigments. Proc Natl Acad

Sci USA 1991;88:325-329.

Smith AW, Hendrickse RG, Harrison C, Hayes RJ, Greenwood BM. The effects on malaria of treatment of iron-deficiency anaemia with oral iron in Gambian children. Ann Trop Paedriat 1979;9:17-23.

Steinman RM, Mellman IS, Muller WA, Cohn ZA. Endocytosis and the recycling of plasma membrane. J Cell Biol 1983;96:1-27.

Studier FW. Analysis of bacteriophage T7 early RNA's and proteins on slab gels. J Mol Biol 1973;79:237-248.

Sturrock A, Alexander J, Lamb J, Craven CM, Kaplan J. Characterization of a transferrin-independant uptake system for iron in HeLa cells. J Biol Chem 1990;265(Pt 6):3139-3145.

Sullivan DJ, Gluzman IY, Goldberg DE. Plasmodium hemozoin formation mediated by histidine-rich proteins. Science 1996;271:219-222.

Sullivan SG, Baysal E, Stern A. Inhibition of hemin-induced hemolysis by desferrioxamine: binding of hemin to red cell membranes and the effects of alteration of membrane sulfhydral groups. Biochim Biochem Acta 1992;1104:38-44.

Surolia N, Padmanaban G. *De novo* biosynthesis of heme offers a new chemotherapeutic target in the human malarial parasite. Biochem Biophys Res Comm 1992;187(2):744-750.

Swartz RD. Deferoxamine and aluminum removal. Am J Kidney Dis 1985;VI(Pt 5):358-364.

Tabak A, Hoffer E, Taitelman H. Evaluation of a liposome system for the delivery of desferrioxamine to lungs in rats. J Pharm Pharmacol 1994;46:789-796.

Taraschi TF, Parashar A, Hooks M, Rubin H. Perturbation of red cell membrane structure during intracellular maturation of *Plasmodium falciparum*. Science 1986;232:102-104.

Theakston RDG, Fletcher KA, Maegraith BG. The use of electron microscopy autoradiography for examining the uptake and degradation of haemoglobin by *P. berghei*. Ann Trop Med Parasitol 1970;64(Pt 1):63-71.

Thorstensen K, Romslo I. Uptake of iron from transferrin by isolated rat hepatocytes. A redox-mediated plasma membrane process? J Biol Chem 1988;263(Pt 18):8844-8850.

Thorstensen K, Romslo I. The role of transferrin in the mechanism of cellular iron uptake. Biochem J 1990;271:1-10.

Toole-Simms W, Sun IL, Morre DJ, Crane FL. Transplasma membrane electron and proton transport is inhibited by chloroquine. Biochem Int 1990;21(Pt 4):761-769.

Traore O, Carnevale P, Kaptue-Noche L, M'Bede J, Desfontaine M, Elion J, Labie D, Nagel RL. Preliminary report on the use of DFO in the treatment of *Plasmodium falciparum* malaria. Am J Haematol 1991;37:206-208.

Tsafack A, Golenser J, Libman J, Shanzeer A, Cabantchik ZI. Mode of action of iron (III) chelators as antimalarials. III. Overadditive effects in the combined action of hydroxamate-based agents on *in vitro* growth of *Plasmodium falciparum*. Molec Pharmacol 1995;47:403-409.

Tsafack A, Loyevsky M, Ponka P, Cabantchik ZI. Mode of action of iron (III) chelators as antimalarials. IV. Potentiation of desferal action by benzoyl and isonicotinoyl hydrazone derivatives. J Lab Clin Med 1996;127:574-582.

Vander Jagt DL, Hunsaker LA, Campos NM. Characterization of a haemoglobin-degrading, low molecular weight protease from *Plasmodium falciparum*. Molec Biochem Parasitol 1986;18:389-400.

Vander Jagt DL, Hunsaker LA, Campos NM, Baack BR. D-Lactate production in erythrocytes infected with *Plasmodium falciparum*. Molec Biochem Parasitol 1990;42:277-284.

Vyoral D, Hradilek A, Neuwirt J. Transferrin and iron distribution in subcellular fractions of K562 cells in the early stages of transferrin endocytosis. Biochim Biophys Acta 1992;137:148-154.

Wapnick AA, Lynch SR, Krawitz P, Seftel HC, Charlton RW, Bothwell TH. Effects of iron overload on ascorbic acid metabolism. Br Med J 1968;3:704-709.

Ward SA, Bray PG, Mungthin M, Hawley SR. Current views on the mechanisms of

resistance to quinoline-containing drugs in *Plasmodium falciparum*. Ann Trop Med Parasitol 1995;89(Pt 2):121-124.

Warhurst DC. Mechanism of chloroquine resistance in malaria. Parasitol 1988;4(Pt 8):211-213.

Warrell DA, Molyneux ME, Beales PF. Severe and complicated malaria. Trans Royal Soc Trop Med Hyg 1990;84(Pt 2):1-65.

Waxman HS, Brown EB. Clinical usefulness of iron chelating agents. Prog Hematol 1969;VI:338-373.

Weaver J, Zhan H, Pollack S. Erythrocyte haemolysate interacts with ATP-Fe to form a complex containing iron, ATP and 13800 molecular weight polypeptide. Br J Haematol 1993;83:138-144.

Weinberg ED. Nutritional immunity: Host's attempt to withhold iron from microbial invaders. JAMA 1975;231(Pt 1):39-41.

White GP, Bailey-Wood R, Jacobs A. Yhe effect of chelating agents on cellular iron metabolism. Clin Sci Molec Med 1976;50:145-152.

White NJ, Warrell DA. The management of severe malaria. In: Wernsdorfer WH, McGregon I, editors. **Malaria: Principles and practice of malariology**. New York: Churchill Livingstone, 1988:880.

Whitehead S, Peto TEA. Stage-dependant effect of deferoxamine on growth of *Plasmodium falciparum in vitro*. Blood 1990;76(Pt 6):1250-1255.

Wilson CM, Smith AB, Baylon RV. Characterization of the δ-aminolevulinate synthase gene homologue in *P. falciparum*. Molec Biochem Parasitol 1996;75:271-276.

Wolfe LC. Desferrithiocin. Semin Hematol 1990;27(Pt 2):117-120.

Wood PA, Rock LM, Eaton JW. Chloroquine resistance and host cell hemoglobin catabolism in *Plasmodium berghei*. In: Evered D, Whelan J, editors. **Malaria and the Red Cell**, New York: Alan R. Liss, Inc., 1984:159-169.

Wright TL, Fitz JG, Weisiger RA. Non-transferrin-bound iron uptake by rat liver. J Biol Chem 1988;263(Pt 4):1842-1847.

Yamada KA, Sherman IW. *Plasmodium lophurae*: Composition and properties of hemozoin, the malarial pigment. Exp Parasitol 1979;48:61-74.

Yang F, Lum JB, McGill JR, Moore CM, Naylor SL, van Bragt PH, Baldwin WD, Bowan BH. Human transferrin: cDNA characterization and chromosomal localization. Proc Natl Acad Sci USA 1984;81:2752-2756.

Yang Y-Z, Ranz A, Pan H-Z, Zhang Z-N, Lin X-B, Meshnick SR. Daphnetin: A novel antimalarial agent with *in vitro* and *in vivo* activity. Am J Trop Med Hyg 1992;46(Pt 1):15-20.

Yayon A, Bauminger ER, Ofer S, Ginsburg H. The malarial pigment in rat infected erythrocytes and its interaction with chloroquine. J Biol Chem 1984a;259(Pt 13): 8163-8167.

Yayon A, Timberg R, Friedman S, Ginsburg H. Effects of chloroquine on the feeding mechanism of the intraerythrocytic human malarial parasite *Plasmodium falciparum*. J Protozool 1984b;31(Pt 3):367-372.

Zarchin S, Krugliak M, Ginsburg H. Digestion of the host erythrocyte by malaria parasites is the primary target for quinoline-containing antimalarials. Biochem Pharmacol 1986;35(Pt 14):2435-2442.

Zhang Y, Hempelmann E. Lysis of malarial parasites and erythrocytes by ferriprotoporphyrin IX-chloroquine and the inhibition of this effect by proteins. Biochem Pharmacol 1987;36(Pt 8):1267-1273.

Zolg JW, Plitt JR, Chen G-X, Palmer S. Point mutations in the dihydrofolate reductase-thymidylate synthase gene as the molecular basis for pyrimethamine resistance in *Plasmodium falciparum*. Molec Biochem Parasitol 1989;36:253-262.